PIKY EATERS:

How PIKfyve and PI(3,5) P_2 Regulate Macropinosome and Phagosome Maturation in *Dictyostelium*

By:
James H. Vines

Thesis submitted in partial fulfilment of the requirements for the degree of Doctor of Philosophy

The University of Sheffield
Faculty of Science
Department of Biomedical Science

March 2023

PIKY EATERS:

How PIKfyve and PI(3,5) P_2 Regulate Macropinosome and Phagosome Maturation in *Dictyostelium*

By:
James H. Vines

Abstract

Endocytosis is the uptake of extracellular material into the cell. Once internalized, endosomes undergo a series of complex regulatory steps to facilitate the breakdown and/or delivery of different cargoes to different cellular locations - a process called maturation. Successful maturation relies upon phosphoinositide signalling lipids (PIPs) and regulatory proteins to aid in membrane identity and coordinate complex trafficking events. PIKfyve is phosphoinositide 5-kinase essential for efficient maturation of phagosomes and is responsible for synthesis of PI(3,5) P_2, a key membrane marker in endocytic pathways including phagocytosis and macropinocytosis. Despite its importance, PI(3,5) P_2 is one of the least well understood regulators of trafficking. Here, we have used the model professional phagocyte *Dictyostelium discoideum* to identify a novel PI(3,5) P_2 biosensor, SnxA, which can faithfully report PI(3,5) P_2 dynamics in live cells. We find PI(3,5) P_2 binding is conferred through a PX-domain within the reporter, and validate the probe in mammalian cells and *D. discoideum*, showing it is recruited to macropinosomes in a PIKfyve-dependent manner. In *D. discoideum* we employ an automated image analysis pipeline to examine SnxA enrichment to phagosomal membranes over time. We quantify PI(3,5) P_2 arrival ∼3-minutes after phagosome engulfment and show this is completely lost in ΔPIKfyve cells. To further characterise the role of PIKfyve and PI(3,5) P_2, we quantify the enrichment of other phagosomal maturation regulators. We find that, while Rab5 and PI(3)P dynamics are unchanged in ΔPIKfyve cells, Rab7 delivery to phagosomal membranes is severally perturbed. By co-expressing fusion proteins, we go on to delineate a subpopulation of Rab7/PI(3,5) P_2-positive vesicles which are delivered to phagosomes. We find these vesicles contain macropinocytic material which is delivered to phagosomes shortly after their engulfment in a PIKfyve-dependant manner. These findings uncover key mechanistic details of the role and regulation of PIKfyve and PI(3,5) P_2.

To my Grandparents

Clive & Muriel

Declaration

This thesis has been submitted in partial fulfilment of the requirements for the degree of doctor of philosophy. In accordance with the University of Sheffield's thesis format guidelines, it includes two results chapters in the form of draft manuscripts which are intended for publication in the near future.

Please note, both these draft manuscripts bear high similarity to a pre-print we submitted to BioRχiv in late 2022. After submission to The Journal of Cell Biology, reviewers comments led us to split this original manuscript into two halves: the first half for re-submission to JCB Tools and the second half for submission elsewhere. These two halves comprise Chapter's 2 and 3 of this thesis and large parts remain unchanged from the pre-print.

Following the University of Sheffield's pagination guidelines, the text of these manuscripts has been formatted to match the overall style of the thesis. Additionally, for ease of reading, figures and supplementary figures have been embedded within the text and re-numbered. Citation formatting has also been changed in accordance with the rest of this work, and heading numbers have been kept consistent throughout the document. The text itself remains largely unchanged from that which is intended to be submitted. A declaration specifying the exact contributions of James H. Vines is provided before each manuscript.

Many figures within the thesis introduction are closely adapted from Vines & King (2019), a review written by James H Vines and Jason S King with diagrams principally created by James H. Vines.

While this work was disrupted by the Covid-19 pandemic, the Royal Society's kind 6-month project extension has meant many of the potential negative impacts of this have been mitigated.

Acknowledgements

I am extremely grateful to my supervisor Jason King, who without doubt is the friendliest, most supportive, most chilled-out, most overly-optimistic supervisor I could ever have hoped for. Thank you for teaching me techniques, proof-reading all my work, putting up with all my complaining, and most importantly teaching me how to ~~forge scientific data~~ do good science. Our week in California with Phil was awesome, even if everyone I knew thought holidaying with my supervisor was an odd choice. The care, fun and commitment you ooze as a supervisor has made my years as a PhD student some of the best of my life. Thank you.

Of course, I am also grateful to the collection of people who have been part of King Lab over the years. From Ben, who put up with all my naive questions when I first started, to Joe, Zhou, and Meg, who have made my final year in the lab a real joy. A special thanks should go to George for teaching me so much about western blotting, and to Chris, for being unfailingly willing to take my plates out of the incubator on Saturday's. You were both fantastic to work with, even during a world-wide pandemic! I should also thank the ultimate race-to-work runner-up, Ana Paula, for being so incredibly funny, entertaining, and annoying throughout the past two years.

Thanks also to Ilona, my wonderful summer student, who I hope might one day be reading through this to steal a paragraph for her thesis when she completes her own PhD in King Lab. With that in mind, I am also extremely grateful to Cat, the supervisor of my own summer studentship in 2016, without whom I should never have been exposed to the wonders of *Dictyostelium*. I am also appreciative of the kind members from the Erdmann, Peden, Humphries and Smythe Labs who have supported my work along the way too.

My time at Sheffield would not have been the same without the BMSquad, who made lunchtime the best part of every day. To Ash, James, Grag, Laura, Juliana, Anna, Curtis Rom-Chains, Ruth, Ellen, and anyone else I have temporarily forgotten, thanks for eating with a guy who likes butter sandwiches. To Katie, Henry, Dan and Keivan, thanks for your friendship over the past 4-years. I have relished painting your houses, enduring your long walks, and laughing at your damaged knees.

I should also thank my friends from Malvern (the best town in the world), my Improvised Comedy troupe, the BMS football squad, and the Gamerboiks (except for Connor), for their friendship over the past few years, and providing me with things other than science to occupy my mind with.

Keivan will be pleased to know he the only person to get name dropped twice in these acknowledgements, as he, along with Mike and my brother Sam had the unfortunate honour of being my flatmates during my PhD. Thanks for putting up with me and following my strict rules about Sunday Chore Days and Andrew Marr. I guess I should also thank Clement for wetting my bathroom floor on all of his many visits to 4RR - I'd know nothing about *Dictyostelium* if it wasn't for you.

To my parents, Adrian and Liz, thank you for supporting me throughout my studies, and letting me stay in your lovely Sheffield flat for the past 4-years. It is only through your support that I've been able to produce this tome which sits before you now, and I am very grateful for it.

Last, but certainly not least, I should thank the main source of joy in my life, my friend, and my partner: Emma. Without her encouragement, optimism, intellect, love and charm, none of this would have been possible. Thanks you for putting up with me.

Contents

List of Figures

List of Supplementary Figures

List of Videos

Chapter 1

Introduction

1.1 Endocytosis, Endosomes and the Endolysosomal System

Endocytosis is the internalization of extracellular material into the cell. Through controlled manipulation of the plasma membrane, cells can capture a variety of cargoes which are then internalized to form intracellular vesicles called endosomes (Rieger et al., 1991). Endocytosis is important for all eukaryotic cells but different cell types employ specialized forms of endocytosis to fulfil specific functional requirements.

1.1.1 The Formation and Function of Different Endosomes

For an endosome to form cargo must be captured, but different cargoes require the use of different cellular machinery for uptake. The cargo captured within an endosome, and its size, define different forms of endocytosis. For example, fluid is captured by pinocytosis, whereas solid particles are captured by phagocytosis, and cargoes of different sizes are captured by either micro- or macro- endocytosis (**Figure 1.1**).

Microendocytosis is the internalization of membrane. This process was first identified in the 1960s when advances in electron microscopy allowed microendosomes <100 nm in diameter to be seen for the first time (Roth & Porter, 1964) (Reviewed in: Elkin et al., 2016). Due to their size, microendosomes have a high *surface-area:volume* ratio; thus, they are optimized for membrane turnover or retrieval of specific proteins on the plasma membrane rather than fluid uptake.

A range of proteins can be employed to form microendosomes. The best studied of these proteins is clathrin, which can form a self-assembling lattice along the plasma membrane after recognizing adaptor proteins bound to cargo, such as activated cell surface receptors (Pearse, 1976). Clathrin oligomerisation leads to membrane curvature, and allows downstream proteins to further invaginate the membrane, leading to the formation of a small clathrin-coated endosome (Reviewed in: McMahon & Boucrot, 2011). A variety of other proteins can also facilitate the formation of small vesicles through micropinocytosis, including caveolin and ARF6 (Reviewed in: Kumari et al., 2010).

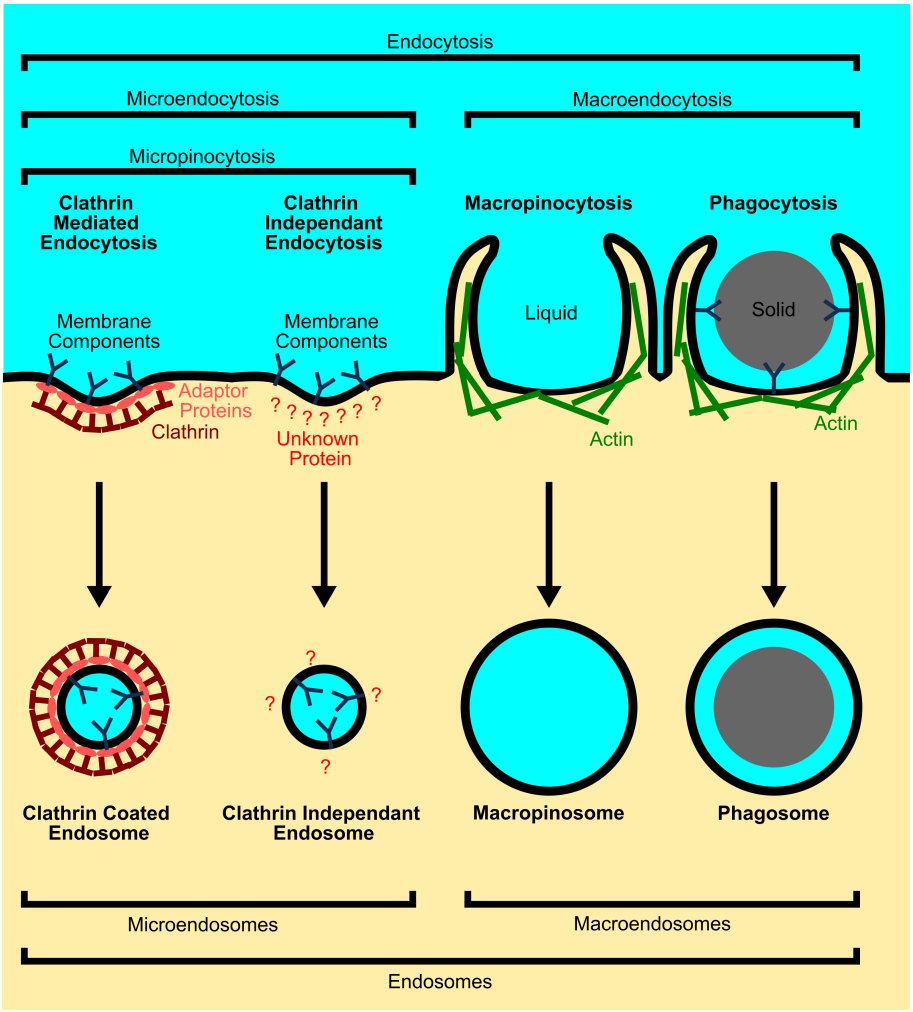

Figure 1.1: **Four Types of Endocytosis.** Adapted from Vines & King (2019). From left to right: (1) In clathrin mediated endocytosis, membrane components to be internalized bind to adaptor proteins, which in turn bind intracellular clathrin. This creates an intracellular coat of clathrin, and an invagination of the plasma membrane. This results in the formation of a small intracellular endosome known as a clathrin coated endosome. (2) In clathrin independent endocytosis, other proteins like caveolin, create small intracellular endosome not associated with clathrin. (3) In macropinocytosis, extracellular fluid is taken up in large cups formed from spontaneous actin polymerization at the cell surface. This forms a large intracellular vesicle known as a macropinosome. (4) In phagocytosis, an extracellular solid (ie bacteria, yeast or latex bead) is taken up upon binding and activation of a cell surface receptor, which in turn causes the formation of a large cup by stimulating actin polymerisation. This forms a large intracellular endosome known as a phagosome.

Macropinocytosis is the uptake of extracellular fluid. It was first identified by Lewis in 1931, when he saw macrophages forming large fluid-filled macroendosomes called macropinosomes (Reviewed in: Chapman-Andresen, 1984). Macropinosomes are >200 nm in diameter, so unlike micropinosomes have a low *surface-area:volume* ratio and are optimized to collect and sort large quantities of extracellular fluid. Because there is no solid cargo, they must initiate formation and determine their shape and size independently of ligand binding.

In mammalian cells, macropinosomes can arise spontaneously from the inward folding of cell-surface membrane ruffles and their subsequent fusion back to the basal membrane. This process is driven by actin nucleation, which occurs non-specifically along the plasma membrane and it is maintained at constitutively low levels in most mammalian cells. Macropinocytosis can be upregulated, however, through activation of receptor tyrosine kinases by growth factors such as colony stimulating factor or epidermal growth factor (Racoosin & Swanson, 1989; Yoshida et al., 2015; Nakase et al., 2015). These promote actin nucleation, increasing ruffling and macropinosome formation (Kaplan, 1977; Hacker et al., 1997). In unicellular organisms macropinocytosis evolved for nutrient acquisition (Reviewed in: King & Kay, 2019). Multicellular organisms have adapted macropinocytosis to aid in immune surveillance, cell motility, and antigen presentation.

Phagocytosis is the capture of large solids. It was first identified by Metchnikoff in 1882, who observed motile cells in starfish larvae internalizing solid particles and forming large, particle-containing, macroendosomes which he called phagosomes (Reviewed in: Tauber, 2003; Gordon, 2016).

Like macropinocytosis, actin nucleation is required to drive phagosome formation, but, unlike macropinocytosis, receptor binding is required. Classical phagocytosis relies upon Fcγ receptors on the cell surface which recognise characteristic motifs on a cargoes surface which promotes actin nucleation at the plasma membrane to driving its extension around the solid and facilitate its engulfment (Levin et al., 2016). Complement mediates phagocytosis, however, uses receptors which recognise targets coated in complement from blood plasma. Here, cargo is internalised by *sinking* into the cell without any protrusions (Reviewed in: Aderem & Underhill, 2003).

While phagosomes can engulf indigestible solids, the primary function of phagocytosis is to ingest and digest other cells or cellular debris. In multicellular organisms, this can include destroying pathogens and clearing apoptotic cells. Professional phagocytes, including macrophages, neutrophils, and dendritic cells, are especially adept at these processes as they are specialized in efficient intracellular killing (Reviewed in: Krause, 2000). Other mammalian cells can also perform non-professional phagocytosis, but this happens at a low frequency and is poorly characterised (Seeberg et al., 2019). Phagocytosis is also crucial for preventing infection in protists and unicellular life forms, which also need to eliminate opportunistic pathogens to survive (Molmeret et al., 2005). Like macropinocytosis, species optimized for phagocytic uptake and digestion can also utilize it as a source of nutrients.

Phagocytosis is often studied in parallel with macropinocytosis, as both macroendocytic pathways rely upon the actin cytoskeleton to manipulate the plasma membrane to form large macroendosomes. Both phagocytosis and macropinocytosis are also crucial for the presentation of exogenously acquired

antigens to T-cells in professional phagocytes of multicellular organisms. Antigens for presentation can be acquired from the extracellular environment through macropinocytosis or by breaking down phagocytosed pathogens (Reviewed in: Roche & Furuta, 2015). These antigens are then displayed on the surface of major histocompatibility complex class II molecules. Hindrance of endosomal processing, however, decreases the overall efficiency of antigen presentation and compromises the development of a robust immune response (Granboulan et al., 2003; Halici et al., 2008; Neumeister et al., 2005).

1.1.2 The Maturation of Endosomes

Endocytic pathways feed into the endolysosomal system. After the formation of an endosome, its cargo must be sorted and the vesicle matured. Using marker proteins and lipids, endocytic compartments can be differentially labelled. Sorting proteins use these markers to establish a network of pathways to move and sort cargo. The resulting web of trafficking endosomes is the endolysosomal system (Reviewed in: Klumperman & Raposo, 2014).

Although it can be entered from phagocytosis, macropinocytosis and microendocytosis, which have distinct differences, many of the proteins and lipids facilitating endolysosomal sorting are the same. This is because every vesicle, big or small, is delivering cargo to one of three exit points: (1) return to the plasma membrane via a recycling pathway, (2) degradation via a lysosomal pathway, or (3) delivery to another location via the trans-golgi network (Reviewed in: Klumperman & Raposo, 2014).

The inositol phospholipid content of an endosomal membrane is central to identifying its position in the endolysosomal system. Inositol phospholipids are made of an inositol head group, a glycerol backbone, and two non-polar fatty acid tails connected to the backbone through an ester linkage(**Figure 1.2 A**). The head group can be phosphorylated at any of three positions (3, 4 or 5) to form one of eight different phosphatidylinositide species (PIPs) (**Figure 1.2 B-I**).

These phosphorylated forms are essential markers for the endolysosomal system. Each can recruit effector proteins, which specifically recognise different phosphorylation patterns through their PIP binding domains. One of the best characterised is the Fab1, YOTB, Vac1, and EEA1 (FYVE) domain, which specifically binds PI(3)P. FYVE-domains consist of two small β-sheets and an α-helix stabilized by two zinc ions, and are often found in proteins requiring recruitment to early endosomes (Reviewed in: Gillooly et al., 2001). The PI(3)P biosensor, 2xFYVE is a tandem repeat FYVE-domain isolated from the human Hrs gene. It is a well characterised PI(3)P reporter used extensively in live cell fluorescence imaging to study PI(3)P synthesis and turnover (Gillooly et al., 2000; Clarke et al., 2010). Other PIP sensing domain include phox homology (PX) domains and pleckstrin homology (PH)domains.

Using kinases and phosphatase the cell is able to convert between each PIP type as maturation progresses to recruit different effectors (Reviewed in: Bohdanowicz & Grinstein, 2013). For example, on early endosomes PI(3)P is phosphorylated at the 5-position to form PI(3,5) P_2 by the kinase PIKfyve (see: **1.4.3 PIKfyve is essential for coordinating maturation**). This results in an elegant system to sort and identify compartments.

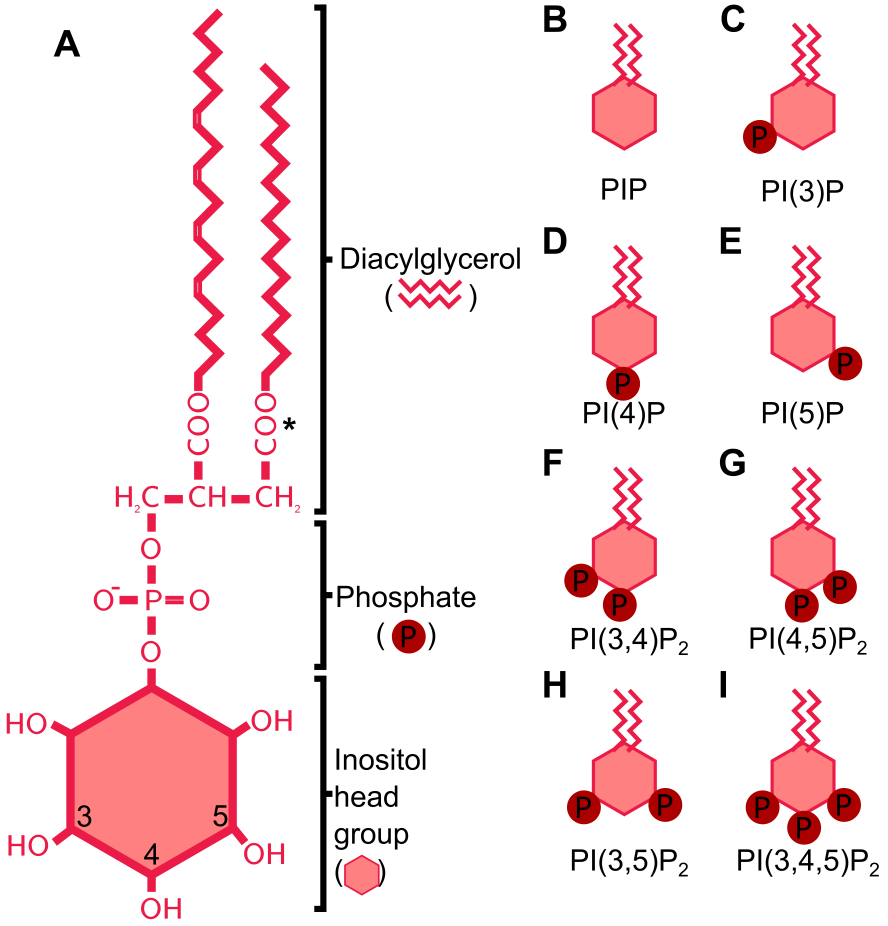

Figure 1.2: **Phosphatidyl-inositol Phosphate Structures.** **(A)** Detailed structure of a phosphatidylinositid consisting of a inositol head group connected to a diacylglycerol by a phosphate linker. 3, 4, and 5 mark the sites at which the inositol head can be phosphorylated by various kinases. Asterisk marks the ester link which is replaced by an ether link in *D. discoideum* to make a plasmanylinositide. **(B)-(I)** Representations of all eight forms which phosphatidyl-inositol phosphates can take. As detailed in (A), the hexagon represents the inositol head group, the lines represent the diacylglycerol, and P represents the sites of phosphorylation for each structure.

Rabs are regulatory guanosine triphosphatases which, like PIPs, act as key endosomal markers and regulators of vesicular transport. Rabs function as switchable molecular triggers which are active in their GTP-bound form and inactive in their GDP-bound form. This activity can be controlled by specific guanine nucleotide exchange factors (GEFs) and GTPase-activating proteins (GAPs), which promote GTP or GDP binding, respectively (**Figure 1.3**) (Levin et al., 2016). In humans, there are around 60 different Rab GTPases, each of which associates with specific intracellular membranes, many of which are part of the endolysosomal system (Zhen & Stenmark, 2015). Using GEFs and GAPs, Rabs can communicate between one another to manage trafficking. For example, the early endosomal marker Rab5 is deactivated by a Rab5-GAP, which also recruits and activates the late endosomal marker, Rab7 (see: **1.4.2 Rab7 Coordinates Later Delivery Events**).

Rab effectors encompass a wide range of proteins, including vesicle tethers, motors, kinases, phosphatases, and various adaptor proteins. It is through these effectors that they can regulate endosome trafficking. They also have roles in a variety of physiological processes, including immunity, hormone secretion, and neurotransmission (Reviewed in: Stenmark, 2009).

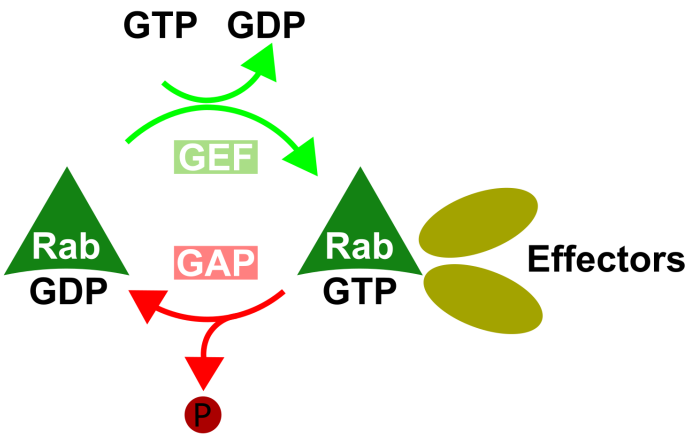

Figure 1.3: **Rab GTPase Switch.** Rabs can interact with effectors in their active GTP-bound form. This is facilitate by GEFs which remove GDP and promote GTP binding. Rabs are deactivated by GAPs which catalyse the breakdown of GTP into GDP + Pi.

The endolysosomal system drives fusion between compartments. Fusion is incredibly important for the maturation of endosomes and the trafficking of cargoes to specific locations in the cell. For example, to breakdown the contents of endosomes, a cocktail of different proteases and hydrolases must be delivered to the endosomal lumen. These are typically delivered via lysosomes which fuse with endosomes to form a single degradative compartment called an endolysosome (or for a phagosomes a phagolysosome). This fusion delivers the digestive cocktail directly the endosome lumen to expedite cargo breakdown.

Fusion is reliant upon PIPs and Rabs to coordinate it. First, fusing vesicles must be tethered to

one another. Tethers are large protein complexes normally present on target membranes. They extend away from the target surface and sample the environment for presence of the vesicles, the identification of which is aided by Rab proteins (Spang, 2016). Upon successful contact, they bring vesicles closer to the target membrane (Reviewed in: Yu & Hughson, 2010). Different tethering complexes are important throughout different stages of maturation. For example, the tethering of vesicles to early endosomes is mediated by the class C core vacuole/endosome tethering (CORVET) complex, while tethering of late endosomes with lysosomes depends on the homotypic fusion and vacuole protein sorting (HOPS) complex (Spang, 2016).

Just because two compartments are tethered does not mean they can automatically fuse. Sometimes, compartments only perform a 'kiss-and-run' event. In these instances, a small portion of material is transferred from one endosome to another, and both endosomes remain independent (Neuhaus et al., 2002). These events have been noted to be especially common in mammalian cells overexpressing a constitutively active Rab5, where short bridges between endosomes are especially easy to observe (Roberts et al., 1999). For complete fusion, SNARE proteins like syntaxin-6 and syntaxin-13 are required (Simonsen et al., 1999; McBride et al., 1999). SNAREs are present in all eukaryotic cells, and fusion between two compartments occurs when one vesicle-SNARE forms a complex with two or three specific target-SNAREs to form an alpha helix coiled-coil bundle (Reviewed in: Ungar & Hughson, 2003; Hong, 2005). This brings membranes into sufficient contact so as to promote their fusion.

Endocytosis is integral to eukaryotic cell function. Although the primary role of endocytosis is uptake of solid, fluid or membrane components, the endolysosomal system as a whole is essential for other cellular processes too (Reviewed in: Repnik et al., 2013). For example, cellular maintenance and repair dependant upon autophagy, which can sequester undesirable proteins, organelles and other cellular debris from the cytosol in membrane abound compartments called autophagosomes. The exocytosis of lysosomes, membrane-bound organelles that contains digestive enzymes, is also important for cell maintenance, including plasma membrane repair (Reddy et al., 2001). Lysosomes can also initiate cell apoptosis by releasing lysosomal proteases into the cytosol.

1.1.3 Macroendocytosis and Human Disease

The array of integral functions the endolysosomal system performs means that its disruption can result a range of cellular abnormalities, many of which are linked to human disease. Many of these are specifically linked with macroendosomes. A full understanding of the endolysosomal system would have significant advantages clinically both for our understanding of disease mechanisms, and for our development of effective therapeutics.

Pathogens can hijack macropinocytosis and phagocytosis to enter host cells. Many pathogens exploit macropinocytosis to promote their own uptake. Pathogens such as *Salmonella* (Rosales-Reyes et al., 2012) and viruses such as Vaccinia and Ebola (Mercer et al., 2010) induce host cell ruffling or blebbing to increase their chances of being taken up in an endosome. Some pathogens are even able to

promote their own phagocytosis; *Listeria monocytogenes*, for example, mimics apoptotic cells to promote its uptake into a phagosome (Czuczman et al., 2014).

Once internalized, hijacking pathogens must inhibit normal maturation or will otherwise be destroyed. Both *Salmonella* and *Legionella* secrete effector proteins through endolysosomal membranes via their type III or type IV bacterial secretion systems, respectively. This allows them to manipulate the identity of their compartments, thereby disrupting normal maturation (Hilbi, 2006). Pathogens can also gain resources by exploiting host cells from within. *Mycobacterium marinum*, for example, actively promotes lipid droplet recruitment to the phagosome from early stages, and continues to accumulate lipids throughout infection to build up its own intra-cytosolic lipid inclusions (Barisch et al., 2015). If pathogens can effectively establish a safe, resource-rich, replication-permissive niche within a host this can be used to promote further infection among neighbouring cells.

This exploitation of endocytosis is a highly effective strategy for human pathogens. For example, *Salmonella typhi*, the primary cause of typhoid fever world-wide affecting about 14 million people annually, exploits endocytosis (Reviewed in : Basnyat et al., 2021). It employs an Arf6-driven actin polymerization pathway to promote its own macropinocytosis (Humphreys et al., 2013). With antimicrobial resistance being common in *Salmonella typhi* infections, new therapeutic strategies, possibly to prohibit *Salmonella* uptake or restore routine maturation, would be highly beneficial for disease prevention.

Macropinocytosis can also be exploited for drug delivery. Finding reliable mechanisms for delivery of large therapeutics to specific target locations within cells is challenging. Endocytosis is an efficient and ubiquitous route into the cell, however. Being receptor-independent, macropinocytosis in particular can be a useful tool for delivery. The size of macropinosomes also means that large or complex molecules like nanoparticles, can be delivered (Reviewed in: Means et al., 2022). Another current example of this is mRNA vaccines, such as those developed to prevent Covid-19, which are most likely taken up via macropinocytosis (Diken et al., 2011).

While macropinocytic entry demonstrates potential, it still has major limitations. Reliably stimulating cells to perform macropinocytosis within different tissue remains challenging. For example, the size, shape, charge, and surface coating of nanoparticles strongly influence their uptake efficiency (Chithrani et al., 2006). Furthermore, creating molecules which reliably escape the macropinosome is difficult, and drugs can become damaged before they reach their target if lysosomal degradation precedes too far (Reviewed in: Desai et al., 2019).

Macropinocytosis is commonly upregulated in cancers. Macropinocytosis can significantly increase nutrient acquisition, which helps to promote tumour growth. Oncogenic mutations in the regulatory protein K-Ras are commonly associated with this,and lead to increased rates of macropinocytic uptake and therefore entry of extracellular protein into the cell (Commisso et al., 2013). In addition, oncogenic mutations can also occur upstream of Ras in the proteins that regulate it, for example mutations in the RasGAP NF1 are found in neurofibromatosis (Li et al., 1992). Helpfully, upregulation of macropinocytosis, in combination with macropinocytic drug delivery does point to a potential mechanism for targetting cancer therapeutics (Reviewed in: Liu & Qian, 2022).

Macroendocytosis is linked with neurodegenerative disease. Ineffective phagocytosis of amyloid-β plaques has been observed in blood samples of Alzheimer's patients (Fiala et al., 2005), and inappropriate phagocytosis of myelin has been observed in macrophages from Multiple Sclerosis patients (Reviewed in: Smith, 1999).

Macropinocytosis has also been linked with cell-to-cell spread of prions (Reviewed in: Zeineddine & Yerbury, 2015). For example, Amyotrophic Lateral Sclerosis is caused by the spread of SOD1 mutant aggregates between cells. This spread is enhanced by their uptake via macropinocytosis. Once internalized, the mutant aggregates can rapidly escape from macropinosomes and promote aggregation of otherwise stable SOD1 mutant protein, leading to a self-perpetuating cycle (Münch et al., 2011).

In 2016, neurological disorders were second leading cause of deaths globally, being linked with 9 million fatalities (Feigin et al., 2019). In the succeeding years, this value will only have increased, as the prevalence of neurological disorders increases as population become proportionally older.

Overall, endocytosis is a complex field of study which is relevant to disease prevention. This work focuses primarily on improving our understanding of how macropinosome/phagosome maturation is regulated. An improved understanding of macropinocytosis and phagocytosis could provide us greater insight into how our immune system functions, and highlight new mechanisms to potentially improve its function. Moreover, both processes are closely implicated with infectious disease, cancers and neurodegeneration: three of the most prevalent areas of human diseases which require our attention. This makes the macroendosome maturation a valuable area to study with significant potential to improve human disease outcomes in the future.

1.2 *Dictyostelium discoideum* as a Model for the Study of Macroendocytosis

A useful model to investigate macroendosomes, and the principal organism used throughout this study, is the soil dwelling amoeba *Dictyostelium discoideum*.

***D. discoideum* have a complex life cycle.** When there is an abundance of nutrients *D. discoideum* grow as single, free-living, cells which reproduce asexually. During this stage of their life cycle they act as professional phagocytes, engulfing and digesting environmental bacteria for food. When food is scarce, however, they initiate a multicellular developmental cycle (**Figure 1.4**): Large numbers of amoebae chemotax towards one another, forming a large aggregate of approximately 100,000 cells (Bonner & Savage, 1947). *D. discoideum* use both intra- and extra- cellular signals, most notably pulses of cAMP (Konijn et al., 1967), to coordinate this process. Once aggregated, cells subsequently differentiate to form a multicellular structure called a slug. When in its natural environment, a slug moves towards the soil surface by sensing heat and light. From there, cells differentiate further, to form an elongated stalk which rises away from the soil surface, with a spore head at its tip. This structure aids dispersal of spores away

from the stalk. Spores scattered to new nutrient rich soils return to their single-celled form to feed on bacteria before repeating the process (Reviewed in: Loomis, 2014).

While this complex lifecycle has been a boon for the study of multicellular development in *D. discoideum*, when studying phagocytosis and macropinocytosis *D. discoideum* are grown in nutrient rich conditions in their single celled, phagocytic, form.

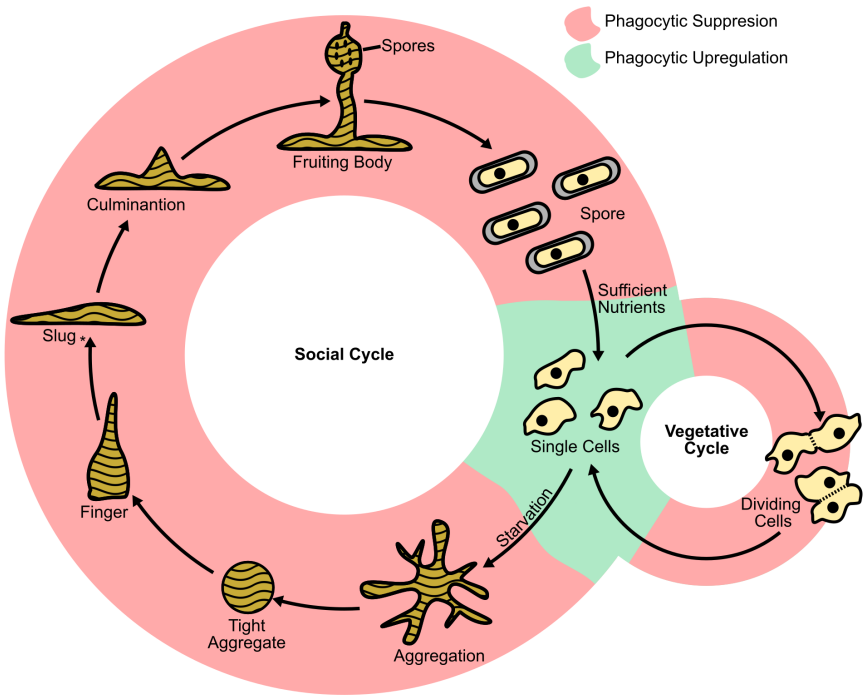

Figure 1.4: ***Dictyostelium* Life Cycle.** Adapted from Vines & King (2019). In nutrient-replete conditions, *D. discoideum* will grow in the vegetative cycle where they feed through phagocytosis and macropinocytosis, as highlight by the green background. Upon starvation, macroendocytosis is largely suppressed and large numbers of cells aggregate by chemotaxis and undergo differentiation to form a multicellular structure consisting of >100,000 cells. The purpose of this structure is to aid the distribution of spores to a more nutrient rich environment.

***D. discoideum* is a well characterized model organism.** Wild-type strains of *D. discoideum* were first isolated in the 1930s (Raper & Thom, 1932; Raper, 1935); however, these strains are uncommonly used in labs today, as they only grow through phagocytosis on solid food. Through sub-culturing in the 1960s to increase macropinocytic rates, the first axenic strain, Ax1, was generated and able to grown in liquid media supplemented with liver extract and fetal calf serum (Sussman & Sussman, 1967). In the 1970s, two more axenic strains, Ax2 and Ax3, were independently generated and eliminated the need for any supplement (Watts & Ashworth, 1970; Loomis, 1971).

The Ax1 strain has since been lost; however, both Ax2 and Ax3 are commonly used as laboratory wild-

type strains today. Ax3 is known to carry a large duplication of chromosomes 2 and 5 within its genome, which are not present in Ax2 (Bloomfield et al., 2008). In this work, an Ax2 wild-type background has been used throughout.

Both axenic strains contain a key mutation in a RasGAP, Neurofibromin (NF1), which allows them to grow axenicly. NF1 regulates Ras, and its disruption ultimately leads to excessive Ras activity, the increased size and frequency of macropinosomes, and excessive fluid uptake - all of which are beneficial for feeding on extracellular liquid nutrients. NF1 mutants can also ingest larger than normal solid particles due to enlargement of phagocytic cups (Bloomfield et al., 2015).

The mechanisms of macropinocytosis and phagocytosis are conserved between *D. discoideum* and higher eukaryotes. Most cells within multicellular eukaryotes have no requirement to be phagocytic; they are in large, static tissues with ready supplies of nutrients. A subset of cells, most notably macrophages and neutrophils, do rely on phagocytosis for immune functions, however. Immune cells also upregulate macropinocytosis, which is important for immune surveillance and antigen presentation.

Despite differences in function, the machinery governing macroendosomal maturation is largely conserved. Comparative phagosome proteome studies between *D. discoideum* and higher multicellular organisms highlights a shared core of phagosomal proteins across species, suggestive of an evolutionary conserved pathway (Boulais et al., 2010) which initially evolved for cell feeding and was later adapted for innate immune roles (Reviewed in: King & Kay, 2019).

The PIP structure in *D. discoideum* is different to other eukaryotes. An ether linkage, not an ester linkage, joins the glycerol backbone to the tails, technically forming a rare plasmanylinositide phospholipid species (asterisk in **Figure 1.2 A**) (Clark et al., 2014). Because inositol phospholipid interactions are mediated through the inositol head-group rather than the lipid chain, however, these slight differences in chemistry do not affect downstream signalling in practice. As such, for this work, both plasmanylinositide and phosphatidylinositide have been treated interchangeably and are both referred to as phosphoinositol phosphates (PIPs).

***D. discoideum* are an ideal model for studying membrane trafficking.** Like other professional phagocytes, *D. discoideum* are able to phagocytose a range of solids including bacteria, yeasts, other cells, and indigestible solids like glass microspheres and latex beads. They also constitutively make large, distinct macropinosomes. Unlike many mammalian cell lines, however, they have small haploid genomes, making them amenable to genetic manipulation (Eichinger et al., 2005). They often lack the redundancy that can be problematic in higher eukaryotes. In addition, their ability to grow in large numbers, and their amenability for biochemical studies and fluorescence microscopy, make them an ideal system for the study of membrane trafficking and macroendosome maturation.

1.3 Maturation of Macropinosomes and Phagosomes

The maturation of a macroendosome is a complex and dynamic process that begins with an initial engulfment event and ends with the degradation of its luminal contents. This process is tightly regulated by the cell to ensure that cargo is processed efficiently. Different types of cargo require different maturation profiles, which the cell will optimize to account for cargo types (Souza et al., 1997; Lamrabet et al., 2020b; Nasser et al., 2013). For example, the requirements to kill and breakdown a yeast are different to that of an *E.coli*. Maturation profiles also vary between cell types. Most notably, *D. discoideum* macropinosomes and phagosomes mature much faster than their mammalian counter-parts (Reviewed in: Vines & King, 2019). This can make it hard to compare timings between cell types, which is further complicated by any differences in regulatory proteins too.

Despite these differences, maturation can be divided into a broad set of events, which cells follow to complete maturation. These include: the nascent stage, recycling events, delivery events, and post-lysosomal formation & exocytosis (Reviewed in: Levin et al., 2016).

This study primarily concerns maturation in *D. discoideum*. Therefore, the events discussed below draw from work on this organism; however, where appropriate, studies from yeast, nematodes worms, and mammalian cells have also been incorporated, as these can help provide broader insights into maturation as a whole. For reference, **Figure 1.5** contains an overview of this process, and **Figure 1.6** contains an approximate timeline for the markers discussed in *D. discoideum*.

1.3.1 Nascent Macroendosomes

Nascent macropinosomes and phagosomes are those which have just formed and separated from the plasma membrane. They have an internal pH equal to that of the extracellular environment, and their membranes contain proteins and lipids which were required for cup formation, closure, and scission, as well as those which were non-specifically incorporated from the plasma membrane.

Actin is the key driver of macroendosome formation. Both formation and closure require actin, so nascent macroendosomes are initially surrounded by actin filaments (Maniak et al., 1995; Kaplan, 1977; Hacker et al., 1997). These filaments rapidly de-polymerize and dissociate following cup closure, along with actin-associated proteins, such as coronin. This typically occurs 30-60 seconds after closure in *D. discoideum* and mammalian macrophages (Maniak et al., 1995; Hacker et al., 1997; Lu & Clarke, 2005; Clarke et al., 2010; Henry et al., 2004). This process coincides with the movement of the macroendosome away from the plasma membrane.

The removal of actin is essential for maturation. In ΔAbp1 *D. discoideum* actin enrichment is sustain due to stalled de-polymerization, and this results in an array of generalized maturation defects, including a decrease proteolytic activity later in maturation (Dieckmann et al., 2012). Abp1 is normally enriched along with MyoK at closing *D. discoideum* phagosomes where both proteins are thought to help regulate formation (Dieckmann et al., 2010); although they remain at phagosomal membranes throughout later stages of maturation (Dieckmann et al., 2012). Actin de-polymerization can also be perturbed in human

neutrophils by lowering calcium ion concentrations, which likewise leads to a perturbation in phagosome maturation (Bengtsson et al., 1993).

PI(3,4,5) P_3 and then PI(3,4) P_2 mark the nascent macroendosome. PI(3,4,5) P_3 appears at sites of forming macroendosomes, but is rapidly de-phosphorylated following cup closure by a PI-5 phosphatase, Dd5P4 (OCRL in mammals), to generate PI(3,4) P_2 (Dormann et al., 2004; Loovers et al., 2007; Luscher et al., 2019). On *D. discoideum* phagosomes, PI(3,4) P_2 enrichment peaks immanently following cup closure, and is typically lost in the successive 60-120 seconds (Dormann et al., 2004; Giorgione & Clarke, 2008). This time period, however, is dependent upon phagosomal contents. Phagocytosis of latex beads shows PI(3,4) P_2 can be maintained for upwards of 360-seconds (Giorgione & Clarke, 2008), possibly due to their indigestible nature.

Plasma membrane proteins are present on nascent macroendosomes. Several studies have shown that cell surface proteins are non-specifically internalised on macropinosomes and phagosomes (Ravanel, 2001; Gotthardt et al., 2002; Buckley et al., 2016). Most appear in the same concentrations as on the plasma membrane (Ravanel, 2001; Mercanti et al., 2006); although, some are excluded from the macroendosome (Mercanti et al., 2006). Thus, mechanisms must exist for preventing certain proteins being captured in macroendosomes during cup formation; however, how these proteins are determined and how they are excluded is not clear.

Some surface proteins also play roles in initiation or formation. For example, LmpB, a glycoprotein, is known to mediate uptake of mycobacteria and is taken up on forming phagosomes (Sattler et al., 2018). Any proteins like this need to be recycled almost immediately following closure, to maintain acceptable levels at the plasma membrane.

1.3.2 Recycling Events

One of the first key events in maturation is the rapid recycling of plasma membrane components back to the cell surface. This occurs immediately after internalization, and in *D. discoideum* most proteins are recycled within 2-minute (Neuhaus & Soldati, 2000).

Many proteins of the nascent macroendosome are rapidly returned to the plasma membrane. LmpB and the copper transporter p25, are just two examples of proteins which are rapidly removed from macroendosomes and recycled back to the plasma membrane (Ravanel, 2001; Gotthardt et al., 2002). This rapid recycling indicates that the return of proteins to the cell surface is important for continued cell function. Indeed, prohibiting recycling of SibA, an integrin-β-like protein important for cell adhesion and phagocytic reception, causes sever phagocytic uptake defects in *D. discoideum* (Cornillon et al., 2006; Buckley et al., 2016).

The return of cell surface proteins is controlled through the combined action of sorting and recycling complexes. WASP and SCAR homologue (WASH) complex is one such complex which is

recruited in patches to macroendosome membranes, where it activates the Arp2/3 complex to generate the small patches of actin which leads to tubule formation (Buckley et al., 2016; Derivery et al., 2009; Gomez & Billadeau, 2009). These tubules can then be pinched off into vesicles and trafficked back to the plasma membrane. Without WASH, cells have severe recycling defects and reduced rates of phagocytosis (Buckley et al., 2016).

WASH co-localizes with the Retromer Sorting Complex (RSC) through interaction of its FAM21 subunit with the VPS35 subunit of RSC (Jia et al., 2012; Buckley et al., 2016). RSC is thought to act as a recruiting hub for a large number of proteins involved in tubule formation, including sorting nexins.

In mammals, sorting nexins are recruited to the RSC to aid sorting of receptors (Reviewed in: Worby & Dixon, 2002; Carlton et al., 2005b,a). SNX1 and SNX2 are two well characterised mammalian sorting nexins which localize to PI(3)P and PI(3,5) P_2 on early macropinosomes. Like most sorting nexins, they contain a phox homology (PX) domain, which aids their recruitment to PIPs, and a BAR domain, which senses and induces membrane curvature (Carlton et al., 2005b). Along with WASH they can enhance the formation of tubules and connect to microtubule motors, further promoting tubule extension ready for scission (Derivery et al., 2009). *D. discoideum* contains a variety of sorting nexins, although most are relatively poorly characterised.

For tubules to become recycling endosomes they must be pinched off. This requires scission machinery such as Dynamin, a large GTPase known to be important in the scission of vesicles from elongated endosomal tubules in mammalian cells and yeast (Reviewed in: Ferguson & Camilli, 2012). Knockouts of the *D. discoideum* dynamin orthologue, DymA, disrupts many membrane scission events causing a wide range of phenotypes (Wienke et al., 1999; Gopaldass et al., 2012). This makes it hard to differentiate between direct and indirect roles of dynamin; nonetheless, DymA localises to phagosomes early and ΔDymA cells have slow acidification, reduced proteolysis rates, and hyper-tubulation throughout maturation (Gopaldass et al., 2012).

Eps15 homology domain (EHD) containing proteins are structurally and functionally related to dynamin. The *D. discoideum* orthologue of EHD is recruited independently of dynamin, but both proteins bind one-another (Gueho et al., 2016). Like with DymA, disruption of EHD results in hyper-tubulation of endosomal compartments; however, each protein appears to play functionally independent roles in phagosome maturation, as EHD knockout phagosomes acidify at normal rates (Gueho et al., 2016).

Whilst it is easy to imagine a role for Dynamin and EHD in the scission of recycling vesicles from nascent phagosomes and macropinosomes, this is yet to be directly tested. As WASH and the retromer are only present for the first 2-3 minutes following engulfment, but DymA and EHD remain for as long as 30 minutes, there are also likely to be a number of additional trafficking steps regulated by this membrane cleavage machinery (Wienke et al., 1999; Buckley et al., 2016; Gueho et al., 2016).

Recycling endosomes are trafficked to target membranes. In mammalian cells, recycling endosomes are marked by Rab4 and Rab11 GTPases as they recycle. Rab11 is specifically associated with exocytosis events at the plasma membrane (Ward et al., 2005). In *D. discoideum*, however, protein markers of recycling endosomes remain unclear, as both Rab4 and Rab11 homologs principally localize to the

contractile vacuole (Bush et al., 1996; Harris et al., 2001). Additionally, whether recycling endosomes always return directly to the plasma membrane, or whether they must travel via the golgi apparatus is unclear; both types of retrograde transport occur in mammalian cells, but there is limited research in *D. discoideum*.

1.3.3 Delivery Events

For maturation to progress, protein and lipids must be delivered to macroendosomes. This delivery can occur directly from the cytosol or from fusion with other endolysosomal compartments. Delivery begins immediately following internalization alongside the recycling events discusses above (Clarke et al., 2010; Tu et al., 2022). It is regulated spatially and temporally by Rab proteins, PIPs and fusion machineries, which serve to identify compartments and control delivery events.

Vacuolar-type H^+-ATPase (V-ATPase) is delivered to macroendosomes to acidify cargo. V-ATPase is a proton pump which actively transports hydrogen ions across endolysosomal membranes (Nolta et al., 1996). It is enriched at the contractile vacuole and on endosomes. While enrichment leads to the acidification of luminal contents inside endosomes, the pH of the contractile vacuole itself remains close to neutral (Stock et al., 2002). V-ATPase consists of a peripheral V1 domain that performs ATP hydrolysis and an integral V0 domain. V-ATPases work through rotary motion, where ATP hydrolysis in V1 causes rotation of a central rotary domain across the membrane, which results in active proton transport into the lumen (Reviewed in: Cipriano et al., 2008).

In *D. discoideum*, V-ATPase is rapidly delivered to phagosomes via early endosomes which begin to fuse within the first 120-second after engulfment (Adessi et al., 1995; Clarke et al., 2002a, 2010). By tagging a large 100kDa transmembrane subunit of the V0 domain, VatM, it is possible to identify small, highly acidic, VatM-positive vesicles clustering early phagosome before fusing (Clarke et al., 2002a). These likely arise from pre-existing acidic compartments of the endolysosomal system, and can be loaded with extracellular dyes which become visible in phagosomal lumens as V-ATPase is delivered and is indicative of fusion (Clarke et al., 2002a, 2010).

In *D. discoideum*, V-ATPase delivery continues until a peak around 4 minutes. Acidification of the lumen continues to increase, however, eventually dropping to pH 3.5 after 30-minutes (Gopaldass et al., 2012). Rapid acidification is important for digestion and killing any live contents of phagosomes. pH is only re-neutralized when the V-ATPase is retrieved from the compartment much later in the pathway (see: **1.3.4 Post-lysosomal Transition & Exocytosis**) (Gopaldass et al., 2012).

VatM is essential for cell viability, and *D. discoideum* knock-downs have slow cell growth, perturbed phagosome acidification, and a mis-localization of other V-ATPase subunits including the catalytic subunit, VatA (Liu et al., 2002). It is likely that a failure to acidify has consequences downstream for hydrolases and proteases which require a low pH to function effectively.

The release of calcium ions from intracellular stores, such as the endoplasmic reticulum (ER), has been found to be essential for the maturation of phagosomes (Stossel, 1973).

This has been demonstrated through studies on the stromal interaction molecule 1 (STIM1), which promotes the recruitment of ER cisternae to phagosomes and is essential for the release of calcium ions into the cytosol (Reviewed in: Nunes & Demaurex, 2010). Studies in phagocytic mouse embryonic fibroblasts (MEFs) have shown decreased phagocytosis and more prominent peri-phagosomal actin rings when STIM1 is disrupted (Nunes et al., 2012). This likely results from observed decreases in ER-phagosome contacts and reductions in peri-phagosomal calcium, both of which have roles in mediating fusion between early endosome with phagosomes (Reviewed in: Nunes-Hasler & Demaurex, 2017).

The exact timing and nature ER-phagosome interaction during maturation is somewhat controversial, however. Early research in *D. discoideum* used two calcium-binding ER proteins, calnexin and calreticulin, as markers for ER protein delivery to phagosomes. Both localized to the forming phagocytic cup, and continued to localize throughout maturation of *Legionella pneumonia*-containing-phagosomes (Mu et al., 2001; Fajardo et al., 2004). Other studies, however, only saw calreticulin enrichment after cup closure (Dieckmann et al., 2012), and some saw no ER proteins at nascent phagosomes at all, only observing calnexin at much later stages (Lu & Clarke, 2005). In mammalian cells, electron microscopy has shown phagosomal-ER interaction throughout maturation in J774 macrophages when phagocytosing *Leishmania*, *Salmonella typhimurium*, and red blood cells; however, in neutrophils neither latex bead or *Leishmania* containing phagosomes displayed any ER interaction (Gagnon et al., 2002). Additionally, studies to assess the lipid origins of the phagosomal membrane during maturation found no significant contribution of ER membrane to the phagosome, suggesting the ER does not play a role in membrane delivery (Touret et al., 2005).

Overall, the contribution of the ER to macroendosome maturation remains unclear. While it is likely that ER proteins are important throughout maturation, exactly when, how, and under what conditions ER contact become essential remains unclear. Furthermore, how ER proteins more generally contribute to phagosomes maturation, with the exception of STIM1, is unknown (Reviewed in: Levin-Konigsberg & Grinstein, 2020).

Macroendosomes are actively trafficked along mirotubules. In *D. discoideum*, phagosomes traffic bi-directionally along microtubules (Lu & Clarke, 2005). Macropinosomes traffic similarly, but also deform as they are moving, demonstrating a characteristic 'stretching' phenotype. Large endosomes, like phagosomes and macropinosomes, also bridge gaps between microtubules, crossing from one to another.

Macroendosomes are pulled along by dynein motors, which cluster into microdomains on surfaces. By clustering they can work cooperatively to move persistently along a microtubule (Rai et al., 2016). This allows for rapid, directional movement of macroendosomes around the cell, which, in *D. discoideum*, persists for around 35-minutes after internalization (Clarke et al., 2002b). Cells treated with nocodozole, a microtubule disruptor, lose this rapid movement, and small endosomes cluster in the cell centre rather than around macroendosomes (Clarke et al., 2002b). This suggests microtubule movement or binding is important for early delivery events. Rapid movement around the cell may bring early macroendosomes into contact with a greater number of endosomes, possibly facilitating more fusion events. Additionally,

characteristic stretching and tubulation of macropinosomes may be important for recycling events.

Macropinosomes shrink as maturation progresses. Because macropinosomes are fluid-filled, their contents can be concentrated by decreasing their size. This is beneficial, as a small compartment will be easier to acidify due to its smaller volume. This means, as maturation progresses, macropinosomes become largely indistinguishable from late endosomes. Phagosomes, however, remain easily identifiable due to their large solid contents which cannot be concentrated until digestion is complete.

The contents of maturing macropinosomes are also delivered back to early macropinosomes. The mixing of macropinosomes from different stages of maturation was first demonstrated in *D. discoideum* by Clarke et al. (2002b). Fusion between mature and early macropinosomes starts from around 2-minutes following engulfment, and is aided by microtubule transport. It is likely that mixing is an efficient mechanism for accumulating maturation machinery to new macropinosomes. The ability to mix is eventually lost as maturation progresses to later stages (Clarke et al., 2002b).

Lysosomes are delivered to macroendosomes to digest cargo. Lysosomes are small, spherical endosomes that contain a range of digestive enzymes. Their delivery to macroendosomes marks the beginning of a later stage of maturation focussed on killing and digestion. Once lysosomal contents are delivered to macropinosomes or phagosomes, the fused compartments are sometimes referred to as either endolysosomes or phagolysosomes. Contrary to a model in which a lysosome contains the entire gamut of digestive enzymes needed to complete maturation, proteomics of purified phagolysosomes in *D. discoideum* indicate multiple phases of delivery and retrieval throughout a long digestive period (Gotthardt et al., 2002). This sequential delivery may aid cargo breakdown or killing.

In mammalian cells, lysosomal integrity is maintained by lysosomal-associated membrane protein 1 (LAMP-1)and lysosomal-associated membrane protein 2 (LAMP-2) (Reviewed in: Eskelinen, 2006). Disruption of either results in mammalian phagosomes being unable to recruit key regulatory proteins, such as Rab7, and a failure of them fuse with lysosomal compartments (Huynh et al., 2007).

While LAMPs are essential for maturation in mammalian cells, *D. discoideum* has no true LAMP homologs. However, two lysosomal proteins do share a key LAMP-1-like sorting motif: LmpA and LmpC (Janssen et al., 2001). Both localize to phagolysosomes, becoming enriched throughout lysosomal delivery (Gotthardt et al., 2002; Sattler et al., 2018). Knockdowns of LmpA are defective in phagocytic uptake, have impaired acidification, and lower levels of lysosomal hydrolases, while LmpC knockouts appear to little effect on maturation (Sattler et al., 2018).

Phagocytosis of living cells requires the cell to activate a variety of killing strategies. The killing of intracellular cargo is achieved through combined actions: The low pH caused by V-ATPase (Aubry et al., 1993; Adessi et al., 1995; Clarke et al., 2002a; Gotthardt et al., 2002) , the delivery of metal ions (Buracco et al., 2018), the production of reactive oxygen species (ROS), and the delivery of lysosomal enzymes all contribute (Reviewed in: Dunn et al., 2018).

The coordination required for each of these steps is energetically intensive for the cell; therefore, it is unlikely that all killing and digestion strategies are employed for both macropinocytosis and phagocytosis.

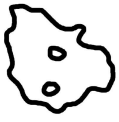

Macropinocytosis is less likely to result in uptake of living cells, and many nutrients may already be broken down. Conversely, phagocytosis can result in the uptake of living pathogens adapt in avoiding many killing mechanisms. As such a larger array of killing methods may be employed for phagosomes. Because of this, studies on killing focus primarily on phagocytosis, not macropinocytosis. Furthermore, because different pathogens are vulnerable to different killing mechanisms, the methods of killing may vary depending on prey. As such, studies frequently show large variations in delivery timings and intensities of different lysosomal components depending upon the cargo. Exactly how the cell is able to distinguish between cargo types and recognise the best killing mechanisms requires further research.

An imbalance of trace metals can inhibit intracellular cell growth. Concentrating or sequestering metal ions, such as iron, zinc and copper, is a pathogen killing mechanism used in mammalian phagocytes, and similar mechanisms exist in *D. discoideum*.

Iron is transported out of phagolysosomes. Low iron concentration reduces the growth rate of intraluminal *L. pneumonia* cells (Buracco et al., 2018). The natural resistance-associated membrane protein 1 (Nramp1) is a metal ion transporter which localizes to macroendosomal membranes in *D. discoideum* cells (Peracino et al., 2006). Overexpression of GFP-Nramp1 protects cells from *L. pneumonia* infection. Its delivery begins around 95 seconds after-engulfment, but only peaks after 15 minutes (Peracino et al., 2006). It localizes with V-ATPase throughout the lysosomal stage, but remains post V-ATPase removal, being present on exocytotic vesicles (Peracino et al., 2006; Buracco et al., 2018). ΔNramp1 cells are defective at killing mycobactreria and *L. pneumonia*, but can kill *Klebsiella aerogenes*, suggesting Nramp1 may only be important for killing some bacterial strains (Peracino et al., 2006).

Zinc is transported into phagolysosomes. Excess levels of zinc may inhibit bacterial ATP production, or replace other metals in the active site of bacterial enzymes. In *D. discoideum*, free zinc is compartmentalized into the endolysosomal system (Barisch et al., 2018; Buracco et al., 2018). It is then delivered to phagolysosomes, either by fusion, or through active transport by zinc transporters, such as ZntB (Barisch et al., 2018). ΔZntB cells have a 60% reduction in intra-luminal zinc levels inside *Escherichia coli* or *M. smegmatis* phagolysosomes (Barisch et al., 2018). Excess levels of zinc are known to contribute to bacterial killing; however, in ΔZntB cells bacterial killing was unaffected. Thus, loss of zinc poisoning can probably be compensated for by killing mechanisms (Barisch et al., 2018).

Copper is transported into phagolysosomes. p80, a Ctr-type copper permease, is present at low levels on the macroendosome membrane from early stages, but is not enriched until post-lysosomal transition (Ravanel, 2001). Copper translocators are upregulated upon bacterial uptake and are to contribute to killing (Hao et al., 2016).

Overall, changes in iron, zinc and copper concentrations appear to be important for killing; however, none are completely essential for phagocytosis.

Reactive oxygen species facilitate killing. In mammals, the NADPH-oxidase, Nox2, is essential to produce the ROS required for an oxidative burst which aids killing during maturation. It produces a superoxide radical from oxygen and NADPH (Reviewed in: Dunn et al., 2018).

D. discoideum contains three catalytic orthologs of mammalian Nox2 (NoxA, NoxB and NoxC). NoxA is the only one expressed in vegetative cells, along with its regulator, CybA (Lardy et al., 2005). Whether NoxA and CybA, or their resulting ROS, are delivered to phagosomes is unclear. ΔNoxA cells show no defects in growth on *K. aerogenes*, and NADPH oxidase activity does not appear to be affected in the knockouts (Lardy et al., 2005). *D. discoideum*, however, has a high general resistance to oxidative stress (Katoch & Begum, 2003), which could suggest that ROS are widely used in killing.

Delivery of a range of lysosomal enzymes contribute to killing. The delivery of lysosomal enzymes to phagolysosomal lumens is complex, and evidence suggests that different enzymes are delivered and retrieved sequentially.

D. discoideum has two main types of lysosomal hydrolases: those with glucosamine-1-phosphate modifications, which are delivered to phagosomes early within the first 3-minutes of maturation, and those with mannose-6-sulfate modifications, which are delivered later (Souza et al., 1997). They are sorted into different lysosomal compartments, but all function to catalyse the breakdown phagolysosomal contents in some way.

Glucosamine-1-phosphate hydrolases include: proteinase I, CP-p34, and CP-p36 (Adessi et al., 1995; Mehta et al., 1995; Gotthardt et al., 2002; Rupper et al., 2001a). All of these enzymes are classified as cysteine proteases, which catalyse the breakdown of peptide bonds. CP-p34 and CP-p36 are amongst some of the first delivered, coinciding with delivery of LmpA and LmpC (Gotthardt et al., 2002; Rupper et al., 2001a). CP-p34 is retrieved before the delivery of mannose-6-sulfate modified hydrolases (Gotthardt et al., 2002), but CP-p36 continues to accumulate as maturation progresses (Rupper et al., 2001a). In Rab7 dominant negative cells, immature forms of cysteine proteinases are delivered to phagosomes instead, highlighting Rab7 as a key lysosomal delivery coordinator (see **1.4.2 Rab7 Coordinates Later Delivery Events**) (Rupper et al., 2001a).

Mannose-6-sulfate hydrolases include: Cathepsin D (CatD), another protease, and α-mannosidase and β-glucosidase, which are both involved in the breakdown of sugars and oligosaccharides, including cellulose (Reviewed in: Dunn et al., 2018). All three are delivered later in maturation, with CatD only accumulating following retrieval of CP-p34 (Journet et al., 1999). CatD remains until just before exocytosis, along with the LmpA and LmpC (Gotthardt et al., 2002).

Other hydrolases, such lysozymes, are also delivered from separate compartments (Cosson & Lima, 2014). Lysozymes are glycoside hydrolases that catalyse the breakdown of Gram-positive bacterial cell walls. AlyA is a member of a family of lysozymes found in *D. discoideum*, and its disruption halves the overall level of lysozyme activity in cells. This significantly affects the cells ability to grow slowly on solid food; although this phenotype can be rescued through continued culturing, suggesting a loss of AlyA can be compensated through increased phagocytic uptake (Müller et al., 2005).

Overall, there is a large range digestive enzymes which can be delivered to phagolysosomes. *D. discoideum* alone has more than 30 genes predicted to be cysteine proteases, and 22 genes predicted to be lysozymes (Cosson & Lima, 2014; Lamrabet et al., 2020a). How each of these enzymes are selectively trafficked is not fully understood, and the benefits of sequential delivery and retrieval are unclear, but

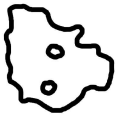

it's possible digestion is more efficient if early hydrolases partially digest the luminal contents for later ones with different cleavage specificity. It's also clear that not all phagolysosomes require every lysosomal enzyme. For bacteria, at least, vastly different mechanisms of killing are used depending on the species (Lamrabet et al., 2020b).

1.3.4 Post-lysosomal Transition & Exocytosis

In *D. discoideum*, the final stage of maturation ends in the expulsion of indigestible luminal contents into extracellular space. Before this can happen, various proteins must be retrieved from the endolysosomal compartment as it transitions into a post-lysosomal.

Proteins are recovered from post-lysosomes before their exocytosis. The transition from a digestive compartment to a post-lysosome is precipitated by retrieval of V-ATPase. Over a three minute time period, it is sequestered from the post-lysosomal membrane into small vesicles and recycled (Clarke et al., 2010). As V-ATPase is removed, the luminal pH begins to re-neutralize and other components, such as Rab7, CatD, LmpA, and LmpC are retrieved (Gotthardt et al., 2002).

Actin polymerization and the WASH complex are essential for this process (Clarke et al., 2010). In ΔWASH mutants V-ATPase cannot be retrieved from post-lysosomal compartments, presumably due to a failure to nucleate actin (Carnell et al., 2011), and exocytosis is unable to resolve in either the absence of WASH or in the presence of an actin de-polymerizing agents (Rauchenberger et al., 1997; Carnell et al., 2011).

Phagosomes fuse with one another before exocytosis. In *D. discoideum*, phagosome-phagosome fusion occurs around 45-minutes after initial engulfment (Rupper et al., 2001b). RabD, a mammalian Rab14 homolog, and PI-3 kinase activity, is required to mediate this fusion. Cells with hyperactive RabD have a five-fold increase in phagosome-phagosome fusion, whereas fusion is halved when expressing dominant negative RabD (Harris & Cardelli, 2002).

Furthermore, treatment of hyperactive RabD cells with LY294002, a PI 3-kinase inhibitor, have a reduction in multi-particle phagosomes. This confirms early evidence that PI03 kinases also play a role downstream, or in parallel with, RabD to mediate phagosome-phagosome fusion (Rupper et al., 2001b; Harris & Cardelli, 2002).

The benefits of phagosome-phagosome fusion are unclear. More recent work has demonstrated in macrophages the process is correlated with impaired degradation. This is also true of bead containing phagosomes, which show reduced degradation when forming multi-bead phagosome - indicating the process is not an evasion response promoted by pathogens (Yu et al., 2022).

Some proteins are retained on the post-lysosome. p80, the Ctr copper transporter, is retained and reaches high concentrations at the point of exocytosis, and thus provides a useful marker for monitoring exocytosis (Ravanel, 2001). In *D. discoideum* a TRPML1 homolog, Mucolipin-1 is delivered to the

post-lysosome too (Lima et al., 2012). Δmcl1 cells have increased exocytosis, and decreased calcium concentration within the lumen (Lima et al., 2012).

Post-lysosomes have unique lipid properties. In *D. discoideum*, Vacuolins (orthologous of flotillin) accumulate on post-lysosomes in detergent-resistant lipid micro-domains known as lipid rafts (Bosmani et al., 2019; Rauchenberger et al., 1997). Vacuolin decorates post-lysosomal compartments just before their exocytosis when the luminal pH is neutral approximately 60-seconds post-engulfment (Rauchenberger et al., 1997). Despite their predominantly post-lysosomal localisation, disruption of vacuolins causes defects throughout the endocytotic cycle, including faster maturation and defective recycling of membrane proteins (Bosmani et al., 2019). It is therefore likely that lipid-micro-domain mediated sorting and recycling has pleiotropic functions throughout the endocytotic pathway.

1.4 Regulation of Maturation

The maturation of macroendosomes described above requires by PIPs, kinases, phosphatases and Rab GTPases to coordinate the delivery and fusion of compartments.

1.4.1 Rab5 and PI(3)P Coordinate Early Delivery Events

Rab5 marks early endosomal compartments. In mammalian macrophages Rab5 becomes enriched on phagosomal membranes within the first 60 seconds following engulfment (Henry et al., 2004; Lippuner et al., 2009). In *D. discoideum* Rab5 marks endosomal membranes even earlier, being present on forming macropinosomes and enriching a few seconds after engulfment (Bucci et al., 1992; Dieckmann et al., 2012; Tu et al., 2022).

Rab5 must be activated to coordinate maturation. GEFs, such as Rabex-5 and Rabaptin-5, work together to create a positive feedback loop for robust activation of Rab5 (Lippé et al., 2001). Continued activation will promote endosome fusion events via Rab5 effectors, including Vps34, EEA1, and CORVET (Reviewed in: Borchers et al., 2021). Rab5 is removed from macroendosomal membranes within a few minutes of its arrival; however, its recruitment and activation is essential for the next stages of maturation (Vieira et al., 2003).

PI(3)P is recruited downstream of Rab5. Like Rab5, PI(3)P is a marker of the early macroendosome. It is enriched on macroendosome membranes within 60 seconds following internalization, immediately after actin de-polymerization (Clarke et al., 2010; Henry et al., 2004). In yeasts and mammalian cells, a PI-3 kinase, Vps34, catalyses PI(3)P production (Christoforidis et al., 1999; Vieira et al., 2001), and its inhibition stalls phagosome maturation. Recruitment of Vps34 is directly linked to Rab5 activation, meaning the co-enrichment of Rab5 and PI(3)P distinguishes the early macroendosome (Fratti et al., 2001).

A Vps34 homologue, DdPIK5, synthesises PI(3)P in *D. discoideum* and rescues yeast lacking the Vps34 protein (Zhou et al., 1995). Few other studies have directly assessed DdPIK5's role in macroendo-

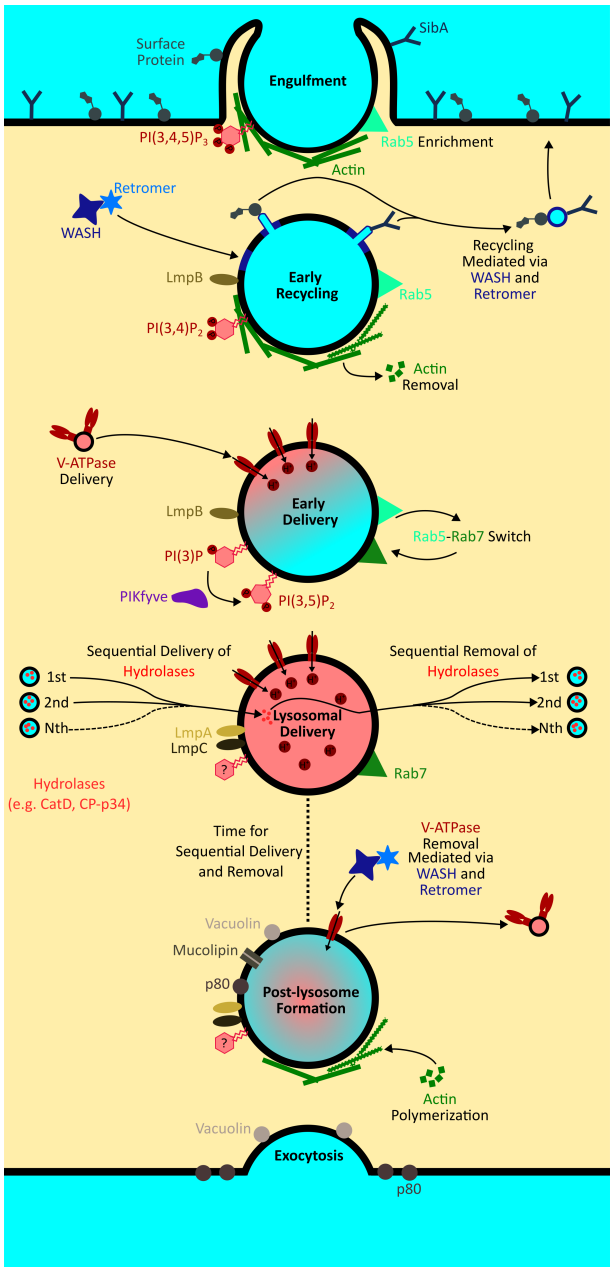

Figure 1.5: **Macropinosome and phagosome maturation in *D. discoideum*.** Adapted from Vines & King (2019). The cartoon shows the progress of macroendosomes as they mature. Upon engulfment, the Rab5 and PI(3,4) P_2 positive nascent vesicle is surrounded by actin which is rapidly removed. In an early recycling phase, plasma membrane proteins are rapidly recycled back to the plasma membrane by the WASH and retromer complexes. During this process, the compartment accumulates PI(3)P, and an early delivery phase also begins as the V-ATPase is delivered on small acidic vesicles. V-ATPase activity causes acidification of the vesicle lumen (represents by red colouring), and over time PI(3)P is converted to PI(3,5)P2 by the activity of PIKfyve. As maturation progresses, Rab5 is retrieved and Rab7 enriched on the membrane, which triggers the lysosomal delivery phase. Here, the lumen is acidified and hydrolases such as CatD and CP-p34 are sequentially delivered over an extended digestive period. Finally, after digestion is complete, the macroendosome is prepared for exocytosis in a late recycling phase. Here, WASH-stimulated actin re-forms around the compartment to retrieve the V-ATPase and form a neutral post-lysosome. The retromer complex is also present and potentially plays a role in hydrolase retrieval. Other important proteins such as vacuolin and mucolipin also accumulate on this late compartment, although are most probably retrieved before exocytosis, unlike p80 which is present during exocytosis and can be seen in high concentrations at the plasma membrane immediately after.

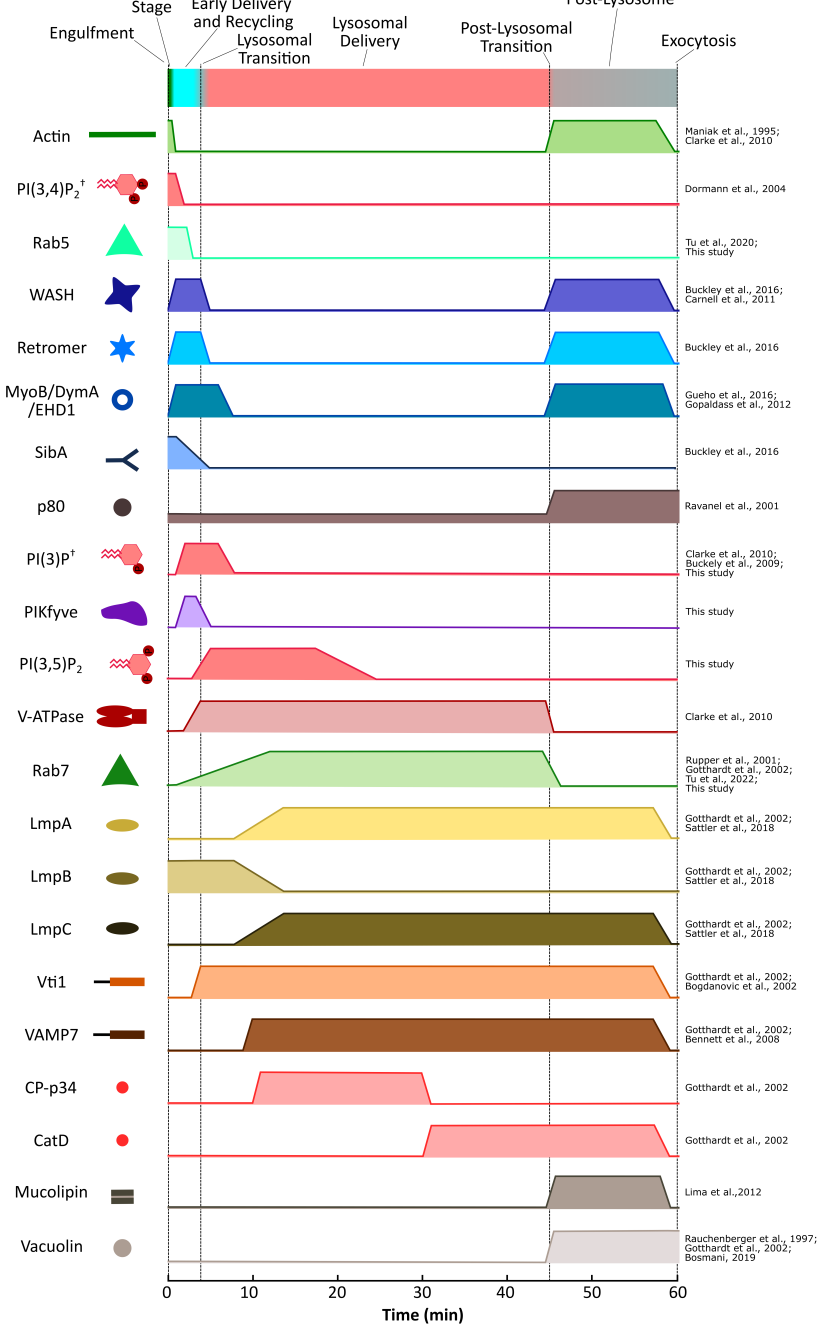

Figure 1.6: **Timings of Components of Phagosome and Macropinosome Maturation in *D. discoideum*.** Adapted from Vines & King (2019). Each line represents the dynamics of the components (protein or lipid) over a 60-minute maturation event. When the line of the time-courses is high, the respective component is at/on/in the endosome at this time-point. When the line of the time-course is low, the component is not present. This diagram has been pieced together from the existing literature, combining both microscopy and biochemical data. It assumes that phagosome and macropinosome maturation are comparable and integrates data from studies of both pathways. It should be noted that in general, biochemical analysis of purified phagosomes often indicates slower maturation than that observed by live-cell imaging, with maturation occurring over an almost 3 hour period (Buckley et al., 2016; Gopaldass et al., 2012; Gotthardt et al., 2002). Microscopy studies in contrast, indicate exocytosis of yeast and bead-containing phagosomes, as well as macropinosomes occurs at around 60-90 minutes after engulfment (Clarke et al., 2010; Lima et al., 2012; Ravanel, 2001). The data has been consolidated from both techniques to an "average" 60-minute transit. With this in mind, this figure is best viewed in the context of this work as a whole and combined with the references provided for each individual component. "†" indicates that retrieval phase is known to be longer in phagosomes containing yeast.

some maturation; although, it likely performs similar functions to its mammalian counterpart following recruitment by Rab5.

PI(3)P typically remains on *D. discoideum* macroendosomes for the next 360-seconds. Bacteria-containing-phagosomes and macropinosome both gradually loose PI(3)P over this time until undetectable (Clarke et al., 2010). Yeast-containing-phagosomes, however, show more sustained levels of PI(3)P, for upwards of 28-minutes (Clarke et al., 2010; Buckley et al., 2019). This reflects how cargo-type can drastically change maturation profiles even relatively early in maturation.

Activated Rab5 and PI(3)P promote early endosome fusion. The movement of macroendosomes around the cell on microtubules helps promote fusion between other compartments. In mammalian cells, Rab5 directly regulates early endosome motility along microtubules, and their movement is dependent upon Rab5 and recruitment of Vps34 (Nielsen et al., 1999).

Furthermore, Rab5 co-localizes and interacts with components of the CORVET tethering complex to contact and tether vesicles ready for fusion (Perini et al., 2014). Following tethering, activated PI(3)P and Rab5 recruit, early endosomal antibody 1 (EEA1) through its FYVE-domain and a Rab5-GTPase binding domain. In mammals, EEA1 interacts directly with syntaxin-6, a SNARE which mediates membrane fusion following tethering (Simonsen et al., 1999). In mammals, this tethering of early endosomes is significantly reduced upon disruption of Rab-GTPase function, PI(3)P synthesis, or EEA1 function (Geumann et al., 2008).

D. discoideum has no EEA1 homolog to recruit SNAREs, but a similar PI(3)P/Rab5 controlled cascade is thought to occur which eventually leads to early endosomes fusion. As in mammals, fusion is still mediated by SNAREs. The first target-SNARE found in *D. discoideum* was syntaxin-7, which is essential for endosome-endosome fusion (Bogdanovic et al., 2002). In complex with its co-target-SNARES, syntaxin 8 and Vti1, it is able to bind a single vesicle-SNARE, VAMP7 (Bogdanovic et al., 2002). Binding facilitates the fusion of the two respective compartments. VAMP7-GFP labels all *D. discoideum* early endocytotic compartments, suggesting that these SNAREs mediate most early fusion events (Bennett et al., 2008).

1.4.2 Rab7 Coordinates Later Delivery Events

Rab7 is an essential marker of later compartments including late endosomes, lysosomes, and autophagosomes (Reiveiwed in: Borchers et al., 2021). Rab7 helps regulate fusion of these later compartments with macroendosomes.

Rab7 activation is coupled with the deactivation and removal of Rab5 (Henry et al., 2004). This is sometimes called the Rab5-Rab7 switch, and requires Rab5-GTP hydrolysis, its release from the membrane and recruitment and activation of Rab7. In mammalian cells, this is mediated by the Mon1-Ccz1 complex. Mon1 interacts with active Rab5 on early endosome membranes, where it can associate with a Rab5-GAP to deactivate Rab5. The whole Mon1-Ccz1 complex, in association with inactive Rab5 can then bind Rab7, and activate it (Kinchen & Ravichandran, 2010; Langemeyer et al., 2020).

Disruption of either Mon1 or Ccz1 results in perturbed phagosome maturation, as phagosomes fail to recruit Rab7 (Kinchen & Ravichandran, 2010; Langemeyer et al., 2020). ΔMon1 cells also have elevated and prolonged enrichment of active Rab5, reflecting the failure to recruit a Rab5-GAP. Interestingly, this ΔMon1 phenotype can be rescued through overexpression of a Rab5-GAP, TBC1D18, which deactivates Rab5 but does not restore Rab7 activity (Hiragi et al., 2022). This does not restore maturation overall, however, suggesting that both de-activation of Rab5 and activation of Rab7 are important requirements for maturation.

D. discoideum have a mon1 homolog and a ccz1 homolog, but both are extremely poorly characterised with unknown roles. Recently, however, a PripA-TbcrA complex which localizes to *D. discoideum* macropinosomes was identified as important for Rab5-Rab7 switching (Tu et al., 2022). PripA can link two membrane compartments, interacting with Rab7 on later macropinosomes and PI(4,5) P_2, a marker of nascent macroendosomes. PripA can then interact with a Rab5 GAP, TbcrA, linking Rab7 recruitment with Rab5 inactivation (Tu et al., 2022).

Rab7 regulates later lysosomal delivery events. In *D. discoideum* Rab7 enrichments occurs within the first couple of minutes following engulfment (Buczynski et al., 1997; Rupper et al., 2001a; Tu et al., 2022). A dominant negative disruption of the Rab7 gene in *D. discoideum* results in reduced delivery of lysosomal markers, such as LmpA, to maturing phagosomes and a complete abolition of macropinocytosis. Delivery of proteins further downstream in maturation, such as the hydrolase α-mannosidase, is also perturbed (Rupper et al., 2001a). Delivery of V-ATPase is unaffected, however, and early acidification profiles are identical, but do re-neutralize much quicker (Rupper et al., 2001a). This indicates Rab7 mediated delivery is downstream of the early fusion events likely mediated by Rab5.

In mammalian phagocytes, Rab7 is delivered to endosomal compartments slightly later, first arriving on phagosomes and macropinosomes around 10-minutes after engulfment, but just before LAMP-1 and LAMP-2 (Henry et al., 2004). Rab7 continues to enrich macroendosomal membranes, peaking after approximately 40-minutes (Henry et al., 2004; Yasuda et al., 2016; Vieira et al., 2003). This gradual accumulation of Rab7 suggests many delivery events from Rab7-positive lysosomal compartments occur over a prolonged period (Reiveiwed in: Borchers et al., 2021).

In yeast, this delivery and fusion is mediated via Rab7 through direct binding of the HOPS complex. This promotes tethering to vesicles and helps regulate SNARE-dependant fusion events. In higher eukaryotes, however, Rab7 does not interact directly with HOPs. Thus, other Rab7-dependant pathways presumably meditate fusion. One possibility is through other Rab7 interactors such as RILP which binds both microtubule motors and HOPS (Jordens et al., 2001).

In *D. discoideum*, Rab7 is maintained on phagosomes until compartments reach a post-lysosomal stage (Temesvarisp et al., 1994; Gotthardt et al., 2002).

1.4.3 PIKfyve is essential for coordinating maturation

PIKfyve is a PI-5 kinase essential for efficient macroendosome maturation and transition into later stages. It is sole enzyme responsible for synthesises of PI(3,5) P_2 through phosphorylation of PI(3)P, and can

also generate PI(5)P from PI.

PIKfyve is a large, evolutionary conserved protein. At its N-terminus, a conserved FYVE-domain functions to localize PIKfyve to PI(3)P (**Figure 1.7 A**). Immunofluorescence microscopy studies show PIKfyve mutants with truncated FYVE-domains a have lower affinity for PI(3)P enriched liposomes (Sbrissa et al., 2002). Similar results have been shown *in vivo*, with truncated PIKfyve mutants unable to localize to PI(3)P positive endosomes in COS cells (Shisheva et al., 1999). Likewise, PIKfyve is unable to localize to endosomes in the presence of the PI-3 kinase inhibitor, wortmannin (Sbrissa et al., 2002).

In higher eukaryotes, a dishevelled egl-10 and pleckstrin (DEP) domain flanks the FYVE-domain, but is absent from yeast, plant and *D. discoideum* genomes, and its function remains largely uncharacterised (Reviewed in: Ikonomov et al., 2009; Lang et al., 2017).

The central region of the PIKfyve protein is comprised of two regions: a chaperonin domain, which has homology to other molecular chaperones, and the CHK homology region of about 300 base pairs, which contains conserved cysteins, histidines and lysines unique to PIKfyve orthologs (Reviewed in: Shisheva, 2008). These two regions are essential for the binding of PIKfyve to other proteins with which it co-localizes (Ikonomov et al., 2009; Lees et al., 2020). One such protein is the Rab9 effector, p40, which is phosphorylated by PIKfyve and aids late endosome transport toward the golgi (Ikonomov et al., 2003) .

Finally, at the C-terminus of PIKfyve is a conserved kinase domain responsible for both PI(3,5) P_2, and PI(5)P synthesis, as well as protein kinase activity (Sbrissa et al., 2000).

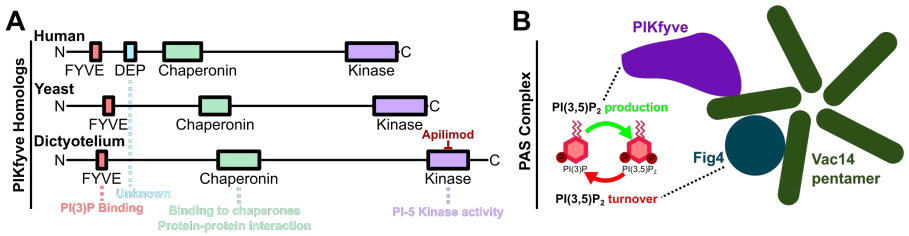

Figure 1.7: **Structure of PIKfyve. A.** Comparison between PIKfyve homologues in human, yeast and *D. discoideum*. Show key domains and their functions. **B.** Structure of the PAS complex. A Vac14 pentameter binds to PIKfyve and Fig4, which together regulate the synthesis and turnover of PI(3,5) P_2.

PIKfyve is in complex with its own phosphatase. *In vivo*, PIKfyve is complexed with two other proteins: Fig4 and Vac14 (**Figure 1.7 B**) (Sbrissa et al., 2007; Ikonomov et al., 2009; Lees et al., 2020). Fig4 is a 5-phosphatase responsible for hydrolysis and turnover of PI(3,5) P_2 back into PI(3)P (Sbrissa et al., 2007). Its function is the complete reverse of PIKfyve, and introduction of siRNAs for Fig4 in HEK293 cells results in increased levels of PI(3,5) P_2, presumably due to reduced turnover (Sbrissa et al., 2007).

Vac14 is a regulatory scaffold protein. It forms a homo-pentameric structure, which couples with both PIKfyve and Fig4 to form the PAS complex. This complex functions to regulate PI(3,5) P_2 synthesis and turnover, and as a positive regulator for PIKfyve (Sbrissa et al., 2008; Lees et al., 2020). Biochemical

analysis shows the pentameric structure orientates Fig4 and PIKfyve to avoid simultaneous access to membrane. This is suggestive of a switching mechanism that controls PI(3,5) P_2 synthesis/turnover and prevents futile cycles of phosphorylation and de-phosphorylation (Lees et al., 2020). Exactly how this switch may be controlled is unknown.

Without the PAS complex, PIKfyve is inactive. Expression of Vac14 siRNA in HEK293 cells results in enlarged endosomes characteristic of PIKfyve dysfunction. Likewise, *in vitro*, forced disassembly of the complex results in an overall reduction of PIKfyve activity (Sbrissa et al., 2004, 2008). These observations likely stem from PIKfyve autoinhibition: While removed from the complex, PIKfyve can autophosphorylate to reduce its own lipid kinase activity. Fig4 phosphatase activity from within the PAS complex is speculated to be required for release of PIKfyve from autoinhibition, and restoration of kinase activity (Sbrissa et al., 2000; Lees et al., 2020).

PIKfyve is a regulator of maturation. In HeLa cells, PIKfyve localizes with EEA1-positive endosomes, but is largely absent from late endosomes (Cabezas et al., 2006). This suggests a role for PIKFyve during early stages of maturaiton, and aligns with the recruitment of other FYVE-domain containing proteins to high concentrations of PI(3)P. The complexity of the PAS complex, however, may impose additional regulation on PIKfyve activity, even after its enrichment. In *D. discoideum*, GFP fusions of PIKfyve have proven challenging to express (Buckley, 2018).

PIKfyve's role in endosomal trafficking is best examined through its inhibition or removal. Apilimod is a potent PIKfyve inhibitor. It is a small organic chemical which blocks PIKfyve's phosphotransferase activity (Cai et al., 2013; Sbrissa et al., 2018). In combination with siRNA knockdowns and conditional knockouts, these inhibitors are commonly employed in studies at the whole organism level, where generation of a complete ΔPIKfyve knockout results in embryonic lethalities. Likewise, homozygous ΔPIKfyve knockout mammalian cell lines are largely unviable (Ikonomov et al., 2011; Krishna et al., 2016; Min et al., 2019).

Across a range of organisms, inhibition or knockdown of PIKfyve results in a substantial PI(3,5) P_2 reduction, a characteristic enlarged endosome phenotype and delays or aberrations in endosome maturation. For example, in *Drosophila*, PIKfyve disruption causes reduced levels of PI(3,5) P_2, increases in cell and organ size, and enlarged late endosomes which are poorly acidified (Rusten et al., 2006). In *C.elegans* a loss of a PIKfyve homolog, PPK-3, again causes impaired production of PI(3,5) P_2, enlarged endosomes, and an embryonic lethality (Nicot et al., 2006; Krishna et al., 2016). Yeast with kinase-deficient Fab1, a PIKfyve homolog, have attenuated vacuole acidification linked with destabilisation of yeast V-ATPase. Hyperactive Fab1 mutants have a reverse phenotype, causing vacuoles to hyper-acidify (Zhang et al., 2022). There are also links between Fab1 in yeast endosome-lysosome fusion events mediated by the HOPS and CORVET complexes (Dove et al., 2009). Finally, macrophage cell lines also have enlarged endosomes and delays in macropinosome shrinkage. Their phagosomes have a reduced degradative capacity and aberrant lysosomal marker accumulation upon PIKfyve inhibition or knockdown (Kim et al., 2014; Krishna et al., 2016).

There is a link between PIKfyve disruption and macroendosomal acidification, although this is not

always consistent between studies. For example, Isobe et al. (2019) demonstrate that PIKfyve disruption causes perturbed phagosome acidification in macrophages. Conflicting studies in both yeast and macrophage, however, suggest disruption of PIKfyve has no effect on phagosome acidity (Kim et al., 2014; Ho et al., 2015), with some even finding inhibition causes hyper-acidification of lysosomes (Leray et al., 2022).

The cause of the swollen endosome phenotype is also unclear. In RAW macrophages treated with apilimod, the swollen endosomes phenotype can be suppressed through generation of ROS which prevent lysosome-lysosome fusion events (Saffi et al., 2021). The mechanisms for this occur independently of PI(3,5) P_2 synthesis, but vary depending upon the ROS. For example, H_2O_2 appears to disrupt movement along microtubules, whereas other ROS have no influence on movement but still rescue the phenotype (Saffi et al., 2021). This is highlights a complexity in the sequence of events which lead to enlarged endosomes, which is challenging to pin on one specific disruption.

Complete ΔPIKfyve knockouts are viable in *D. discoideum*. Similar to higher eukaryotes, they have enlarged endosomes, slow macropinosome shrinkage, slow phagosome movement, and a reduced degradative capacity (Buckley, 2018). Their phagosomes also acidify slowly and have massively reduced levels of proteolysis. Surprisingly, acidification and proteolysis is unaffected in macropinosomes (Buckley, 2018). This is suggestive of an as yet uncharacterised regulatory difference between phagosome and macropinosome maturation, or, possibly, a more general cargo-related dependence. This finding could also help account for some of the differences seen in other organisms, which are inconclusive about PIKfvye's role in endolysosomal acidification.

ΔPIKfyve *D. discoideum* cells also show delayed recruitment of a range of proteins involved in all stages of maturation. These include early markers, such as V-ATPase and Dynamin A, and later markers, such as LmpA and CatD to phagosomes (Buckley, 2018). These observations suggest that PIKfyve, and in turn PI(3,5) P_2, are essential for normal maturation.

Why such a broad range of proteins from different stages of maturation are affected is not clear. One possibility is that PI(3,5) P_2 may be a key-player in phagosome-endosome fusion events similar to Rab5 or Rab7, resulting in a generalized delivery defect upon its removal. PIKfyve itself could also play a role in recruiting and regulating maturation, and the yeast homolog, Fab1, has been shown to act as a substrate of the Target of Rapamycin Complex 1 (mTORC1), a master regulator involved in nutrient and energy and regulating protein synthesis. In yeast, it phosphorylates PIKfyve proximal to its FYVE-domain. Synthesis of PI(3,5) P_2 supports further mTORC1 activation, and together both proteins a feedback loop to regulate overall PI(3,5) P_2 production and signalling (Chen et al., 2021). Whether such mechanism also exist in higher eukaryotes is unclear; however, this highlights the possibility that PIKfyve itself could be involved in signalling cascades in other organisms.

1.4.4 PI(3,5) P_2 plays an important, but uncharacterised role, in maturation

Despite PI(3,5) P_2's relatively low abundance, making up only 0.04% to 0.08% of the total cell inositol phospholipid content, its absence has a large impact on the endolysosomal system (Reviewed in: Dove

et al., 2009). This is, in part, due to the role it plays in directly regulating endolysosomal ion channels during macroendosome maturation.

Transient receptor potential (TRP) protein of the mucolipin sub family (TRPML) is one of the best characterised PI(3,5) P_2 effectors. There are three TRPML paralogs in mammals (TRPML1-3). All are calcium ion channels involved in signalling across endolysosomal membranes to help mediate endosome fusion events (Reviewed in: Cheng et al., 2010). Of these three only TRPML1 binds to, and is activated by, PI(3,5) P_2(**Figure 1.8**).

Macrophages with inactive or deficient TRPML1 exhibit an enlarged endosome phenotype similar to ΔPIKfyve cells. Their phagosomes also show decreased uptake efficiency, slower maturation, reduced killing, perturbed exocytosis, and become surrounded by lysosomal vesicles which cluster but do not fuse (Dong et al., 2010; Samie et al., 2013; Dayam et al., 2015). The fusion defect can be rescued through forced calcium ion release, pertaining to a role for TRPML1 and calcium ions in phagosome-lysosome fusion (Dayam et al., 2015). Furthermore, in yeast, calcium ion concentration in the cytosol increases during phagocytosis, which is dependent upon both TRPML1 and PIKfyve (Dayam et al., 2015).

Overexpression of TRPML1 rescues the characteristic enlarged endosome phenotype caused by PIKfyve inhibition (Dong et al., 2010), suggesting TRPML1 inactivation may be the principal cause of endosome enlargement. Other ΔPIKfyve phenotypes could be accounted for by the requirement for TRPML1 activity during calcium-ion dependant movement of lysosomes along microtubules (Li et al., 2016). TRPML1 itself localizes to phagosomes within 5 minutes of engulfment (although, surprisingly, smaller phagosomes have delayed TRPML1 arrival) (Samie et al., 2013).

Evidence from whole endosome patch clamping suggests the N-terminus of TRPML1 binds PI(3,5) P_2 which activates the channel to facilitate calcium ion efflux (Dong et al., 2010). Conversely, structural studies indicate that TRPML1 remains closed when bound to PI(3,5) P_2, and it's only through binding of co-factors, such as the drug rapamycin, that the channel opens with high efficacy (Fine et al., 2018; Gan et al., 2022). This suggest a more complex regulation of TRPML1 than initially characterised by Dong et al. (2010). The channel is also regulated by other PIPs, such as PI(4,5) P_2, which deactivates the channel at the plasma membrane (Zhang et al., 2012).

The extent to which additional co-factors are important for channel opening *in vivo* remains unclear. Regardless, the evidence above supports a link between PI(3,5) P_2 synthesis, TRPML1 activation and calcium release, leading to phagosome-lysosome fusion. Calcium ion signalling has been linked to SNARE function, providing a possible explanation for these observations (Bharat et al., 2014).

D. discoideum possess a single TRPML ortholog, mcln; however, it is only present on post-lysosomes at exocytosis and Δmcln *D. discoideum* don't exhibit the same ΔPIKfyve-like phenotypes as mammalian cells (Lima et al., 2012). Thus, there must be additional macroendosomal regulators with a requirement for PI(3,5) P_2 in *D. discoideum*.

Two-pore channels (TPCs) are also regulated by PI(3,5) P_2. Like TRPMLs, TPCs are a family of calcium ion channels that localize to endosomes. There are two paralogs in mammals: TPC1 localizes to early endosomes, binding both PI(3)P and PI(3,5) P_2, and TPC2 localizes to lysosomes, binding

exclusively PI(3,5) P_2 (Feng et al., 2022). This binding is thought to activate the channels to facilitate ion movement.

TPCs can also be activated by a calcium ion releasing secondary messenger, nicotinic acid adenine dinucleotide phosphate (NAADP). The respective roles of NAADP and PI(3,5) P_2 in TPC2 activation are somewhat contested. Calcraft et al. (2009) identified NAADP as the only requirement for channel activation, as measured by calcium ion release. Wang et al. (2012), however, found PI(3,5) P_2 alone to be sufficient for channel activation as measured, not by calcium ion release, but by sodium ion release (Wang et al., 2012). Recent research suggests that TPCs are in fact a rare form of ion channel which can vary ion selectivity in a ligand-dependent manner, releasing more calcium ions on NAADP binding, and more sodium ions upon PI(3,5) P_2 binding (Gerndt et al., 2020). Binding of both ligands appears to result in increased calcium, but not sodium efflux (Yuan et al., 2022). Importantly, TPC2 in its PI(3,5) P_2 bound form produces only small calcium ion signals, speculated to be sufficient for fusion events or exocytosis. In contrast, NAADP binding may result in more generalized calcium signalling, possibly leading to ER interaction (Reviewed in: Jaślan et al., 2023).

D. discoideum have a single TPC protein, tpc2, which is similar to its mammalian counterpart. Δtpc2 *D. discoideum* show a higher rate of calcium ion uptake into vesicles, suggesting TPC2 may normally acts as a calcium ion leak. Δtpc2 cells also show reduced acidity of intracellular vesicles, and have been noted to have an accumulation of autophagosomes (Chang et al., 2020). It is unclear whether or not they have enlarged endosomes. Additional research on tpc2 during maturaion is lacking, with most research focusing instead on its role during multicellular development (Chang et al., 2020). In particular, whether *D. discoideum* TPC2 is activated by PI(3,5) P_2, when it is present on endolysosomal membranes, and whether its disruption results in any ΔPIKfyve-like phenotypes all still need to be established.

A chlorine/hydrogen antiporter, ClC-7, also directly interacts with PI(3,5) P_2. ClC-7 is present on late lysosomes, and has principally been studied in human osteosarcoma U2OS cell lines. Inhibition of PIKfyve causes hyperacidfication of these lysosomes, which is rescued in ΔClC-7 knock-outs. Interestingly, the enlarged endosome phenotype is not rescued, indicating they are likely caused independently (Leray et al., 2022).

ClC-7 itself exports 1 hydrogen ion from the lysosomal lumen in exchange for importing two chloride ions (Graves et al., 2008). Chlorine ion influx likely acts to negate large voltage differences which build up within acidified lysosomes, and would perturb further hydrogen ion pumping (Reviewed in: Mindell, 2012). PI(3,5) P_2 is hypothesised to regulate chlorine ion flux by inhibiting ClC-7 and thus chlorine efflux, which would prevent hyper-acidification. This provides a link from PIKfyve, through PI(3,5) P_2, to regulation of lysosomal pH.

The interplay between PI(3,5) P_2 and ClC-7 requires further characterisation, however. In earlier endolysosomal compartments, PIKfyve inhibition is typically associated with slower acidification and a failure to re-neutralize (Buckley, 2018; Rusten et al., 2006; Isobe et al., 2019). Other ClC family proteins localize to early endosomes in mammals across a range of cell types, but none have yet been identified as PI(3,5) P_2 interactors (Reviewed in: Mindell, 2012). ClC-7 has several chloride channel orthologs

(ClCA-F) in *D. discoideum*; however, they are all poorly characterised.

V-ATPase activity and assembly is influenced by PI(3,5) P_2 levels. In yeast, elevated levels of PI(3,5) P_2 increases recruitment of V1 subunits from the cytosol to the vacuolar membrane, and *in vivo* the purified V0 subunit has a preference for PI(3,5) P_2 binding (Li et al., 2014). Additionally, in isolated vacuolar vesicles, exogenous PI(3,5) P_2 enhances V-ATPase activity, possibly by stabilizing the enzyme (Banerjee et al., 2019). There is also evidence that calcium ion transporters, like those discussed above, interact with the V-ATPase in yeast (Zhang et al., 2022). There is little evidence on how PI(3,5) P_2 affects V-ATPase assembly outside of yeast.

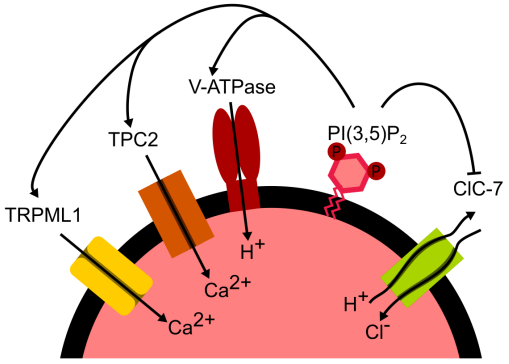

Figure 1.8: **PI(3,5) P_2 Effectors.** Summarizes the four ion transporters thought to be regulated by PI(3,5) P_2. Those on the left are activated by PI(3,5) P_2, while those on the right are suppressed.

Other proteins, which are not ion channels, also bind PI(3,5) P_2, but their links with maturation are less clear. For example, activation of mTORC1, a regulator of cell growth and metabolism, has been linked with PI(3,5) P_2 binding through Raptor (Bridges et al., 2012). ATP13A2, a lysosomal transporter implicated in Parkinsons disease, is thought to be activate by PI(3,5) P_2 also (Holemans et al., 2015). Finally, Sorting Nexin 2 localizes to early endocytic compartments and non-specifically binds PI(3,5) P_2. It localizes to tubular elements on endosomes hypothesised to play roles in early recycling via the retromer sorting complex (Carlton et al., 2005b).

The downstream effects of PIKfyve activity are hard to establish due to the lack of any reliable PI(3,5) P_2 reporter. In 2013, a tandem repeat of the N-terminal region of TRPML was reported to exhibit PI(3,5) P_2 binding *in vitro* and in cells (Li et al., 2013). Later work, however, found evidence of non-specific endolysosomal recruitment and retention after PI(3,5) P_2 depletion (Hammond et al., 2015).

The lack of a reliable reporter means it is challenging to unpick the functions of PIKfyve from the effects of PI(3,5) P_2 synthesis. While the PI(3,5) P_2 effectors discussed above can account for some of the

phenotypes observed in ΔPIKfyve cells, it is probable that PIKfyve itself also plays a regulatory role in macroendosomal maturation aside from it's PI(3,5) P_2 synthesis.

1.4.5 Summary Remarks

In summary, macroendosome maturation is a highly regulated and complex process requires coordination of several different delivery and retrieval events over a prolonged period of time to successfully process macroendosomal contents. The description of maturation above is not complete, and instead is meant to provide a generalized overview of the process, focusing particularly on core regulatory proteins and lipids which control normal maturation. The cascade of early markers leading from Rab5, to PI(3)P, and then PIKfyve onto Rab7 and PI(3,5) P_2 is particularly significant, as disruption to any one of these results in downstream maturation defects.

In particular, the role of PIKfyve in macroendosome maturation is still poorly understood. Buckley (2018) successfully characterised a ΔPIKfyve cell line in *D. discoideum*; however, understanding the mechanisms by which PIKfyve acts still requires further research.

In recent years research into PIKfyve has garnered greater interest due to discoveries highlighting it as a target for treatment of neurodegenerative diseases and viral infections. For example, inhibition of PIKfyve reduces the induction of tau aggregation in mouse neurons at the early stages of Alzheimer's disease (Soares et al., 2021). Furthermore, in Amyotrophic Lateral Sclerosis PIKfyve inhibition activates a protein clearance mechanism to remove proteins likely to form aggregates and extends the survival of a patient-derived motor neurons (Hung et al., 2023). Treatment of cells with PIKfyve inhibitors, like apilimod, has also been shown to disrupt viral infection. Both enterovirus-71 (Luo et al., 2023) and SARS-CoV-2 (Kang et al., 2020) have perturbed replication upon PIKfyve inhibition, and inhibitors also reduce uptake of the SARS-CoV-2 spike protein (Drewry et al., 2022). Apilimod is already an approved anti-cancer drug for B-cell malignancies (Ikonomov et al., 2019; Gayle et al., 2017), making it a strong therapeutic candidate.

Therefore, understanding the function of PIKfyve is of considerable clinical interest. Moreover, understanding PIKfyve function is relevant to our current understanding of the endolysosomal system and macroendosome maturation more generally.

1.5 Project Aims

This work seeks to further characterise PIKfyve's role in macroendosomal maturation by investigating its product, PI(3,5) P_2, and by examining how PIKfyve influences other core endolysosomal regulators.

Aim 1: To Characterise and Deploy a novel PI(3,5) P_2 probe

Previous unpublished work in the King Lab identified a novel PI(3,5) P_2 binding probe, SnxA. To be employed as a reliable biosensor, however, the probe required further characterization. Here, the probe was dissected to optimise binding: A tandem repeat of probe's PX-domain (2xPX), predicted to be

responsible for its localization, was cloned and further examined for PI(3,5) P_2 binding *in vitro* alongside the full length protein. Both probes were also deployed *in vivo*, in both *D. discoideum* and a range of mammalian cell lines, where they localize to early endocytic compartments. Finally, the probe has been examined alongside a PIKfyve-GFP probe to better characterise PI(3,5) P_2 formation during maturation.

Aim 2: To Establish how PIKfyve Disruption Leads to ΔPIKfyve Phenotypes

While the effects of disrupting PIKfyve during phagosome and macropinosome maturation have been well characterised by Buckley (2018), how PIKfyve or PI(3,5) P_2 cause these phenotypes remains poorly understood. To assess how PIKfyve disruption affects maturation more broadly, endolysosomal maturation markers Rab5, PI(3)P, PI(3,5) P_2, and Rab7 were tagged and followed during maturation of ΔPIKfyve *D. discoideum*. Rab7 recruitment to phagosomes was severally reduced in ΔPIKfyve cells, which likely leads to perturbed downstream processing including a reduction in phagosome-macropinosome mixing.

Chapter 2

Declaration:

In accordance with the University of Sheffield's thesis format guidelines, this chapter has been submitted for examination in the form of a draft manuscript, which is intended for re-submission to the Journal of Cell Biology in the near future.

This work results from revisions to an original pre-print (Vines et al., 2022) which also included data from my second thesis chapter. Consequently, this work bears marked similarity to the original manuscript. Changes were requested by reviewers to focus more concisely on the PI(3,5) P_2 probe and its use as a novel tool for a JCB tools paper, with other parts of the work being moved to a second paper.

All of the experiments, unless stated below, were carried out by James H Vines. All analysis, unless stated below, was carried out by James H Vines. The manuscript was written by James H Vines and Jason S King, with feedback from other co-authors.

The following data is not my own work:

1. The discovery and initial characterization of the PI(3,5) P_2 probe was carried out by Jason S. King.
2. Further characterisation and creation of the integrating SnxA *Dictyostelium* cell line was performed by Catherine M. Buckley.
3. Images in **Figure 2.1 A-B** were collected by Jason S. King.
4. Data in **Figure 2.1 C-E** was collected and analysed by Catherine M. Buckley.
5. Images in **Figure 2.5 A** were collected by Catherine M. Buckley, but analysed by James H Vines (**Figure 2.5 B**).
6. All data in **Figure 2.S3** was collected by Catherine M. Buckley and Aurelie Gueho while in the lab of Thierry Soldati.
7. Data in **Figure 2.2 A-F** and **Figure 2.S1 B-E** was collect by Hannes Maib while in the lab of David H. Murray. James H. Vines assisted only in the cloning steps to create the required expression plasmids.

Work on this project started long before I joined King Lab in 2018, so I am especially grateful to those who let me continue their work for my PhD.

Draft Manuscript:

A PI(3,5) P_2 Reporter Reveals PIKfyve Activity and Dynamics on Macropinosomes and Phagosomes

James H. Vines[1], Hannes Maib[2],Catherine M. Buckley[1,4], Aurelie Gueho[3], Thierry Soldati[3], David H. Murray[2] and Jason S. King[1]✉

[1]School of Biosciences, University of Sheffield, Firth Court Western Bank, Sheffield, UK.

[2]Division of Cell and Developmental Biology, School of Life Sciences, University of Dundee.

[3]Department of Biochemistry, Faculty of Sciences, University of Geneva, Switzerland.

[4]Current address: Department of Medicine, Cambridge University, UK.

✉Corresponding author: Jason.King@sheffield.ac.uk

Abstract

The phosphoinositide signalling lipids (PIPs) are key regulators of membrane identity and vesicle trafficking. Of these, PI(3,5) P_2 is one of the least well understood, despite key roles in many endocytic pathways including phagocytosis and macropinocytosis. PI(3,5) P_2 is generated by the phosphoinositide 5-kinase PIKfyve, and is critical for phagosomal digestion and killing of engulfed microbes. However PI(3,5) P_2 dynamics and regulation remain unclear due to the lack of a reliable reporters. Using the model professional phagocyte *Dictyostelium discoideum* we have identified SnxA as a highly selective PI(3,5) P_2-binding protein that allows faithful observation of PI(3,5) P_2 dynamics in live cells for the first time. We validate this probe in mammalian cells and show that it is also recruited to macropinosomes in a PIKfyve-dependent manner. Using SnxA-GFP we demonstrate that both phagosomes and macropinosomes accumulate PI(3,5) P_2 three minutes after engulfment, but then differ with PI(3,5) P_2 retained for 25-minutes on phagosomes but lost after 5-minutes from macropinosomes. We further find that PIKfyve recruitment and activity are separable, and that PIKfyve activation stimulates its own dissociation. We therefore describe a new tool for observing PI(3,5) P_2 dynamics in live cells that reveals key mechanistic details of the role and regulation of PIKfyve/PI(3,5) P_2 with broad relevance across endocytic pathways.

Phagocytosis | PIKfyve | *Dictyostelium* | Phosphatidylinositol(3,5)-bisphosphate | Macropinocytosis

2.1 Introduction

The inositol phospholipids are a family of interconvertible signals that define distinct endocytic compartments. Differential phosphorylation at three positions on the inositol headgroup allows seven different signalling species to be generated. These are used to recruit specific effector proteins to membranes and are interconverted by a large family of lipid kinases and phosphatases. Transitions between different phosphoinositides (PIPs) are thus central components of the identity, sorting and progression of almost all membrane compartments.

One of the least understood PIP transitions is the generation of PI(3,5) P_2 by the phosphoinositide 5-kinase PIKfyve (Fab1p in yeast). PIKfyve is recruited to early endosomes via its FYVE (Fab1, YOTB, Vac1 and EEA1) domain that binds PI(3)P and subsequently phosphorylates it at the 5-position to produce PI(3,5) P_2 (Cabezas et al., 2006; Sbrissa et al., 1999; Yamamoto et al., 1995). PIKfyve is in a complex with the scaffolding regulator Vac14 (ArPIKfyve) and the 5-phosphatase Fig4 (Sac3) which catalyses the reverse reaction (Botelho et al., 2008; Rudge et al., 2004; Sbrissa et al., 2007). This complex is under intricate regulation and while genetic, biochemical and structural studies have provided some mechanistic insight (Berwick et al., 2004; Ikonomov et al., 2009; Lees et al., 2020; Sbrissa et al., 2000), the dynamics of PI(3,5) P_2 formation in vivo have remained elusive due to the lack of a reliable live-cell reporter.

Disruption of PIKfyve causes severe and widespread defects in endocytic trafficking in all organisms studied, typified by the formation of swollen endosomes and defects in lysosomal degradation (Buckley et al., 2019; Choy et al., 2018; de Lartigue et al., 2009; Dove et al., 2009; Ikonomov et al., 2001; Kim et al., 2014; Krishna et al., 2016; Nicot et al., 2006). PIKfyve activity is therefore critical for several physiologically important pathways such as the digestion of autophagic and phagocytic cargo and of endocytosed receptors (Buckley et al., 2019; de Lartigue et al., 2009; Demirsoy et al., 2017; Ferguson et al., 2009; Kim et al., 2014; McCartney et al., 2014; Rusten et al., 2006). Unsurprisingly, disrupted PI(3,5) P_2 signalling is implicated in a broad range of diseases (Mccartney et al., 2014; Shisheva, 2012).

How these phenotypes result from PI(3,5) P_2 deficiency is not clear. Several studies have indicated that PI(3,5) P_2 can directly regulate lysosomal ion channels such as mucolipin (TRPML1), Two-Pore calcium channels (TPCs), and the chloride channel ClC7 (Dong et al., 2010; Leray et al., 2022; Samie et al., 2013; Wang et al., 2012). PI(3,5) P_2 has also been shown to regulate association of the two vacuolar ATPase (V-ATPase) subcomplexes on the yeast vacuole, although this has not yet been confirmed in other organisms (Li et al., 2014). Loss of PI(3,5) P_2 can also affect lysosomal transport and delivery to the compartments targeted for degradation (Li et al., 2016). Each mechanism can potentially contribute to the phenotypes observed, but our understanding is limited by poor knowledge of where and when PI(3,5) P_2 is generated.

We and others have previously demonstrated a key role for PIKfyve during phagosome maturation. Phagocytosis is used by cells to engulf large extracellular particles such as microbes, dead cells and debris and is highly related to the process of macropinocytosis, whereby cells take up bulk extracellular fluid (King & Kay, 2019). After engulfment, both pathways follow a complex series of maturation steps to deliver antimicrobial and digestive components in order to defend against potential pathogens, recycle nutrients or generate antigens for presentation (Buckley et al., 2016; Chen et al.,

2010; Levin et al., 2016).

PIKfyve plays an evolutionarily conserved role during phagosome maturation, and is important for phagosome-lysosome fusion in macrophages, neutrophils and the amoeba *Dictyostelium discoideum* (Buckley et al., 2019; Dayam et al., 2015, 2017; Isobe et al., 2019; Kim et al., 2014). We recently showed that loss of PIKfyve in *Dictyostelium* severely disrupts phagosomal proteolysis and killing, rendering them hypersensitive to infection with *Legionella pneumophila* (Buckley et al., 2019). Whilst this demonstrates the importance of PIKfyve in innate immunity, its regulation remains poorly understood.

A major obstacle to understanding PI(3,5) P_2 function and regulation has been the lack of a reliable reporter to visualise when and where it is generated in cells. Although a tandem repeat of the N-terminal lipid-binding region of TRPML1 showed PI(3,5) P_2 specificity in vitro and looked promising in cells (Li et al., 2013), others found clear evidence of non-specific endosomal recruitment and retention after PI(3,5) P_2 depletion (Hammond et al., 2015). We therefore set out to identify and validate an alternative reporter to faithfully describe PI(3,5) P_2 dynamics within live cells. Here, we identify and characterise SnxA as a highly-selective PI(3,5) P_2-binding protein. Using phagosome and macropinosomes maturation as accessible endocytic pathways we then use fluorescent SnxA fusions as reporters to visualise and describe PI(3,5) P_2 dynamics in live cells for the first time and uncover key regulatory steps in both PIKfyve recruitment and activity.

2.2 Materials and Methods

2.2.1 *Dictyostelium* Culture

All *Dictyostelium discoideum* cells were derived from the Ax2 (Kay) laboratory strain background and were grown in adherent culture in filter sterilised HL5 medium (Formedium) at 22°C. Cells expressing extrachromosomal plasmids were transformed by electroporation and grown in appropriate antibiotic selection by addition of either 20 µg/ml hygromycin (Invitrogen) or 10 µg/ml G418 (Sigma). The PIKfyve knockout strain in Ax2 background generated as previously described (Buckley et al., 2019). Live cell imaging was performed in defined SIH medium (Formedium).

Growth on bacterial lawns was performed by seeding ∼20 *Dictyostelium* cells with suspension of *Klebsiella aerogenes* on SM agar plates (Formedium). Colonies were visible after 5 days and colony size measured each day. Tests of growth on a panel of bacteria were performed as described by Froquet et al. (2009). Dilutions from 1 to 1×10^4 cells were seeded on agarose in wells of a 96-well plate containing the relevant bacteria. After several days (dependent on bacterial strain) wells were scored for the presence of *Dictyostelium* colonies. Bacteria used were a gift from Pierre Cosson and were: *K. pneumoniae* laboratory strain and 52145 isogenic mutant (Benghezal et al., 2006), *M. luteus* (Wilczynska & Fisher, 1994), the isogenic *P. aeruginosa* strains PT5 and PT531 (rhlR-lasR avirulent mutant) (Cosson et al., 2002), *E. coli* B/r (Gerisch, 1959), non-sporulating *B. subtilis* 36.1 (Ratner & Newell, 1978) and *E.coli* DH5α (Fisher Scientific). An avirulent strain of *K. pneumoniae* was obtained from ATCC (Strain no. 51697).

2.2.2 Mammalian Cell Culture

HEK293, MIA PaCa-2 (gifted from Helen Matthews) and RPE-1 cells were cultured in DMEM supplemented with 10% FBS, 2 mM L-glutamine and 50 µg/mL penicillin/streptomycin at 37 °C in a humidified incubator with 5% CO_2. For transient transfection with SnxA-GFP or 2xPX-GFP probes, cells were seeded in glass-bottomed dishes or coverslips at 200,000 cells/mL and grown overnight before treatment with Lipofectamine 3000 Transfection Reagent (ThermoFisher) as per manufactures guidelines. For apilimod treatment, 1000 nM apilimod (USBiological) was added 24-hours after transfection, for at least 1-hour before imaging.

To score the number of GFP-positive vesicles in live cells, ten images were captured per condition. Cells were scored for the number of identifiable vesicles within the cell. A Z-stack was used to help identify vesicles, although single Z-stacks are shown in figures for clarity. Untransfected cells, or those with extremely high levels of expression, were not counted. To see dextran uptake in live cells, media was removed and 2.5 mg/mL 70kDa TexasRed dextran added throughout (see preparation of dextran for more info). Images were captured every 60 s for up to an hour. For fixing, cells on coverslips were first washed twice in PBS and treated with 4% PFA for 10-minutes before another wash and mounting. All images were captured using a Nikon W1 Spinning Disk Confocal.

2.2.3 Cloning

All gene sequences used for cloning were obtained from dictybase (http://www.dictybase.org/) (Fey et al., 2013). PX domain containing proteins encoded within the *Dictyostelium* genome were identified by BLAST. Full-length SnxA-GFP (pJSK619), and PIKfyve-GFP (pJV0025) plasmids were generated by PCR of the respective coding sequences from cDNA using primeSTAR max DNA polymerase (Clontech), subcloning into Zero Blunt TOPO II vector (Life Technologies) and then cloning into the BglII/SpeI sites of the pDM1045 expression vector (Paschke et al., 2018; Veltman et al., 2009). To generate 1x and 2xPX expression plasmids, the sequence for the PX domain was synthesised by DC Biosciences with a 3'BglII sites and a 5'BamHI and SpeI sites. This was cloned into the Bglll/SpeI sites of pDM1043 to give the 1xPX-GFP expression vector pJV0010. A second copy of the PX domain was then inserted into the BglII sites of this as a BglII/BamHI fragment of the synthesised gene to give the 2xPX-GFP construct pJV0016. The same procedure was used to generate the mammalian expression vectors. The full-length and PX domain coding sequences were human codon optimised, synthesised and cloned as a BamHI/EcoRI fragments into pEGFP-C1. The full-length, 1xPX and 2xPX constructs are pJSK659, pJSK663 and pJSK664 respectively. These will be available at Addgene.com.

2xFYVE-GFP (pJSK418) uses the sequence from the human Hrs gene and was previously described (Calvo-Garrido et al., 2014). Co-expression plasmids were created by first cloning the RFP-fusion sequence into the pDM series shuttle vectors (pDM1042 and pDM1121), before cloning as an NgoMIV fragment into the appropriate GFP-expression vector. The SnxA-GFP integrating vector was made by cloning full-length SnxA into the integrating C-terminal GFP vector pDM1053 (Paschke et al., 2018). Prior to transformation, the plasmid was linearised with BamHI, and transformation performed with 100 U of BamHI, producing a 5-10 fold increase in the number of colonies compared to controls. Colonies were selected and screened by confocal microscopy for a cell line with

low-expression and high contrast.

2.2.4 PIP arrays

PIP arrays were performed using whole cell lysates from *Dictyostelium* cells expressing the GFP-fusion constructs. $\sim 2 \times 10^8$ cells were lysed in RIPA buffer (50 mM Tris HCL pH 7.5, 150 mM NaCl, 0.1% SDS, 2 mM EDTA, 0.5% sodium deoxycholate, 1x HALT protease inhibitor cocktail (Pierce)). PIP arrays (Echelon Biosciences) were blocked for 1 hour at room temperature in 3% fatty acid free BSA in TBS-T, and then incubated with lysates for 1 hour. Membranes were probed with anti-GFP antibody as for Western blots.

2.2.5 Purification of recombinant proteins

All SnxA probes were expressed as N-terminal 6xHis and eGFP fusion proteins in BL21 cells in LB media containing Ampicillin and 1.7 g Lactose per litre for 7 h at 37°C before lowering down to 18°C for ∼10-12 h. Cells were pelleted and lysed by ultrasound before clearing by centrifugation at 60,000 x g for 1 h. Cleared lysates were filtered through a 0.22 µm filter and purified using a 5 mL His trap HP column followed by anion exchange using a 5 ml Capto-Q column and size exclusion chromatography using a Superdex 200 16/60 pg column. All probes were snap frozen in liquid nitrogen and stored at -80°C.

2.2.6 Lipid binding experiments

Performed as previously (Maib & Murray, 2022). 1 mg liposomes, containing each of the seven different PIPs were produced by mixing 95 mol percent POPC (1-palmitoyl-2-oleoyl-sn-glycero-3-phosphocholine) with 5 mol % of the respective phosphatidylinositol together with 0.1% Atto647N-DOPE. The mixtures were evaporated under nitrogen and dried overnight in a vacuum extruder. Dried lipids were resuspended in 1 mL buffer containing 150 mM NaCl, 20 mM HEPES and 0.5 mM TCEP and subjected to 6 freeze-thaws in liquid nitrogen. Liposomes ∼100 nm diameter were generated by passing the lipid mixture 11 times through a 100 nm filter (Whatman Nuclepore). Liposomes were aliquoted, snap frozen and stored at -20 °C.

Membrane coated beads were generated by adding 10 µg of liposomes to $\sim 0.5 \times 10^6$ 10 µm silica beads (Whitehouse Scientific) in 100 µl of 200 mM NaCl for 30 min rotation at room temperature. Beads were washed twice and resuspended in buffer containing 150 mM NaCl, 20 mM HEPES, 0.5 mM TCEP (tris(2-carboxyethyl)phosphine hydrochloride) and blocked with 10% goat serum for 30 min. Drops of 7.5 µl beads were added into the corners of uncoated µ-Slide 8 well chambers (Ibidi) and 7.5 µl of the purified SnxA probes were added and mixed by pipetting at indicated final concentrations. Lipid binding kinetics were allowed to equilibrate for 30 min at room temperature before imaging close to the equator of the beads.

Confocal images were acquired using a Leica SP8 Confocal Microscope with a Leica HC PL APO CS2 63x/1.40 Oil objective at 0.75 base zoom with 1024x1024 pixels scan. GFP and Atto647N-DOPE fluorescence were imaged simultaneously without any measurable bleed through. Data was analysed using a custom ImageJ script that segments the Atto647N-DOPE channel to create a mask around the outer circumference for each bead. Segmented masks were then used to measure GFP fluorescence around each bead.

2.2.7 Mass photometry

Mass photometry measurements were performed as described in (Sonn-Segev et al., 2020). Briefly, cover slips were cleaned in 50% isopropanol and 5 µl of sample was applied to a culture well gasket. Samples were diluted to a concentration of between 25-50 nM in buffer containing 250 mM NaCl, 20 mM HEPES and 0.5 M Tris(2-carboxyethyl)phosphine hydrochloride (TCEP) immediately before measurements. Data was acquired using OneMP mass photometer (Refeyn Ltd, Oxford, UK) AcquireMP (Refeyn Ltd,) and data analysis was performed using DiscoverMP (Refeyn Ltd). Calibration was carried out using standards of known molecular weight. For each sample, between 1,315 and 10,380 individual events were recorded and analysed.

2.2.8 Preparation of fluorescent yeast and dextran

Saccharomyces cerevisiae were used for phagocytosis assays. Yeast were grown for 3 days at 37 ˚C in standard YPD media (Formedium) until stationary phase before centrifugation at 1000 x g for 5 minutes and resuspension at a final concentration of 1×10^9 cells/mL in PBS pH 7, and frozen until use. Yeast were fluorescently labelled using either pHrodo red succinimidyl ester (Life Technologies), or Alexa-405 succinimidyl ester (Life Technologies) at a final concentration of 0.25 mM and 2.5 mM, respectively. 0.5×10^9 yeast were resuspended in 200 µL PBS at pH 8.5 and incubated with 10 µL of prepared dye for 30-minutes at 37 ˚C with gentle shaking. After, cells were pelleted and sequentially washed in 1 ml of PBS pH 8.5, 1 ml of 25 nM Tris-HCl pH 8.5, and 1 ml of PBS pH 8.5 again. Finally, cells were resuspended in 500 µl of KK2 pH 6.1 and kept at -20 ˚C. Yeast were diluted in SIH medium (Formedium) to a working concentration of 1×10^8 yeast/mL before use. TexasRed 70kDa Dextran (Life Technologies) was resuspended in water and diluted to a working concentration of 2 mg/mL.

2.2.9 Microscopy and image analysis

For fluorescence microscopy $\sim 1 \times 10^6$ *Dictyostelium* cells were seeded in 35 mm glass-bottomed microscopy dishes (Mat tek P35G-1.5-14-C) and left to grow overnight in SIH medium (Formedium). Cells were imaged on a Zeiss LSM880 AiryScan Confocal with x63 Plan Apochromat oil objective and processed using the Zeiss microscope software, unless otherwise stated.

For timelapses of phagocytosis, most of the medium was aspirated immediately before imaging, and 20 µL of 1×10^8 dyed yeast added. After 60 seconds, cells were overlaid with a thin layer of 1% agarose in SIH and excess medium removed. For normal timelapses, images were captured every 10 seconds for up to 10 minutes. For extended timelapses, images were captured every 60 seconds. Automated analysis of the fluorescent intensity around each phagosomal membrane was performed using the Python plugin pyimagej (https://pypi.org/project/pyimagej/). Images where phagosomal entry could be seen were manually selected. To segment out the phagosome, the yeast channel was thresholded and particles larger than 1.5 µm^2 selected. Particles on time-adjacent frames were automatically scored for similarity based on position and size, and high similarity particles categorized into the same event. Then, throughout each event, the phagosome area was monitored for fluorescence change of pHrodo-labelled-yeast as a proxy for phagosomal pH. The selection perimeter was enlarged into two rings of $\sim$ 0.35 µm thickness: an inner ring 0.2 µm enlarged, to measure enrichment at the phagosomal membrane, and an outer ring 0.85 µm enlarged, to monitor background

cytosol fluorescence. Each event was then manually screened for errors before mean fluorescence intensity was recorded for each frame, normalized to intracellular background, and fold enrichment from -10 s calculated. Because addition of an agarose overlay appeared to suppress the effects of apilimod, cells treated with 5 µM apilimod (added > 2 hours before imaging) (USBiological) were imaged without overlay through a larger Z range every 10s using a Nikon W1 Spinning Disk Confocal. The automated analysis pipeline was not sensitive enough to detect PIKfyve-GFP enrichment, so events were manually followed and scored as either GFP positive or negative using ImageJ.

Dextran pulse-chases were performed by aspirating most of the medium, then adding 50 µl of 2 mg/ml 70kDaTexas Red dextran for the indicated time. Dextran was the removed by washing thrice in SIH medium, leaving ∼1 ml of SIH in the dish. Cells were immediately imaged, with multiple fields of view taken every 2-minutes for 10-minutes. GFP co-localisation at each timepoint was then scored manually.

2.2.10 Generating SnxA knockouts

The SnxA (DDB_G0289833) locus was disrupted by homologous recombination, inserting a blasticidin resistance cassette within the gene and deleting 550 bp of coding sequence. The knockout construct was made using a one-step recombination method into the pKOSG-OBA-Dicty vector as previously described (Wiegand et al., 2011). The 5' recombination arm was generated with the primers agcgcgtctc caatgACCACCCAGGTTAAAAATAATTCC/ agc gcgtctcccttcTTCCTTTTCTAAGAGAATATATT TGG, and the 3' arm with agcgcgtctccgttgCCTTA AAAGAGACGAAGGT/ agcgcgtctcctcccCTGGC TTTGTTTTTATAAAACAG. PCR products were recombined with the vector using StarCombinase (IBA GmbH, Göttingen, Germany). The resulting vector was used to transform Ax2 *Dictyostelium*, and the resulting blasticidin-resistant clones were screened for successful gene disruption by PCR using the primers GCACTGGGAGTTCCAATATC AATATCATC/ATAATTAATTCAACATCTTG CAAAT. Multiple independent clones were isolated and used for functional characterisation.

2.2.11 Endocytosis and fluid phase proteolysis

Macropinocytosis and exocytosis (Maniak, 2001), were measured by incubating 5×10^6 cells/mL in HL5 medium containing 2 mg/mL 70 kDa FITC dextran (Sigma). 500 µl of cells was then removed at each timepoint and added to 1 mL ice-cold KK2 (0.1 M potassium phosphate, pH 6.1). Cell pellets were then washed once and lysed in 50 mM Na_2HPO_4 (pH 9.3) with 0.2% Triton X-100 before FITC fluorescence was measured in a fluorimeter. Exocytosis was measured in the same way, except cells were pre-incubated with FITC-dextran for at least 2 hours, before washing out and measuring the decrease in fluorescence over time.

2.2.12 Phagocytosis assays

Bead uptake, proteolysis and acidification were performed as previously described in detail in (Sattler et al., 2013). Briefly, phagocytosis was measured by uptake of 1 µm YG-green beads (Polysciences Inc.). Cells were incubated with beads for the times indicated and fluorescence measured by flow cytometry. pH and proteolysis were measured using 3 µm silica beads (Kisker Biotech) conjugated to either FITC or BSA respectively as well as alexa594 as a reference dye. Synchronous phagocytosis was caused by centrifuging beads onto confluent cells in a 96-well plate (1,200 RPM for 10 seconds) before washing

and measuring changes in the fluorescence intensities over time. All samples were measured in triplicate.

2.2.13 Statistics

Statistical analysis was performed using Graphpad Prism 9. Biological replicate numbers and statistical tests used for each experiment are detailed in each figure legend. A p-value of < 0.05 was deemed significant with * indicating $p < 0.05$, $**p < 0.01$ and $***p < 0.005$ throughout.

2.3 Results

2.3.1 Identification of SnxA as a PI(3,5) P_2-binding protein in Dictyostelium

To identify a specific PI(3,5) P_2-binding protein that could be used as a reporter, we started with the assumption that such proteins would only be recruited to membranes in the presence of PIKfyve. As PX-domains are frequently used by proteins to bind specific PIPs, we searched the *Dictyostelium* genome for proteins containing a PX domain and screened C-terminally tagged GFP fusions of these for PIKfyve-dependent localization, by expression in both wild-type and ΔPIKfyve cells.

Of the proteins cloned, most localised to membranes irrespective of the presence or absence of PIKfyve (e.g. **Figure 2.1 A**). However, one (DDB_G0289833) clearly localised to large vesicles with the appearance of macropinosomes in wild-type but was completely cytosolic in ΔPIKfyve cells (**Figure 2.1 B**). DDB_G0289833 is previously unstudied and contains a coiled-coil domain in addition to the PX-domain. As this domain combination is found in many mammalian sorting nexins we named the *Dictyostelium* protein SnxA. To further confirm the dependence of SnxA recruitment on PIKfyve we applied the PIKfyve inhibitor apilimod (Cai et al., 2013) to wildtype cells expressing SnxA-GFP. This caused rapid dissociation of SnxA-GFP from all membranes, becoming completely cytosolic within 10 minutes (**Figure 2.1 C-D**).

PIKfyve activity is required for the formation of both PI(3,5) P_2 and PI(5)P. To determine the lipid-binding specificity of SnxA we examined binding to PIP arrays using lysates from SnxA-GFP expressing *Dictyostelium* cells. In this assay SnxA-GFP bound with at least a 20-fold preference to PI(3,5) P_2 over all other PIPs with almost no non-specific binding at even the highest lipid concentrations (**Figure 2.1 E**).

To optimise lipid binding and reporter characteristics, we then tested GFP-fusions of either the PX-domain alone, or a tandem repeat of this domain (1xPX-GFP) and 2xPX-GFP respectively, **Figure 2.1 F**). 1xPX-GFP had low contrast, localising poorly to large vesicles in some cells but was completely cytosolic in many others. Contrast was significantly enhanced in the 2xPX-GFP construct, which localised with similar characteristics and PIKfyve-dependence as full-length SnxA-GFP (**Figure 2.1 G**). The 2xPX-GFP construct also bound similarly to PIP arrays, localizing specifically to PI(3,5) P_2(**Figure 2.S1 A**).

To confirm PI(3,5) P_2-specificity to more physiologically-relevant membranes, all three GFP fusions were produced recombinantly (**Figure 2.S1 B**) and screened for binding to beads coated with bilayers consisting of 5% phosphoinositide and 95% POPC. Lipid binding and affinities were then determined by measuring GFP recruitment by microscopy (Maib & Murray, 2022). As anticipated, both SnxA-GFP and 2xPX-GFP probes showed high specificity for PI(3,5) P_2, while 1xPX showed very little binding (**Figure 2.2 A-D**). By

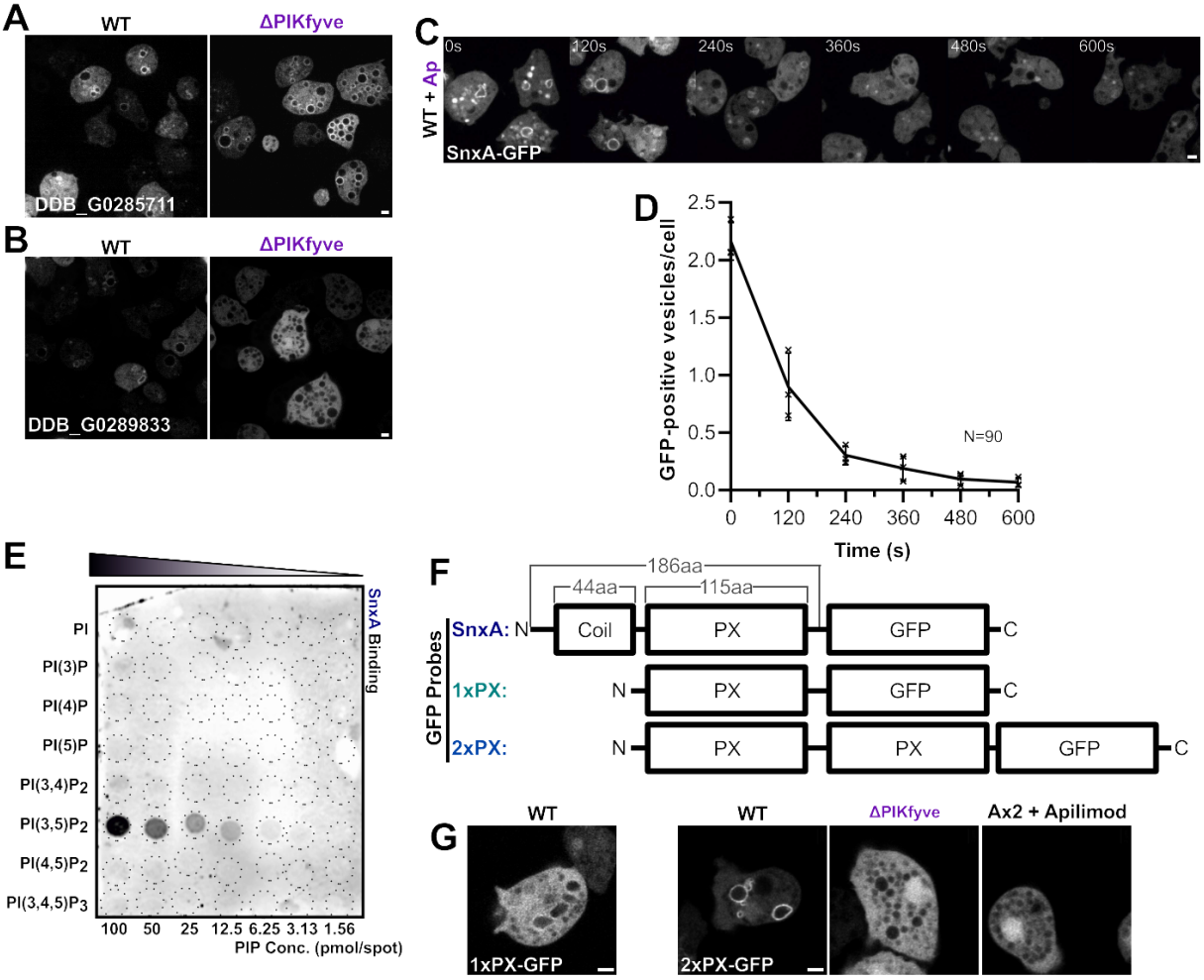

Figure 2.1: **Identification of SnxA as a PI(3,5)P_2 reporter.** **(A)** and **(B)** Expression of GFP-fusions of PX-domain containing proteins in wildtype and ΔPIKfyve Ax3 Dictyostelium. (A) DDB_G0285711 localised to large vesicles in both cells, whereas DDB_G0289833 (B) was completely cytosolic in ΔPIKfyve. **(C)** Timelapse of DDB_G0289833 (SnxA)-GFP localisation in Ax2 cells after addition of the PIKfyve inhibitor apilimod (3 µM). Quantification of number of SnxA-GFP vesicles per cell is shown in **(D)**. >90 cells measured per time-point. Data shows mean ±SEM of 3 independent experiments. **(E)** PIP array using lysates from wildtype cells expressing SnxA-GFP and probed with anti-GFP antibody. **(F)** Schematics of SnxA-GFP, 1xPX-GFP and 2xPX-GFP. **(G)** Representative images of their localisation in the cells indicated. 1xPX-GFP remained predominately cytosolic in wildtype cells, whereas 2xPX-GFP localised strongly to large vesicles, which was lost in ΔPIKfyve and apilimod treated cells. All scale bars = 2 µm.

titrating the probe concentration at a fixed amount of membrane, we determined an apparent K_D of 187.3 nM for full-length SnxA and 217.5 nM for 2xPX (**Figure 2.2 E-F**). Importantly, no binding to PI(5)P, the other product of PIKfyve, was observed under any conditions (**Figure 2.S1 C-D**).

These data demonstrate that the PX-domain of SnxA is a highly selective PI(3,5) P_2-binding domain. Whilst a tandem repeat of this domain increases binding affinity, this unexpectedly provides no improvement over the full-length protein. We therefore tested whether the full-length protein dimerises by measuring the mass distribution of the recombinant fusion proteins by mass photometry (Sonn-Segev et al., 2020). While the 1x and 2xPX GFP fusions existed as a single population with apparent molecular weights of 92 and 104 kDa respectively, 85% of the full-length SnxA protein had an apparent molecular weight of 181 kDa – approximately double that expected for a monomer (**Figure 2.S1 E**). Full-length SnxA therefore dimerises via its coiled-coil domain, providing an avidity similar to the 2xPX construct. This may be advantageous for imaging as it will incorporate 2 GFP-moieties into each dimer and increase brightness, although it is also possible that full-length SnxA could dimerise with other proteins.

2.3.2 Validation of SnxA as a PI(3,5) P_2 reporter in mammalian cells

Our data in *Dictyostelium* indicate that SnxA has both high selectivity for PI(3,5) P_2 and fast off-kinetics, indicated by rapid dissociation upon PIKfyve inhibition. To test whether it could be universally used as a PI(3,5) P_2 reporter in other organisms, we made human codon-optimised versions of both the full-length SnxA and the 2xPX construct to express as N-terminal GFP-fusions in a panel of mammalian cell lines.

In all cell lines examined, both full-length SnxA and 2xPX GFP fusions localised clearly to large intracellular vesicles (**Figure 2.3 A**). Localisation was almost completely lost upon inhibition of PIKfyve with apilimod and whilst a small number of GFP-positive puncta were observed in some cells, these were much smaller and resembled aggregates, with no visible lumen (see **Figure 2.3 A,C and E** zoom panels). Effective inhibition of PIKfyve was confirmed by the presence of the typical swollen vacuoles visible in these cells (Cai et al., 2013).

We also noted that upon paraformaldehyde (PFA) fixation, SnxA-GFP was also partly enriched near the plasma membrane (**Figure 2.S2 A**). This was insensitive to apilimod treatment and did not occur with the 2xPX-GFP probe. A similar localisation was also never visible in unfixed cells (e.g. **Figure 2.3**). Plasma membrane enrichment is therefore due to non-specific binding via the coiled-coil domain rather than an additional pool of PI(3,5) P_2. As this localisation is sufficiently distinct from endosomal PI(3,5) P_2 pools this does not prevent use of SnxA-GFP as a probe for experiments where fixation is necessary, however we advocate caution interpreting any observations at or near the cell surface and the use of appropriate controls.

Although both fusion proteins were recruited to vesicles of comparable size, fewer structures were often observed in cells expressing 2xPX-GFP than those expressing the full-length SnxA-GFP. This varied between cell lines; both reporters behaved similarly in MIA PaCa-2 pancreatic cancer cells, whereas the 2xPX-GFP was recruited to very few structures in both retinal pigment epithelial (RPE-1) or human embryonic kidney (HEK293) cells. We also noticed that these cells grew more slowly and

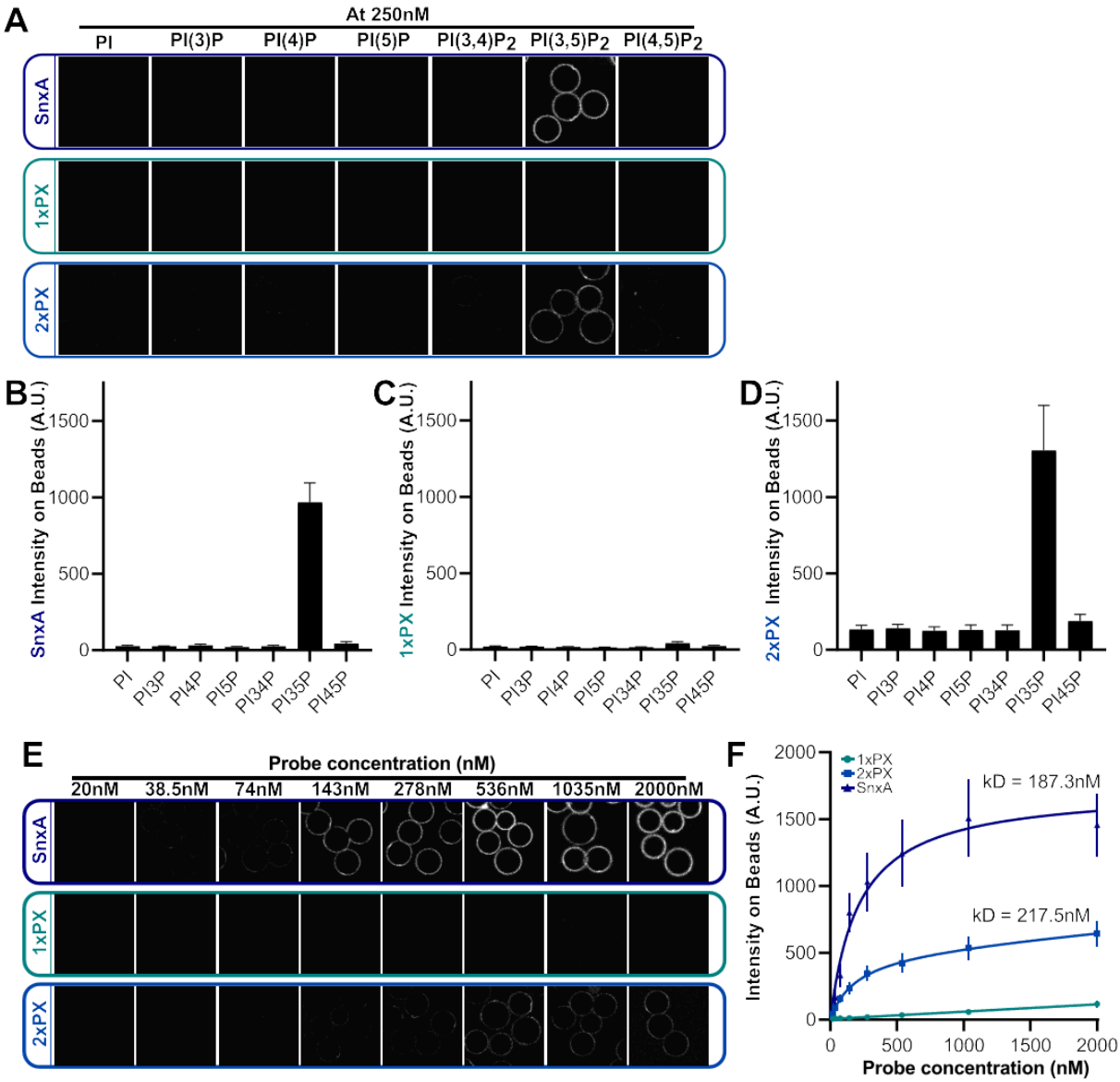

Figure 2.2: **PI(3,5) P_2 binding specificity. (A-D)** Representative images and quantification of binding of recombinant SnxA-GFP probes to membrane coated beads containing the indicated PIPs. **(E)** Binding of each SnxA probe titrated against beads harbouring PI(3,5) P_2. Intensities and apparent K_D's are shown in **(F)**. All graphs show the mean ±standard deviation from 3 independent experiments.

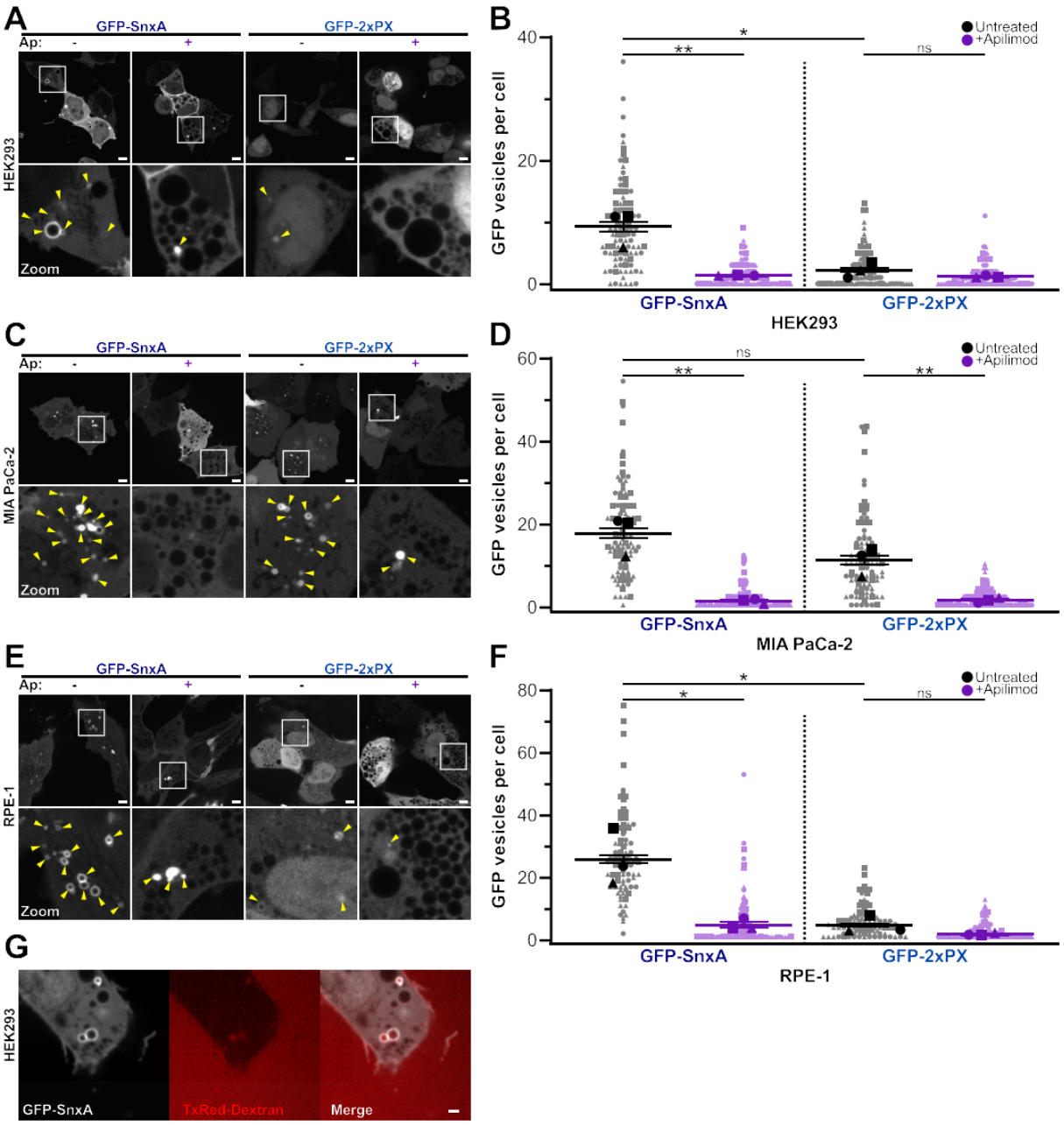

Figure 2.3: **Expression of SnxA fusions in mammalian cells.(A-F)** Representative images and quantification of either full-length SnxA or 2xPX GFP fusions expressed in either HEK293, MIA-PaCa-2 or RPE-1 cells. Images are single slices of a spinning disc Z-stack, with enlargements in the boxed regions below. Cells were either left untreated (-) or pretreated with 1 µM apilimod (Ap) for 1 hour prior to imaging. Arrowheads indicate the GFP-positive structures that were quantified over 3 independent experiments in (B), (D) and (F). 30 cells were scored for each condition for each and P-values calculated by an unpaired T-Test, scalebars represent 10 µm. **(G)** Shows an image from a timeseries (Video 2.1) of a HEK293 cell expressing SnxA-GFP just after addition of Texas-red dextran.

generally appeared less healthy than untransfected or SnxA-GFP expressing cells . Expression of 2xPX-GFP may therefore cause cytotoxicity in some cells – most likely dependent on expression levels.

As the large vesicles observed resemble macropinosomes, we tested this by incubating HEK293 cells with 70kDa Texas-red dextran, which is predominantly taken up by this route. Dextran clearly labelled all SnxA-GFP positive vesicles indicating that they are macropinocytic in origin. However, not all dextran-containing vesicles had SnxA-GFP, indicating that PI(3,5) P_2 is only transiently present (**Figure 2.3 G**, and **Video 2.1**). Although PI(3,5) P_2 is thought to be a general component of late endosomal/lysosomal pathways we never observed any small puncta that could represent classical endocytic pathways. See the discussion for potential explanations for this.

2.3.3 SnxA-probes do not disrupt PIKfyve signalling in *Dictyostelium*

To characterise SnxA as a PI(3,5) P_2 reporter in detail we returned to the *Dictyostelium* model system. As disruption of PIKfyve blocks both phagosomal proteolysis and the concentration of macropinosome contents we started by testing whether expression of SnxA-GFP fusions also affected these pathways (Buckley et al., 2019). Neither full-length SnxA, 1xPX nor 2xPX GFP-fusions had deleterious effects in either assay and we did not notice any obvious changes to cell morphology or growth (**Figure 2.S2 B-C**). Therefore none of the SnxA probes appear to disrupt PI(3,5) P_2 signalling in *Dictyostelium*.

We also generated multiple independent SnxA knockouts and asked whether it played an important function in phagosome maturation itself. Unlike ΔPIKfyve cells, ΔSnxA mutants had no significant defects in growth on bacteria, bulk fluid uptake, phagocytosis, phagosome proteolysis or acidification (**Figure 2.S3 A-G**). Following extensive investigation, the only differences we could observe between wild-type and ΔSnxA cells was a subtle but reproducible alteration in the dynamics of macropinosome shrinkage after internalisation: whilst wild-type macropinosomes transiently enlarge after internalisation before shrinking and concentrating, the expansion phase does not occur in ΔSnxA cells and can be rescued by re-expression of SnxA-GFP (**Figure 2.S3 H-I**). Despite this, bulk fluid uptake is unaffected and no axenic growth defect was observed. We speculate the transient swelling indicates SnxA-dependent fusion of another endocytic compartment to very early macropinosomes, but this requires further investigation. In any case, SnxA is not necessary for maturation of either phagosomes or macropinosomes.

2.3.4 PI(3,5) P_2 dynamics during phagosome and macropinosomes maturation

To test whether the large SnxA-GFP-positive vesicles observed in *Dictyostelium* were also macropinosomes, and determine at which point PI(3,5) P_2 is present we labelled macropinosomes with a 2-minute pulse of Texas Red-dextran and then imaged different fields of view at time intervals after dextran removal. For optimal imaging and uniform expression we generated a stably integrated SnxA-GFP cell line selecting for a clone with low expression/high contrast for microscopy experiments. This allows the percentage of macropinosomes positive for GFP to be measured for up to 10 minutes of maturation (Buckley et al., 2016).

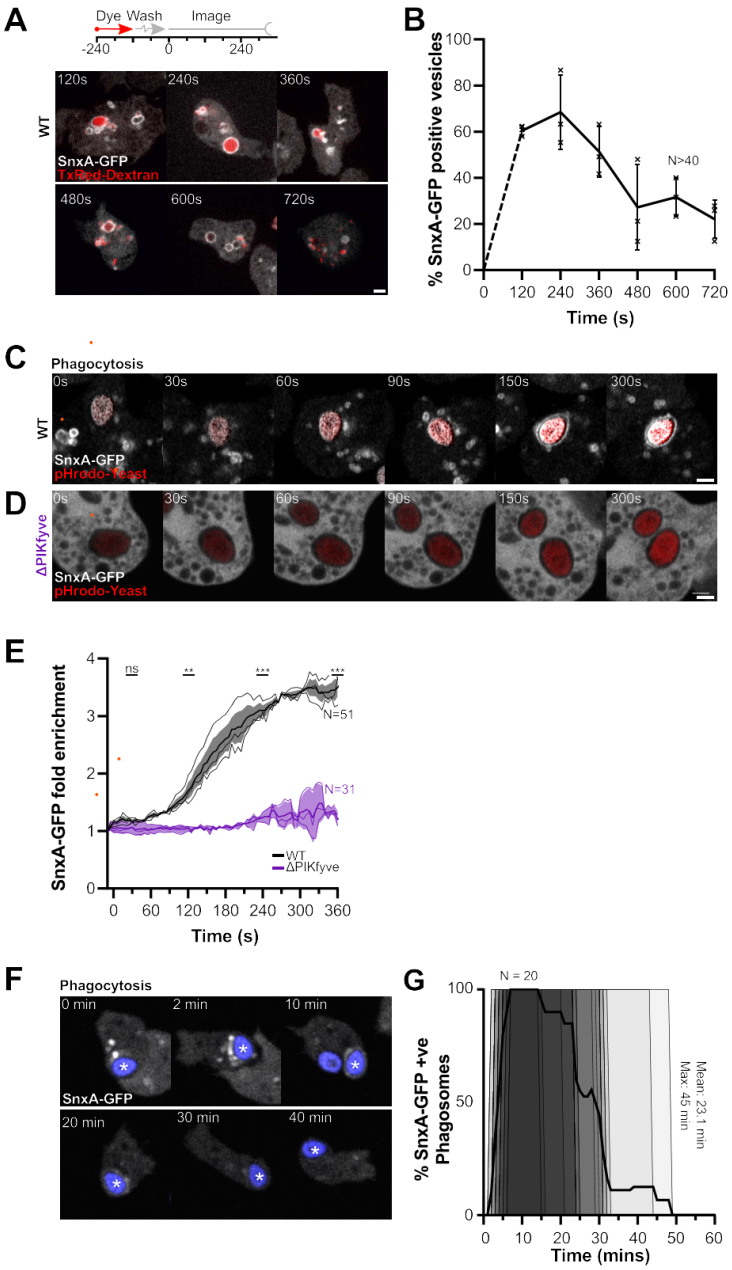

Figure 2.4: **PI(3,5)P_2 dynamics during macropinosome and phagosome maturation.** **(A)** Recruitment of SnxA-GFP in *Dictyostelium* cells following a 2-minute dextran pulse-chase to label macropinosomes. Different fields of view were taken at time points after dextran wash-out. **(B)** The proportion of macropinosomes positive for SnxA-GFP at each time after dextran addition. >40 vesicles were scored per time-point for 3 independent experiments. **(C)** Images from a timelapse of SnxA-GFP during phagocytosis of pHrodo-yeast (red) in wildtype and **(D)** ΔPIKfyve cells. See Video 2.2 for the complete sequence. **(E)** Quantification of SnxA-GFP enrichment at the phagosomal membrane averaged over 51 wildtype and 31 ΔPIKfyve phagosomes across 3 independent experiments. Fold enrichment normalised to 10s before engulfment. **(F)** Example of a long-term timelapse of SnxA-GFP recruitment to phagosomes. **(G)** Shows quantification of 20 phagocytic events followed in this way and scored for SnxA-GFP localisation over time. All scale bars = 2 µm and all graphs show the mean ±SEM of 3 independent experiments unless otherwise stated.

This demonstrated that SnxA-GFP is transiently recruited to macropinosomes within 2-minutes of engulfment, peaking at 4-minutes before removal after 5-6 minutes (**Figure 2.4 A and B**).

We then observed SnxA-GFP recruitment to phagosomes using timelapse confocal microscopy of cells engulfing pHrodo labelled yeast. Unlike macropinosomes, individual yeast containing phagosomes could be reliably followed over time, so we also developed an automated image analysis pipeline to measure the fluorescence intensity in a ring around the yeast and average over multiple events (**Figure 2.S4 A-C**). This showed that phagosomes also acquire SnxA-GFP 2-minutes after engulfment, with no enrichment observed in ΔPIKfyve controls (**Figure 2.4 C-E** and **Video 2.2**). In contrast to the rapid loss from macropinosomes, longer-term timelapses indicated that SnxA-GFP then remained on the phagosomal membrane for a further 20-minutes (**Figure 2.4 F-G**). Therefore, although the early stages of macropinosome and phagosome maturation appear identical, the timing then appears to diverge.

The quantitative analysis of phagosome maturation also allowed us to compare recruitment of 2xPX-GFP to full-length SnxA-GFP. This showed that 2xPX-GFP was recruited to phagosomes with identical dynamics to the full-length SnxA but whilst SnxA-GFP remained stably associated with the phagosome (**Figure 2.4 E**), the intensity of 2xPX-GFP slowly decreased after 3-minutes (**Figure 2.S4 D-F**). Co-expression of 2xPX-RFP in expressing cells SnxA-GFP showed that this effect was dominant, as both reporters were then lost with comparable dynamics (**Figure 2.S4 G-H** and **Video 2.3**). Therefore, 2xPX expression again exhibited a greater tendency to interfere with $PI(3,5)P_2$ signalling than SnxA-GFP, consistent with our observations in mammalian cells. However in *Dictyostelium* at least, this was relatively minor and insufficient to detectably perturb phagosomal digestion. As 2xPX had superior contrast to full-length SnxA as an RFP fusion, with indistinguishable initial recruitment it is therefore still useful in some circumstances, with appropriate caution.

2.3.5 The SnxA reporter reveals complex coordination of PIKfyve recruitment and activity

$PI(3,5)P_2$ is generated by phosphorylation of PI(3)P, which is both the substrate of PIKfyve and responsible for its recruitment via the FYVE-domain. SnxA allows us to observe $PI(3,5)P_2$ accumulation in live cells for the first time, so we next asked how this relates to both PI(3)P and PIKfyve dynamics.

To compare the relative dynamics of PI(3)P and $PI(3,5)P_2$, we co-expressed SnxA-GFP with the PI(3)P reporter RFP-2xFYVE (Gillooly et al., 2000) and followed early phagosome maturation. Although RFP-2xFYVE expression caused a delay in SnxA-GFP recruitment compared to our previous experiments, it was clearly recruited first, immediately following engulfment (**Figure 2.5 A-B** and **Video 2.4**). SnxA-GFP was then enriched on the phagosome several minutes later (**Figure 2.5 A-B** and **Video 2.4**). In this experiment, this was accompanied by a partial drop in RFP-2xFYVE intensity; this is consistent with PIKfyve depleting PI(3)P as indicated in mammalian cells (Hazeki et al., 2012; Kim et al., 2014), although our previous studies show that PI(3)P dynamics are unaffected by loss of PIKfyve in *Dictyostelium* (Buckley et al., 2019). Either way, our observations confirm the early formation of PI(3)P and subsequent conversion to $PI(3,5)P_2$ by phago-

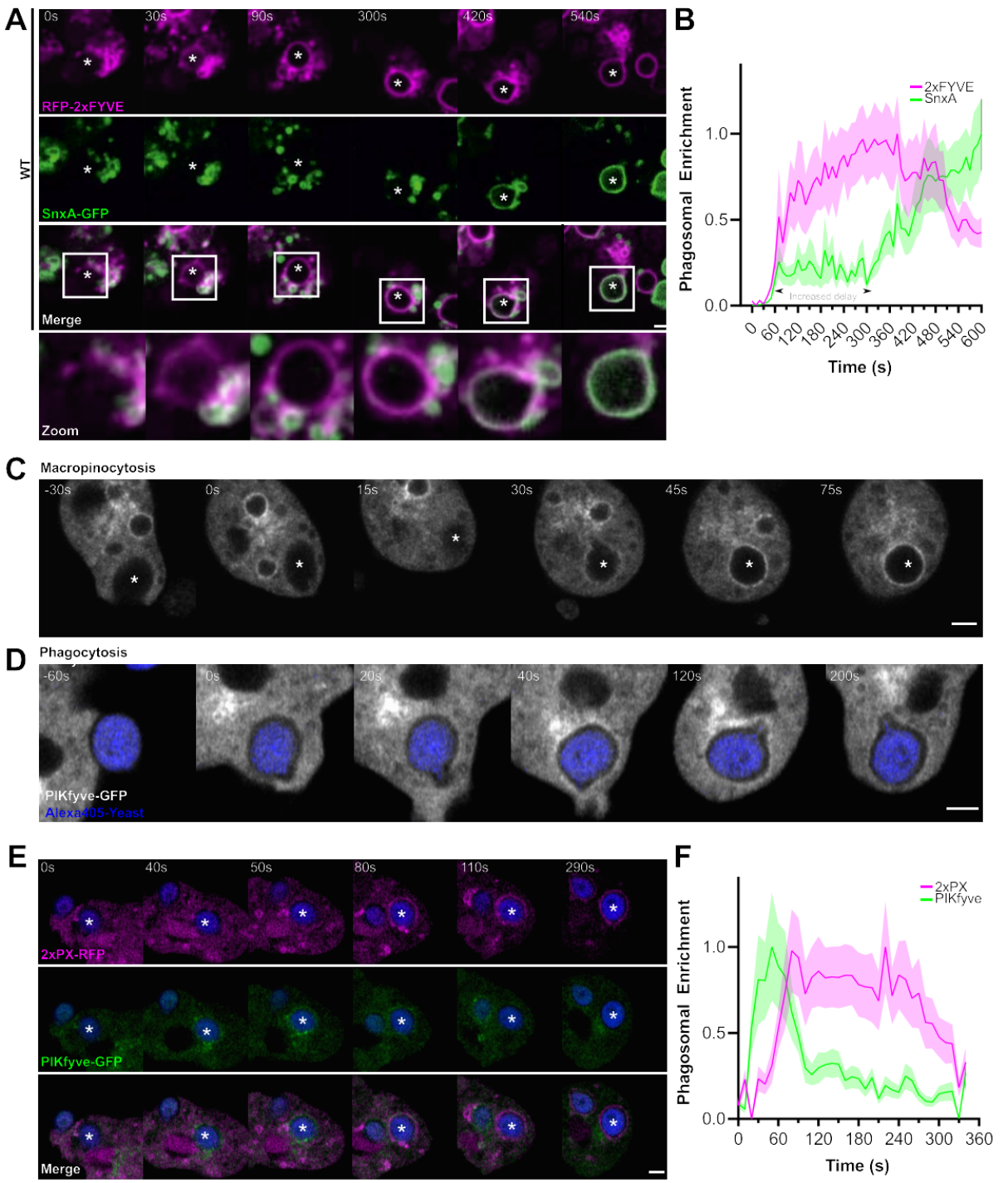

Figure 2.5: **Recruitment of SnxA relative to PI(3)P and PIKfyve.** **(A)** Timelapse of cells co-expressing 2xFYVE-RFP (magenta) and SnxA-GFP (green) during phagocytosis of an unlabelled yeast. Engulfed yeast is indicated with an asterisk, scale bar = 2 µm. See Video 2.4 for full time series. Quantification of the fluorescence intensities of both channels around the yeast in this video is shown in **(B)**. **(C)** and **(D)** show recruitment of PIKfyve-GFP to a newly-formed macropinosome and phagosome respectively. The full timelapse is shown in Video 2.5 and Video 2.6. **(E)** Timelapse of cells co-expressing 2xPX-RFP (magenta) and PIKfyve-GFP (green) during phagocytosis of Alexa405-yeast (blue). The full timelapse is shown in Video 2.7 **(F)** Quantification of the fluorescence intensities around the phagosome in (E). Data shown is the mean intensity ±the standard deviation around the phagosomal membrane normalised between minimum and maximum intensities observed.

somal PIKfyve (Ellson et al., 2001; Hazeki et al., 2012).

We then investigated how the dynamics of PIKfyve related to PI(3,5) P_2 accumulation by expression of PIKfyve-GFP. Although PIKfyve-GFP expressed poorly in wild-type cells, it was clearly visible on large vesicles that resembled macropinosomes. A diffuse perinuclear cluster of presumably sub-resolution vesicles could also be observed in some cells (**Figure 2.S5 A**). Contrast was improved by expression in ΔPIKfyve cells, which also rescued the swollen endosomal phenotype (**Figure 2.S5 B**). This allowed PIKfyve-GFP dynamics to be observed over time, demonstrating recruitment to both macropinosomes and phagosomes within 60-seconds of engulfment (**Figure 2.5 C and D** and **Video 2.5** and **Video 2.6**). This is consistent with the role for PIKfyve in the early maturation and its initial recruitment by PI(3)P. Whilst low signal and movement in the Z-axis meant it was not possible to reliably follow individual macropinosomes much beyond 2 minutes, we observed removal of PIKfyve-GFP from phagosomes approximately 3-minutes post engulfment.

To examine how PIKfyve recruitment and dissociation relates to PI(3,5) P_2 production, we co-expressed PIKfyve-GFP with the SnxA probe (2xPX-RFP) in cells engulfing alexa-405 labelled yeast. This confirmed that PIKfyve is recruited 1-2 minutes prior to PI(3,5) P_2 accumulation but also showed that they only co-localise fleetingly, with PIKfyve-GFP dissociating immediately after the SnxA probe arrives (**Figure 2.5 E-F** and **Video 2.7**). PIKfyve is therefore recruited early during phagosome maturation, but dissociates rapidly upon activation and accumulation of PI(3,5) P_2.

As PI(3)P is present throughout the first 10-minutes of both macropinosome and phagosome maturation (Buckley et al., 2019; King & Kay, 2019), dissociation of PIKfyve at 2-3 minutes indicates an additional layer of regulation. As PIKfyve dissociation coincides with PI(3,5) P_2 accumulation, we used the inhibitor apilimod to test whether PIKfyve activity is required for its release. Consistent with this, PIKfyve-GFP appeared to accumulate more strongly on phagosomes in aplimod treated cells. Timelapse microscopy then confirmed that apilimod treatment caused PIKfyve to be retained on phagosomes for significantly longer compared with untreated controls (**Figure 2.6 A-C**). This demonstrates PIKfyve dissociation is promoted by its catalytic activity, providing a mechanism to couple activation and release.

2.4 Discussion

In this study we identify the *Dictyostelium* protein SnxA as a highly selective PI(3,5) P_2-binding protein, and demonstrate its utility as a reporter for PIKfyve signalling in both *Dictyostelium* and mammalian cells. Using this, we have been able to visualise PI(3,5) P_2 dynamics in live cells for the first time and provide insight into the complex regulation of PIKfyve and the early regulation of phagosome and macropinosome maturation.

Whilst we find that both full-length SnxA and tandem PX domain constructs are selective for PI(3,5) P_2, we note several caveats that should be considered with their use. Firstly, the full-length protein also contains a coiled-coil domain in addition to the PI(3,5) P_2-binding PX domain. The primary function of this appears to be mediating homodimerization which is highly advantageous in increasing binding avidity, but we cannot completely exclude interactions with other proteins. Nonetheless, with the exception of the moderate PI(3,5) P_2-independent enrichment at the plasma

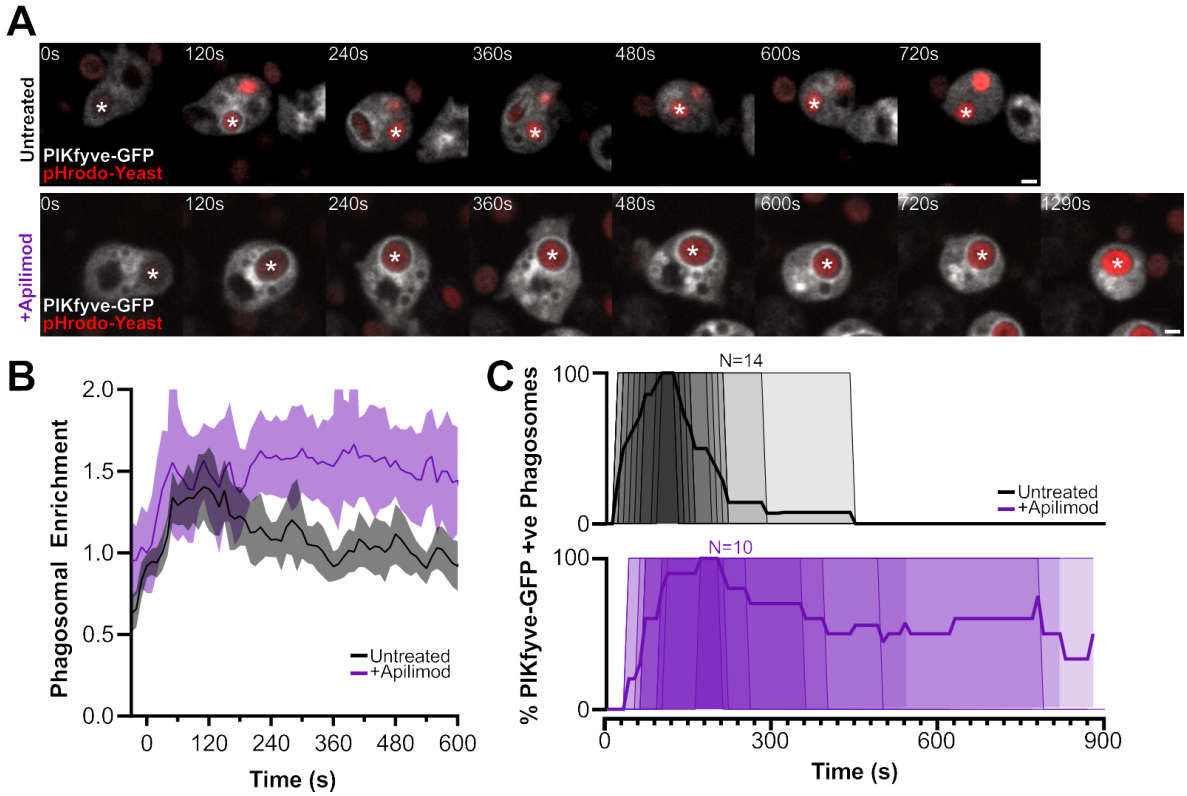

Figure 2.6: **PIKfyve activity is required for its dissociation from phagosomes. (A)** Timelapses of PIKfyve-GFP expressing cells during phagocytosis of pHrodo-yeast (red) before (top) and after (bottom) addition of 5 µM apilimod. The PIKfyve-GFP intensity around the phagosome in these movies is quantified in **(B)**. **(C)** Shows PIKfyve-GFP dynamics over multiple events, by manually scoring the time of PIKfyve-GFP delivery and release. 14 untreated events and 10 apilimod-treated events were scored with the thick line indicating the proportion of GFP-positive phagosomes at each time after engulfment. Thin lines represent individual events. All scale bars = 2 µm.

membrane observed upon paraformaldehyde fixation, full-length SnxA is recruited to the same compartments with similar dynamics to a 2xPX construct lacking the coiled-coil domain. Therefore any additional interactions appear to have minor or no effects on localisation.

The 2xPX construct is theoretically superior as it has the same K_D as a SnxA dimer and should be more specific. However, we observed 2xPX fusions also have a greater tendency to disrupt PI(3,5) P_2 signalling in both *Dictyostelium* and mammalian cells. Whilst disruption was minor in *Dictyostelium*, cell morphology, growth and macropinocytosis were clearly perturbed in some mammalian cell lines. This is most likely due to the 2xPX probe outcompeting endogenous PI(3,5) P_2 effectors or regulators. We speculate this is due to a slower off-rate of a constitutive tandem fusion compared to a SnxA dimer connected by transient electrostatic interactions.

Despite this caveat, we found the 2xPX probe often had better contrast for microscopy. This was especially evident when expression levels varied over a large range or when imaging parameters were challenging, such as in co-expression experiments. In *Dictyostelium* cells expressing SnxA-GFP from an extrachromosomal vector, vesicular localisation was only visible above the background signal in lower expressing cells whereas 2xPX-GFP and particularly 2xPX-RFP performed much better than their counterparts. Deleterious effects of 2xPX expression in mammalian cells was also not evident in all cell lines tested and are likely to be minimised by low expressing using weaker promoters than those used in this study. It is also possible to bypass probe expression artefacts altogether by using recombinant probes to strain fixed cells (Hammond et al., 2009; Maib & Murray, 2022). The choice of full-length SnxA or 2xPX probes therefore depends on individual experimental conditions. We recommend future users carefully test both, using appropriate controls including treatment with PIKfyve inhibitors and functional read outs of the pathways under investigation where possible.

The ability to observe the localisation and dynamics of both the PIKfyve enzyme and its product has provided several new mechanistic insights. Combined, our data support a model whereby PIKfyve is regulated in a series of coordinated steps. Initially, inactive PIKfyve is recruited by binding PI(3)P via its FYVE domain before subsequent activation causes rapid PI(3,5) P_2 accumulation. Finally, PIKfyve dissociates dependent on its own activity.

Complex regulation is not unexpected. PIKfyve is unusual in that its catalytic substrate (PI(3)P) also mediates its recruitment via additional interactions with the FYVE domain. Whilst PIKfyve could be released from the membrane by simply using up all the PI(3)P (Kerr et al., 2010), this is unlikely to be the case in this system as significant PI(3)P is retained on phagosomes long after PIKfyve dissociates and loss of PIKfyve does not affect PI(3)P dynamics (Buckley et al., 2019). There is therefore likely to be an additional regulation of the FYVE domain binding. This is supported by a recent study demonstrating recruitment of the yeast PIKfyve orthologue Fab1 is regulated by phosphorylation near its FYVE domain by TORC1, causing translocation between the yeast vacuole and signalling endosomes (Chen et al., 2021). Whilst it is unclear whether this mechanism is conserved in other endocytic pathways or organisms, the finding that PIKfyve recruitment to PI(3)P is also conditionally regulated during *Dictyostelium* phagosome maturation shows strong similarities.

A further complication is that PIKfyve is complexed with the phosphatase Fig4 which can po-

tentially break down PI(3,5) P_2 as soon as it is generated. As PI(3,5) P_2 accumulates in a burst almost 2 minutes after PIKfyve arrival, either PIKfyve or Fig4 catalytic activity must also be regulated. The crystal structure of the PIKfyve complex suggests that PIKfyve can be inhibited by auto-phosphorylation, requiring a protein dephosphorylation activity of Fig4 for activation (Lees et al., 2020). Fig4 may therefore also be temporally regulated during phagosome maturation, or an additional unknown regulatory mechanism may exist. Our observations that PIKfyve dissociates as soon as PI(3,5) P_2 accumulates but is retained if pharmacologically inactivated indicates that catalytic activity also affects membrane association. This is consistent with a previous study in mammalian cells, where catalytically inactive PIKfyve was also reported to be retained on macropinosomes (Kerr et al., 2010). Whilst the FYVE domain is not well resolved in the crystal structure, it is suggested to lie near the kinase domain (Lees et al., 2020). This may provide potential for an additional level of regulation to explain the coordination of recruitment and activity in vivo but needs more investigation.

Many aspects of maturation are shared between phagosomes, macropinosomes, and other endocytic pathways, such as classical clathrin-mediated endosomes. These also transition from a Rab5/PI(3)P-positive early form to later compartments demarked by Rab7, V-ATPase and lysosomal components. Furthermore, degradation of classically endocytosed receptors, autophagosomes and entotic vesicles are also sensitive to PIKfyve inhibition (de Lartigue et al., 2009; Krishna et al., 2016; Qiao et al., 2021). A significant limitation of SnxA as a PI(3,5) P_2 probe is that we were not able to see any significant recruitment to these smaller endocytic compartments. There are several potential explanations for this; for example PI(3,5) P_2 may not be present in sufficient abundance in other endocytic pathways due to their limited membrane surface, or a limited pool of PI(3,5) P_2 may already be fully occupied by endogenous binding proteins. Low levels of SnxA recruitment onto small compartments may also simply not be visible over the cytosolic background with standard confocal imaging.

Whatever the reason, it is likely that at our observations with phagosomes and macropinosomes are applicable to other endocytic routes and overcomes the technical challenges in following ∼100nm vesicles in sufficient detail over time. Using *Dictyostelium* SnxA to report PI(3,5) P_2 dynamics in live cells we have harnessed an experimentally-tractable approach to define the complex sequence of events that occur in the first minutes of phagosome maturation with key mechanistic insights into regulation of PIKfyve and PI(3,5) P_2.

2.5 Acknowledgments

The authors thank Douwe Veltman and Peggy Paschke for their continued development of his expression system and Robert Insall for his support in the early days of this project. DHM is supported by the Wellcome Trust grant 211193/Z/18/Z and Royal Society RGS\R2\180284. AG and TS were supported by the Swiss National Science Foundation research grants 310030_149390, 310030_169386 and 310030_188813 to TS. JHV is funded by Royal Society grant RGF\EA\180126, JSK is funded by a Royal Society University Research Fellowship URF\R\201036. Imaging work was performed in the Wolfson Light Microscopy Facility at Sheffield.

2.6 Bibliography

Benghezal, M., Fauvarque, M.-O., Tournebize, R., Froquet, R., Marchetti, A., Bergeret, E., Lardy,

B., Klein, G., Sansonetti, P., Charette, S. J., & Cosson, P. (2006). Specific host genes required for the killing of klebsiella bacteria by phagocytes. *Cellular Microbiology*, 8, 139–148.

Berwick, D. C., Dell, G. C., Welsh, G. I., Heesom, K. J., Hers, I., Fletcher, L. M., Cooke, F. T., & Tavaré, J. M. (2004). Protein kinase b phosphorylation of pikfyve regulates the trafficking of glut4 vesicles. *Journal of cell science*, 117, 5985–5993.

Botelho, R. J., Efe, J. A., Teis, D., & Emr, S. D. (2008). Assembly of a fab1 phosphoinositide kinase signaling complex requires the fig4 phosphoinositide phosphatase. *Molecular Biology of the Cell*, 19, 4273–4286.

Buckley, C. M., Gopaldass, N., Bosmani, C., Johnston, S. A., Soldati, T., Insall, R. H., & King, J. S. (2016). Wash drives early recycling from macropinosomes and phagosomes to maintain surface phagocytic receptors. *Proceedings of the National Academy of Sciences of the United States of America*, 113, E5906.

Buckley, C. M., Heath, V. L., Guého, A., Bosmani, C., Knobloch, P., Sikakana, P., Personnic, N., Dove, S. K., Michell, R. H., Meier, R., Hilbi, H., Soldati, T., Insall, R. H., & King, J. S. (2019). Pikfyve/fab1 is required for efficient v-atpase and hydrolase delivery to phagosomes, phagosomal killing, and restriction of legionella infection. *PLoS Pathogens*, 15.

Cabezas, A., Pattni, K., & Stenmark, H. (2006). Cloning and subcellular localization of a human phosphatidylinositol 3-phosphate 5-kinase, pikfyve/fab1. *Gene*, 371, 34–41.

Cai, X., Xu, Y., Cheung, A. K., Tomlinson, R. C., Alcázar-Román, A., Murphy, L., Billich, A., Zhang, B., Feng, Y., Klumpp, M., Rondeau, J.-M., Fazal, A. N., Wilson, C. J., Myer, V., Joberty, G., Bouwmeester, T., Labow, M. A., Finan, P. M., Porter, J. A., Ploegh, H. L., Baird, D., Camilli, P. D., Tallarico, J. A., & Huang, Q. (2013). Pikfyve, a class iii pi kinase, is the target of the small molecular il-12/il-23 inhibitor apilimod and a player in toll-like receptor signaling. *Chemistry and Biology*, 20, 912–21.

Calvo-Garrido, J., King, J. S., Muñoz-Braceras, S., & Escalante, R. (2014). Vmp1 regulates ptdins3p signaling during autophagosome formation in dictyostelium discoideum. *Traffic (Copenhagen, Denmark)*, 15, 1235–1246.

Chen, D., Xiao, H., Zhang, K., Wang, B., Gao, L., Jian, Y., Qi, X., Sun, J., Miao, L., & Yang, C. (2010). Retromer is required for apoptotic cell clearance by phagocytic receptor recycling. *Science*, 327, 1261–1264.

Chen, Z., Malia, P. C., Hatakeyama, R., Nicastro, R., Hu, Z., Péli-Gulli, M. P., Gao, J., Nishimura, T., Eskes, E., Stefan, C. J., Winderickx, J., Dengjel, J., Virgilio, C. D., & Ungermann, C. (2021). Torc1 determines fab1 lipid kinase function at signaling endosomes and vacuoles. *Current biology : CB*, 31, 297–309.e8.

Choy, C. H., Saffi, G., Gray, M. A., Wallace, C., Dayam, R. M., Ou, Z. Y. A., Lenk, G., Puertollano, R., Watkins, S. C., & Botelho, R. J. (2018). Lysosome enlargement during inhibition of the lipid kinase pikfyve proceeds through lysosome coalescence. *Journal of Cell Science*, 131.

Cosson, P., Zulianello, L., Join-Lambert, O., Faurisson, F., Gebbie, L., Benghezal, M., Delden, C. V., Curty, L. K., & Köhler, T. (2002). Pseudomonas aeruginosa virulence analyzed in a dictyostelium

discoideum host system. *Journal of bacteriology*, 184, 3027–3033.

Dayam, R. M., Saric, A., Shilliday, R. E., & Botelho, R. J. (2015). The phosphoinositide-gated lysosomal ca2+ channel, trpml1, is required for phagosome maturation. *Traffic*, 16, 1010–1026.

Dayam, R. M., Sun, C. X., Choy, C. H., Mancuso, G., Glogauer, M., & Botelho, R. J. (2017). The lipid kinase pikfyve coordinates the neutrophil immune response through the activation of the rac gtpase. *Journal of immunology (Baltimore, Md. : 1950)*, 199, 2096–2105.

de Lartigue, J., Polson, H., Feldman, M., Shokat, K., Tooze, S. A., Urbé, S., & Clague, M. J. (2009). Pikfyve regulation of endosome-linked pathways. *Traffic (Copenhagen, Denmark)*, 10, 883–893.

Demirsoy, S., Martin, S., Motamedi, S., van Veen, S., Holemans, T., den Haute, C. V., Jordanova, A., Baekelandt, V., Vangheluwe, P., & Agostinis, P. (2017). Atp13a2/park9 regulates endo-/lysosomal cargo sorting and proteostasis through a novel pi(3, 5)p2-mediated scaffolding function. *Human molecular genetics*, 26, 1656–1669.

Dong, X. P., Shen, D., Wang, X., Dawson, T., Li, X., Zhang, Q., Cheng, X., Zhang, Y., Weisman, L. S., Delling, M., & Xu, H. (2010). Pi(3,5)p2 controls membrane traffic by direct activation of mucolipin ca2+ release channels in the endolysosome. *Nature communications*, 1.

Dove, S. K., Dong, K., Kobayashi, T., Williams, F. K., & Michell, R. H. (2009). Phosphatidylinositol 3,5-bisphosphate and fab1p/pikfyve underppin endo-lysosome function. *The Biochemical journal*, 419, 1–13.

Ellson, C. D., Anderson, K. E., Morgan, G., Chilvers, E. R., Lipp, P., Stephens, L. R., & Hawkins, P. T. (2001). Phosphatidylinositol 3-phosphate is generated in phagosomal membranes. *Current biology : CB*, 11, 1631–1635.

Ferguson, C. J., Lenk, G. M., & Meisler, M. H. (2009). Defective autophagy in neurons and astrocytes from mice deficient in pi(3,5)p2. *Human Molecular Genetics*, 18, 4868–4878.

Fey, P., Dodson, R. J., Basu, S., & Chisholm, R. L. (2013). One stop shop for everything dictyostelium: dictybase and the dicty stock center in 2012. *Methods in molecular biology (Clifton, N.J.)*, 983, 59–92.

Froquet, R., Lelong, E., Marchetti, A., & Cosson, P. (2009). Dictyostelium discoideum: a model host to measure bacterial virulence. *Nature protocols*, 4, 25–30.

Gerisch, G. (1959). Ein submerskulturverfahren für entwicklungsphysiologische untersuchungen andictyostelium discoideum. *Naturwissenschaften 1959 46:23*, 46, 654–656.

Gillooly, D. J., Morrow, I. C., Lindsay, M., Gould, R., Bryant, N. J., Gaullier, J. M., Parton, R. G., & Stenmark, H. (2000). Localization of phosphatidylinositol 3-phosphate in yeast and mammalian cells. *The EMBO Journal*, 19, 4577.

Hammond, G. R., Schiavo, G., & Irvine, R. F. (2009). Immunocytochemical techniques reveal multiple, distinct cellular pools of ptdins4p and ptdins(4,5)p(2). *The Biochemical journal*, 422, 23–35.

Hammond, G. R., Takasuga, S., Sasaki, T., & Balla, T. (2015). The ml1nx2 phosphatidylinositol 3,5-bisphosphate probe shows poor selectivity in cells. *PLOS ONE*, 10, e0139957.

Hazeki, K., Nigorikawa, K., Takaba, Y., Segawa, T., Nukuda, A., Masuda, A., Ishikawa, Y., Kubota, K., Takasuga, S., & Hazeki, O. (2012). Essential roles of pikfyve and pten on phagosomal phosphatidylinositol 3-phosphate dynamics. *FEBS letters*, 586, 4010–4015.

Ikonomov, O. C., Sbrissa, D., Fenner, H., & Shisheva, A. (2009). Pikfyve-arpikfyve-sac3 core complex: contact sites and their consequence for sac3 phosphatase activity and endocytic membrane homeostasis. *The Journal of biological chemistry*, 284, 35794–806.

Ikonomov, O. C., Sbrissa, D., & Shisheva, A. (2001). Mammalian cell morphology and endocytic membrane homeostasis require enzymatically active phosphoinositide 5-kinase pikfyve. *The Journal of biological chemistry*, 276, 26141–26147.

Isobe, Y., Nigorikawa, K., Tsurumi, G., Takemasu, S., Takasuga, S., Kofuji, S., & Hazeki, K. (2019). Pikfyve accelerates phagosome acidification through activation of trpml1 while arrests aberrant vacuolation independent of the ca2+ channel. *The Journal of Biochemistry*, 165, 75–84.

Kerr, M. C., Wang, J. T., Castro, N. A., Hamilton, N. A., Town, L., Brown, D. L., Meunier, F. A., Brown, N. F., Stow, J. L., & Teasdale, R. D. (2010). Inhibition of the ptdins(5) kinase pikfyve disrupts intracellular replication of salmonella. *The EMBO journal*, 29, 1331–1347.

Kim, G. H., Dayam, R. M., Prashar, A., Terebiznik, M., & Botelho, R. J. (2014). Pikfyve inhibition interferes with phagosome and endosome maturation in macrophages. *Traffic (Copenhagen, Denmark)*, 15, 1143–1163.

King, J. S. & Kay, R. R. (2019). The origins and evolution of macropinocytosis. *Philosophical Transactions of the Royal Society B*, 374.

Krishna, S., Palm, W., Lee, Y., Yang, W., Bandyopadhyay, U., Xu, H., Florey, O., Thompson, C. B., & Overholtzer, M. (2016). Pikfyve regulates vacuole maturation and nutrient recovery following engulfment. *Developmental cell*, 38, 536–47.

Lees, J. A., Li, P. Q., Kumar, N., Weisman, L. S., & Reinisch, K. M. (2020). Insights into lysosomal pi(3,5)p2 homeostasis from a structural-biochemical analysis of the pikfyve lipid kinase complex. *Molecular cell*, 80, 736–743.e4.

Leray, X., Hilton, J. K., Nwangwu, K., Becerril, A., Mikusevic, V., Fitzgerald, G., Amin, A., Weston, M. R., & Mindell, J. A. (2022). Tonic inhibition of the chloride/proton antiporter clc-7 by pi(3,5)p2 is crucial for lysosomal ph maintenance. *eLife*, 11.

Levin, R., Grinstein, S., & Canton, J. (2016). The life cycle of phagosomes: formation, maturation, and resolution. *Immunological Reviews*, 273, 156–179.

Li, S. C., Diakov, T. T., Xu, T., Tarsio, M., Zhu, W., Couoh-Cardel, S., Weisman, L. S., & Kane, P. M. (2014). The signaling lipid pi(3,5)p2 stabilizes v1–vo sector interactions and activates the v-atpase. *Molecular Biology of the Cell*, 25, 1251.

Li, X., Rydzewski, N., Hider, A., Zhang, X., Yang, J., Wang, W., Gao, Q., Cheng, X., & Xu, H. (2016). A molecular mechanism to regulate lysosome motility for lysosome positioning and tubulation. *Nature cell biology*, 18, 404–417.

Li, X., Wang, X., Zhang, X., Zhao, M., Tsang, W. L., Zhang, Y., Yau, R. G. W., Weisman, L. S.,

& Xu, H. (2013). Genetically encoded fluorescent probe to visualize intracellular phosphatidylinositol 3,5-bisphosphate localization and dynamics. *Proceedings of the National Academy of Sciences of the United States of America*, 110, 21165–21170.

Maib, H. & Murray, D. H. (2022). A mechanism for exocyst-mediated tethering via arf6 and pip5k1c-driven phosphoinositide conversion. *Current Biology*, 32, 2821–2833.e6.

Maniak, M. (2001). Fluid-phase uptake and transit in axenic dictyostelium cells. *Biochimica et Biophysica Acta - General Subjects*, 1525, 197–204.

Mccartney, A. J., Zhang, Y., & Weisman, L. S. (2014). Phosphatidylinositol 3,5-bisphosphate: low abundance, high significance. *BioEssays : news and reviews in molecular, cellular and developmental biology*, 36, 52–64.

McCartney, A. J., Zolov, S. N., Kauffman, E. J., Zhang, Y., Strunk, B. S., Weisman, L. S., & Sutton, M. A. (2014). Activity-dependent pi(3,5)p2 synthesis controls ampa receptor trafficking during synaptic depression. *Proceedings of the National Academy of Sciences of the United States of America*, 111, E4896–E4905.

Nicot, A.-S., Fares, H., Payrastre, B., Chisholm, A. D., Labouesse, M., & Laporte, J. (2006). The phosphoinositide kinase pikfyve/fab1p regulates terminal lysosome maturation in caenorhabditis elegans. *Molecular Biology of the Cell*, 17, 3062–3074.

Paschke, P., Knecht, D. A., Silale, A., Traynor, D., Williams, T. D., Thomason, P. A., Insall, R. H., Chubb, J. R., Kay, R. R., & Veltman, D. M. (2018). Rapid and efficient genetic engineering of both wild type and axenic strains of dictyostelium discoideum. *PLOS ONE*, 13, e0196809.

Qiao, Y., Choi, J. E., Tien, J. C., Simko, S. A., Rajendiran, T., Vo, J. N., Delekta, A. D., Wang, L., Xiao, L., Hodge, N. B., Desai, P., Mendoza, S., Juckette, K., Xu, A., Soni, T., Su, F., Wang, R., Cao, X., Yu, J., Kryczek, I., Wang, X. M., Wang, X., Siddiqui, J., Wang, Z., Bernard, A., Fernandez-Salas, E., Navone, N. M., Ellison, S. J., Ding, K., Eskelinen, E. L., Heath, E. I., Klionsky, D. J., Zou, W., & Chinnaiyan, A. M. (2021). Autophagy inhibition by targeting pikfyve potentiates response to immune checkpoint blockade in prostate cancer. *Nature Cancer 2021 2:9*, 2, 978–993.

Ratner, D. I. & Newell, P. C. (1978). Linkage analysis in dictyostelium discoideum using multiply marked tester strains: establishment of linkage group vii and the reassessment of earlier linkage data. *Journal of general microbiology*, 109, 225–236.

Rudge, S. A., Anderson, D. M., & Emr, S. D. (2004). Vacuole size control: regulation of ptdins(3,5)p2 levels by the vacuole-associated vac14-fig4 complex, a ptdins(3,5)p2-specific phosphatase. *Molecular biology of the cell*, 15, 24–36.

Rusten, T. E., Rodahl, L. M., Pattni, K., Englund, C., Samakovlis, C., Dove, S., Brech, A., & Stenmark, H. (2006). Fab1 phosphatidylinositol 3-phosphate 5-kinase controls trafficking but not silencing of endocytosed receptors. *Molecular Biology of the Cell*, 17, 3989–4001.

Samie, M., Wang, X., Zhang, X., Goschka, A., Li, X., Cheng, X., Gregg, E., Azar, M., Zhuo, Y., Garrity, A. G., Gao, Q., Slaugenhaupt, S., Pickel, J., Zolov, S. N., Weisman, L. S., Lenk, G. M., Titus, S., Bryant-Genevier, M., Southall, N., Juan, M., Ferrer, M., & Xu, H. (2013). A trp channel in the lysosome regulates large particle

phagocytosis via focal exocytosis. *Developmental cell*, 26, 511–524.

Sattler, N., Monroy, R., & Soldati, T. (2013). Quantitative analysis of phagocytosis and phagosome maturation. *Methods in Molecular Biology*, 983, 383–402.

Sbrissa, D., Ikonomov, O. C., Fu, Z., Ijuin, T., Gruenberg, J., Takenawa, T., & Shisheva, A. (2007). Core protein machinery for mammalian phosphatidylinositol 3,5-bisphosphate synthesis and turnover that regulates the progression of endosomal transport. *Journal of Biological Chemistry*, 282, 23878–23891.

Sbrissa, D., Ikonomov, O. C., & Shisheva, A. (1999). Pikfyve, a mammalian ortholog of yeast fab1p lipid kinase, synthesizes 5-phosphoinositides. effect of insulin. *The Journal of biological chemistry*, 274, 21589–21597.

Sbrissa, D., Ikonomov, O. C., & Shisheva, A. (2000). Pikfyve lipid kinase is a protein kinase: downregulation of 5'-phosphoinositide product formation by autophosphorylation. *Biochemistry*, 39, 15980–9.

Shisheva, A. (2012). Pikfyve and its lipid products in health and in sickness. *Current topics in microbiology and immunology*, 362, 127–162.

Sonn-Segev, A., Belacic, K., Bodrug, T., Young, G., VanderLinden, R. T., Schulman, B. A., Schimpf, J., Friedrich, T., Dip, P. V., Schwartz, T. U., Bauer, B., Peters, J. M., Struwe, W. B., Benesch, J. L., Brown, N. G., Haselbach, D., & Kukura, P. (2020). Quantifying the heterogeneity of macromolecular machines by mass photometry. *Nature Communications 2020 11:1*, 11, 1–10.

Veltman, D. M., Akar, G., Bosgraaf, L., & Haastert, P. J. V. (2009). A new set of small, extrachromosomal expression vectors for dictyostelium discoideum. *Plasmid*, 61, 110–118.

Wang, X., Zhang, X., Dong, X. P., Samie, M., Li, X., Cheng, X., Goschka, A., Shen, D., Zhou, Y., Harlow, J., Zhu, M. X., Clapham, D. E., Ren, D., & Xu, H. (2012). Tpc proteins are phosphoinositide-activated sodium-selective ion channels in endosomes and lysosomes. *Cell*, 151, 372.

Wiegand, S., Kruse, J., Gronemann, S., & Hammann, C. (2011). Efficient generation of gene knockout plasmids for dictyostelium discoideum using one-step cloning. *Genomics*, 97, 321–325.

Wilczynska, Z. & Fisher, P. R. (1994). Analysis of a complex plasmid insertion in a phototaxis-deficient transformant of dictyostelium discoideum selected on a micrococcus luteus lawn. *Plasmid*, 32, 182–194.

Yamamoto, A., DeWald, D. B., Boronenkov, I. V., Anderson, R. A., Emr, S. D., & Koshland, D. (1995). Novel pi(4)p 5-kinase homologue, fab1p, essential for normal vacuole function and morphology in yeast. *Molecular biology of the cell*, 6, 525–539.

2.7 Supplementary Figures and Videos

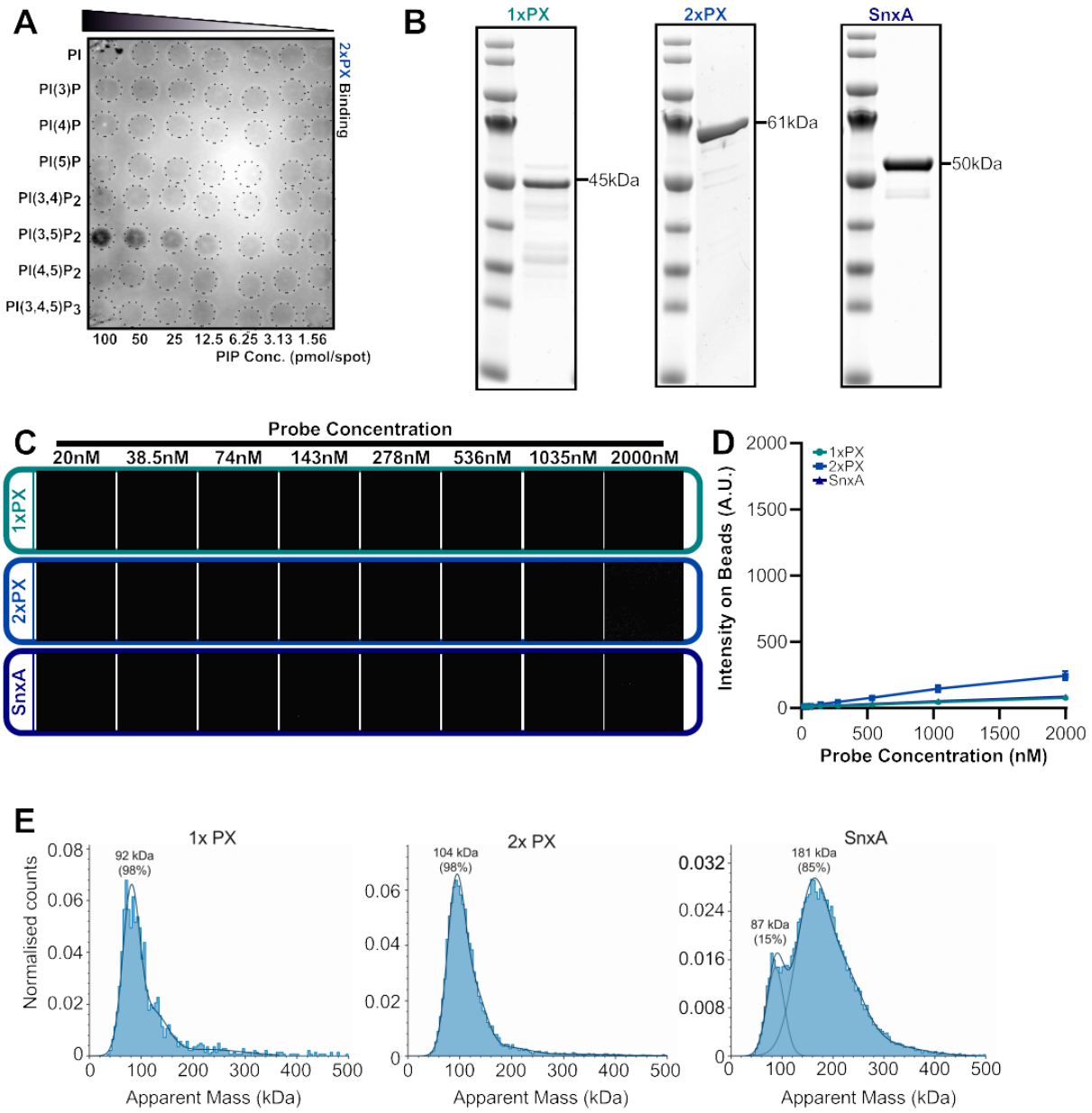

Supplementry Figure 2.S1: **SnxA does not bind PI(5)P. (A)** PIP array performed using lysates from wildtype cells expressing 2xPX-GFP and probed with anti-GFP antibody. **(B)** Coomassie stained SDS-PAGE gels of recombinant GFP fusion SnxA probes used for lipid binding assays. **(C)** Representative images of SnxA probe titrated against PI(5)P-containing membrane coated beads, quantified in **(D)**. (E)**(E)** Mass photometry analysis of recombinant SnxA fusions. Note that exact molecular weights of native proteins are inaccurate below ∼100 kDa using this technique.

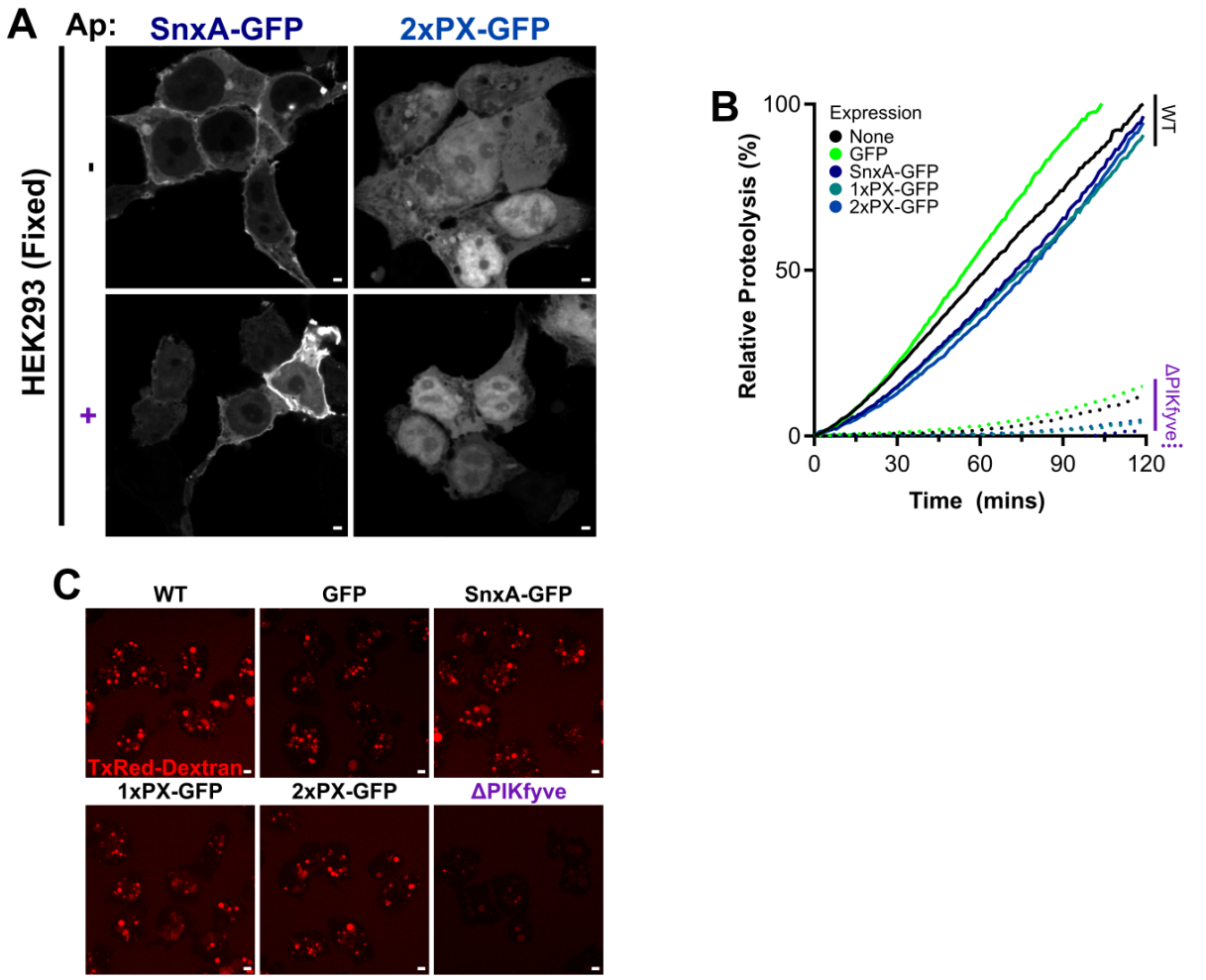

Supplementry Figure 2.S2: **Characterisation of SnxA probes.** **(A)** Confocal images of HEK293 cells transfected with either full-length or 2xPX GFP fusions after fixation with paraformaldehyde. **(B)** Phagosomal proteolysis of both Ax2 and ΔPIKfyve *Dictyostelium* cells expressing different SnxA-derived probes, measured by digestion of bead-conjugated DQ-BSA. **(C)** Images of macropinosomes in Ax2 cells expressing each probe, or ΔPIKfyve cells after overnight incubation in TxRed-dextran. The bright vesicles indicate concentration of macropinosomes contents. All scale bars represent 2 µm

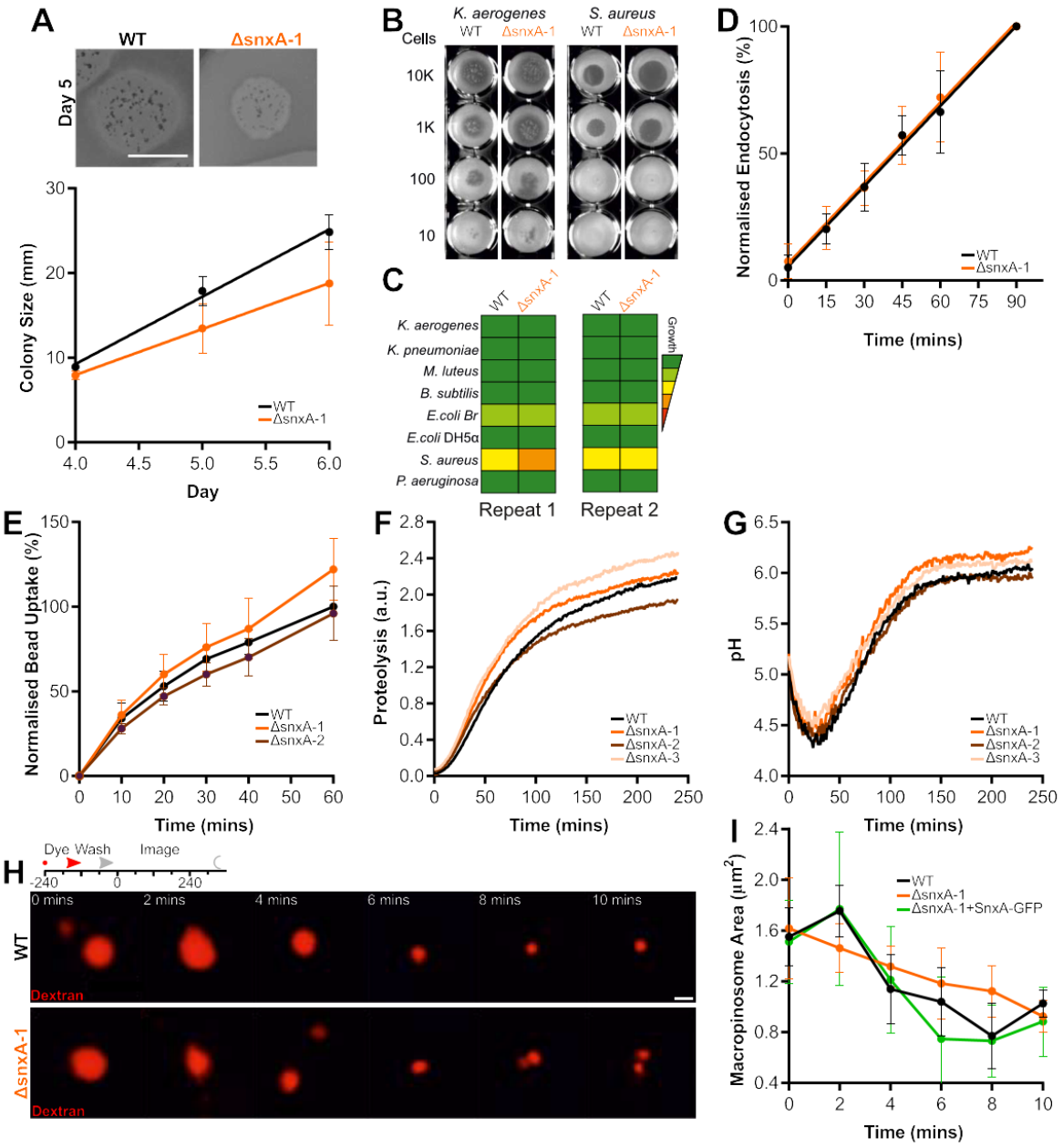

Supplementry Figure 2.S3: **Loss of SnxA has little effect on phagosome or macropinosome maturation.** **(A)** Images of wildtype and ΔsnxA-1 colonies growing on a lawn of K. aerogenes. Average colony diameter over time is shown below. Scale bar = 10 mm. **(B)** Growth of mutant cells in different bacteria. Numbers indicate the number of *Dictyostelium* cells seeded on each well. **(C)** Summary of growth on a range of bacteria screened as in (B). **(D)** Quantification of endocytosis calculated by FITC dextran uptake. **(E)** Phagocytosis of 1 µm fluorescent beads, measured by flow cytometry and normalised to wildtype cells at 60 mins. **(F)** Phagosomal proteolysis and **(G)** pH over time, measured by fluorescence changes after engulfment of either DQ-BSA or FITC/Alexa594 reporter beads respectively. **(H)** Representative images of macropinosomes shrinking after a 2 minute pulse of TRITC-dextran, Scale bar = 2 µm. Size is quantified in **(I)**. All data shown are the mean± SD of at least 3 independent experiments. ΔsnxA-1, 2 and 3 indicate independent knockout clones.

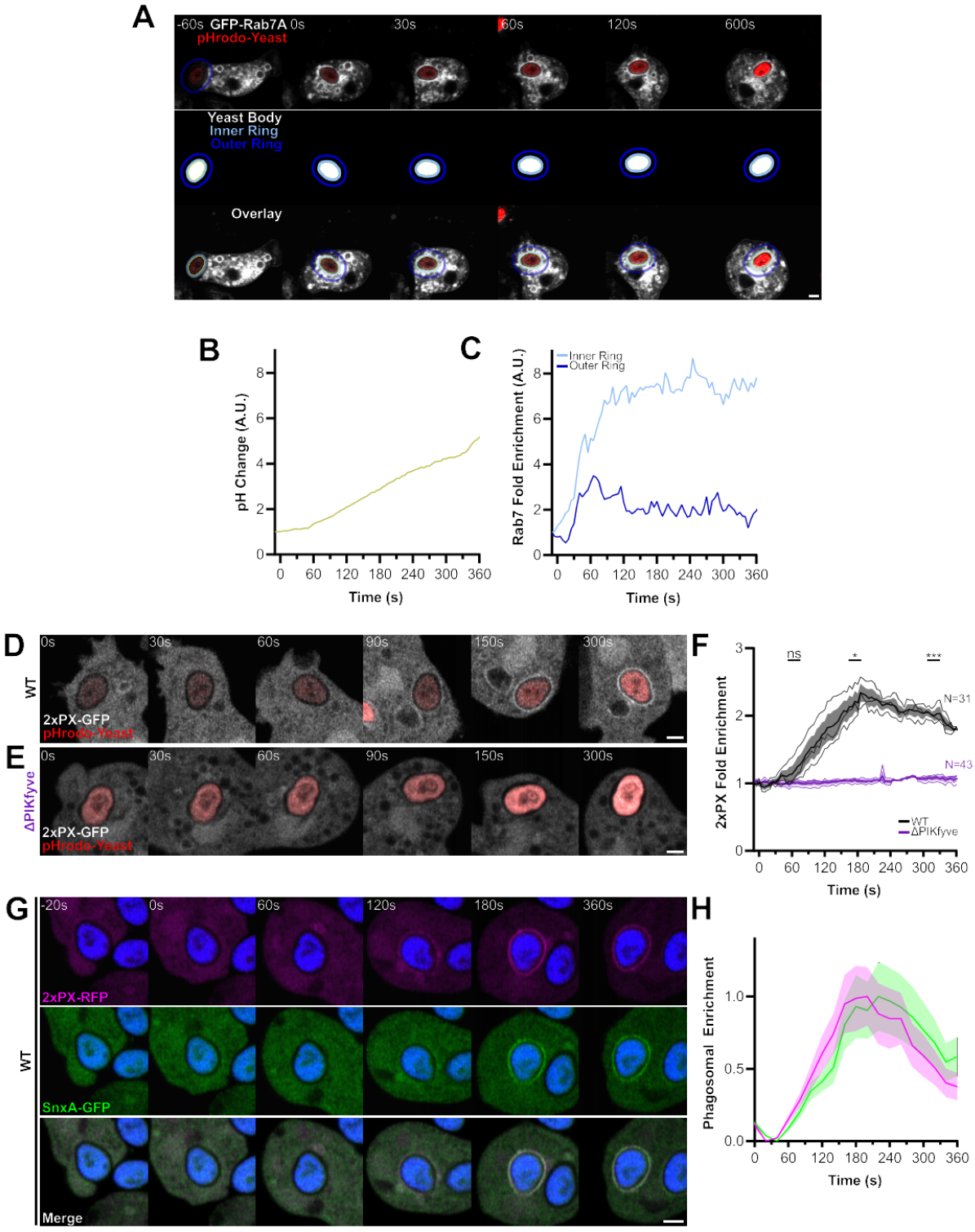

Supplementry Figure 2.S4: **Quantification of phagosomal recruitment and comparison of SnxA and 2xPX. (A)** Shows automated methodology to quantify fluorescent reporter recruitment to a phagocytic event. Channel containing yeast (red) is thresholded and particles larger than 1.5 µm^2 are segmented (white circles). This area is used to monitor fluorescence change of pHrodo-labelled-yeast, a proxy for phagosomal pH, shown in **(C)**. The perimeter is enlarged by 0.2 µm to generate a ring of 0.3 µm thickness over the phagosomal membrane (inner ring). As a control, and additional ring further away from the yeast (outer ring, expanded by 0.85 µm from the yeast) was also generated, to give a measure of background cytosol fluorescence that should remain constant. **(D)** Timelapse of 2xPX-GFP recruitment to a pHrodo-labelled yeast containing phagosome in wild-type cells. **(E)** Shows an identical experiment in ΔPIKfyve mutants. **(F)** Shows quantification of phagosomal enrichment in both cell lines, averaged over multiple cells. **(G)** Timelapse of phagocytosis in wild-type cells co-expressing SnxA-GFP and 2xPX-RFP (see Video 3 for full timeseries). **(H)** Quantification of probe intensities over time in this video.

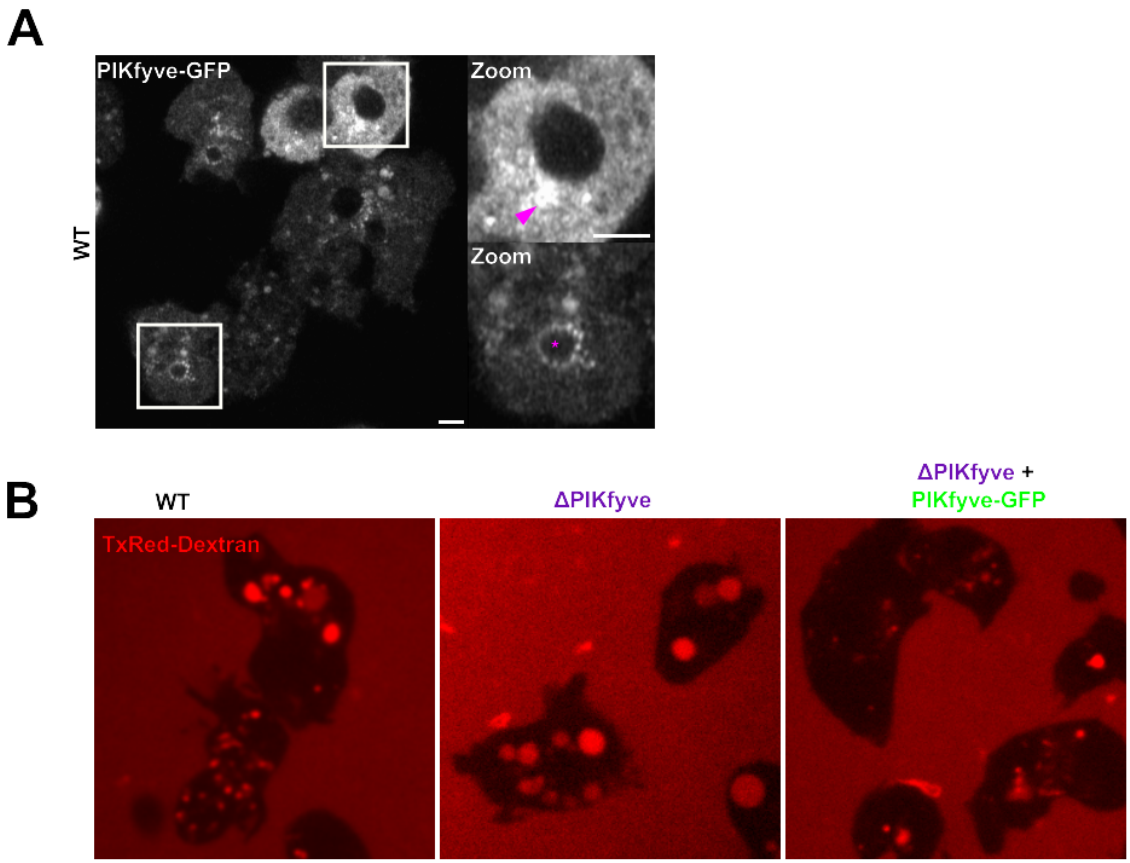

Supplementry Figure 2.S5: **Expression of PIKfyve-GFP in *Dictyostelium*.** **(A)** Localisation of PIKfyve-GFP in wild-type cells. Boxes indicate regions enlarged in the panels on the right. **(B)** Rescue of the macropinosome concentration defect by PIKfyve-GFP expression in ΔPIKfyve cells. The cell lines indicted were incubated overnight in TxRed Dextran overnight prior to confocal microscopy.

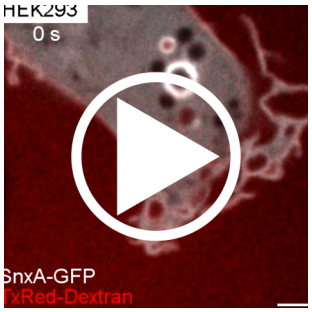

Video 2.1: Macropinocytosis in HEK293 cells expressing SnxA-GFP directly following addition of txRed dextran. Scale bar = 2 µm

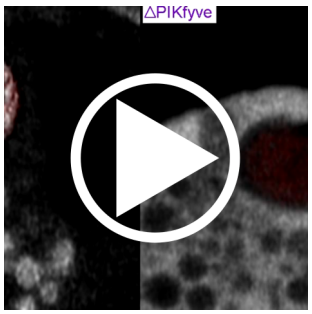

Video 2.2: PI(3,5) P_2 dynamics during phagosome maturation. Wildtype (left) and ΔPIKfyve(right) cells expressing the SnxA-GFP probe for PI(3,5) P_2. Note the complete loss of localisation in the mutants. Scale bar = 2 µm

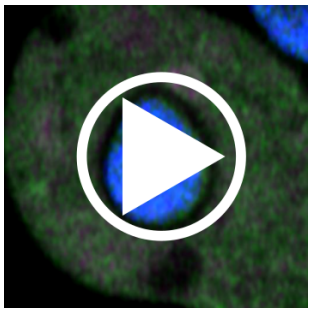

Video 2.3: Co-localisation of SnxA-GFP and 2xPX-RFP to a newly formed phagosome in a wild-type *Dictyostelium* cell. Scale bar = 2 µm

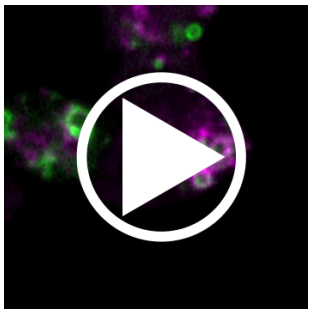

Video 2.4: Simultaneous imaging of PI(3)P (RFP-2xFYVE, magenta) and PI(3,5) P_2(SnxA-GFP) recruitment to phagosomes in wildtype cells. Scale bar = 2 µm

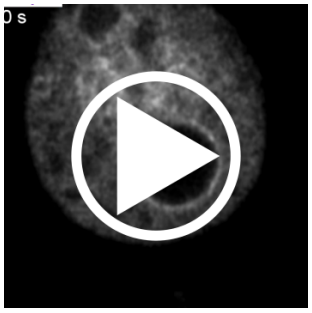

Video 2.5: Recruitment of PIKfyve-GFP to a newly formed macropinosome (asterisk). PIKfyve-GFP expressed in a ΔPIKfyve cell. Scale bar = 2 µm

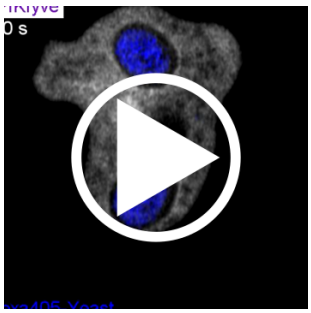

Video 2.6: Recruitment of PIKfyve-GFP to phagosomes. Engulfment of an alexa405-labelled yeast by a GFP-PIKfyve expressing ΔPIKfyve cell. Scale bar = 2 µm

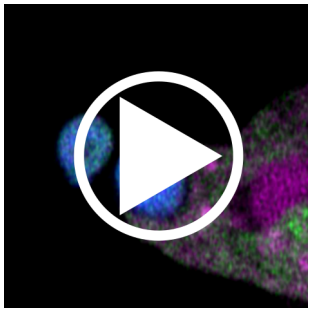

Video 2.7: Simultaneous imaging of PIKfyve-GFP and PI(3,5) P_2(RFP-2xPX) in magenta), in wildtype cells. Scale bar = 2 µm

Chapter 3

Declaration:

In accordance with the University of Sheffield's thesis format guidelines, this chapter has been submitted for examination in the form of a draft manuscript, which is intended for submission to an unknown journal in the near future.

This work results from revisions to an original manuscript (Vines et al., 2022) which also included data from my first thesis chapter. Consequently, this work bears marked similarity to the original pre-print. This manuscript contains everything unrelated to PI(3,5) P_2 probe as a tool. That includes examining how PIKfyve interacts with other key macroendosomal regulators.

All of the experiments, unless stated below, were carried out by James H Vines. All analysis, unless stated below, was carried out by James H Vines. The manuscript was written by James H Vines and Jason S King.

The following data is not my own work:

1. Data in **Figure 3.3 D-G** was collected and analysed by Catherine M. Buckley.

2. Data in **Figure 3.4 E and H** was collected by Catherine M. Buckley, but analysed by James H Vines.

Draft Manuscript:

PIKfyve is Required for Phagosomal Rab7 Acquisition and the Delivery and Fusion of Early Macropinosomes to Phagosomes

James H. Vines[1], Catherine M. Buckley[2] and Jason S. King[1]✉

[1]School of Biosciences, University of Sheffield, Firth Court Western Bank, Sheffield, UK.

[2]Current address: Department of Medicine, Cambridge University, UK.

✉Corresponding author: Jason.King@sheffield.ac.uk

Abstract

The maturation of a phagosomes requires complex coordination and regulation of processing machineries. Like other endocytic pathways, phagosome maturation is regulated by a combination of Rab GTPases and phosphoinositide signalling lipids (PIPs) which define membrane identity and control vesicle trafficking. PIKfyve, a PI-5 kinase, plays a key role in regulating endocytic traffic, and its disruption results in severe defects in phagosomal digestion and the killing of engulfed microbes. How PIKfyve, and its product PI(3,5) P_2, control phagosome maturation remains unclear. Using the model professional phagocyte, *Dictyostelium discoideum*, we show PIKfyve is required for the phagosomal Rab5-Rab7 transition. Using PIP markers, including our recently characterized PI(3,5) P_2-probe, SnxA (Vines et al., 2022), we delineate subpopulations of Rab7-positive endosomes which are marked by PI(3,5) P_2 and describe their sequential delivery to phagosomes in a PIKfyve dependent manner. Furthermore, we find PIKfyve is required for fusion between macropinosomes and phagosomes, which enables phagosomes to efficiently accumulate lysosomal components. These findings uncover key mechanistic details on the role and regulation of PIKfyve/PI(3,5) P_2 likely to have general relevance across endocytic pathways.

Phagocytosis | Macropinocytosis | PIKfyve | Rab7 | *Dictyostelium*

3.1 Introduction

The degradation of endocytic cargo is a highly regulated cellular process. Endosomes must acquire

the correct markers with temporal accuracy to facilitate their maturation. This is achieved through sequential regulatory steps, which identify compartments in different stages of maturation. In this way, effector proteins and lysosomal compartments are recruited over the course of maturation to expedite the trafficking or degradation luminal contents. Disruption of any one of these key regulators can result in aberrant endosomal trafficking and severe physiological defects.

Inositol phospholipids define specific compartment membranes during endosomal maturation. They contain a glycerol backbone, two non-polar fatty acid tails, and an inositol head group which can be phosphorylated at any of three positions (3, 4 or 5) to form one of eight different phosphoinositide (PIP) species. Each PIP can recruit different effector proteins, allowing for spatially segregated protein enrichment to different membranes. Because PIP species can be inter-converted through phosphorylation or de-phosphorylation, their binding proteins and effectors are also recruited temporally throughout maturation (Bohdanowicz & Grinstein, 2013).

PIKfyve is a phosphoinositide 5-kinase recruited via a FYVE (Fab1, YOTB, Vac1 and EEA1) domain to PI(3)P concentrated on early endosomes. Here, it phosphorylates PI(3)P to produce PI(3,5) P_2, a low abundance phosphoinositide required for routine endosome maturation (Yamamoto et al., 2017; Sbrissa et al., 2002; Cabezas et al., 2006). Across an array of organisms, disruption of PIKfyve causes a range of endocytic trafficking defects, including characteristic swollen endosomes and defects in lysosomal degradation (Ikonomov et al., 2001; Dove et al., 2009; de Lartigue et al., 2009; Choy et al., 2018; Kim et al., 2014; Buckley et al., 2019; Nicot et al., 2006; Krishna et al., 2016). Precisely how PIKfyve disruption leads to these phenotypes in unclear; although several PI(3,5) P_2 activated ion channels on endosomal membranes have been identified, including TRPML1 and TPC2, and have both been implicated in endosome-endosome fusion events (Leray et al., 2022; Samie et al., 2013; Wang et al., 2012; Dong et al., 2010).

The Rab family of small GTPases also plays key roles in regulating endolysosomal traffic (Borchers et al., 2021). Early endosomes are marked by Rab5, which recruits effector proteins essential for early endosome fusion events (Henry et al., 2004; Lippuner et al., 2009). This includes Vps34, the class III PI-3 kinase responsible for PI(3)P synthesis. As maturation progresses, Rab5 is exchanged with the lysosomal marker, Rab7. In both yeast and mammals, this switch is mediated by the Mon1-Ccz1 complex, which both deactivates and dissociates Rab5, and recruits and activates Rab7 to endosomes (Kinchen & Ravichandran, 2010; Langemeyer et al., 2020; Nordmann et al., 2010). Accumulation of Rab7 on late endosomes promotes fusion with lysosomal compartments, and its disruption result in severely perturbed lysosomal delivery to phagosomes (Rupper et al., 2001).

Our previous work, using the soil-dwelling amoeba, *Dictyostelium discoideum*, showed that PIKfyve is critical for phagosome maturation (Buckley et al., 2019). *Dictyostelium* is a well-characterized model organism which feeds through phagocytosis of bacteria or bulk uptake of media by macropinocytosis. The maturation of phagosomes and macropinosomes is highly related and is studied extensively in a range of professional phagocytes, including macrophages. *Dictyostelium* is well-suited for the study of these processes, being a genetically pliable model which is amenable to biochemical analysis and fluorescence microscopy studies. Additionally, comparative phagosome pro-

teome studies between *Dictyostelium* and higher multicellular organisms indicates a shared core of phagosomal proteins across species (Boulais et al., 2010).

Using a PIKfyve-null (ΔPIKfyve) *Dictyostelium* cell line, we previously characterized a defect in phagosomal proteolysis and killing, which rendered cells hypersensitive to infection with *Legionella pneumophila*, and demonstrated the physiological importance of PIKfyve in innate immunity (Buckley et al., 2019). These defects were, in part, caused by perturbed V-ATPase and protease delivery to newly formed phagosomes. PIKfyve is also important for phagosome-lysosome fusion in both macrophages and neutrophils (Dayam et al., 2017, 2015; Kim et al., 2014; Isobe et al., 2019). This indicates a central and conserved role, but how PIKfyve activity is regulated and integrates with other components of the phagosomal maturation machinery such as Rab signalling and fusion with other endosomal compartments is poorly understood.

Here, we dissect how disruption of PIKfyve leads to defective phagosome maturation. By examining key maturation markers: Rab5, PI(3)P, V-ATPase, and Rab7, we find that whilst PIKfyve-deficient phagosomes can acquire and recycle Rab5, they accumulate almost no Rab7, which appears to be normally delivered by vesicle fusion. Furthermore, using our recently characterised molecular biosensor, SnxA which binds to PI(3,5) P_2 with high specificity (Vines et al., 2022), we identify an additional route for PI(3,5) P_2 enrichment to phagosomes and macropinosomes on small, Rab7-positive macropinosomes. Finally, we find PIKfyve has a specific role in regulating heterotypic fusion between phagosomes and a temporally defined population of macropinosomes, which we suggest plays a previously unappreciated role in maintaining digestive efficiency.

3.2 Materials and Methods

3.2.1 *Dictyostelium* Culture

All *Dictyostelium discoideum* cells were derived from the Ax2 (Kay) laboratory strain background unless stated otherwise and were grown in adherent culture in filter sterilised HL5 medium (Formedium) at 22°C. Cells expressing extrachromosomal plasmids were transformed by electroporation and grown in appropriate antibiotic selection by addition of either 20 µg/mL hygromycin (Invitrogen) or 10 µg/mL G418 (Sigma). PIKfyve knockout strain in Ax2 background generated as previously described (Buckley et al., 2019). Live cell imaging was performed in defined SIH medium (Formedium).

3.2.2 Cloning

All gene sequences used for cloning were obtained from dictybase (Fey et al., 2013). The generation of SnxA-GFP (pJSK619), PIKfyve-GFP (pJV0025) and integrating SnxA-GFP plasmids has been described previously (Vines et al., 2022). GFP-Rab5A (pJV0054) was generated similarly: cDNA was cloned via PCR using primeSTAR max DNA polymerase (Clontech). This was followed by subcloning into a zero blunt TOPO II vector (Life Technologies), before cloning into the appropriate BglII/SpeI sites of the pDM expression plasmid (Paschke et al., 2018; Veltman et al., 2009). The coding sequence was confirmed by restriction digest. 2xFYVE-GFP (pJSK418) uses the sequence from the human Hrs gene and was previously described (Calvo-Garrido et al., 2014). A GFP-Rab7A (pTH70) plasmid was kindly gifted by Huaquing Cai (Tu et al., 2022). Co-expression plasmids were created by first cloning the RFP-fusion sequence into the pDM series shuttle vectors (pDM1042 and pDM1121), before

cloning as an NgoMIV fragment into the appropriate GFP-expression vector.

3.2.3 Preparation of fluorescent yeast and dextran

Saccharomyces cerevisiae were used for phagocytosis assays. To obtain non-budded yeast, cells were grown for 3 days at 37°C in standard YPD media (Formedium) until in stationary phase. For a budded population, growth was halted while yeast were still in log phase. Both populations were then centrifuged at 1000 x g for 5-minutes and resuspended to a final concentration of 1×10^9 cells/mL in PBS pH7, then frozen until use. Yeast were fluorescently labelled using either pHrodo red succinimidyl ester (Life Technologies), or Alexa-405 succinimidyl ester (Life Technologies) at a final concentration of 0.25 mM and 2.5 mM, respectively. 0.5×10^9 yeast were resuspended in 200 µL PBS at pH8.5 and incubated with 10 µL of prepared dye for 30-minutes at 37°C with gentle shaking. After, cells were pelleted and sequentially washed in 1 m: of PBS pH 8.5, 1 mL of 25 nM Tris-HCl pH 8.5, and 1 mL of PBS pH 8.5 again. Finally, cells were resuspended in 500 µL of KK2 pH 6.1 and kept at -20°C. Yeast were diluted in SIH to a working concentration of 1×10^8 yeast/mL before use.

Texas-Red 70kDa Dextran (Life Technologies) was resuspended in water and diluted to a working concentration of 2 mg/mL. Far-red dextran was generated by labelling 70 kDa dextran (Invitrogen) with Alexa Fluor 680 NHS Ester (Invitrogen) as above, removing unbound dye by dialysis in KK2.

3.2.4 Microscopy and image analysis

Approximately 1×10^6 *Dictyostelium* cells were seeded into 35 mm microscopy dishes with glass bottoms (Mattek P35G-1.5-14-C) for fluorescence microscopy, and left to grow overnight in SIH medium (Formedium). Imaging was conducted using a Zeiss LSM880 AiryScan Confocal microscope equipped with a 63× Plan Apochromat oil objective.

To perform dual colour timelapse phagocytosis assays, most of the medium was removed just prior to imaging, and 20 µL of 1×10^8 dyed yeast added. After 60-seconds, a thin layer of 1% agarose in SIH was overlaid on the cells, and excess medium was removed. For normal timelapses, images were captured every 10-seconds for up to 10-minutes. For extended timelapses, images were captured every 60-seconds. Fluorescent intensity analysis around each phagosomal membrane was carried out automatically using the Python plugin pyimagej, which has been described previously (Vines et al., 2022). In brief, phagosomal contents were identified and segmented by using the fluorescent yeast, which are large and easy to follow. The fluorescence channel containing the yeast was thresholded, and large yeast-sized particles identified to be followed over time by examining similar particles on adjacent frames. This allowed individual phagosomes to be followed over the course of a few minutes. Increases in membrane fluorescence were then calculated by expanding the particle perimeter and taking average fluorescence readings in a banded area.

To perform dextran pulse-chases, the majority of the medium was removed and replaced with 50 µL of 2 mg/mL 70kDa Texas Red dextran for the specified duration. Dextran was then removed by washing three times in SIH medium, leaving ∼1 mL of SIH in the dish. Cells were immediately imaged, with multiple fields of view captured every 2-minutes for 10-minutes. An ImageJ script was used for the automated quantification of macropinosome number and size. GFP co-localization at each time point was scored manually.

For macropinosomes-phagosome fusion assays,

50 µL of 2 mg/mL Texas Red dextran was added to cells for the time indicated for macropinosomes to form. The dish was then washed as above, before addition of 20 µL of 1×10^8 dyed yeast and then agarose overlay after a further 60-seconds. Clustering analysis was performed using a modified version of the automated analysis pipeline described above. For macropinosome/macropinosome mixing a second dye, 50 µL of Alexa680 70kDa Dextran, was added instead of yeast. For macropinosome/phagosome fusion assays, budded yeast were used instead and analysis of fusion performed manually in ImageJ by measuring the mean intensity across the yeast neck over time. For analysis of clustering macropinosomes, macropinosomes within 1 µm of the phagosome were manually scored as GFP positive or negative, and binned into 2-minute intervals.

3.2.5 Western Blotting

Wildtype and ΔPIKfyve cells expressing GFP-Rab5A, GFP-2xFYVE, or GFP-Rab7A were analysed by SDS-PAGE and Western blot using a rabbit anti-GFP primary antibody (gift from Andrew Peden) and a fluorescently conjugated anti-rabbit 800 secondary antibody, using standard techniques. The endogenous biotinylated mitochondrial protein methylcrotonoyl-CoA Carboxylase 1 was used as a loading control using Alexa680-conjugated streptavadin (Davidson et al., 2013).

3.2.6 Statistics

Graphpad Prism 9 was used for statistical analysis. The figure legends provide details on the number of biological replicates and the statistical tests used for each experiment. A p-value of <0.05 was considered significant, with * indicating $p>0.05$, ** indicating $p>0.01$, and *** indicating $p>0.005$ throughout.

3.3 Results

3.3.1 Loss of PIKfyve specifically affects Rab7 delivery to phagosomes

To understand the functional role of PIKfyve, we examined how its loss affected other core components of the phagosome maturation pathway. Previously, we observed that PIKfyve-GFP is transiently recruited to *Dictyostelium* phagosomes between 30 to 120-seconds following engulfment (Vines et al., 2022), so we focused our analysis on components likely to be active within this time frame. During classical endocytosis, Rab5 accumulates at early stages and exchanges with Rab7 as endosomes mature (Rink et al., 2005). A similar Rab5-Rab7 exchange has been described during both phagosome and macropinosome maturation around the same time we observe PIKfyve-GFP recruitment (Kerr et al., 2006; Poteryaev et al., 2010; Tu et al., 2022; Vieira et al., 2003).

Co-expression of RFP-Rab5A and GFP-Rab7A allowed us to follow the dynamics of both proteins to newly formed phagosomes in wildtype and ΔPIKfyve cells (**Figure 3.1 A-B** and **Video 3.1**). In wild-type cells, as previously reported (Tu et al., 2022), RFP-Rab5A was highly enriched on perinuclear endosomes, and to a lesser extent at the plasma membrane. RFP-Rab5A was recruited to phagosomes following internalization before its removal in the following minutes. As expected, this coincided with a gradual accumulation of GFP-Rab7A, which also localized to a large pool of small endosomes which continuously clustered around phagosomes and appeared to fuse from approximately 30-seconds post-engulfment. In contrast, although RFP-Rab5A dynamics appeared identical in ΔPIKfyve cells phagosomes, they only ever ac-

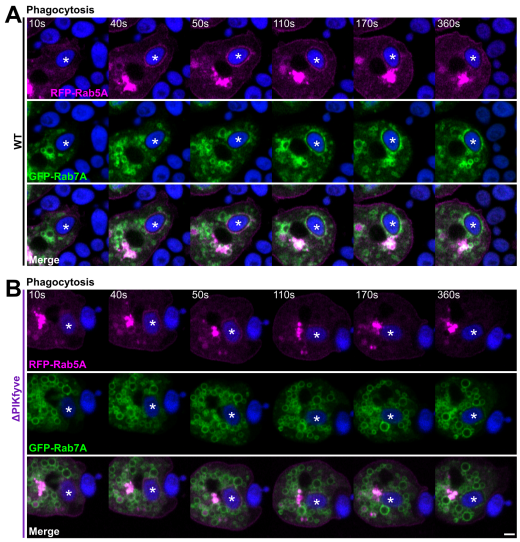

Figure 3.1: **Simultaneous analysis of RFP-Rab5 and GFP-Rab7 recruitment** Timelapse movies of **(A)** Wildtype and **(B)** ΔPIKfyve cells co-expressing RFP-Rab5A (magenta) and GFP-Rab7A (green) during phagocytosis of Alexa405-yeast (blue). Rab7A only arrives on wildtype phagosomes. The followed phagosome is indicted by and asterisk. The full timeseries is shown in **Video 3.1**. All scale bars = 2 µm

cumulated very low levels of GFP-Rab7A, despite its strong recruitment to other enlarged endocytic compartments (**Figure 3.1 B**).

To quantify changes in protein enrichment around engulfed particles over multiple events, we employed an automated image analysis pipeline which we have previously described (Vines et al., 2022). This segments the yeast and measures the fluorescence intensity of fluorescent fusion proteins around the periphery at each time point. To reduce the possibility of artefacts from overexpressing both proteins during quantification, Rab5A and Rab7A were expressed individually as GFP-fusions and multiple events averaged, normalised to the completion of engulfment (**Figure 3.2**).

This analysis confirmed the enrichment of GFP-Rab5A just prior to phagocytic cup closure (**Figure 3.2 A-C** and **Video 3.2**). This was independent of successful internalization (**Video 3.3**), suggesting a potential role for Rab5 before engulfment is complete in *Dictyostelium*. Rab5A-GFP then intensified following internalization and peaked 30-seconds after engulfment (**Figure 3.2 A**). Although expression levels were lower in the mutants (**Figure 3.S1 A**), the timing of Rab5A-GFP dynamics was not significantly changed in ΔPIKfyve cells (**Figure 3.2 B-C**).

As Rab5 is also responsible for PI(3)P synthesis, due to the recruitment and activation of the Class 2 PI3-kinase Vps34, we also quantified PI(3)P using the well characterised reporter GFP-2xFYVE ((Gillooly et al., 2000)). In wildtype cells, GFP-2xFYVE became enriched on phagosomes in a uniform ring within 60 seconds of engulfment (**Figure 3.S1 B-D** and **Video 3.4**), and was maintained for at least 50-minutes (**Figure 3.S1 E**). PI(3)P also localized to a set of small vesicles throughout the cytosol (arrows in **Figure 3.S1 B**). In ΔPIKfyve cells, however, these vesicles were replaced with large numbers of characteristically swollen endosomes which moved slowly around the cell (**Figure 3.S1 C**). Nonetheless, there were no quantifiable differences in phagosomal PI(3)P dynamics in ΔPIKfyve cells consistent with normal Rab5 dynamics (**Figure 3.S1 D**).

Quantification of GFP-Rab7A in wildtype cells showed a continuous accumulation to phagosomes over the first 6 minutes of maturation following its initial arrival around 30-seconds post-

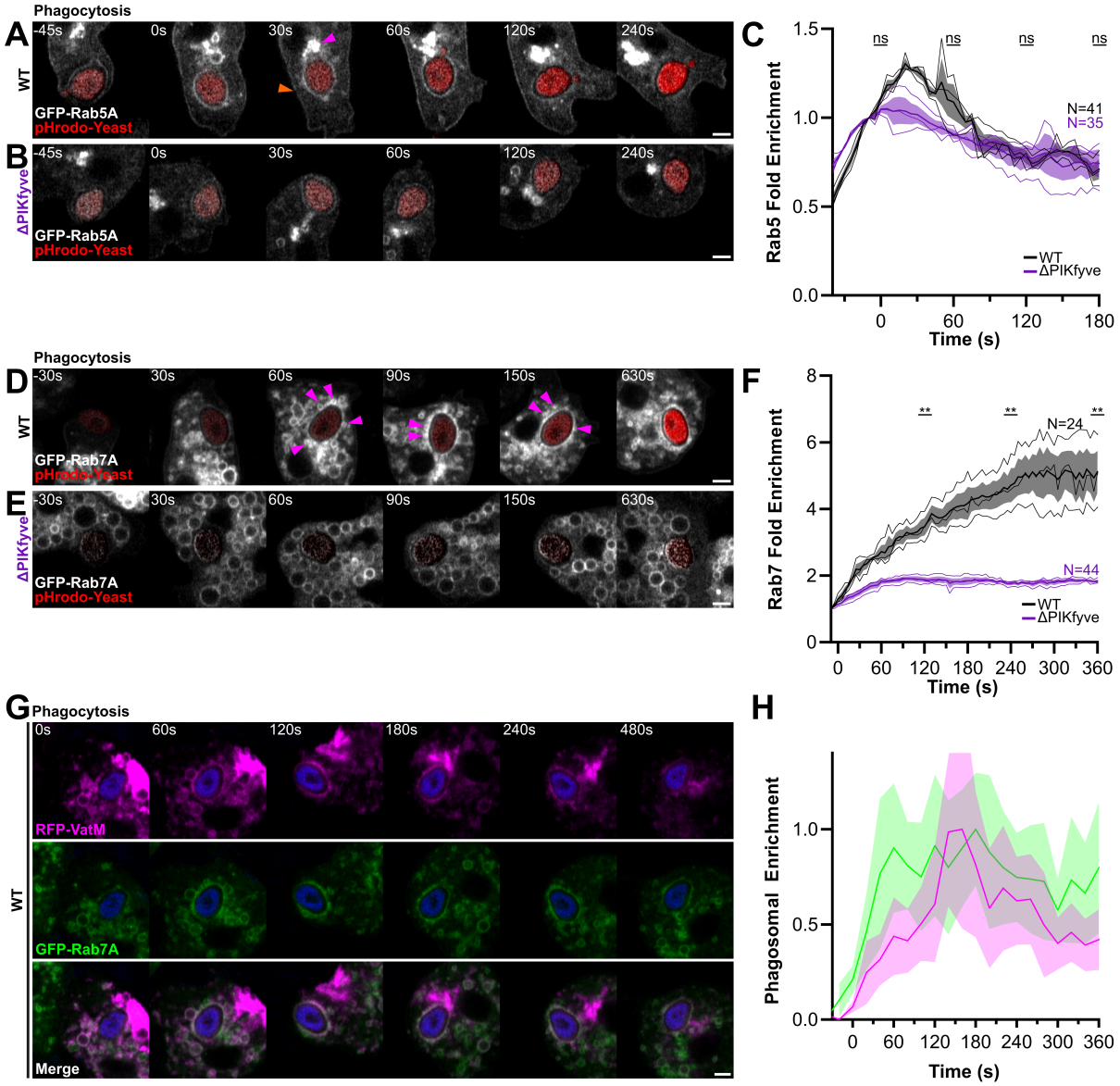

Figure 3.2: **Loss of PIKfyve affects Rab7 recruitment to phagosomes. (A)** and **(B)** Timelapses of GFP-Rab5A during phagocytosis of pHrodo-yeast (red) in wildtype (A) and ΔPIKfyve(B) cells. GFP-Rab5A is constitutively enriched on a peri-nuclear pool (pink arrow) and the plasma membrane (orange arrow) as well as the phagosomal envelope for 0s-60 s. Quantification of GFP-Rab5A enrichment at the phagosomal membrane is shown in **(C)**. Rab5 has similar dynamics in both cell types, with no significant differences at all timepoints tested. **(D)** and **(E)** show GFP-Rab7A recruitment to phagosomes in wild-type and ΔPIKfyve cells respectively. Arrowheads indicate the clustered GFP-Rab7A-enriched vesicles only observed in wildtype cells. **(F)** Quantification of phagosomal GFP-Rab7A enrichment, demonstrating a significant decrease in ΔPIKfyve mutants. **(G)** Timelapse movie of wildtype cells co-expressing RFP-VatM (magenta) and GFP-Rab7A (green). Fluorescence intensity around phagosome in G is shown in (H). Data is mean intensity ± SD of a linescan along the phagosomal membrane normalised between minimum and maximum intensities observed. All scale bars = 2 µm.

engulfment (**Figure 3.2 D-F** and **Video 3.5**). GFP-Rab7A was maintained for at least 50-minutes (**Figure 3.S1 F-G**), most likely until the transition to a post-lysosome (Buczynski et al., 1997). In contrast, although very low levels of GFP-Rab7A were visible at some timepoints, quantitative analysis confirmed the majority of GFP-Rab7A delivery to phagosomes was lost in ΔPIKfyve cells (**Figure 3.2 F**). In these experiments, it was notable that whilst GFP-2xFYVE appeared as a smooth ring directly on the phagosomal membrane, in wild-type cells GFP-Rab7A-positive vesicles appeared to cluster around the phagosome before fusing. This was apparent by analysis of the variance in fluorescence along the phagosome membrane (**Figure 3.S1 H**), and indicates that phagosomal Rab7 accumulation is predominately driven by fusion with other Rab7-containing compartments, rather than recruitment from a cytosolic pool. In contrast, although the cytosol of ΔPIKfyve cells was full of swollen GFP-Rab7A positive vesicles, there was no obvious clustering around the nascent phagosome (**Figure 3.2 D**).

We have previously shown that disruption of PIKfyve causes a reduction in V-ATPase-delivery to phagosomes (Buckley et al., 2019). We therefore asked whether Rab7 and V-ATPase were delivered on the same vesicles by co-expressing GFP-Rab7A with RFP-VatM (a component of the V-ATPase complex) in wildtype cells (**Figure 3.2 G**). This showed that all VatM-positive vesicles were also Rab7A-positive, and both proteins accumulated on the phagosomal membrane with similar timings (**Figure 3.2 H**). This indicates that PIKfyve is required for the delivery of Rab7A/VatM-positive endosomes to the early phagosome, and its absence causes a generalized loss in the delivery of the lysosomal components required for normal maturation.

3.3.2 PIKfyve is not important for Rab7 delivery to macropinosomes

Although GFP-Rab7A did not accumulate on ΔPIKfyve phagosomes, it clearly still localised to other large endocytic compartments (**Figure 3.2 E**). As these resemble the swollen macropinosomes previously observed in these cells (Buckley et al., 2019), we asked whether the defect in GFP-Rab7A delivery was specific to phagosome maturation. As individual macropinosomes are difficult to follow for more than 2-3 minutes by timelapse microscopy, we labelled macropinosomes with a 2-minute pulse of TexasRed-dextran (**Figure 3.3 A-B**). Different fields of view were then captured at time intervals after dextran removal allowing the percentage of macropinosomes positive for GFP to be measured for up to 10-minutes (Buckley et al., 2016). In this assay, GFP-Rab7A recruitment to macropinosomes was indistinguishable between ΔPIKfyve cells and wild-type controls, accumulating within 2-minutes of internalisation (**Figure 3.3 C**).

Although GFP-Rab7A dynamics appeared normal, the macropinosomes in ΔPIKfyve cells did still appear much larger. Quantification of the size and fluorescence intensity of these demonstrated that although macropinosomes started off the same size in both ΔPIKfyve and control cells, the normal shrinkage and concentration of their lumen was significantly impaired in *PIKfyve* mutants (**Figure 3.3 D-F**). Therefore shrinkage and Rab7 accumulation are functionally separable, indicating different roles of PIKfyve.

To functionally assess macropinosome maturation, we also measured proteolysis of the reporter dye DQ-BSA over time. Although loss of PIKfyve almost completely blocks proteolysis of DQ-BSA

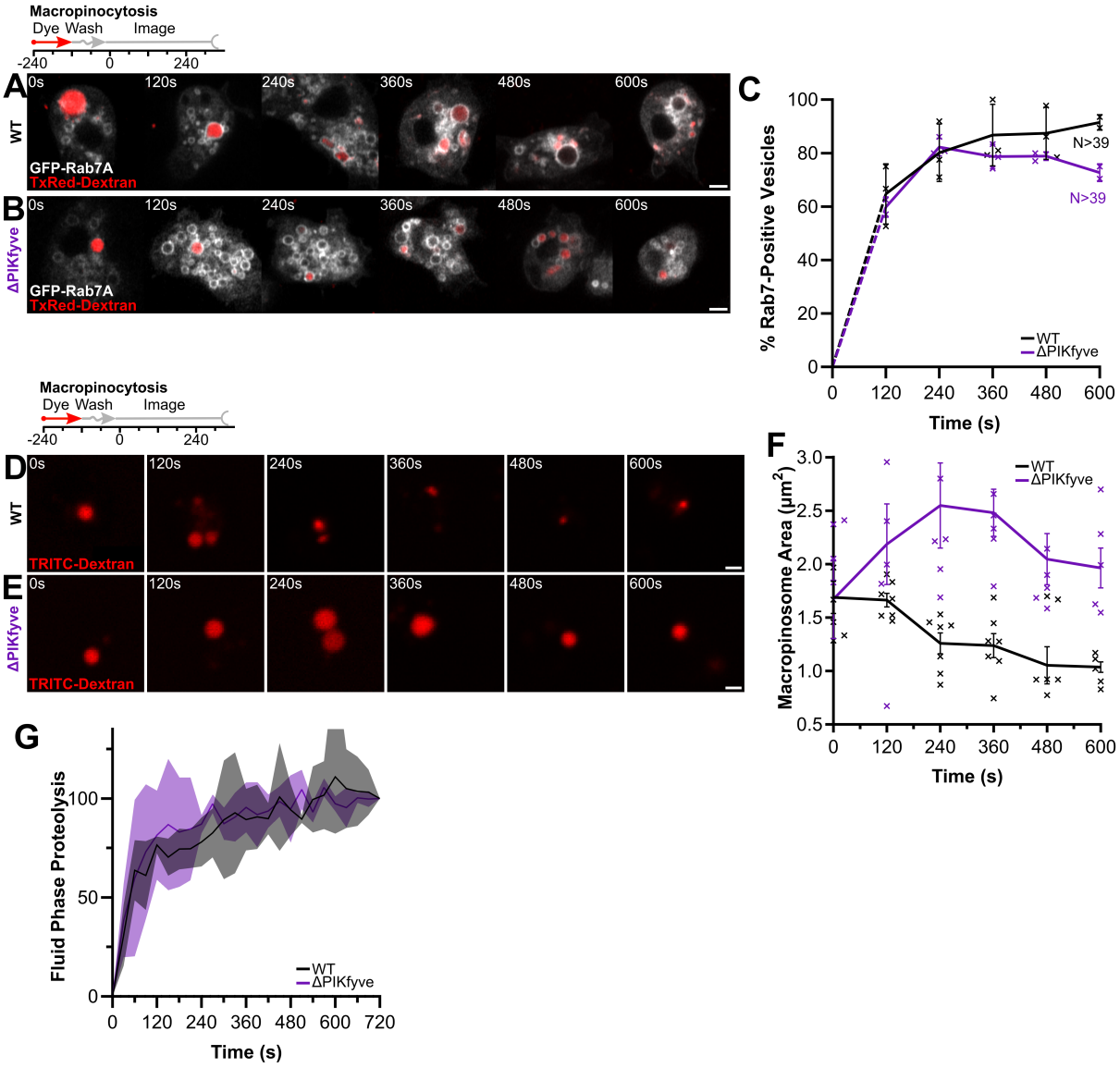

Figure 3.3: **PIKfyve is not important for Rab7 delivery to macropinosomes (A)** and **(B)** GFP-Rab7A recruitment to macropinosomes labelled by a 2-minute pulse of TxRed dextran (red) in wildtype (A) and ΔPIKfyve(B) cells. **(C)** Quantification by scoring the percentage of GFP-positive macropinosomes at each time point after dextran wash out. GFP-Rab7A dynamics are similar in both cell types. Data shown is mean ± SEM of 3 independent experiments, with N indicating the total number of cells measured. Biological replicates shown by crosses. **(D)** and **(E)** labelling of macropinosomes by a 2-minute pulse of TRITC dextran (red) in wildtype (D) and ΔPIKfyve(E) cells. **(F)** Quantification of macropinosome shrinkage during early maturation. Whilst wild-type macropinosomes lose approximately half their volume within 5 minutes, this is disrupted in ΔPIKfyve cells. Graph represents the mean ± SEM of six independent experiments. Biological replicates shown by crosses. **(G)** Fluid phase proteolytic activity in wildtype and ΔPIKfyve cells measured by increase in fluorescence after a 2-minute pulse of DQ-BSA. Data shown is mean ± SD of three independent experiments. All scale bars = 2 μm.

when conjugated to beads (Buckley et al., 2019), degradation of the fluid-phase dye was completely unaffected (**Figure 3.3 G**). Therefore, despite generally similar maturation pathways, PIKfyve plays a specific role in the fusion of lysosomes to phagosomes, but not macropinosomes.

3.3.3 PI(3,5) P_2 is delivered by fusion of small Rab7-positive vesicles

The evidence above suggests that PIKfyve or production of PI(3,5) P_2 is required for lysosomal fusion with phagosomes. To better understand how Rab7 is recruited relative to PI(3,5) P_2, we co-expressed RFP-Rab7A with PIKfyve-GFP in ΔPIKfyve cells (Figure **Figure 3.4 A**). As expected, PIKfyve-GFP expression restored Rab7A recruitment to phagosomes and recruitment of PIKfyve-GFP overlapped with the start of Rab7 enrichment (**Figure 3.4 B**). As we recently showed, PIKfyve recruitment was only transient and lost from the phagosomal membrane within 2-minutes. The sustained presence of its product, PI(3,5) P_2, may therefore function to maintain continued Rab7 recruitment.

To observe PI(3,5) P_2 dynamics, we used our recently identified biosensor, SnxA, which specifically binds this lipid with high affinity (Vines et al., 2022). In *Dictyostelium*, we showed SnxA-GFP is enriched on both phagosomes and macropinosomes approximately 120-seconds after engulfment, around the same time PIKfyve itself leaves the phagosome. Upon disruption of PIKfyve, SnxA-GFP becomes completely cytosolic. For clarity, the dynamics of PI(3,5) P_2 during phagosome maturation relative to other markers from this and other studies is shown in **Figure 3.4 C**.

Closer examination of SnxA-GFP recruitment to phagosome and macropinosomes by timelapse microscopy indicated that accumulation of SnxA-GFP is accompanied by the docking and fusion of multiple smaller SnxA-GFP-positive vesicles less than 1 µm in size. These cluster around macropinosomes and phagosomes several seconds before they themselves acquire the SnxA-GFP (arrows in **Figure 3.4 D-E** and **Video 3.6**). This implies that PI(3,5) P_2 accumulates through both *in situ* synthesis by PIKfyve and delivery via fusion with another PI(3,5) P_2 compartment. This suggests a role for PIKfyve in regulating the clustering or fusion of a specific subset of vesicles to the phagosome.

We then asked whether the small PI(3,5) P_2-positive vesicles also contained Rab7, by co-expressing SnxA-GFP with RFP-Rab7A. This demonstrated that all docked SnxA-positive vesicles were also positive for Rab7A (White arrows **Figure 3.4 F** and **Figure 3.S2 A**). However, RFP-Rab7A also localised to additional populations of vesicles that start to cluster and fuse much earlier than those marked by SnxA, as is evident in the quantification of intensity (**Figure 3.4 G**). Co-expression of SnxA-GFP alongside RFP-VatM yielded similar results, with SnxA vesicles representing a later-fusing subset of VatM-positive endosomes (**Figure 3.4 H-I**).

Together, our data demonstrate the presence of a Rab7/VatM/PI(3,5) P_2-positive compartment which is delivered to early phagosomes following PIKfyve recruitment, approximately 120-seconds post-engulfment. This compartment can be distinguished from an additional population of Rab7/V-ATPase-positive endosomes which cluster earlier and do not contain PI(3,5) P_2. This is indicative of the sequential delivery of lysosomal components and depends on PIKfyve for its regulation.

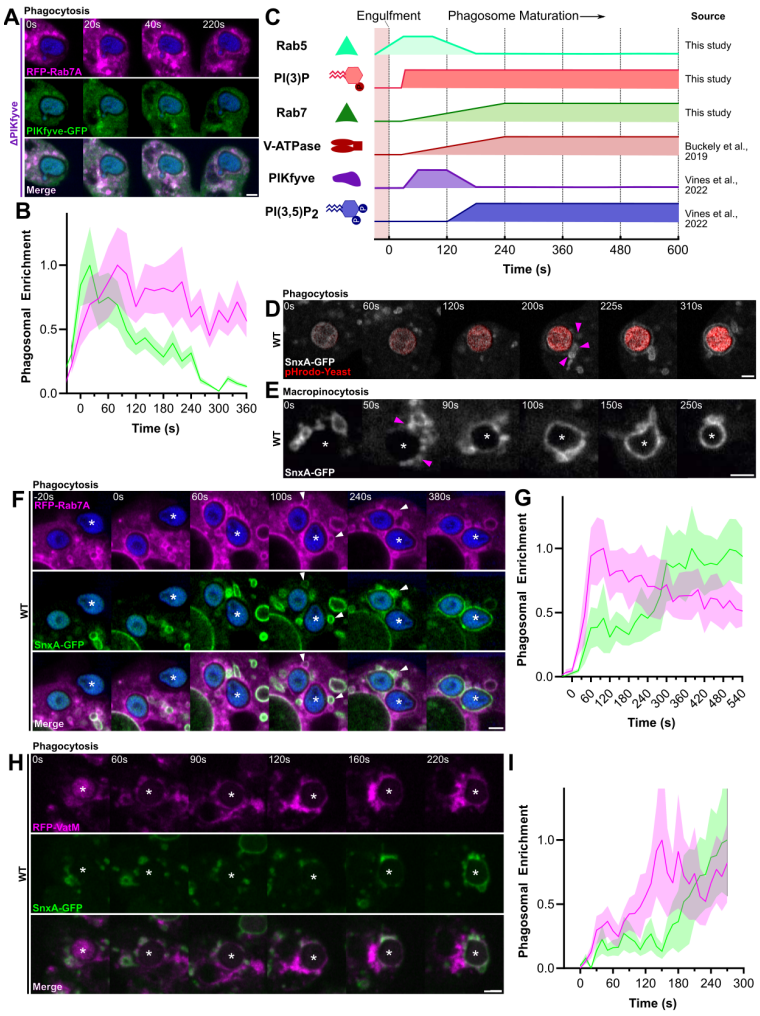

Figure 3.4: **PI(3,5) P_2 is delivered after Rab7 to both macropinosomes and phagosomes. (A)** Timelapse of RFP-Rab7A in ΔPIKfyve cells with PIKfyve-GFP rescue expression. Fluorescence intensity around phagosome in A is shown in **(B)**. **(C)** and **(D)** Timelapses of SnxA-GFP during phagocytosis of pHrodo-yeast (red) (C) and macropinocytosis (D) in wildtype cells. Pink arrowheads indicate clustering SnxA vesicles. **(E)** The arrival of maturation components to the phagosomal membrane summarised from this study and our previous work. When the line is low, the respective component is absent from the phagosomal membrane, when the line is high the component is enriched. **(F)** Timelapses of RFP-Rab7A (magenta) and SnxA-GFP (green) during phagocytosis of Alexa405-yeast (blue) in wildtype cells. SnxA and Rab7 co-localize on many clustering vesicles (arrowheads). Fluorescence intensity around phagosome in F is shown in **(G)**. **(H)** Timelapses of RFP-VatM (magenta) and SnxA-GFP (green) during phagocytosis in wildtype cells. Fluorescence intensity around phagosome in H is shown in **(I)**. For all intensity graphs, data is mean intensity ± SD of a linescan along the respective phagosomal membrane normalised between minimum and maximum intensities observed. All scale bars = 2 µm.

3.3.4 The clustering PI(3,5) P_2-positive vesicles are macropinosomes

We next investigated the origin of the pool of Rab7/V-ATPase/PI(3,5) P_2-positive vesicles that fuse with phagosomes. Our previous work shows the primary compartment marked by SnxA in *Dictyostelium* and mammalian cells are macropinosomes (Vines et al., 2022) (**Figure 3.4 E**) and this overlaps with the accumulation of Rab7 (**Figure 3.3 A**). Others have also shown that macropinosomes can undergo homotypic fusion (Dolat & Spiliotis, 2016; Hamasaki et al., 2004; Neuhaus et al., 2002; Tu et al., 2022) and using sequential pulses of different coloured dextrans, we were also able to observe macropinosomes fusing with one another from relatively early stages of maturation (**Figure 3.S2 B**). Therefore, we hypothesized that Rab7/V-ATPase/PI(3,5) P_2 macropinosomes fuse with phagosomes in a PIKfyve-dependent manner.

To test this, we labelled macropinosomes by incubating cells with a 5-minute pulse of 70kDa dextran, before washing and addition of yeast. In this way, we were able to follow interactions between a defined population of dextran-filled macropinosomes and nascent phagosomes. Using cells co-expressing 2xFYVE-RFP and SnxA-GFP, we observed that the SnxA-positive vesicles clustered around the nascent phagosome contained dextran and were also positive for RFP-2xFYVE (white arrows **Figure 3.5 A** and **Video 3.7**). We previously showed that both lipids are only present on macropinosomes between 3-8 minutes of maturation (Vines et al., 2022; King & Kay, 2019). This matches the timings of our pulse-chase experiment and indicates macropinosomes cluster phagosomes at a defined point in their maturation.

In addition to SnxA macropinosomes, we also identified additional populations of SnxA-GFP negative macropinosomes, which clustered earlier. To determine the identities of these macropinosomes and how they changed over time, we imaged macropinosome clustering in cells expressing different GFP-fusion reporters. At 2-minute intervals post-phagocytosis, all dextran-labelled macropinosomes within 1 µm of the phagosomal membrane were scored for the presence of each reporter (**Figure 3.5 B-C**). In each experiment, the number of phagosome-proximal macropinosomes started low (initially ~2 per phagosome) but increased to ~6 per phagosome by 2-minutes. There is, therefore, temporal regulation of the interaction between the two compartments.

Consistent with our timelapses of SnxA-GFP delivery, only 33% of proximal macropinosomes were positive for SnxA-GFP at initial timepoints. This likely indicates the background false-positive rate for this method caused by macropinosomes that are near phagosomes by chance. In contrast, ~80% of macropinosomes clustered around phagosomes at 6-8 minutes were clearly marked by SnxA-GFP. At all timepoints, 80% of proximal macropinosomes were positive for GFP-Rab7A. Therefore the increased population of macropinosomes that actively cluster around phagosomes around 5-minutes is defined by PI(3,5) P_2, rather than Rab7.

3.3.5 PIKfyve is required for fusion of macropinosomes with phagosomes

As the clustering of macropinosomes correlates with the presence of PI(3,5) P_2, we tested whether this was perturbed by PIKfyve disruption. For this, we repeated the dextran and yeast pulse chase described above in both wildtype and ΔPIKfyve

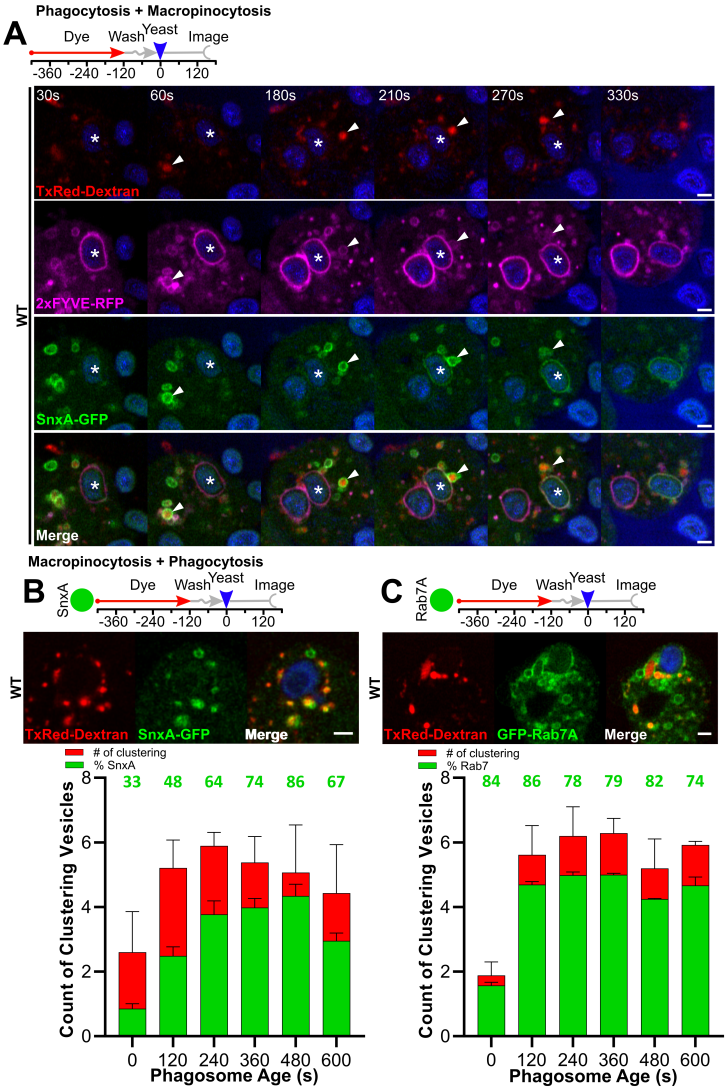

Figure 3.5: **Clustering Rab7/PI(3)P/PI(3,5)P2 positive compartments are macropinosomes. (A)** Timelapse of cells co-expressing 2xFYVE-RFP (magenta) and SnxA-GFP (green) during phagocytosis of Alexa405-yeast (blue) in wildtype cells. Schematic shows experimental procedure: Cells were pre-incubated for 5 minutes with a 70kDa Txred-dextran (red) to load macropinosomes before dextran washout and addition of yeast. White arrow indicates a 2xFYVE and SnxA positive macropinosome which docks and fuses with the phagosome during acquisition of SnxA to the phagosomal membrane. **(B-D)** Images and quantification of clustering macropinosome identity. Wildtype cells expressing GFP-Rab7A, GFP-2xFYVE or SnxA-GFP were treated with a dextran pulse-chase before phagocytosis of yeast. Macropinosomes within 1 µm of the phagosome were identified at each timepoint and both total number (red bars) and proportion colocalizing with the respective GFP-reporter (green bars and numbers) were scored manually. Frames were binned into 2- minute groups, data shown are the mean ±SEM of three independent experiments. Note increased clustering from 2 minutes, with high Rab7 colocalization, followed by an increase in SnxA-GFP positive macropinosomes after 4 mins. All scale bars = 2 µm.

cells. As before, in wildtype cells, macropinosomes began clustering around phagosomes from within 30-seconds of engulfment (**Figure 3.6 A**). This was completely lost in ΔPIKfyve cells, where the enlarged macropinosomes were never clearly observed interacting with the phagosome (**Figure 3.6 B**). We quantified this by measuring the average dextran signal within 0.5 µm of the yeast, showing that this failure to cluster was persistent throughout maturation (**Figure 3.6 C**).

To determine whether macropinosomes were just clustering around phagosomes or fusing with them, we also examined delivery of dextran to the phagosomal lumen. Using GFP-2xFYVE to highlight the bounding phagosomal membrane, it was occasionally possible to observe dextran accumulation in small pockets that appeared to be within the phagosomal envelope (**Figure 3.6 D**). This was difficult to reliably quantify, but we noticed that when budding yeast were used, dextran accumulated prominently within the bud neck region of the phagosome due to its negative curvature (**Figure 3.6 E**). Using budded yeast therefore enabled us to reproducibly observe and quantify dextran delivery within the phagosome. This demonstrated fusion of early macropinosomes to phagosomes in wild-type cells, and was again completely lost in ΔPIKfyve cells (**Figure 3.6 F**). Therefore, PIKfyve is required for both clustering and delivery of macropinosomes to early phagosomes.

As both PI(3)P and PI(3,5) P_2 are only present on macropinosomes for the first 7-8 minutes of maturation (Vines et al., 2022), we asked if macropinosomes were only fusion-competent over this period. To test this, cells were again exposed to a 5-minute pulse of dextran, but were then incubated for 10-minutes for these macropinosomes to mature to a later stage before addition and phagocytosis of yeast. This delay significantly decreased accumulation of dextran at the yeast neck, although not as much as observed in ΔPIKfyve cells with ∼20% of the dextran delivery remaining (**Figure 3.6 G**).

As macropinosomes also fuse with each other (**Figure 3.S2 B**), this residual macropinosome-phagosome fusion can potentially be attributed to older macropinosomes fusing to newer macropinosomes which are then able to fuse with the nascent phagosome. Macropinosomes are therefore only competent to fuse with phagosomes at a specific early stage (2-8 minutes old), when they possess both PI(3)P and PI(3,5) P_2.

Our data demonstrate a specific role for PIKfyve in the delivery of macropinosomes to newly formed phagosomes. As these macropinosomes are enriched in V-ATPase, Rab7 and lysosomal enzymes, this provides a mechanism for their rapid delivery to early phagosomes, which is physiologically important for effective bacterial killing and protection from pathogens (Buckley et al., 2016).

3.4 Discussion

In this study we expand our understanding of the complex dynamics of Rab and phosphoinositide signalling that underpin the processing of phagosomes and macropinosomes. We describe a complex pathway in which distinct pools of endosomes are sequentially delivered to maturing phagosomes over the first few minutes of maturation.

We have shown a portion of these endosomes are early macropinosomes which cluster around phagosomes before heterotopic fusion. While the delivery of lysosomal contents to phagosomes is well studied (Dayam et al., 2017, 2015; Kim et al., 2014; Isobe et al., 2019), fusion with early macropinosomes (less than 8-minutes old) is much less well understood. However, studies in both *Dictyostelium* and mammalian cells have also shown early macropino-

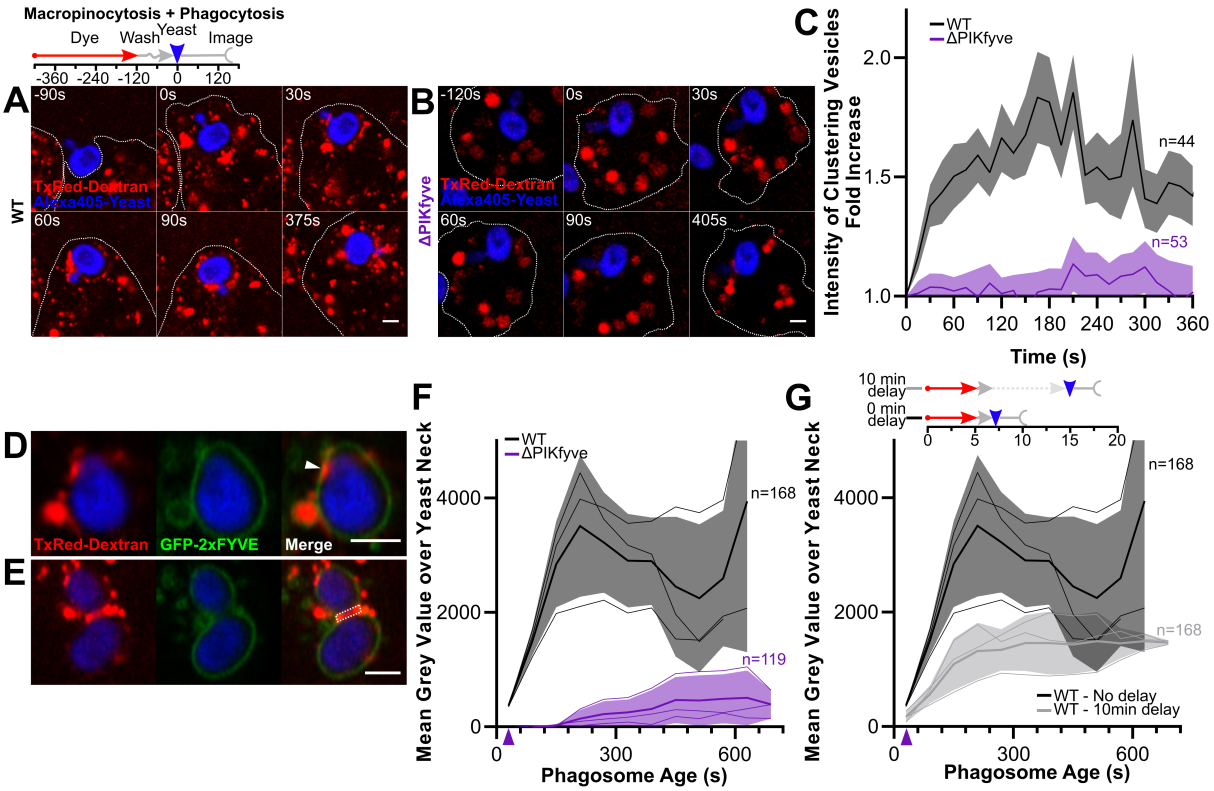

Figure 3.6: **PIKfyve drives fusion between macropinosomes and phagosomes.** **(A)** and **(B)** Timelapses of interactions between early macropinosomes (red) and phagosomes (blue) in wildtype and ΔPIKfyve cells, after sequential addition of fluorescent dextran and yeast. Schematic shows experimental procedure. Macropinosomes cluster around phagosomes in wildtype but not in ΔPIKfyve cells. **(C)** Quantification of dextran intensity around phagosomes, averaged over multiple events. Graph shows fold enrichment normalised to 10s before engulfment ± SEM. **(D)** TxRed-dextran (red) accumulation within the phagosomal membrane (green) marked by 2xFYVE (arrowhead). **(E)** Shows the same, using a budded yeast. Note strong dextran accumulation around the bud neck (dashed box). **(F)** Quantification of dextran intensity in this area averaged across multiple events ± SEM, binned by the age of the phagosome. **(G)** Quantification of dextran delivery (as in F) after a 10-minute delay before addition of yeast (see schematic, same control data as in F). Older macropinosomes show less delivery to phagosomes. All purple arrows on graphs indicate the time of PIKfyve arrival. All scale bars = 2 µm.

somes fuse with one another in the first few minutes after formation, although it is unclear whether aged macropinosomes also possess this ability (Hamasaki et al., 2004; Schink et al., 2021).

Fusion between macropinosomes and phagosomes has also been observed in mammalian cells and implicated during infection. Both *Salmonella enterica* and *Shigella flexineri* induce macropinosome formation from the ruffles formed during their entry into non-phagocytic host cells (Adam et al., 1996; Francis et al., 1993). These macropinosomes cluster around the bacteria-containing vacuole and appear to facilitate the rupture and escape of *Shigella* (Weiner et al., 2016) whereas they appear to stabilise and support the vacuolar lifestyle of *Salmonella* (Stévenin et al., 2019). Interestingly, inhibition of PIKfyve also disrupts *Salmonella* replication (Kerr et al., 2006). Whilst it is unclear how infection-associated macropinosomes relate to those made constitutively by professional phagocytes like macrophages or *Dictyostelium*, this highlights a common role for macropinosome delivery in the remodelling of microbe-containing compartments.

The observation that macropinosomes undergo continuous retrograde fusion with subsequent newly-formed macropinosomes and phagosomes challenges the view of maturation as a linear process. Our data indicate a cyclic model whereby nascent macropinosomes fuse with a slightly older population, distinguished through PIPs such as PI(3,5) P_2. A proportion of these will again fuse with the next round of macropinosomes whilst the rest presumably progress further and lose fusogenicity and enter a terminally digestive phase (**Figure 3.7**). We speculate that these retrograde fusion events provide a mechanism to rapidly deliver a large volume of hydrolases, V-ATPase and other digestive machinery to newly internalised vesicles. Rapid enzyme delivery may be particularly important for both macropinosomes and phagosomes due to their large size and low surface area-to-volume ratio.

We find that fusion between macropinosomes and phagosomes depends on PIKfyve, and coincides with the presence of PI(3,5) P_2 on the macropinosomes. Loss of PIKfyve blocked both the clustering of macropinosomes around phagosomes and the delivery of macropinocytic material. Previous studies have also implicated PIKfyve during endosome fusion events. For example, fusion of macropinosomes with lysosomes is at least partially regulated by recruitment of the septin cytoskeleton in a PIKfyve-dependent manner (Dolat & Spiliotis, 2016). However, *Dictyostelium* do not possess septins, and we find no defect in macropinosomes maturation in these cells, indicating that fusion of phagosomes with lysosomes uses an alternative PIKfyve-dependent mechanism. Nonetheless, PIKfyve appears to have a conserved role in regulating endosomal mixing, and the disruption of this fusion between macropinosomes and phagosomes likely accounts for some of the acidification and proteolysis defects we previously observed (Buckley et al., 2019).

PIKfyve disruption also results in an almost complete block in Rab7 delivery to phagosomes. In wildtype cells, Rab7A-positive vesicles continually clustered around the surface of nascent phagosomes, with Rab7A intensifying on the phagosomal membrane gradually over a period of several minutes. This indicates that on *Dictyostelium* phagosomes at least, the majority of Rab7 accumulates by fusion with Rab7-positive compartments. This is consistent with the recent work by Tu et al. (2022), who also describe fusion of Rab7-positive vesicles with early-Rab5 positive macropinosomes, but contrasts with the canonical view of Rab7 recruitment from

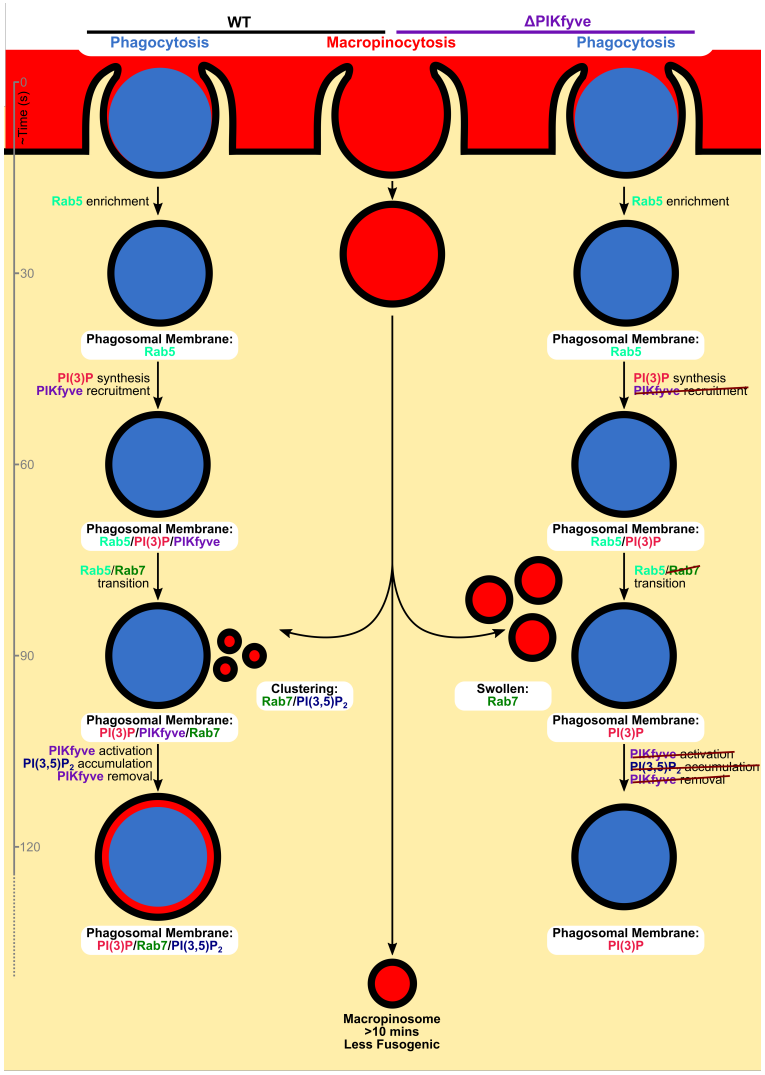

Figure 3.7: **Model for the first 2 minutes of phagosome maturation.** The left side indicates the maturation of phagosomes in wild-type cells, with PIKfyve-deficient cells on the right. Macropinosome maturation in the centre. Wild-type phagosomes accumulate each of the proteins and lipids indicated as per Figure 5G, with PIKfyve becoming activated approximately 1 minute after recruitment, at the point that macropinosomes of a similar age fuse and PIKfyve itself dissociates. In the absence of PIKfyve, macropinosomes do not shrink as efficiently, and do not cluster around, or fuse with phagosomes.

a cytosolic pool via the activities of the Mon1/Ccz complex.

Importantly however, although Rab7A is markedly decreased on ΔPIKfyve phagosomes, it is not completely absent with roughly 10% still recruited compared to macropinosomes in the same cell. Therefore some Rab7A can accumulate on phagosomes independently of PIKfyve. In the absence of obvious vesicles clustering around the phagosomes, we speculate that this small pool of PIKfyve-independent Rab7 is acquired from a cytosolic pool via classical Rab5-Rab7 exchange. However, this alone appears inadequate to facilitate subsequent fusion with other Rab7A-positive compartments, further Rab7 enrichment, and lysosomal fusion.

The loss of Rab7A-positive vesicles clustering around phagosomes in ΔPIKfyve cells suggests the failure for phagosomes to enrich in Rab7A is due to disruption of heterotypic docking and/or fusion. While the PIKfyve protein complex could be directly mediating fusion with Rab7A-positive compartments, it is more likely that PI(3,5) P_2 plays a role. In yeast, the Rab7 homolog, Ypt7, directly interacts with the HOPS complex which itself mediates endosomal fusion (Ostrowicz et al., 2010; Brett et al., 2008). A similar, less direct interaction between Rab7 and HOPS occurs in higher eukaryotes through the Rab7 effector RILP (Lin et al., 2014; van der Kant et al., 2013). Furthermore, disruption of Rab7A in *Dictyostelium* results in severe defects in lysosomal activity and delivery of premature lysosomal enzymes (Rupper et al., 2001).

How PI(3,5) P_2 mediates fusion between phagosomes and macropinosomes remains unclear. PI(3,5) P_2 is a calcium ion channel activator on phagosomal membranes, and in mammalian cells, overexpression of the PI(3,5) P_2-activated calcium ion channel TRPML1 partially rescues the characteristic ΔPIKfyve swollen endosome phenotype (Dong et al., 2010). Whether a reduction in swollen endosomes would also restore heterotypic fusion remains to be tested, although the *Dictyostelium* TRPML1 homolog, mcln1, does not localize to phagosomes until after post-lysosome transition (Lima et al., 2012), meaning there must be a slightly different mechanism in this organism.

Nearly all clustering PI(3,5) P_2-positive macropinosomes were also Rab7/PI(3)P-positive, which further supports their identification as macropinosomes less than 8-minutes old and distinct from younger, PI(3,5) P_2-negative, macropinosomes. This finding helps to identify multiple pools of Rab7-positive vesicles which can fuse with phagosomes and indicates a more complex picture than the canonical view of a single lysosomal population being delivered. Analyses of *Dictyostelium* phagosomes purified at different stages of maturation also showed different proteases were delivered and recovered over time (Souza et al., 1997; Gotthardt et al., 2006). The timescale in our experiments is much shorter, but both studies suggest that multiple endosomal populations are involved in phagosome maturation. The sequential fusion of different endosomal and lysosomal populations was also observed in studies of macropinosome maturation in macrophages (Racoosin & Swanson, 1993) indicating that this is likely a universal phenomenon.

A further interesting aspect of our studies is the clear differences between phagosome and macropinosome maturation in *Dictyostelium*. Whilst early steps such as the Rab5-Rab7 transition and acquisition of PI(3)P followed by PI(3,5) P_2 appear identical, only phagosomal degradation is strongly affected by loss of PIKfyve. In contrast, PIKfyve-deficient macropinosomes digest normally and still acquire Rab7, even though their shrinkage is reduced similar to observations in mammalian cells

(Freeman et al., 2020; Kerr et al., 2010). PIKfyve therefore appears to play independent roles in shrinkage and degradation, and in *Dictyostelium* at least, only phagosomes require PIKfyve for Rab7 and lysosomal delivery. These differences are likely driven by signalling from phagocytic receptors, but how this is mediated and how it functionally affects killing and digestion remain unclear.

Many aspects of maturation are shared between phagosomes, macropinosomes, and other endocytic pathways, such as classical clathrin-mediated endosomes. These also transition from a Rab5/PI(3)P-positive early form to later compartments demarked by Rab7, V-ATPase and lysosomal components. Furthermore, degradation of classically endocytosed receptors, autophagosomes and entotic vesicles are also sensitive to PIKfyve inhibition (Qiao et al., 2021; Krishna et al., 2016; de Lartigue et al., 2009). It is therefore likely that at least some of our observations on phagosomes are applicable to other endocytic routes, although the differences with macropinosomes indicate previously unexpected complexity. Nonetheless, in this study we further define the complex sequence of events that occur in the first minutes of a phagosome, and describe key mechanistic insights in to the roles and regulation of PIKfyve and PI(3,5) P_2.

3.5 Acknowledgements

The authors thank Huaqing Cai for Rab expression plasmids, Douwe Veltman and Peggy Paschke for their continued development of his expression system and Robert Insall for his support in the early days of this project. JHV is funded by Royal Society grant RGF\EA\180126, JSK is funded by a Royal Society University Research Fellowship URF\R\201036. Imaging work was performed in the Wolfson Light Microscopy Facility at Sheffield.

3.6 Bibliography

Adam, T., Giry, M., Boquet, P., & Sansonetti, P. (1996). Rho-dependent membrane folding causes shigella entry into epithelial cells. *The EMBO Journal*, 15, 3315.

Bohdanowicz, M. & Grinstein, S. (2013). Role of phospholipids in endocytosis, phagocytosis, and macropinocytosis. *Physiological Reviews*, 93, 69–106.

Borchers, A. C., Langemeyer, L., & Ungermann, C. (2021). Who's in control? principles of rab gtpase activation in endolysosomal membrane trafficking and beyond. *Journal of Cell Biology*, 220.

Boulais, J., Trost, M., Landry, C. R., Dieckmann, R., Levy, E. D., Soldati, T., Michnick, S. W., Thibault, P., & Desjardins, M. (2010). Molecular characterization of the evolution of phagosomes. *Molecular Systems Biology*, 6, 423.

Brett, C. L., Plemel, R. L., Lobinger, B. T., Vignali, M., Fields, S., & Merz, A. J. (2008). Efficient termination of vacuolar rab gtpase signaling requires coordinated action by a gap and a protein kinase. *The Journal of cell biology*, 182, 1141–1151.

Buckley, C. M., Gopaldass, N., Bosmani, C., Johnston, S. A., Soldati, T., Insall, R. H., & King, J. S. (2016). Wash drives early recycling from macropinosomes and phagosomes to maintain surface phagocytic receptors. *Proceedings of the National Academy of Sciences of the United States of America*, 113, E5906–E5915.

Buckley, C. M., Heath, V. L., Guého, A., Bosmani, C., Knobloch, P., Sikakana, P., Personnic, N., Dove, S. K., Michell, R. H., Meier, R., Hilbi, H., Soldati, T., Insall, R. H., & King, J. S. (2019). Pikfyve/fab1 is required for efficient v-atpase and hydrolase delivery to phagosomes, phagosomal killing, and restriction of legionella infection. *PLoS Pathogens*, 15.

Buczynski, G., Bush, J., Zhang, L., Rodriguez-Paris, J., & Cardelli, J. (1997). Evidence for a recycling role for rab7 in regulating a late step in endocytosis and in retention of lysosomal enzymes in dictyostelium discoideum. *Molecular biology of the cell*, 8, 1343–1360.

Cabezas, A., Pattni, K., & Stenmark, H. (2006). Cloning and subcellular localization of a human phosphatidylinositol 3-phosphate 5-kinase, pikfyve/fab1. *Gene*, 371, 34–41.

Calvo-Garrido, J., King, J. S., Muñoz-Braceras, S., & Escalante, R. (2014). Vmp1 regulates ptdins3p signaling during autophagosome formation in dictyostelium discoideum. *Traffic (Copenhagen, Denmark)*, 15, 1235–1246.

Choy, C. H., Saffi, G., Gray, M. A., Wallace, C., Dayam, R. M., Ou, Z. Y. A., Lenk, G., Puertollano, R., Watkins, S. C., & Botelho, R. J. (2018). Lysosome enlargement during inhibition of the lipid kinase pikfyve proceeds through lysosome coalescence. *Journal of Cell Science*, 131.

Davidson, A. J., King, J. S., & Insall, R. H. (2013). The use of streptavidin conjugates as immunoblot loading controls and mitochondrial markers for use with dictyostelium discoideum. *BioTechniques*, 55, 39–41.

Dayam, R. M., Saric, A., Shilliday, R. E., & Botelho, R. J. (2015). The phosphoinositide-gated lysosomal ca2+ channel, trpml1, is required for phagosome maturation. *Traffic*, 16, 1010–1026.

Dayam, R. M., Sun, C. X., Choy, C. H., Mancuso, G., Glogauer, M., & Botelho, R. J. (2017). The lipid kinase pikfyve coordinates the neutrophil immune response through the activation of the rac gtpase. *Journal of immunology (Baltimore, Md. : 1950)*, 199, 2096–2105.

de Lartigue, J., Polson, H., Feldman, M., Shokat, K., Tooze, S. A., Urbé, S., & Clague, M. J. (2009). Pikfyve regulation of endosome-linked pathways. *Traffic (Copenhagen, Denmark)*, 10, 883–893.

Dolat, L. & Spiliotis, E. T. (2016). Septins promote macropinosome maturation and traffic to the lysosome by facilitating membrane fusion. *The Journal of cell biology*, 214, 517–527.

Dong, X. P., Shen, D., Wang, X., Dawson, T., Li, X., Zhang, Q., Cheng, X., Zhang, Y., Weisman, L. S., Delling, M., & Xu, H. (2010). Pi(3,5)p2 controls membrane traffic by direct activation of mucolipin ca2+ release channels in the endolysosome. *Nature communications*, 1.

Dove, S. K., Dong, K., Kobayashi, T., Williams, F. K., & Michell, R. H. (2009). Phosphatidylinositol 3,5-bisphosphate and fab1p/pikfyve underppin endolysosome function. *The Biochemical journal*, 419, 1–13.

Fey, P., Dodson, R. J., Basu, S., & Chisholm, R. L. (2013). One stop shop for everything dictyostelium: dictybase and the dicty stock center in 2012. *Methods in molecular biology (Clifton, N.J.)*, 983, 59–92.

Francis, C. L., Ryan, T. A., Jones, B. D., Smith, S. J., & Falkow, S. (1993). Ruffles induced by salmonella and other stimuli direct macropinocytosis of bacteria. *Nature 1993 364:6438*, 364, 639–642.

Freeman, S. A., Uderhardt, S., Saric, A., Collins, R. F., Buckley, C. M., Mylvaganam, S., Boroumand, P., Plumb, J., Germain, R. N., Ren, D., & Grinstein, S. (2020). Lipid-gated monovalent ion fluxes regulate endocytic traffic and support immune surveillance. *Science*, 367, 301–305.

Gillooly, D. J., Morrow, I. C., Lindsay, M., Gould, R., Bryant, N. J., Gaullier, J. M., Parton, R. G., & Stenmark, H. (2000). Localization of phosphatidylinositol 3-phosphate in yeast and mammalian cells. *The EMBO Journal*, 19, 4577.

Gotthardt, D., Blancheteau, V., Bosserhoff, A., Ruppert, T., Delorenzi, M., & Soldati, T. (2006). Proteomics fingerprinting of phagosome maturation and evidence for the role of a galpha during uptake. *Molecular and cellular proteomics : MCP*, 5, 2228–2243.

Hamasaki, M., Araki, N., & Hatae, T. (2004). Association of early endosomal autoantigen 1 with macropinocytosis in egf-stimulated a431 cells. *The anatomical record. Part A, Discoveries in molecular, cellular, and evolutionary biology*, 277, 298–306.

Henry, R. M., Hoppe, A. D., Joshi, N., & Swanson, J. A. (2004). The uniformity of phagosome maturation in macrophages. *The Journal of Cell Biology*, 164, 185.

Ikonomov, O. C., Sbrissa, D., & Shisheva, A. (2001). Mammalian cell morphology and endocytic membrane homeostasis require enzymatically active phosphoinositide 5-kinase pikfyve. *The Journal of biological chemistry*, 276, 26141–26147.

Isobe, Y., Nigorikawa, K., Tsurumi, G., Takemasu, S., Takasuga, S., Kofuji, S., & Hazeki, K. (2019). Pikfyve accelerates phagosome acidification through activation of trpml1 while arrests aberrant vacuolation independent of the ca2+ channel. *The Journal of Biochemistry*, 165, 75–84.

Kerr, M. C., Lindsay, M. R., Luetterforst, R., Hamilton, N., Simpson, F., Parton, R. G., Gleeson, P. A., & Teasdale, R. D. (2006). Visualisation of macropinosome maturation by the recruitment of sorting nexins. *Journal of cell science*, 119, 3967–3980.

Kerr, M. C., Wang, J. T., Castro, N. A., Hamilton, N. A., Town, L., Brown, D. L., Meunier, F. A., Brown, N. F., Stow, J. L., & Teasdale, R. D. (2010). Inhibition of the ptdins(5) kinase pikfyve disrupts intracellular replication of salmonella. *The EMBO journal*, 29, 1331–1347.

Kim, G. H., Dayam, R. M., Prashar, A., Terebiznik, M., & Botelho, R. J. (2014). Pikfyve inhibition interferes with phagosome and endosome maturation in macrophages. *Traffic (Copenhagen, Denmark)*, 15, 1143–1163.

Kinchen, J. M. & Ravichandran, K. S. (2010). Identification of two evolutionarily conserved genes regulating processing of engulfed apoptotic cells. *Nature 2010 464:7289*, 464, 778–782.

King, J. S. & Kay, R. R. (2019). The origins and evolution of macropinocytosis. *Philosophical Transactions of the Royal Society B*, 374.

Krishna, S., Palm, W., Lee, Y., Yang, W., Bandyopadhyay, U., Xu, H., Florey, O., Thompson, C. B., & Overholtzer, M. (2016). Pikfyve regulates vacuole maturation and nutrient recovery following engulfment. *Developmental cell*, 38, 536–47.

Langemeyer, L., Borchers, A. C., Herrmann, E., Füllbrunn, N., Han, Y., Perz, A., Auffarth, K., Kümmel, D., & Ungermann, C. (2020). A conserved and regulated mechanism drives endosomal rab transition. *eLife*, 9.

Leray, X., Hilton, J. K., Nwangwu, K., Becerril, A., Mikusevic, V., Fitzgerald, G., Amin, A., Weston, M. R., & Mindell, J. A. (2022). Tonic inhibition of the chloride/proton antiporter clc-7 by pi(3,5)p2 is crucial for lysosomal ph maintenance. *eLife*, 11.

Lima, W. C., Leuba, F., Soldati, T., & Cosson, P. (2012). Mucolipin controls lysosome exocytosis in dictyostelium. *Journal of Cell Science*, 125, 2315–2322.

Lin, X., Yang, T., Wang, S., Wang, Z., Yun, Y., Sun, L., Zhou, Y., Xu, X., Akazawa, C., Hong, W., & Wang, T. (2014). Rilp interacts with hops complex via vps41 subunit to regulate endocytic trafficking. *Scientific Reports*, 4.

Lippuner, C., Paape, D., Paterou, A., Brand, J., Richardson, M., Smith, A. J., Hoffmann, K., Brinkmann, V., Blackburn, C., & Aebischer, T. (2009). Real-time imaging of leishmania mexicana-infected early phagosomes: a study using primary macrophages generated from green fluorescent protein-rab5 transgenic mice. *The FASEB Journal*, 23, 483–491.

Neuhaus, E. M., Almers, W., & Soldati, T. (2002). Morphology and dynamics of the endocytic pathway in dictyostelium discoideum. *Molecular Biology of the Cell*, 13, 1390–1407.

Nicot, A.-S., Fares, H., Payrastre, B., Chisholm, A. D., Labouesse, M., & Laporte, J. (2006). The phosphoinositide kinase pikfyve/fab1p regulates terminal lysosome maturation in caenorhabditis elegans. *Molecular Biology of the Cell*, 17, 3062–3074.

Nordmann, M., Cabrera, M., Perz, A., Bröcker, C., Ostrowicz, C., Engelbrecht-Vandré, S., & Ungermann, C. (2010). The mon1-ccz1 complex is the gef of the late endosomal rab7 homolog ypt7. *Current biology : CB*, 20, 1654–1659.

Ostrowicz, C. W., Bröcker, C., Ahnert, F., Nordmann, M., Lachmann, J., Peplowska, K., Perz, A., Auffarth, K., Engelbrecht-Vandré, S., & Ungermann, C. (2010). Defined subunit arrangement and rab interactions are required for functionality of the hops tethering complex. *Traffic*, 11, 1334–1346.

Paschke, P., Knecht, D. A., Silale, A., Traynor, D., Williams, T. D., Thomason, P. A., Insall, R. H., Chubb, J. R., Kay, R. R., & Veltman, D. M. (2018). Rapid and efficient genetic engineering of both wild type and axenic strains of dictyostelium discoideum. *PLOS ONE*, 13, e0196809.

Poteryaev, D., Datta, S., Ackema, K., Zerial, M., & Spang, A. (2010). Identification of the switch in early-to-late endosome transition. *Cell*, 141, 497–508.

Qiao, Y., Choi, J. E., Tien, J. C., Simko, S. A., Rajendiran, T., Vo, J. N., Delekta, A. D., Wang, L., Xiao, L., Hodge, N. B., Desai, P., Mendoza, S., Juckette, K., Xu, A., Soni, T., Su, F., Wang, R., Cao, X., Yu, J., Kryczek, I., Wang, X. M., Wang, X., Siddiqui, J., Wang, Z., Bernard, A., Fernandez-Salas, E., Navone, N. M., Ellison, S. J., Ding, K., Eskelinen, E. L., Heath, E. I., Klionsky, D. J., Zou, W., & Chinnaiyan, A. M. (2021). Autophagy inhibition by targeting pikfyve potentiates response to immune checkpoint blockade in prostate cancer. *Nature Cancer 2021 2:9*, 2, 978–993.

Racoosin, E. L. & Swanson, J. A. (1993). Macropinosome maturation and fusion with tubular lysosomes in macrophages. *The Journal of cell biology*, 121, 1011–1020.

Rink, J., Ghigo, E., Kalaidzidis, Y., & Zerial, M. (2005). Rab conversion as a mechanism of progression from early to late endosomes. *Cell*, 122, 735–749.

Rupper, A., Grove, B., & Cardelli, J. (2001). Rab7 regulates phagosome maturation in dictyostelium. *J. Cell Sci.*, 109, 1479–1495.

Samie, M., Wang, X., Zhang, X., Goschka, A., Li, X., Cheng, X., Gregg, E., Azar, M., Zhuo, Y., Garrity, A. G., Gao, Q., Slaugenhaupt, S., Pickel, J., Zolov, S. N., Weisman, L. S., Lenk, G. M., Titus, S., Bryant-Genevier, M., Southall, N., Juan, M., Ferrer, M., & Xu, H. (2013). A trp channel in the lysosome regulates large particle phagocytosis via focal exocytosis. *Developmental cell*, 26, 511–524.

Sbrissa, D., Ikonomov, O. C., & Shisheva, A. (2002). Phosphatidylinositol 3-phosphate-interacting domains in pikfyve. *Journal of Biological Chemistry*, 277, 6073–6079.

Schink, K. O., Tan, K. W., Spangenberg, H., Martorana, D., Sneeggen, M., Stévenin, V., Enninga, J., Campsteijn, C., Raiborg, C., & Stenmark, H. (2021). The phosphoinositide coincidence detector phafin2 promotes macropinocytosis by coordinating actin organisation at forming macropinosomes. *Nature Communications 2021 12:1*, 12, 1–17.

Souza, G., Mehta, D., Lammertz, M., Rodriguez-Paris, J., Wu, R., Cardelli, J., & Freeze, H. (1997). Dictyostelium lysosomal proteins with different sugar modifications sort to functionally distinct compartments. *Journal of Cell Science*, 110, 2239–2248.

Stévenin, V., Chang, Y. Y., Toquin, Y. L., Duchateau, M., Gianetto, Q. G., Luk, C. H., Salles, A., Sohst, V., Matondo, M., Reiling, N., & Enninga, J. (2019). Dynamic growth and shrinkage of the salmonella-containing vacuole determines the intracellular pathogen niche. *Cell reports*, 29, 3958–3973.e7.

Tu, H., Wang, Z., Yuan, Y., Miao, X., Li, D., Guo, H., Yang, Y., & Cai, H. (2022). The pripa-tbcra complex-centered rab gap cascade facilitates macropinosome maturation in dictyostelium. *Nature Communications 2022 13:1*, 13, 1–15.

van der Kant, R., Fish, A., Janssen, L., Janssen, H., Krom, S., Ho, N., Brummelkamp, T., Carette, J., Rocha, N., & Neefjes, J. (2013). Late endosomal transport and tethering are coupled processes controlled by rilp and the cholesterol sensor orp1l. *Journal of cell science*, 126, 3462–74.

Veltman, D. M., Akar, G., Bosgraaf, L., & Haastert, P. J. V. (2009). A new set of small, extrachromosomal expression vectors for dictyostelium discoideum. *Plasmid*, 61, 110–118.

Vieira, O. V., Bucci, C., Harrison, R. E., Trimble, W. S., Lanzetti, L., Gruenberg, J., Schreiber, A. D., Stahl, P. D., & Grinstein, S. (2003). Modulation of rab5 and rab7 recruitment to phagosomes by phosphatidylinositol 3-kinase. *Molecular and Cellular Biology*, 23, 2501.

Vines, J. H., Buckley, C. M., Maib, H., Gueho, A., Soldati, T., Murray, D., & King, J. S. (2022). A pi(3,5)p2 probe reveals pikfyve is required for rab7 acquisition and the delivery and fusion of early macropinosomes to phagosomes. *bioRxiv*, (pp. 2022.09.19.508510).

Wang, X., Zhang, X., Dong, X. P., Samie, M., Li, X., Cheng, X., Goschka, A., Shen, D., Zhou, Y., Harlow, J., Zhu, M. X., Clapham, D. E., Ren, D., & Xu, H. (2012). Tpc proteins are phosphoinositide-activated sodium-selective ion channels in endosomes and lysosomes. *Cell*, 151, 372.

Weiner, A., Mellouk, N., Lopez-Montero, N., Chang, Y. Y., Souque, C., Schmitt, C., & Enninga, J. (2016). Macropinosomes are key players in early shigella invasion and vacuolar escape in epithelial cells. *PLOS Pathogens*, 12, e1005602.

Yamamoto, A., DeWald, D. B., Boronenkov, I. V., Anderson, R. A., Emr, S. D., & Koshland, D. (2017). Novel pi(4)p 5-kinase homologue, fab1p, essential for normal vacuole function and morphology in yeast. *https://doi.org/10.1091/mbc.6.5.525*, 6, 525–539.

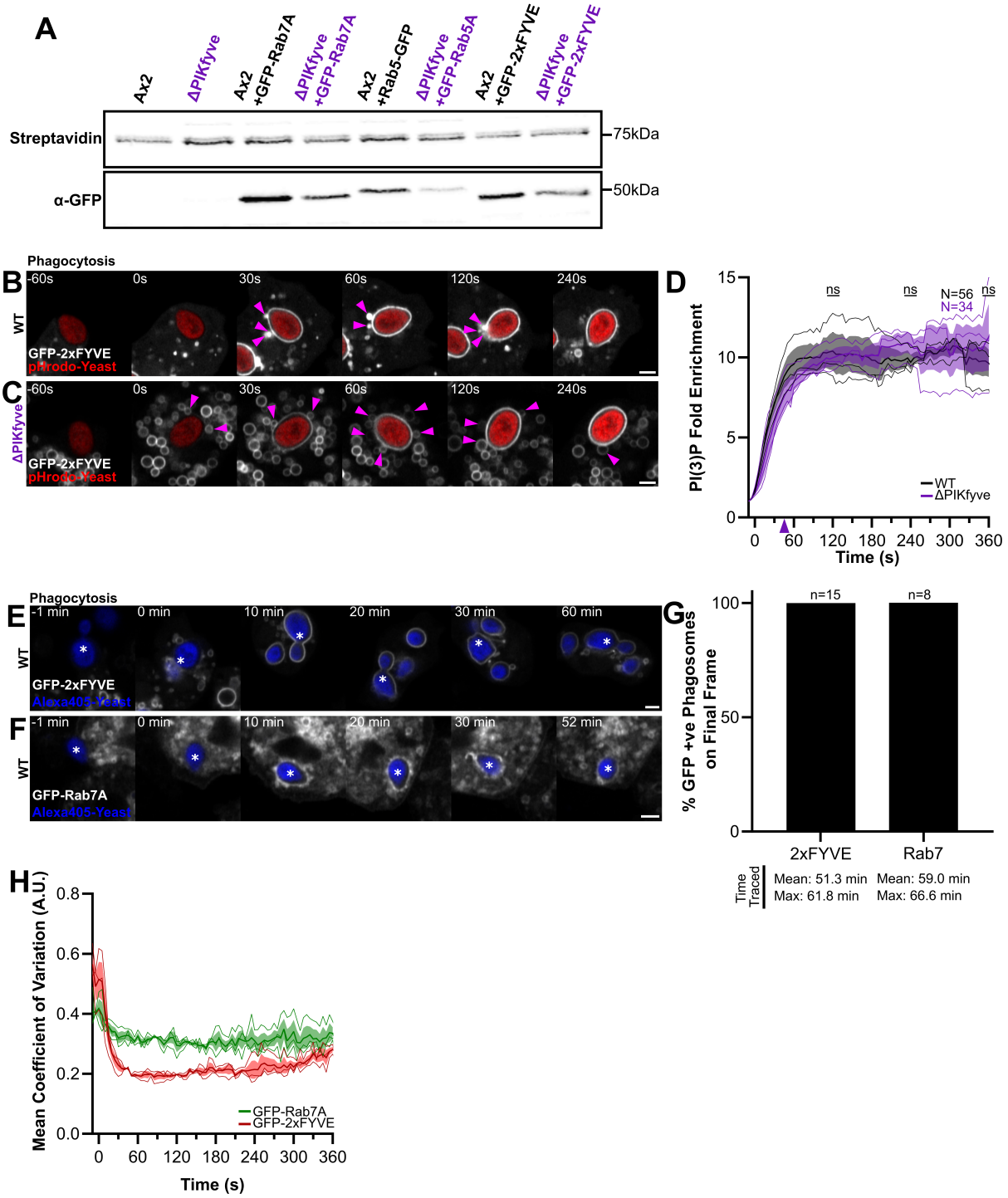

Supplementry Figure 3.S1: **Delivery of reporters to phagosomes and macropinosomes.** **(A)** Expression levels of GFP-reporter levels in wildtype and ΔPIKfyve cells. Western blot of whole cell lysates probed with anti-GFP antibody. Streptavidin staining of endogenously biotinylated proteins used as loading control. **(B)** and **(C)** Representative timelapses of the PI(3)P reporter, GFP-2xFYVE, during phagocytosis of pHrodo-yeast (red) in wildtype and ΔPIKfyve cells. Pink arrows indicate GFP-2xFYVE labelled vesicles clustering around the phagosomal membrane from 30s. GFP-2xFYVE enrichment is quantified in **(D)**. There were no statistically significant differences at any timepoints tested. **(E)** and **(F)** Long-term timelapses of GFP-2xFYVE and GFP-Rab7A recruitment to phagosomes. Both reporters remain associated for at least 1 hour after engulfment. The time each event could be tracked varied due to the point in the timelapse at which engulfment occurred but the proportion of phagosomes still positive for each reporter at the end of each movie is shown in **(G)**. Only those able to be tracked for ¿30 minutes were scored. **(E)** Variation in the fluorescent signal around phagosomes of GFP-2xFYVE, and GFP-Rab7A. The coefficient of variation along a linescan around the phagosome was measured at each time point. Graphs show mean coefficients of variation ± SEM. Variation in GFP-Rab7A signal is greater than 2xFYVE, indicating a patchy distribution. All scale bars = 2 µm.

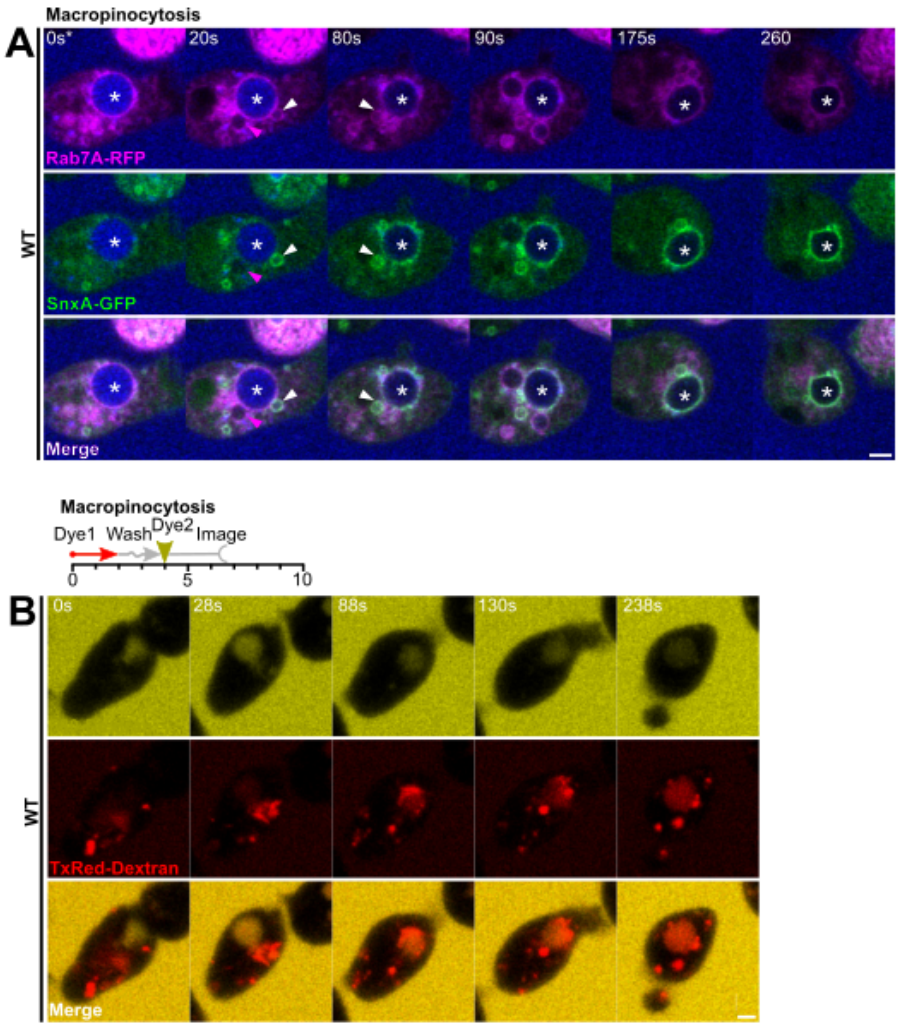

Supplementry Figure 3.S2: **Delivery to Macropinosomes. (A)** Timelapses of RFP-Rab7A (magenta) and SnxA-GFP (green) during macropinocytosis of Alexa405 70kDa dextran in wildtype cells. SnxA and Rab7 co-localize on many clustering vesicles (arrowheads). **(B)** Timelapse of cells after sequential pulses of TxRed and FITC dextran. The older macropinosomes (red) can be seen fusing and mixing contents with a newly formed macropinosome (yellow). All scale bars = 2 µm.

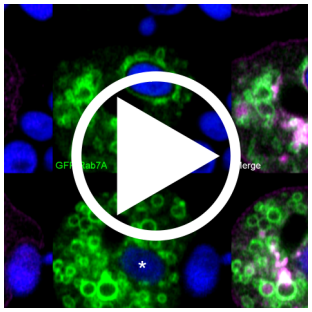

Video 3.1: Simultaneous imaging of RFP-Rab5A and GFP-Rab7A recruitment to phagosomes in wild-type (top) and ΔPIKfyve(bottom) cells. Scale bar = 2 µm

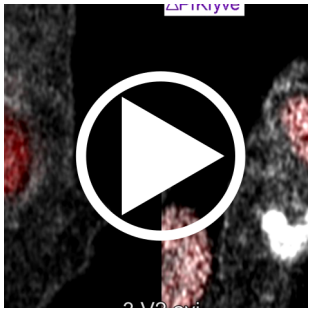

Video 3.2: GFP-Rab5A dynamics at phagosomes in both wildtype (left) and ΔPIKfyve(right) cells. Scale bar = 2 µm

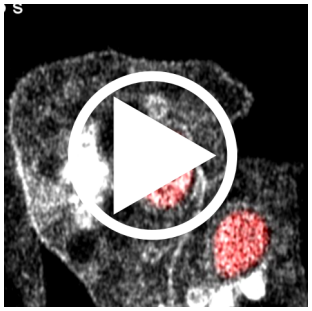

Video 3.3: Enrichment of GFP-Rab5A at phagocytic cups. Multiple failed attempts to complete engulfment of a pHrodo labelled yeast demonstrate that GFP-Rab5A is enriched at the cup before internalisation completes. Scale bar = 2 µm

Video 3.4: PI(3)P dynamics at phagosomes in both wildtype (left) and ΔPIKfyve(right) cell. Cells expressing GFP-2xFYVE reporter for PI(3)P. Scale bar = 2 µm

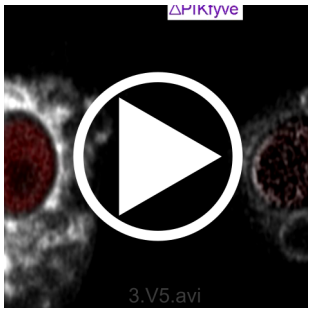

Video 3.5: GFP-Rab7A dynamics at phagosomes in both wildtype (left) and ΔPIKfyve(right) cells. Scale bar = 2 µm

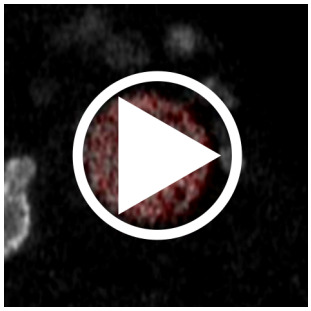

Video 3.6: PI(3,5) P_2 dynamics during phagosome maturation. Wildtype cells expressing the SnxA-GFP probe for PI(3,5) P_2. Note small vesicles clustering before membrane enrichment. Scale bar = 2 µm

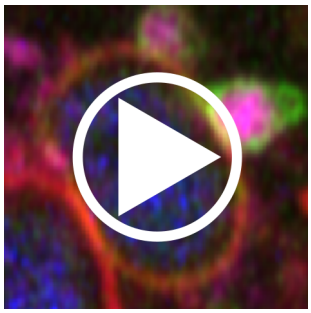

Video 3.7: Texas Red dextran labelled macropinosomes (red) being delivered to yeast containing phagosomes (blue) in cells expressing GFP-SnxA (green) and RFP-2xFYVE (magenta). Note the docking of a Rab7/PI(3)P-positive macropinosome with phagosome. Scale bar = 2 µm

Chapter 4

Discussion

Many of the key aspects for discussion arising from this work have already been covered within the manuscripts above; however, because they are for publication these discussions are fairly conservative in nature. The following discussion expands upon some of the points above, considers more speculative ideas arising from the work, and discusses potential next steps to progress the work further. For this reason, there are some minor repetitions between this discussion and those above. **Figure 1.5** and **Figure 1.6** may be useful in providing a pictorial overview of the maturation process.

4.1 The Characterisation of a PI(3,5) P_2 Probe

By screening PX-domain containing *D. discoideum* proteins, we identified and characterised two related PI(3,5) P_2 binding probes, SnxA-GFP and 2xPX-GFP. *In vitro*, both probes proved specific for PI(3,5) P_2, binding with high affinity even at relatively low PIP concentrations (**Figure 2.2**). Both probes localized to phagosomes and macropinosomes in live *D. discoideum*, and SnxA does not appear to disrupt normal macroendosome trafficking (**Figure 2.4** and **Figure 2.S2**). We observed no major off-target effects of expressing the probes in *D. discoideum*, and the lack of identifiable phenotypes in ΔSnxA cells is also indicative that the protein may only have a minor function (**Figure 2.S3**). A humanized version of the SnxA probe also localized to macropinosomes in HEK293, MIA PaCa-2 and RPE-1 cells, demonstrating its broad applicability in a range of cell types (**Figure 2.3**).

Like most molecular biosensors, both probes have limitations, however. For example, HEK293 and REP-1 cells were very sensitive to 2xPX-GFP expression resulting in poor localization, and in fixed cells the SnxA-GFP probe exhibited significant plasma membrane binding. Fortunately, these limitations can be mitigated by properly evaluating each probes before use in specific cell lines. It would have been preferable to test both probes in mammalian cells further. Trialling a range of transfection conditions may have identified an optimal expression level for the 2xPX-GFP probe in sensitive cells. Furthermore, using an alternative fixation method, less disruptive to intracellular vesicles, may have reduced the level of SnxA-GFP plasma membrane binding in fixed cells. Despite these caveats both probes have demonstrated a specificity for PI(3,5) P_2, and reliable localization across a range of cell types.

How do PI(3,5) P_2 and PIKfyve behave on macroendosomes? Examination of PIKfyve localization alongside our PI(3,5) P_2 reporter revealed an unexpected complexity in PIKfyve regulation. Despite poor expression of the probe, we robustly observed that PIKfyve-GFP was removed from macroendosomal membrane a few minutes after internalization (**Figure 2.S5**), and moreover, only fleetingly co-localized with PI(3,5) P_2(**Figure 2.5**).

PIKfyve is a large 299kDa protein, for this reason previous attempts to tag the protein in King Lab had proven unsuccessful. Here, we cloned sections of the *PIKfyve* gene into the pDM expression system via a TOPO cloning plasmid. While this did *eventually* work, PIKfyve-GFP expresses poorly in wild-type cells, and expression in ΔPIKfyve cells is only marginally better (**Figure 2.S5**). Expression levels are inconsistent between cells, making quantification of many cells challenging.

Given the findings of this project, a Fig4 fusion protein for expression in *D. discoideum* would be desirable. In fact, both binding partners of PIKfyve, Fig4 and Vac14, were successfully N- and C terminally tagged using the pDM expression system (data not shown); however, both express extremely poorly in wild-type and ΔPIKfyve *D. discoideum*. This is unfortunate, as Fig4 localization would have assisted our conclusions on PIKfyve regulation.

It is possible an integrating vector for all three probes may improve their expression levels in cells. Alternatively, in the future, using a HaloTag fusion protein and a synthetic fluorescent ligand may help improve PIKfyve contrast if necessary.

Why is PIKfyve removed from macroendosomal membranes? PIKfyve is unusual, as its catalytic substrate (PI(3)P) also mediates its recruitment. Whilst PIKfyve could be released from the membrane by simply using up all the PI(3)P (Kerr et al., 2010), this cannot be the case in *D. discoideum* as PI(3)P is retained on phagosomes after PIKfyve dissociates (**Figure 3.S1**). Thus, other regulation must exist. Additionally, because PIKfyve is also in complex with its own phosphatase, Fig4 (which can breakdown PI(3,5) P_2 into PI(3)P), maintenance of the complex on the macroendosomal membrane for too long would likely lead to fruitless cycles of phosphorylation and de-phosphorylation. The crystal structure of the PIKfyve complex suggests that PIKfyve can be inhibited by auto-phosphorylation, requiring a protein dephosphorylation activity of Fig4 for activation (Lees et al., 2020). Fig4 may therefore be temporally regulated during phagosome maturation, or an additional unknown regulatory mechanism may exist.

Our observations that PIKfyve normally dissociates as soon as PI(3,5) P_2 accumulates but is retained if pharmacologically inactivated indicates that catalytic activity also affects membrane association. Catalytically inactive PIKfyve is also retained on macropinosomes in mammalian cells (Kerr et al., 2010). Whilst the FYVE domain is not well resolved in the crystal structure, it is suggested to lie near the kinase domain (Lees et al., 2020). This may provide potential for an additional level of regulation to explain the coordination of recruitment and activity *in vivo*, but this requires more investigation.

Is PI(3,5) P_2 synthesised or delivered? A second key observation was that PI(3,5) P_2 is delivered to macroendosomes via small PI(3,5) P_2-positive macropinosomes which cluster immediately before its enrichment (**Figure 3.4** and **Figure 3.5**). These macropinosomes do not appear to co-localize with

PIKfyve-GFP. When we first identified this phenomenon, the origin of these vesicles was unclear to us. Only through observations of other endosomal markers did we consider they may be a form of macropinosome.

We have been unable to see enrichment of PI(3,5) P_2 on macroendosomal membranes before PI(3,5) P_2 delivery via small macropinosome. PIKfyve, however, is present on macroendosomal membranes well before this delivery step. We speculate at least some amount of PI(3,5) P_2 must be synthesised on the macroendosomal membrane before delivery. It may be that our probes are not sensitive enough to detect very small amounts of PI(3,5) P_2. Whether macroendosomes could accumulate significant levels of PI(3,5) P_2 without macropinosome fusion is also unclear. In the future, finding a way to either inhibit fusion without inhibiting PIKfyve may help determine this balance. It is possible that levels of PI(3,5) P_2 are needed on both membranes to promote fusion (Leray et al., 2022; Samie et al., 2013; Wang et al., 2012; Dong et al., 2010). It's also possible that the PIKfyve complex itself may mediate tethering with other PI(3,5) P_2 positive compartments once it has synthesised enough PI(3,5) P_2 on the target membrane.

4.2 The Regulators of Macroendosome Maturation

The latter part of this work focuses on a central pathway which regulates the early stages of phagosome and macropinosome maturation. We characterise this pathway by overexpression of Rab5, Rab7 and PIKfyve GFP-fusions, and probes localizing to PI(3)P and PI(3,5) P_2(**Figure 4.1 A+B**). In wild-type *D. discoideum* we show Rab5 marks the forming and nascent phagosome. Its enrichment is shortly followed by synthesis of PI(3)P, likely through Rab5-dependant activation of Vps34, and delivery of PI(3)P from endosomes within 30-seconds of engulfment. PIKfyve arrives at a similar time, likely through FYVE domain-mediated binding to PI(3)P. Following this, small Rab7-positive vesicles cluster around the phagosome and Rab7 gradually begins to enrich on the phagosomal membrane over the next 360-seconds. Rab5 is removed of the membrane within the first 60-seconds of this enrichment, and PI(3,5) P_2 is synthesised and delivered about 120-seconds later. PI(3,5) P_2 co-localizes only fleetingly with PIKfyve before it is removed. PI(3,5) P_2 remains on phagosomal membranes for approximately 20-minutes, whereas Rab7 and PI(3)P remain for upwards of 50-minutes.

Is this pathway conserved with other endocytotic routes? While our conclusions stem mostly from phagocytosis data, it is likely that our findings are applicable to other endocytotic pathways. Our pulse-chase data (**Figure 2.4 A-B** and **Figure 3.3 A-B**) indicate that all probes arrive with similar dynamics to maturing macropinosomes, although both PI(3)P and PI(3,5) P_2 clearly dissociate much quicker. The pulse chase data is further supported by movies following individual macropinosome (**Figure 3.S2 A** and unpublished).

The key difference between macropinosome and phagosome dynamics was the delayed dissociation of PI(3)P and PI(3,5) P_2 from phagosomes. Bacteria containing phagosomes also have earlier PI(3)P retrieval in *D. discoideum* (Clarke et al., 2010), suggesting the type of cargo (not the type of endosome) may have the greatest impact on maturation dynamics. This has some logic: yeast-containing-phagosomes

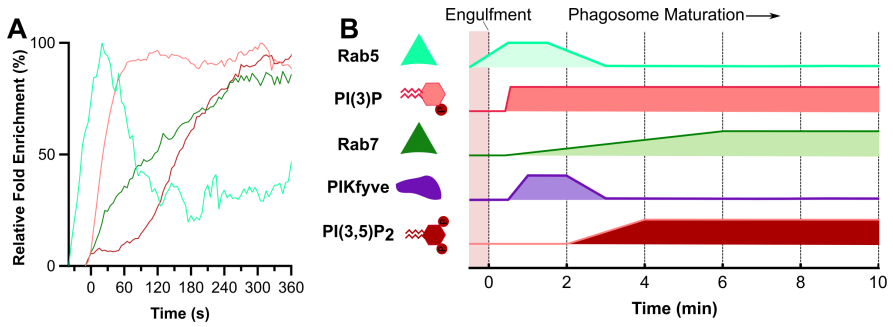

Figure 4.1: **Phagosomal Enrichment Summary.** **(A)** Combination of wildtype data from **Figure 2.4 C**, **Figure 3.2 C,F** and **Figure 3.S1 D**, normalized from 0% to 100% localization for each marker. A simplified version is displayed in **(B)**.

are much larger than either bacteria-containing phagosomes or macropinosomes. They may require a prolonged maturation period to acidify such a large compartment or to digest the large amount of material. Whether bacteria-containing-phagosomes also have a shorter PI(3,5) P_2 enrichment time remains to be tested.

It is likely that at least some of our observations are also applicable to other endocytic routes, such as the maturation of smaller endosomes. In mammalian cells, clathrin mediated endosomes also transition from a Rab5/PI(3)P-positive early form to a later Rab7-positive form following fusion with lysosomal compartments. In our experiments, however, we saw no identifiable SnxA-GFP or PIKfyve-GFP enrichment to small compartments analogous to microendosomes. This may indicate a difference in maturation at this scale, or possibly the sensitivity of our probes is not sufficient to see these small ~100 nm compartments which are technically challenging to study in the detail.

How does PIKfyve disruption affect the pathway? The maturation of phagosomes is severely disrupted in ΔPIKfyve *D. discoideum*. While Rab5 and PI(3)P dynamics remain unchanged, Rab7 fails to accumulate fully on phagosomal membranes and PI(3,5) P_2 is not synthesised or delivered. The Rab7/V-ATPase-vesicles which normally cluster around wild-type phagosomes remain Rab7/V-ATPase-positive, but become enlarged and fail to cluster nascent phagosomes in ΔPIKfyve cells. This provides some explanation for the reduced phagosome acidification and proteolysis profiles we previously observe in these cells (Buckley et al., 2019).

Alongside our data on PIKfyve localization, our data support a model whereby PIKfyve is regulated in a series of coordinated steps: (1) inactive PIKfyve is recruited by binding PI(3)P, (2) acute activation of PIKfyve and PI(3,5) P_2 accumulation, (3) fusion of additional PI(3,5) P_2- containing vesicles, (4) PIKfyve dissociation, dependent on its own activity.

The failure of phagosomes to accumulate Rab7 upon PIKfyve disruption could be either a cause or a symptom of maturation defects. Rab7 is a key lysosomal marker important for lysosome fusion. In yeast, the Rab7 homolog, Ypt7, directly interacts with the HOPS complex to mediate endolysosomal

fusion (Ostrowicz et al., 2010; Brett et al., 2008). A similar, less direct interaction between Rab7 and HOPS occurs in higher eukaryotes through the Rab7 effector RILP(Lin et al., 2014; Kant et al., 2015). Furthermore, disruption of Rab7A in *Dictyostelium* results in sever defects in lysosomal activity and delivery of premature lysosomal enzymes (Rupper et al., 2001a).

Importantly, however, Rab7A is not completely absent from phagosomal membranes when PIKfyve is disrupted. This implies some Rab7A is still able to arrival independently of PIKfyve - perhaps from a cytosolic pool - but it cannot enrich because fusion with other Rab7 compartments is somehow blocked in ΔPIKfyve cells. If Rab7 is important for later fusion events, this blockage would result in a negative feedback loop, whereby reduced Rab7 early results in reduced fusion with Rab7-endosomes later.

The mechanism through which PI(3,5) P_2 reduction causes prohibition of Rab7A-mediated fusion remain unclear, however. One possibility is that PI(3,5) P_2 is required on both membranes to promote fusion, possibility through activation of a ligand gated ion channel (Leray et al., 2022; Samie et al., 2013; Wang et al., 2012; Dong et al., 2010).

Another possibility, is that the increased size of macropinosomes in ΔPIKfyve cells negatively impacts fusogenicity. It is possible that artificially reducing the size of the macropinosomes in ΔPIKfyve cells may restore macropinosome/phagosome fusion. This could be tested in mammalian cells, where overexpression or hyper-activation of the TRPML1 channel eliminates the swollen endosome phenotype (Dong et al., 2010). Unfortunately, as the TRPML orthologue in *D. discoideum* appears to be independent of PIKfyve (Lima et al., 2012) there is no known way to rescue this phenotype in *D. discoideum* without also restoring PI(3,5) P_2.

Interestingly, macropinosome proteolysis was unchanged in ΔPIKfyve cells and Rab7 levels appeared normal. This highlights a previously unappreciated difference between macropinosomes and phagosomes. Again, to understand the cause of this difference it is important to examine Rab7 enrichment to other endosome types during PIKfyve disruption. If bacteria-containing phagosomes show the same phenotype, then this is possibly mediated through ligand binding regulation of Rab7A enrichment may be more related to size.

Is this pathway conserved in other cell types? While a core of phagosomal proteins is shared between *D. discoideum* and higher eukaryotes (Boulais et al., 2010), this study exposes several differences within the maturation pathway. From early on, we saw Rab5 localizing much earlier than previously described in mammalian cells (Lippuner et al., 2009), and its transition with Rab7 occurs much quicker in *D. discoideum* (Henry et al., 2004). This may suggest the speed of PI(3,5) P_2 acquisition is also much faster in these cells. Furthermore, several well characterised regulators, such as the Rab5-interacting protein EEA1 and the Rab7-interacting protein RILP, are absent from the *D. discoideum* genome, making it harder to draw direct comparison with mammalian cells. Nonetheless, the roles of Rab5, Rab7, PIKfyve and PI(3,5) P_2 are likely conserved between cell types.

4.3 The Mixing of Macropinosomes and Phagosomes

Above we present evidence that phagosomes/macropinosome mixing requires PIKfyve activity. These macropinosomes are less than 8-minutes old and are Rab7/V-ATPase/PI(3)P/PI(3,5) P_2-positive. They only fuse with the phagosomes after around 120-second post-engulfment, around the same time as PI(3,5) P_2 acquisition. It is likely these retrograde fusion events enable the rapid delivery of a large volume of hydrolases, V-ATPase, and other digestive machinery to newly internalized vesicles, which is particularly important for both macropinosomes and phagosomes due to their large size and low surface area-to-volume ratio.

It is not clear whether phagosome/macropinosome mixing happens with all cargo. It is possible that smaller, bacteria-containing-phagosomes, do not have the same requirement for fusion due to their decreased size. Detecting fusion in such a small phagosomes may be technically challenging; although, by employing a SNAP-tag-like system it may be possible for bacteria to be selectively fluorescent upon mixing with dextran.

The extent to which this fusion happens in other cell lines in unclear. Many professional phagocytes also maintain high levels of macropinocytosis (Reviewed in: Lim & Gleeson, 2011), but *D. discoideum* perform much more phagocytosis and have much faster killing, so phagosome/macropinosome fusion may not be as important in other cells. True wild-type *D. discoideum*(NC4 or DdB non-axenic strains) have much lower macropinocytic uptake Ax2 lab strain (Bloomfield et al., 2015). Thus, it would be possible to test whether the reduction in macropinocytic material reduced the efficiency of phagosome maturation between these two cell types.

Another interesting question is whether large macropinosomes can ever fuse with a phagosomes. **Figure 3.S2** demonstrates small macropinosomes clustering a large macropinosome, but we never witnessed macropinosomes that large clustering one another. This could suggest the cell has some way to detect a macropinosomes size and determine is suitability for fusion. Of course, this is linked with ΔPIKfyve, as these macropinosomes fail to shrink.

4.4 The Automated Image Analysis Pipeline

Despite its relatively minor appearance in the manuscripts above, the creation of an automated image analysis pipeline made up a sizeable part of this work. Its implementation allowed for an effective and unbiased approach to quantify the enrichment of fluorescence probes around yeast-containing-phagosomes, and it was further adapted to examine macropinosome clustering also.

The pipeline does possess some limitations, however. It is currently limited to the analysis of larger phagosomal particles. Efforts to adapt the pipeline for smaller bacterial sized particles were not successful due their decreased size and increased number. The smaller a particle becomes the more likely it is to move out of focus and be lost. Likewise, attempts to automatically track macropinosomes proved fruitless due to their ever decreasing size and variability in fluorescent dextran levels over time.

While the pipeline successfully accounts for multiple fluorescent markers, the variability in expression

levels between dual-expression vectors, problems with RFP-photobleaching, and interference of probes with one another meant this dual quantification proved unreliable in comparison to single colour GFP quantification. Additionally, poor quality probes, such a PIKfyve-GFP, produced highly variable results which could not be used.

A lot of these issues could have potentially been solved by employing a machine learning model (Reviewed in: Moen et al., 2019). This could have made the pipeline far more adaptable to a broader range of experiments and less error prone. If 3D-particle particle tracking could also have been implemented this would have prevented particles being lost from going out of focus - although, this would have been inordinately more complicated.

Despite these issues, the pipeline has been successfully used throughout this work to quantify and collate data from a large number of phagocytosis events, which would have otherwise been very difficult to do.

4.5 The Future

From discussion points above a few areas for further investigation standout.

Firstly, further characterisation the SnxA and 2xPX probes in mammalian cell lines would aid in their validation as generalized PI(3,5) P_2 reporters. Expression in phagocytic cells would be especially insightful and may aid comparisons with the *D. discoideum* data if enough events could be captured for use with the automated image analysis pipeline.

Secondly, further characterising how different cargoes affect key maturation markers in both wildtype and ΔPIKfyve *D. discoideum* is important. Both of the manuscripts above are limited in only examining yeast containing phagosomes or dextran containing macropinosomes. To find out if our findings can be applied more generally to other endocytic pathways, broadening this range to include bacteria and beads would be beneficial. It would also be interesting to see if the probes ever bound to microendosomes, which may perhaps only be detectable *in vitro*.

Thirdly, finding more interacting partners of PIKfyve or SnxA could be useful in aiding our understanding of the pathway. I have already performed a GFP-trap experiment using the *D. discoideum* PIKfyve-GFP and SnxA-GFP proteins to determine interacting proteins. Unfortunately, due to unforeseeable delays at the mass spectrometry facility, the data was not available to analyse in time for this publication. Nevertheless, once this data is available, it could help provide some useful hits for further investigation.

It would be interesting to examine the roles of HOPS and CORVET in *D. discoideum*. Attempts were made to generate knockout cell lines of both, but we had issues with CRISPR/Cass9 knockout selection (unpublished). We also overexpressed fusion proteins of Vps39 and Vps41, components of the *D. discoideum* CORVETTE complex; however, these expressed poorly and did not localize to phagosomes. Characterization of HOPS recruitment in particular, alongside Rab7A in wildtype and ΔPIKfyve cell lines would be especially insightful and could provide an explanation for vesicle tethering and fusion.

Finally, further investigating the nature of PIKfyve activity and regulation would be interesting.

Others have already created PIKfyve kinase dead mutation in mammalain cells and yeast (Sbrissa et al., 2000; Gary et al., 1998), and we have already begun cloning for *D. discoideum*. The pinnacle would be recapitulation of the whole PIKfyve complex *in vitro* to examine the requirements for PI(3,5) P_2 synthesis.

4.6 Summary

In conclusion, this work provides novel insights into the complex sequence of events that occur during phagosome maturation and sheds light on the critical role of PIKfyve and PI(3,5) P_2 in this process. By utilizing a *Dictyostelium* SnxA reporter and characterising its PX-domain as the key component of PI(3,5) P_2 binding, we have observed PI(3,5) P_2 dynamics in live cells for the first time. In *D. discoideum* we have demonstrated PI(3,5) P_2's involvement in the regulation of phagosomal maturation and linked PIKfyve activity to phagosomal acquisition of Rab7 and fusion with macropinosomes, which we hypothesise drive efficient macroendosomal maturation. Our findings also highlight unexpected difference between macropinosomes and phagosome, uncovering potential new avenues for enquiry. Overall, our study represents an important step towards understanding the fundamental mechanisms underlying endosome maturation and the sequence of steps through which PIKfyve and PI(3,5) P_2 help to coordinate the endolysosomal system.

Chapter 5

Bibliography

Aderem, A. & Underhill, D. M. (2003). Mechanisms of phagocytosis in macrophages. *https://doi.org/10.1146/annurev.immunol.17.1.593*, 17, 593–623.

Adessi, C., Chapel, A. G., Vincon, M., Rabilloud, T., Klein, G., Satre, M., & Garin, J. (1995). Identification of major proteins associated with dictyostelium discoideum endocytic vesicles. *undefined*.

Aubry, L., Klein, G., Martiel, J.-L., & Satre, M. (1993). Kinetics of endosomal ph evolution in dictyostelium discoideum amoebae. study by fluorescence spectroscopy. *Journal of Cell Science*, 105 (Pt 3), 861–6.

Banerjee, S., Clapp, K., Tarsio, M., & Kane, P. M. (2019). Interaction of the late endo-lysosomal lipid pi(3,5)p2 with the vph1 isoform of yeast v-atpase increases its activity and cellular stress tolerance. *Journal of Biological Chemistry*, 294, 9161–9171.

Barisch, C., Kalinina, V., Lefrançois, L. H., Appiah, J., López-Jiménez, A. T., & Soldati, T. (2018). Localization of all four znt zinc transporters in dictyostelium and impact of znta and zntb knockout on bacteria killing. *Journal of Cell Science*, 131.

Barisch, C., Paschke, P., Hagedorn, M., Maniak, M., & Soldati, T. (2015). Lipid droplet dynamics at early stages of mycobacterium marinum infection in dictyostelium. *Cellular microbiology*, 17, 1332–1349.

Basnyat, B., Qamar, F. N., Rupali, P., Ahmed, T., & Parry, C. M. (2021). Enteric fever. *BMJ*, 372.

Bengtsson, T., Jaconi, M., Gustafson, M., Magnusson, K., Theler, J., Lew, D., & Stendahl, O. (1993). Actin dynamics in human neutrophils during adhesion and phagocytosis is controlled by changes in intracellular free calcium. *Eur J Cell Biol.*, 62, 49–58.

Bennett, N., Letourneur, F., Ragno, M., & Louwagie, M. (2008). Sorting of the v-snare vamp7 in dictyostelium discoideum: a role for more than one adaptor protein (ap) complex. *Experimental cell research*, 314, 2822–2833.

Bharat, T. A., Malsam, J., Hagen, W. J., Scheutzow, A., Söllner, T. H., & Briggs, J. A. (2014). Snare and regulatory proteins induce local membrane protrusions to prime docked vesicles for fast calcium-triggered fusion. *EMBO reports*, 15, 308–314.

Bloomfield, G., Tanaka, Y., Skelton, J., Ivens, A., & Kay, R. R. (2008). Widespread duplications in the genomes of laboratory stocks of dictyostelium discoideum. *Genome Biology*, 9, R75.

Bloomfield, G., Traynor, D., Sander, S. P., Veltman, D. M., Pachebat, J. A., & Kay, R. R. (2015). Neurofibromin controls macropinocytosis and phagocytosis in dictyostelium. *eLife*, 4.

Bogdanovic, A., Bennett, N., Kieffer, S., Louwagie, M., Morio, T., Garin, J., Satre, M., & Bruckert, F. (2002). Syntaxin 7, syntaxin 8, vti1 and vamp7 (vesicle-associated membrane protein 7) form an active snare complex for early macropinocytic compartment fusion in dictyostelium discoideum. *The Biochemical journal*, 368, 29–39.

Bohdanowicz, M. & Grinstein, S. (2013). Role of phospholipids in endocytosis, phagocytosis, and macropinocytosis. *Physiological Reviews*, 93, 69–106.

Bonner, J. T. & Savage, L. J. (1947). Evidence for the formation of cell aggregates by chemotaxis in the development of the slime mold dictyostelium discoideum. *The Journal of experimental zoology*, 106, 1–26.

Borchers, A. C., Langemeyer, L., & Ungermann, C. (2021). Who's in control? principles of rab gtpase activation in endolysosomal membrane trafficking and beyond. *Journal of Cell Biology*, 220.

Bosmani, C., Bach, F., Leuba, F., Hanna, N., Burdet, F., Pagni, M., Hagedorn, M., & Soldati, T. (2019). Dictyostelium discoideum flotillin homologues are essential for phagocytosis and participate in plasma membrane recycling and lysosome biogenesis. *biorxiv*.

Boulais, J., Trost, M., Landry, C. R., Dieckmann, R., Levy, E. D., Soldati, T., Michnick, S. W., Thibault, P., & Desjardins, M. (2010). Molecular characterization of the evolution of phagosomes. *Molecular Systems Biology*, 6, 423.

Brett, C. L., Plemel, R. L., Lobinger, B. T., Vignali, M., Fields, S., & Merz, A. J. (2008). Efficient termination of vacuolar rab gtpase signaling requires coordinated action by a gap and a protein kinase. *The Journal of cell biology*, 182, 1141–1151.

Bridges, D., Ma, J.-T., Park, S., Inoki, K., Weisman, L. S., & Saltiel, A. R. (2012). Phosphatidylinositol 3,5-bisphosphate plays a role in the activation and subcellular localization of mechanistic target of rapamycin 1. *Molecular Biology of the Cell*, 23, 2955–2962.

Bucci, C., Parton, R. G., Mather, I. H., Stunnenberg, H., Simons, K., Hoflack, B., & Zerial, M. (1992). The small gtpase rab5 functions as a regulatory factor in the early endocytic pathway. *Cell*, 70, 715–28.

Buckley, C. M. (2018). Macropinocytosis and phagocytosis in the social amoeba dictyosterlium discoideum.

Buckley, C. M., Gopaldass, N., Bosmani, C., Johnston, S. A., Soldati, T., Insall, R. H., & King, J. S. (2016). Wash drives early recycling from macropinosomes and phagosomes to maintain surface phagocytic receptors. *Proceedings of the National Academy of Sciences of the United States of America*, 113, E5906.

Buckley, C. M., Heath, V. L., Guého, A., Bosmani, C., Knobloch, P., Sikakana, P., Personnic, N., Dove, S. K., Michell, R. H., Meier, R., Hilbi, H., Soldati, T., Insall, R. H., & King, J. S. (2019). Pikfyve/fab1 is required for efficient v-atpase and hydrolase delivery to phagosomes, phagosomal killing, and restriction of legionella infection. *PLoS Pathogens*, 15.

Buczynski, G., Bush, J., Zhang, L., Rodriguez-Paris, J., & Cardelli, J. (1997). Evidence for a recycling role for rab7 in regulating a late step in endocytosis and in retention of lysosomal enzymes in dictyostelium discoideum. *Molecular biology of the cell*, 8, 1343–1360.

Buracco, S., Peracino, B., Andreini, C., Bracco, E., & Bozzaro, S. (2018). Differential effects of iron, zinc, and copper on dictyostelium discoideum cell growth and resistance to legionella pneumophila. *Frontiers in Cellular and Infection Microbiology*, 7, 536.

Bush, J., Temesvari, L., Rodriguez-Paris, J., Buczynski, G., & Cardelli, J. (1996). A role for a rab4-like gtpase in endocytosis and in regulation of contractile vacuole structure and function in dictyostelium discoideum. *Molecular Biology of the Cell*, 7, 1623–1638.

Cabezas, A., Pattni, K., & Stenmark, H. (2006). Cloning and subcellular localization of a human phosphatidylinositol 3-phosphate 5-kinase, pikfyve/fab1. *Gene*, 371, 34–41.

Cai, X., Xu, Y., Cheung, A. K., Tomlinson, R. C., Alcázar-Román, A., Murphy, L., Billich, A., Zhang, B., Feng, Y., Klumpp, M., Rondeau, J.-M., Fazal, A. N., Wilson, C. J., Myer, V., Joberty, G., Bouwmeester, T., Labow, M. A., Finan, P. M., Porter, J. A., Ploegh, H. L., Baird, D., Camilli, P. D., Tallarico, J. A., & Huang, Q. (2013). Pikfyve, a class iii pi kinase, is the target of the small molecular il-12/il-23 inhibitor apilimod and a player in toll-like receptor signaling. *Chemistry and Biology*, 20, 912–21.

Calcraft, P. J., Ruas, M., Pan, Z., Cheng, X., Arredouani, A., Hao, X., Tang, J., Rietdorf, K., Teboul, L., Chuang, K. T., Lin, P., Xiao, R., Wang, C., Zhu, Y., Lin, Y., Wyatt, C. N., Parrington, J., Ma, J., Evans, A. M., Galione, A., & Zhu, M. X. (2009). Naadp mobilizes calcium from acidic organelles through two-pore channels. *Nature*, 459, 596–600.

Carlton, J., Bujny, M., Rutherford, A., & Cullen, P. (2005a). Sorting nexins - unifying trends and new perspectives. *Traffic*, 6, 75–82.

Carlton, J. G., Bujny, M. V., Peter, B. J., Oorschot, V. M., Rutherford, A., Arkell, R. S., Klumperman, J., McMahon, H. T., & Cullen, P. J. (2005b). Sorting nexin-2 is associated with tubular elements of the early endosome, but is not essential for retromer-mediated endosome-to-tgn transport. *Journal of cell science*, 118, 4527.

Carnell, M., Zech, T., Calaminus, S. D., Ura, S., Hagedorn, M., Johnston, S. A., May, R. C., Soldati, T., Machesky, L. M., & Insall, R. H. (2011). Actin polymerization driven by wash causes v-atpase retrieval and vesicle neutralization before exocytosis. *Journal of Cell Biology*, 193, 831–839.

Chang, F.-S., Wang, Y., Dmitriev, P., Gross, J., Galione, A., & Pears, C. (2020). A two-pore channel protein required for regulating mtorc1 activity on starvation. *BMC Biology*, 18.

Chapman-Andresen, C. (1984). The early days of pinocytosis. *Carlsberg Research Communications*, 49, 179–186.

Chen, Z., Malia, P. C., Hatakeyama, R., Nicastro, R., Hu, Z., Péli-Gulli, M. P., Gao, J., Nishimura, T., Eskes, E., Stefan, C. J., Winderickx, J., Dengjel, J., Virgilio, C. D., & Ungermann, C. (2021). Torc1 determines fab1 lipid kinase function at signaling endosomes and vacuoles. *Current Biology*, 31, 297–309.e8.

Cheng, X., Shen, D., Samie, M., & Xu, H. (2010). Mucolipins: Intracellular trpml1-3 channels. *FEBS letters*, 584, 2013.

Chithrani, B. D., Ghazani, A. A., & Chan, W. C. (2006). Determining the size and shape dependence of gold nanoparticle uptake into mammalian cells. *Nano Letters*, 6, 662–668.

Christoforidis, S., Miaczynska, M., Ashman, K., Wilm, M., Zhao, L., Yip, S.-C., Waterfield, M. D., Backer, J. M., & Zerial, M. (1999). Phosphatidylinositol-3-oh kinases are rab5 effectors. *NATURE CELL BIOLOGY*, 1.

Cipriano, D. J., Wang, Y., Bond, S., Hinton, A., Jefferies, K. C., Qi, J., & Forgac, M. (2008). Structure and regulation of the vacuolar atpases. *Biochimica et Biophysica Acta (BBA)*, 1777, 599–604.

Clark, J., Kay, R. R., Kielkowska, A., Niewczas, I., Fets, L., Oxley, D., Stephens, L. R., & Hawkins, P. T. (2014). Dictyostelium uses ether-linked inositol phospholipids for intracellular signalling. *The EMBO Journal*, 33, 2188.

Clarke, M., Köhler, J., Arana, Q., Liu, T., Heuser, J., & Gerish, G. (2002a). Dynamics of the vacuolar h+-atpase in the contractile vacuole complex and the endosomal pathway of dictyostelium cells. *Journal of Cell Science*, 115, 2893–2905.

Clarke, M., Köhler, J., Heuser, J., & Gerisch, G. (2002b). Endosome fusion and microtubule-based dynamics in the early endocytic pathway of dictyostelium. *Traffic*, 3, 791–800.

Clarke, M., Maddera, L., Engel, U., & Gerisch, G. (2010). Retrieval of the vacuolar h+-atpase from phagosomes revealed by live cell imaging. *PLoS ONE*, 5, e8585.

Commisso, C., Davidson, S. M., Soydaner-Azeloglu, R. G., Parker, S. J., Kamphorst, J. J., Hackett, S., Grabocka, E., Nofal, M., Drebin, J. A., Thompson, C. B., Rabinowitz, J. D., Metallo, C. M., Heiden, M. G. V., & Bar-Sagi, D. (2013). Macropinocytosis of protein is an amino acid supply route in ras-transformed cells. *Nature*, 497, 633–637.

Cornillon, S., Gebbie, L., Benghezal, M., Nair, P., Keller, S., Wehrle-Haller, B., Charette, S. J., Brückert, F., Letourneur, F., & Cosson, P. (2006). An adhesion molecule in free-living dictyostelium amoebae with integrin beta features. *EMBO Reports*, 7, 617.

Cosson, P. & Lima, W. C. (2014). Intracellular killing of bacteria: Is dictyostelium a model macrophage or an alien? *Cellular Microbiology*, 16, 816–823.

Czuczman, M. A., Fattouh, R., Rijn, J. M. V., Canadien, V., Osborne, S., Muise, A. M., Kuchroo, V. K., Higgins, D. E., & Brumell, J. H. (2014). Listeria monocytogenes exploits efferocytosis to promote cell-to-cell spread. *Nature*, 509, 230–234.

Dayam, R. M., Saric, A., Shilliday, R. E., & Botelho, R. J. (2015). The phosphoinositide-gated lysosomal ca2+ channel, trpml1, is required for phagosome maturation. *Traffic*, 16, 1010–1026.

Derivery, E., Sousa, C., Gautier, J. J., Lombard, B., Loew, D., & Gautreau, A. (2009). The arp2/3 activator wash controls the fission of endosomes through a large multiprotein complex. *Developmental Cell*, 17, 712–723.

Desai, A. S., Hunter, M. R., & Kapustin, A. N. (2019). Using macropinocytosis for intracellular delivery of therapeutic nucleic acids to tumour cells. *Philosophical Transactions of the Royal Society B*, 374.

Dieckmann, R., Guého, A., Monroy, R., Ruppert, T., Bloomfield, G., & Soldati, T. (2012). The balance in the delivery of er components and the vacuolar proton pump to the phagosome depends on myosin ik in dictyostelium. *Molecular and cellular proteomics*, 11, 886–900.

Dieckmann, R., Heyden, Y. V., Kistler, C., Gopaldass, N., Hausherr, S., Crawley, S. W., Schwarz, E. C., Diensthuber, R. P., Côté, G. P., Tsiavaliaris, G., & Soldati, T. (2010). A myosin ik-abp1-pakb circuit acts as a switch to regulate phagocytosis efficiency. *Molecular Biology of the Cell*, 21, 1505–1518.

Diken, M., Kreiter, S., Selmi, A., Britten, C. M., Huber, C., Türeci, O., & Sahin, U. (2011). Selective uptake of naked vaccine rna by dendritic cells is driven by macropinocytosis and abrogated upon dc maturation. *Gene Therapy 2011 18:7*, 18, 702–708.

Dong, X. P., Shen, D., Wang, X., Dawson, T., Li, X., Zhang, Q., Cheng, X., Zhang, Y., Weisman, L. S., Delling, M., & Xu, H. (2010). Pi(3,5)p2 controls membrane traffic by direct activation of mucolipin ca2+ release channels in the endolysosome. *Nature communications*, 1.

Dormann, D., Weijer, G., Dowler, S., & Weijer, C. J. (2004). In vivo analysis of 3-phosphoinositide dynamics during dictyostelium phagocytosis and chemotaxis. *Journal of cell science*, 117, 6497–509. This contains infomation on the PIPs in nascent macropinosomes AND phagosomes immediatley after cup clourse in Dicty.

Dove, S. K., Dong, K., Kobayashi, T., Williams, F. K., & Michell, R. H. (2009). Phosphatidylinositol 3,5-bisphosphate and fab1p/pikfyve underppin endo-lysosome function. *The Biochemical journal*, 419, 1–13.

Drewry, D. H., Potjewyd, F. M., Bayati, A., Smith, J. L., Dickmander, R. J., Howell, S., Taft-Benz, S., Min, S. M., Hossain, M. A., Heise, M., McPherson, P. S., Moorman, N. J., & Axtman, A. D. (2022). Identification and utilization of a chemical probe to interrogate the roles of pikfyve in the lifecycle of beta-coronaviruses. *Journal of medicinal chemistry*, 65, 12860–12882.

Dunn, J. D., Bosmani, C., Barisch, C., Raykov, L., Lefrançois, L. H., Cardenal-Muñoz, E., López-Jiménez, A. T., & Soldati, T. (2018). Eat prey, live: Dictyostelium discoideum as a model for cell-autonomous defenses. *Frontiers in Immunology*, 8, 1906.

Eichinger, I., Pachebat, J. A., Glöckner, G., Rajandream, M. A., Sucgang, R., Berriman, M., Song, J., Olsen, R., Szafranski, K., Xu, Q., Tunggal, B., Kummerfeld, S., Madera, M., Konfortov, B. A., Rivero, F., Bankier, A. T., Lehmann, R., Hamlin, N., Davies, R., Gaudet, P., Fey, P., Pilcher, K., Chen, G., Saunders, D., Sodergren, E., Davis, P., Kerhornou, A., Nie, X., Hall, N., Anjard, C., Hemphill, L., Bason, N., Farbrother, P., Desany, B., Just, E., Morio, T., Rost, R., Churcher, C., Cooper, J., Haydock, S., Driessche, N. V., Cronin, A., Goodhead, I., Muzny, D., Mourier, T., Pain, A., Lu, M., Harper, D., Lindsay, R., Hauser, H., James, K., Quiles, M., Babu, M. M., Saito, T., Buchrieser, C., Wardroper, A., Felder, M., Thangavelu, M., Johnson, D., Knights, A., Loulseged, H., Mungall, K., Oliver, K., Price, C., Quail, M. A., Urushihara, H., Hernandez, J., Rabbinowitsch, E., Steffen, D., Sanders, M., Ma, J., Kohara, Y., Sharp, S., Simmonds, M., Spiegler, S., Tivey, A., Sugano, S., White, B., Walker, D., Woodward, J., Winckler, T., Tanaka, Y., Shaulsky, G., Schleicher, M., Weinstock, G., Rosenthal, A., Cox, E. C., Chisholm, R. L., Gibbs, R., Loomis, W. F., Platzer, M., Kay, R. R., Williams, J., Dear, P. H., Noegel, A. A., Barrell, B., & Kuspa, A. (2005). The genome of the social amoeba dictyostelium discoideum. *Nature*, 435, 43.

Elkin, S. R., Lakoduk, A. M., & Schmid, S. L. (2016). Endocytic pathways and endosomal trafficking: A primer. *Wiener medizinische Wochenschrift (1946)*, 166, 196.

Eskelinen, E. L. (2006). Roles of lamp-1 and lamp-2 in lysosome biogenesis and autophagy. *Molecular Aspects of Medicine*, 27, 495–502.

Fajardo, M., Schleicher, M., Noegel, A., Bozzaro, S., Killinger, S., Heuner, K., Hacker, J. R., & Steinert, M. (2004). Calnexin, calreticulin and cytoskeleton-associated proteins modulate uptake and growth of legionella pneumophila in dictyostelium discoideum. *Microbiology*, 150, 2825–2835.

Feigin, V. L., Nichols, E., Alam, T., Bannick, M. S., Beghi, E., Blake, N., Culpepper, W. J., Dorsey, E. R., Elbaz, A., Ellenbogen, R. G., Fisher, J. L., Fitzmaurice, C., Giussani, G., Glennie, L., James, S. L., Johnson, C. O., Kassebaum, N. J., Logroscino, G., Marin, B., Mountjoy-Venning, W. C., Nguyen, M., Ofori-Asenso, R., Patel, A. P., Piccininni, M., Roth, G. A., Steiner, T. J., Stovner, L. J., Szoeke, C. E., Theadom, A., Vollset, S. E., Wallin, M. T., Wright, C., Zunt, J. R., Abbasi, N., Abd-Allah, F.,

Abdelalim, A., Abdollahpour, I., Aboyans, V., Abraha, H. N., Acharya, D., Adamu, A. A., Adebayo, O. M., Adeoye, A. M., Adsuar, J. C., Afarideh, M., Agrawal, S., Ahmadi, A., Ahmed, M. B., Aichour, A. N., Aichour, I., Aichour, M. T. E., Akinyemi, R. O., Akseer, N., Al-Eyadhy, A., Salman, R. A.-S., Alahdab, F., Alene, K. A., Aljunid, S. M., Altirkawi, K., Alvis-Guzman, N., Anber, N. H., Antonio, C. A. T., Arabloo, J., Aremu, O., Ärnlöv, J., Asayesh, H., Asghar, R. J., Atalay, H. T., Awasthi, A., Quintanilla, B. P. A., Ayuk, T. B., Badawi, A., Banach, M., Banoub, J. A. M., Barboza, M. A., Barker-Collo, S. L., Bärnighausen, T. W., Baune, B. T., Bedi, N., Behzadifar, M., Behzadifar, M., Béjot, Y., Bekele, B. B., Belachew, A. B., Bennett, D. A., Bensenor, I. M., Berhane, A., Beuran, M., Bhattacharyya, K., Bhutta, Z. A., Biadgo, B., Bijani, A., Bililign, N., Sayeed, M. S. B., Blazes, C. K., Brayne, C., Butt, Z. A., Campos-Nonato, I. R., Cantu-Brito, C., Car, M., Cárdenas, R., Carrero, J. J., Carvalho, F., Castañeda-Orjuela, C. A., Castro, F., Catalá-López, F., Cerin, E., Chaiah, Y., Chang, J. C., Chatziralli, I., Chiang, P. P. C., Christensen, H., Christopher, D. J., Cooper, C., Cortesi, P. A., Costa, V. M., Criqui, M. H., Crowe, C. S., Damasceno, A. A. M., Daryani, A., la Cruz-Góngora, V. D., Hoz, F. P. D. L., Leo, D. D., Degefa, M. G., Demoz, G. T., Deribe, K., Dharmaratne, S. D., Diaz, D., Dinberu, M. T., Djalalinia, S., Doku, D. T., Dubey, M., Dubljanin, E., Duken, E. E., Edvardsson, D., El-Khatib, Z., Endres, M., Endries, A. Y., Eskandarieh, S., Esteghamati, A., Esteghamati, S., Farhadi, F., Faro, A., Farzadfar, F., Farzaei, M. H., Fatima, B., Fereshtehnejad, S. M., Fernandes, E., Feyissa, G. T., Filip, I., Fischer, F., Fukumoto, T., Ganji, M., Gankpe, F. G., Garcia-Gordillo, M. A., Gebre, A. K., Gebremichael, T. G., Gelaw, B. K., Geleijnse, J. M., Geremew, D., Gezae, K. E., Ghasemi-Kasman, M., Gidey, M. Y., Gill, P. S., Gill, T. K., Gnedovskaya, E. V., Goulart, A. C., Grada, A., Grosso, G., Guo, Y., Gupta, R., Gupta, R., Haagsma, J. A., Hagos, T. B., Haj-Mirzaian, A., Haj-Mirzaian, A., Hamadeh, R. R., Hamidi, S., Hankey, G. J., Hao, Y., Haro, J. M., Hassankhani, H., Hassen, H. Y., Havmoeller, R., Hay, S. I., Hegazy, M. I., Heidari, B., Henok, A., Heydarpour, F., Hoang, C. L., Hole, M. K., Rad, E. H., Hosseini, S. M., Hu, G., Igumbor, E. U., Ilesanmi, O. S., Irvani, S. S. N., Islam, S. M. S., Jakovljevic, M., Javanbakht, M., Jha, R. P., Jobanputra, Y. B., Jonas, J. B., Józwiak, J. J., Jürisson, M., Kahsay, A., Kalani, R., Kalkonde, Y., Kamil, T. A., Kanchan, T., Karami, M., Karch, A., Karimi, N., Kasaeian, A., Kassa, T. D., Kassa, Z. Y., Kaul, A., Kefale, A. T., Keiyoro, P. N., Khader, Y. S., Khafaie, M. A., Khalil, I. A., Khan, E. A., Khang, Y. H., Khazaie, H., Kiadaliri, A. A., Kiirithio, D. N., Kim, A. S., Kim, D., Kim, Y. E., Kim, Y. J., Kisa, A., Kokubo, Y., Koyanagi, A., Krishnamurthi, R. V., Defo, B. K., Bicer, B. K., Kumar, M., Lacey, B., Lafranconi, A., Lansingh, V. C., Latifi, A., Leshargie, C. T., Li, S., Liao, Y., Linn, S., Lo, W. D., Lopez, J. C. F., Lorkowski, S., Lotufo, P. A., Lucas, R. M., Lunevicius, R., Mackay, M. T., Mahotra, N. B., Majdan, M., Majdzadeh, R., Majeed, A., Malekzadeh, R., Malta, D. C., Manafi, N., Mansournia, M. A., Mantovani, L. G., März, W., Mashamba-Thompson, T. P., Massenburg, B. B., Mate, K. K., McAlinden, C., McGrath, J. J., Mehta, V., Meier, T., Meles, H. G., Melese, A., Memiah, P. T., Memish, Z. A., Mendoza, W., Mengistu, D. T., Mengistu, G., Meretoja, A., Meretoja, T. J., Mestrovic, T., Miazgowski, B., Miazgowski, T., Miller, T. R., Mini, G. K., Mirrakhimov, E. M., Moazen, B., Mohajer, B., Mezerji, N. M. G., Mohammadi, M., Mohammadi-Khanaposhtani, M., Mohammadibakhsh, R., Mohammadnia-Afrouzi, M., Mohammed, S., Mohebi, F., Mokdad, A. H., Monasta, L., Mondello, S., Moodley, Y., Moosazadeh, M., Moradi, G., Moradi-Lakeh, M., Moradinazar, M., Moraga, P., Velásquez, I. M., Morrison, S. D., Mousavi, S. M., Muhammed, O. S., Muruet, W., Musa, K. I., Mustafa, G., Naderi, M., Nagel, G., Naheed, A., Naik, G., Najafi, F., Nangia, V., Negoi, I., Negoi, R. I., Newton, C. R. J., Ngunjiri, J. W., Nguyen, C. T., Nguyen, L. H., Ningrum, D. N. A., Nirayo, Y. L., Nixon, M. R., Norrving, B., Noubiap, J. J., Shiadeh, M. N., Nyasulu, P. S., Ogbo, F. A., Oh, I. H., Olagunju, A. T., Olagunju, T. O., Olivares, P. R., Onwujekwe, O. E., Oren, E., Owolabi, M. O., A, M. P., Pakpour, A. H., Pan, W. H., Panda-Jonas, S., Pandian, J. D., Patel, S. K., Pereira, D. M., Petzold, M., Pillay, J. D., Piradov, M. A., Polanczyk, G. V., Polinder, S., Postma, M. J., Poulton, R., Poustchi, H., Prakash, S., Prakash, V., Qorbani, M., Radfar, A., Rafay, A., Rafiei, A., Rahim, F., Rahimi-Movaghar, V., Rahman, M., Rahman, M. H. U., Rahman, M. A., Rajati, F., Ram, U., Ranta, A., Rawaf, D. L., Rawaf, S., Reinig, N., Reis, C., Renzaho, A. M., Resnikoff, S., Rezaeian,

S., Rezai, M. S., González, C. M. R., Roberts, N. L., Roever, L., Ronfani, L., Roro, E. M., Roshandel, G., Rostami, A., Sabbagh, P., Sacco, R. L., Sachdev, P. S., Saddik, B., Safari, H., Safari-Faramani, R., Safi, S., Safiri, S., Sagar, R., Sahathevan, R., Sahebkar, A., Sahraian, M. A., Salamati, P., Zahabi, S. S., Salimi, Y., Samy, A. M., Sanabria, J., Santos, I. S., Milicevic, M. M. S., Sarrafzadegan, N., Sartorius, B., Sarvi, S., Sathian, B., Satpathy, M., Sawant, A. R., Sawhney, M., Schneider, I. J., Schöttker, B., Schwebel, D. C., Seedat, S., Sepanlou, S. G., Shabaninejad, H., Shafieesabet, A., Shaikh, M. A., Shakir, R. A., Shams-Beyranvand, M., Shamsizadeh, M., Sharif, M., Sharif-Alhoseini, M., She, J., Sheikh, A., Sheth, K. N., Shigematsu, M., Shiri, R., Shirkoohi, R., Shiue, I., Siabani, S., Siddiqi, T. J., Sigfusdottir, I. D., Sigurvinsdottir, R., Silberberg, D. H., Silva, J. P., Silveira, D. G. A., Singh, J. A., Sinha, D. N., Skiadaresi, E., Smith, M., Sobaih, B. H., Sobhani, S., Soofi, M., Soyiri, I. N., Sposato, L. A., Stein, D. J., Stein, M. B., Stokes, M. A., Sufiyan, M. B., Sykes, B. L., Sylaja, P., Tabarés-Seisdedos, R., Ao, B. J. T., Tehrani-Banihashemi, A., Temsah, M. H., Temsah, O., Thakur, J. S., Thrift, A. G., Topor-Madry, R., Tortajada-Girbés, M., Tovani-Palone, M. R., Tran, B. X., Tran, K. B., Truelsen, T. C., Tsadik, A. G., Car, L. T., Ukwaja, K. N., Ullah, I., Usman, M. S., Uthman, O. A., Valdez, P. R., Vasankari, T. J., Vasanthan, R., Veisani, Y., Venketasubramanian, N., Violante, F. S., Vlassov, V., Vosoughi, K., Vu, G. T., Vujcic, I. S., Wagnew, F. S., Waheed, Y., Wang, Y. P., Weiderpass, E., Weiss, J., Whiteford, H. A., Wijeratne, T., Winkler, A. S., Wiysonge, C. S., Wolfe, C. D., Xu, G., Yadollahpour, A., Yamada, T., Yano, Y., Yaseri, M., Yatsuya, H., Yimer, E. M., Yip, P., Yisma, E., Yonemoto, N., Yousefifard, M., Yu, C., Zaidi, Z., Zaman, S. B., Zamani, M., Zandian, H., Zare, Z., Zhang, Y., Zodpey, S., Naghavi, M., Murray, C. J., & Vos, T. (2019). Global, regional, and national burden of neurological disorders, 1990–2016: a systematic analysis for the global burden of disease study 2016. *The Lancet Neurology*, 18, 459–480.

Feng, X., Xiong, J., Cai, W., Tian, J. B., & Zhu, M. X. (2022). The three two-pore channel subtypes from rabbit exhibit distinct sensitivity to phosphoinositides, voltage, and extracytosolic ph. *Cells*, 11, 2006.

Ferguson, S. M. & Camilli, P. D. (2012). Dynamin, a membrane-remodelling gtpase. *Nature Reviews Molecular Cell Biology*, 13, 75–88.

Fiala, M., Lin, J., Ringman, J., Kermani-Arab, V., Tsao, G., Patel, A., Lossinsky, A. S., Graves, M. C., Gustavson, A., Sayre, J., Sofroni, E., Suarez, T., Chiappelli, F., & Bernard, G. (2005). Ineffective phagocytosis of amyloid-beta by macrophages of alzheimer's disease patients. *Journal of Alzheimer's disease : JAD*, 7, 221–232.

Fine, M., Schmiege, P., & Li, X. (2018). Structural basis for ptdinsp2-mediated human trpml1 regulation. *Nature Communications*, 9.

Fratti, R. A., Backer, J. M., Gruenberg, J., Corvera, S., & Deretic, V. (2001). Role of phosphatidylinositol 3-kinase and rab5 effectors in phagosomal biogenesis and mycobacterial phagosome maturation arrest. *Journal of Cell Biology*, 154, 631–644.

Gagnon, E., Duclos, S., Rondeau, C., Chevet, E., Cameron, P. H., Steele-Mortimer, O., Paiement, J., Bergeron, J. J., & Desjardins, M. (2002). Endoplasmic reticulum-mediated phagocytosis is a mechanism of entry into macrophages. *Cell*, 110, 119–131.

Gan, N., Han, Y., Zeng, W., Wang, Y., Xue, J., & Jiang, Y. (2022). Structural mechanism of allosteric activation of trpml1 by pi(3,5)p2 and rapamycin. *Proceedings of the National Academy of Sciences of the United States of America*, 119, e2120404119.

Gary, J. D., Wurmser, A. E., Bonangelino, C. J., Weisman, L. S., & Emr, S. D. (1998). Fab1p is essential for ptdins(3)p 5-kinase activity and the maintenance of vacuolar size and membrane homeostasis. *The Journal of Cell Biology*, 143, 65.

Gayle, S., Landrette, S., Beeharry, N., Conrad, C., Hernandez, M., Beckett, P., Ferguson, S. M., Mandelkern, T., Zheng, M., Xu, T., Rothberg, J., & Lichenstein, H. (2017). Identification of apilimod as a first-in-class pikfyve kinase inhibitor for treatment of b-cell non-hodgkin lymphoma. *Blood*, 129, 1768–1778.

Gerndt, S., Chen, C. C., Chao, Y. K., Yuan, Y., Burgstaller, S., Rosato, A. S., Krogsaeter, E., Urban, N., Jacob, K., Nguyen, O. N. P., Miller, M. T., Keller, M., Vollmar, A. M., Gudermann, T., Zierler, S., Schredelseker, J., Schaefer, M., Biel, M., Malli, R., Wahl-Schott, C., Bracher, F., Patel, S., & Grimm, C. (2020). Agonist-mediated switching of ion selectivity in tpc2 differentially promotes lysosomal function. *eLife*, 9.

Geumann, U., Barysch, S. V., Hoopmann, P., Jahn, R., & Rizzoli, S. O. (2008). Snare function is not involved in early endosome docking. *Molecular biology of the cell*, 19, 5327–5337.

Gillooly, D. J., Morrow, I. C., Lindsay, M., Gould, R., Bryant, N. J., Gaullier, J. M., Parton, R. G., & Stenmark, H. (2000). Localization of phosphatidylinositol 3-phosphate in yeast and mammalian cells. *The EMBO Journal*, 19, 4577.

Gillooly, D. J., Simonsen, A., & Stenmark, H. (2001). Cellular functions of phosphatidylinositol 3-phosphate and fyve domain proteins. *Biochem. J*, 355, 249–258.

Giorgione, J. & Clarke, M. (2008). Heterogeneous modes of uptake for latex beads revealed through live cell imaging of phagocytes expressing a probe for phosphatidylinositol-(3,4,5)-trisphosphate and phosphatidylinositol-(3,4)-bisphosphate. *Cell Motility and the Cytoskeleton*, 65, 721–733.

Gomez, T. S. & Billadeau, D. D. (2009). A fam21-containing wash complex regulates retromer-dependent sorting. *Developmental Cell*, 17, 699–711.

Gopaldass, N., Patel, D., Kratzke, R., Dieckmann, R., Hausherr, S., Hagedorn, M., Monroy, R., Krüger, J., Neuhaus, E. M., Hoffmann, E., Hille, K., Kuznetsov, S. A., & Soldati, T. (2012). Dynamin a, myosin ib and abp1 couple phagosome maturation to f-actin binding. *Traffic*, 13, 120–130.

Gordon, S. (2016). Phagocytosis: The legacy of metchnikoff. *Cell*, 166, 1065–1068.

Gotthardt, D., Warnatz, H. J., Henschel, O., Brückert, F., Schleicher, M., & Soldati, T. (2002). High-resolution dissection of phagosome maturation reveals distinct membrane trafficking phases. *Molecular biology of the cell*, 13, 3508–20.

Granboulan, M., Lankar, D., Raposo, G., Bonnerot, C., & Hivroz, C. (2003). Phosphoinositide 3-kinase activation by igbeta controls de novo formation of an antigen-processing compartment. *Journal of Biological Chemistry*, 278, 4331–4338.

Graves, A. R., Curran, P. K., Smith, C. L., & Mindell, J. A. (2008). The cl-/h+ antiporter clc-7 is the primary chloride permeation pathway in lysosomes. *Nature 2008 453:7196*, 453, 788–792.

Gueho, A., Bosmani, C., Gopaldass, N., Molle, V., Soldati, T., & Letourneur, F. (2016). Dictyostelium ehd associates with dynamin and participates in phagosome maturation. *Journal of Cell Science*.

Hacker, U., Albrecht, R., & Maniak, M. (1997). Fluid-phase uptake by macropinocytosis in dictyostelium. *Journal of Cell Science*, 110, 105–112.

Halici, S., Zenk, S. F., Jantsch, J., & Hensel, M. (2008). Functional analysis of the salmonella pathogenicity island 2-mediated inhibition of antigen presentation in dendritic cells. *Infection and immunity*, 76, 4924–4933.

Hammond, G. R., Takasuga, S., Sasaki, T., & Balla, T. (2015). The ml1nx2 phosphatidylinositol 3,5-bisphosphate probe shows poor selectivity in cells. *PLOS ONE*, 10, e0139957.

Hao, X., Lüthje, F., Rønn, R., German, N. A., Li, X., Huang, F., Kisaka, J., Huffman, D., Alwathnani, H. A., Zhu, Y.-G., & Rensing, C. (2016). A role for copper in protozoan grazing - two billion years selecting for bacterial copper resistance. *Molecular Microbiology*, 102, 628–641.

Harris, E. & Cardelli, J. (2002). Rabd, a dictyostelium rab14-related gtpase, regulates phagocytosis and homotypic phagosome and lysosome fusion. *Journal of Cell Science*, 115, 3703–3713.

Harris, E., Yoshida, K., Cardelli, J., & Bush, J. (2001). Rab11-like gtpase associates with and regulates the structure and function of the contractile vacuole system in dictyostelium. *J. Cell Sci.*, 104, 1119–1127.

Henry, R. M., Hoppe, A. D., Joshi, N., & Swanson, J. A. (2004). The uniformity of phagosome maturation in macrophages. *The Journal of Cell Biology*, 164, 185.

Hilbi, H. (2006). Modulation of phosphoinositide metabolism by pathogenic bacteria. *Cellular Microbiology*, 8, 1697–1706.

Hiragi, S., Matsui, T., Sakamaki, Y., & Fukuda, M. (2022). Tbc1d18 is a rab5-gap that coordinates endosome maturation together with mon1. *The Journal of cell biology*, 221.

Ho, C. Y., Choy, C. H., Wattson, C. A., Johnson, D. E., & Botelho, R. J. (2015). The fab1/pikfyve phosphoinositide phosphate kinase is not necessary to maintain the ph of lysosomes and of the yeast vacuole. *Journal of Biological Chemistry*, 290, 9919–9928.

Holemans, T., Sørensen, D. M., van Veen, S., Martin, S., Hermans, D., Kemmer, G. C., den Haute, C. V., Baekelandt, V., Pomorski, T. G., Agostinis, P., Wuytack, F., Palmgren, M., Eggermont, J., & Vangheluwe, P. (2015). A lipid switch unlocks parkinson's disease-associated atp13a2. *Proceedings of the National Academy of Sciences*, 112, 9040–9045.

Hong, W. (2005). Snares and traffic. *Biochimica et biophysica acta*, 1744, 493–517.

Humphreys, D., Davidson, A. C., Hume, P. J., Makin, L. E., & Koronakis, V. (2013). Arf6 coordinates actin assembly through the wave complex, a mechanism usurped by salmonella to invade host cells. *Proceedings of the National Academy of Sciences of the United States of America*, 110, 16880–16885.

Hung, S. T., Linares, G. R., Chang, W. H., Eoh, Y., Krishnan, G., Mendonca, S., Hong, S., Shi, Y., Santana, M., Kueth, C., Macklin-Isquierdo, S., Perry, S., Duhaime, S., Maios, C., Chang, J., Perez, J., Couto, A., Lai, J., Li, Y., Alworth, S. V., Hendricks, E., Wang, Y., Zlokovic, B. V., Dickman, D. K., Parker, J. A., Zarnescu, D. C., Gao, F. B., & Ichida, J. K. (2023). Pikfyve inhibition mitigates disease in models of diverse forms of als. *Cell*, 186, 786–802.e28.

Huynh, K. K., Eskelinen, E. L., Scott, C. C., Malevanets, A., Saftig, P., & Grinstein, S. (2007). Lamp proteins are required for fusion of lysosomes with phagosomes. *The EMBO Journal*, 26, 313–324.

Ikonomov, O. C., Sbrissa, D., Delvecchio, K., Xie, Y., Jin, J. P., Rappolee, D., & Shisheva, A. (2011). The phosphoinositide kinase pikfyve is vital in early embryonic development: Preimplantation lethality of pikfyve-/- embryos but normality of pikfyve+/- mice. *The Journal of Biological Chemistry*, 286, 13404.

Ikonomov, O. C., Sbrissa, D., Fenner, H., & Shisheva, A. (2009). Pikfyve-arpikfyve-sac3 core complex: contact sites and their consequence for sac3 phosphatase activity and endocytic membrane homeostasis. *The Journal of biological chemistry*, 284, 35794–806.

Ikonomov, O. C., Sbrissa, D., Mlak, K., Deeb, R., Fligger, J., Soans, A., Finley, R. L., & Shisheva, A. (2003). Active pikfyve associates with and promotes the membrane attachment of the late endosome-to-trans-golgi network transport factor rab9 effector p40. *The Journal of biological chemistry*, 278, 50863–50871.

Ikonomov, O. C., Sbrissa, D., & Shisheva, A. (2019). Small molecule pikfyve inhibitors as cancer therapeutics: Translational promises and limitations. *Toxicology and applied pharmacology*, 383.

Isobe, Y., Nigorikawa, K., Tsurumi, G., Takemasu, S., Takasuga, S., Kofuji, S., & Hazeki, K. (2019). Pikfyve accelerates phagosome acidification through activation of trpml1 while arrests aberrant vacuolation independent of the ca2+ channel. *The Journal of Biochemistry*, 165, 75–84.

Janssen, K. P., Rost, R., Eichinger, L., & Schleicher, M. (2001). Characterization of cd36/limpii homologues in dictyostelium discoideum. *Journal of Biological Chemistry*, 276, 38899–38910.

Jaślan, D., Ferro, I. F., Kudrina, V., Yuan, Y., Patel, S., & Grimm, C. (2023). Pi(3,5)p2 and naadp: Team players or lone warriors? – new insights into tpc activation modes. *Cell Calcium*, 109.

Jia, D., Gomez, T. S., Billadeau, D. D., & Rosen, M. K. (2012). Multiple repeat elements within the fam21 tail link the wash actin regulatory complex to the retromer. *Molecular Biology of the Cell*, 23, 2352–2361.

Jordens, I., Fernandez-Borja, M., Marsman, M., Dusseljee, S., Janssen, L., Calafat, J., Janssen, H., Wubbolts, R., & Neefjes, J. (2001). The rab7 effector protein rilp controls lysosomal transport by inducing the recruitment of dynein-dynactin motors. *Current Biology*, 11, 1680–1685.

Journet, A., Chapel, A., Jehan, S., Adessi, C., Freeze, H., Klein, G., & Garin, J. (1999). Characterization of dictyostelium discoideum cathepsin d. *Journal of Cell Science*, 112, 3833–3844.

Kang, Y. L., Chou, Y. Y., Rothlauf, P. W., Liu, Z., Soh, T. K., Cureton, D., Case, J. B., Chen, R. E., Diamond, M. S., Whelan, S. P., & Kirchhausen, T. (2020). Inhibition of pikfyve kinase prevents infection by zaire ebolavirus and sars-cov-2. *Proceedings of the National Academy of Sciences of the United States of America*, 117, 20803–20813.

Kant, R. V. D., Jonker, C. T. H., Wijdeven, R. H., Bakker, J., Janssen, L., Klumperman, J., & Neefjes, J. (2015). Characterization of the mammalian corvet and hops complexes and their modular restructuring for endosome specificity *. *THE JOURNAL OF BIOLOGICAL CHEMISTRY*.

Kaplan, G. (1977). Differences in the mode of phagocytosis with fc and c3 receptors in macrophages. *Scandinavian Journal of Immunology*, 6, 797–807.

Katoch, B. & Begum, R. (2003). Biochemical basis of the high resistance to oxidative stress in dictyostelium discoideum. *Journal of Biosciences*, 28, 581–588.

Kerr, M. C., Wang, J. T., Castro, N. A., Hamilton, N. A., Town, L., Brown, D. L., Meunier, F. A., Brown, N. F., Stow, J. L., & Teasdale, R. D. (2010). Inhibition of the ptdins(5) kinase pikfyve disrupts intracellular replication of salmonella. *The EMBO journal*, 29, 1331–1347.

Kim, G. H., Dayam, R. M., Prashar, A., Terebiznik, M., & Botelho, R. J. (2014). Pikfyve inhibition interferes with phagosome and endosome maturation in macrophages. *Traffic (Copenhagen, Denmark)*, 15, 1143–1163.

Kinchen, J. M. & Ravichandran, K. S. (2010). Identification of two evolutionarily conserved genes regulating processing of engulfed apoptotic cells. *Nature 2010 464:7289*, 464, 778–782.

King, J. S. & Kay, R. R. (2019). The origins and evolution of macropinocytosis. *Philosophical Transactions of the Royal Society B*, 374.

Klumperman, J. & Raposo, G. (2014). The complex ultrastructure of the endolysosomal system. *Cold Spring Harbor Perspectives in Biology*, 6.

Konijn, T. M., Meene, J. G. V. D., Bonner, J. T., & Barkley, D. S. (1967). The acrasin activity of adenosine-3',5'-cyclic phosphate. *Proceedings of the National Academy of Sciences of the United States of America*, 58, 1152–1154.

Krause, K. H. (2000). Professional phagocytes: predators and prey of microorganisms. *Schweizerische Medizinische Wochenschrift*, 130, 97–100.

Krishna, S., Palm, W., Lee, Y., Yang, W., Bandyopadhyay, U., Xu, H., Florey, O., Thompson, C. B., & Overholtzer, M. (2016). Pikfyve regulates vacuole maturation and nutrient recovery following engulfment. *Developmental cell*, 38, 536–47.

Kumari, S., Mg, S., & Mayor, S. (2010). Endocytosis unplugged: Multiple ways to enter the cell. *Cell Research*, 20, 256–275.

Lamrabet, O., Jauslin, T., Lima, W. C., Leippe, M., & Cosson, P. (2020a). The multifarious lysozyme arsenal of dictyostelium discoideum. *Developmental and Comparative Immunology*, 107, 103645.

Lamrabet, O., Melotti, A., Burdet, F., Hanna, N., Perrin, J., Nitschke, J., Pagni, M., Hilbi, H., Soldati, T., & Cosson, P. (2020b). Transcriptional responses of dictyostelium discoideum exposed to different classes of bacteria. *Frontiers in Microbiology*, 11.

Lang, M. J., Strunk, B. S., Azad, N., Petersen, J. L., & Weisman, L. S. (2017). An intramolecular interaction within the lipid kinase fab1 regulates cellular phosphatidylinositol 3,5-bisphosphate lipid levels. *Molecular biology of the cell*, 28, 858–864.

Langemeyer, L., Borchers, A. C., Herrmann, E., Füllbrunn, N., Han, Y., Perz, A., Auffarth, K., Kümmel, D., & Ungermann, C. (2020). A conserved and regulated mechanism drives endosomal rab transition. *eLife*, 9.

Lardy, B., Bof, M., Aubry, L., Paclet, M. H., Morel, F., Satre, M., & Klein, G. (2005). Nadph oxidase homologs are required for normal cell differentiation and morphogenesis in dictyostelium discoideum. *Biochimica et Biophysica Acta - Molecular Cell Research*, 1744, 199–212.

Lees, J. A., Li, P. Q., Kumar, N., Weisman, L. S., & Reinisch, K. M. (2020). Insights into lysosomal pi(3,5)p2 homeostasis from a structural-biochemical analysis of the pikfyve lipid kinase complex. *Molecular cell*, 80, 736–743.e4.

Leray, X., Hilton, J. K., Nwangwu, K., Becerril, A., Mikusevic, V., Fitzgerald, G., Amin, A., Weston, M. R., & Mindell, J. A. (2022). Tonic inhibition of the chloride/proton antiporter clc-7 by pi(3,5)p2 is crucial for lysosomal ph maintenance. *eLife*, 11.

Levin, R., Grinstein, S., & Canton, J. (2016). The life cycle of phagosomes: formation, maturation, and resolution. *Immunological Reviews*, 273, 156–179.

Levin-Konigsberg, R. & Grinstein, S. (2020). Phagosome-endoplasmic reticulum contacts: Kissing and not running. *Traffic*, 21, 172–180.

Li, S. C., Diakov, T. T., Xu, T., Tarsio, M., Zhu, W., Couoh-Cardel, S., Weisman, L. S., & Kane, P. M. (2014). The signaling lipid pi(3,5)p2 stabilizes v1–vo sector interactions and activates the v-atpase. *Molecular Biology of the Cell*, 25, 1251.

Li, X., Rydzewski, N., Hider, A., Zhang, X., Yang, J., Wang, W., Gao, Q., Cheng, X., & Xu, H. (2016). A molecular mechanism to regulate lysosome motility for lysosome positioning and tubulation. *Nature cell biology*, 18, 404–417.

Li, X., Wang, X., Zhang, X., Zhao, M., Tsang, W. L., Zhang, Y., Yau, R. G. W., Weisman, L. S., & Xu, H. (2013). Genetically encoded fluorescent probe to visualize intracellular phosphatidylinositol 3,5-bisphosphate localization and dynamics. *Proceedings of the National Academy of Sciences of the United States of America*, 110, 21165–21170.

Li, Y., Bollag, G., Clark, R., Stevens, J., Conroy, L., Fults, D., Ward, K., Friedman, E., Samowitz, W., Robertson, M., Bradley, P., McCormick, F., White, R., & Cawthon, R. (1992). Somatic mutations in the neurofibromatosis 1 gene in human tumors. *Cell*, 69, 275–281.

Lim, J. P. & Gleeson, P. A. (2011). Macropinocytosis: an endocytic pathway for internalising large gulps. *Immunology and Cell Biology*, 89, 836–843.

Lima, W. C., Leuba, F., Soldati, T., & Cosson, P. (2012). Mucolipin controls lysosome exocytosis in dictyostelium. *Journal of Cell Science*, 125, 2315–2322.

Lin, X., Yang, T., Wang, S., Wang, Z., Yun, Y., Sun, L., Zhou, Y., Xu, X., Akazawa, C., Hong, W., & Wang, T. (2014). Rilp interacts with hops complex via vps41 subunit to regulate endocytic trafficking. *Scientific Reports*, 4.

Lippuner, C., Paape, D., Paterou, A., Brand, J., Richardson, M., Smith, A. J., Hoffmann, K., Brinkmann, V., Blackburn, C., & Aebischer, T. (2009). Real-time imaging of leishmania mexicana-infected early phagosomes: a study using primary macrophages generated from green fluorescent protein-rab5 transgenic mice. *The FASEB Journal*, 23, 483–491.

Lippé, R., Miaczynska, M., Rybin, V., Runge, A., & Zerial, M. (2001). Functional synergy between rab5 effector rabaptin-5 and exchange factor rabex-5 when physically associated in a complex. *Molecular Biology of the Cell*, 12, 2219–2228.

Liu, H. & Qian, F. (2022). Exploiting macropinocytosis for drug delivery into kras mutant cancer. *Theranostics*, 12, 1321.

Liu, T., Mirschberger, C., Chooback, L., Arana, Q., Sacco, Z. D., MacWilliams, H., & Clarke, M. (2002). Altered expression of the 100 kda subunit of the dictyosteliumvacuolar proton pump impairs enzyme assembly, endocytic function and cytosolic ph regulation. *Journal of Cell Science*, 115, 1907–1918.

Loomis, W. F. (1971). Sensitivity of dictyostelium discoideum to nucleic acid analogues. *Experimental cell research*, 64, 484–486.

Loomis, W. F. (2014). Cell signaling during development of dictyostelium. *Developmental biology*, 391, 1.

Loovers, H. M., Kortholt, A., de Groote, H., Whitty, L., Nussbaum, R. L., & van Haastert, P. J. M. (2007). Regulation of phagocytosis in dictyostelium by the inositol 5-phosphatase ocrl homolog dd5p4. *Traffic*, 8, 618–628.

Lu, H. & Clarke, M. (2005). Dynamic properties of legionella-containing phagosomes in dictyostelium amoebae. *Cellular Microbiology*, 7, 995–1007.

Luo, Z., Liang, Y., Tian, M., Ruan, Z., Su, R., Shereen, M. A., Yin, J., Wu, K., Guo, J., Zhang, Q., Li, Y., & Wu, J. (2023). Inhibition of pikfyve kinase interferes escrt pathway to suppress rna virus replication. *Journal of medical virology*, 95.

Luscher, A., Fröhlich, F., Barisch, C., Littlewood, C., Metcalfe, J., Leuba, F., Palma, A., Pirruccello, M., Cesareni, G., Stagi, M., Walther, T. C., Soldati, T., Camilli, P. D., & Swan, L. E. (2019). Lowe syndrome–linked endocytic adaptors direct membrane cycling kinetics with ocrl in dictyostelium discoideum. *Molecular Biology of the Cell*, 30, 2268–2282.

Maniak, M., Rauchenberger, R., Albrecht, R., Murphy, J., & Gerisch, G. (1995). Coronin involved in phagocytosis: Dynamics of particle-induced relocalization visualized by a green fluorescent protein tag. *Cell*, 83, 915–924.

McBride, H. M., Rybin, V., Murphy, C., Giner, A., Teasdale, R., & Zerial, M. (1999). Oligomeric complexes link rab5 effectors with nsf and drive membrane fusion via interactions between eea1 and syntaxin 13. *Cell*, 98, 377–386.

McMahon, H. T. & Boucrot, E. (2011). Molecular mechanism and physiological functions of clathrin-mediated endocytosis. *Nature Reviews Molecular Cell Biology*, 12, 517–533.

Means, N., Elechalawar, C. K., Chen, W. R., Bhattacharya, R., & Mukherjee, P. (2022). Revealing macropinocytosis using nanoparticles. *Molecular Aspects of Medicine*, 83, 100993.

Mehta, D. P., Etchison, J. R., & Freeze, H. H. (1995). Characterization, subcellular localization, and developmental regulation of a cysteine proteinase from dictyostelium discoideum. *Archives of Biochemistry and Biophysics*, 321, 191–198.

Mercanti, V., Charette, S. J., Bennett, N., Ryckewaert, J. J., Letourneur, F., & Cosson, P. (2006). Selective membrane exclusion in phagocytic and macropinocytic cups. *Journal of Cell Science*, 119, 4079–4087.

Mercer, J., Schelhaas, M., & Helenius, A. (2010). Virus entry by endocytosis. *Annual review of biochemistry*, 79, 803–833.

Min, S. H., Suzuki, A., Weaver, L., Guzman, J., Chung, Y., Jin, H., Gonzalez, F., Trasorras, C., Zhao, L., Spruce, L. A., Seeholzer, S. H., Behrens, E. M., & Abrams, C. S. (2019). Pikfyve deficiency in myeloid cells impairs lysosomal homeostasis in macrophages and promotes systemic inflammation in mice. *Molecular and Cellular Biology*, 39.

Mindell, J. A. (2012). Lysosomal acidification mechanisms. *https://doi.org/10.1146/annurev-physiol-012110-142317*, 74, 69–86.

Moen, E., Bannon, D., Kudo, T., Graf, W., Covert, M., & Valen, D. V. (2019). Deep learning for cellular image analysis. *Nature Methods 2019 16:12*, 16, 1233–1246.

Molmeret, M., Horn, M., Wagner, M., Santic, M., & Kwaik, Y. A. (2005). Amoebae as training grounds for intracellular bacterial pathogens. *Applied and Environmental Microbiology*, 71, 20–28.

Mu, A., Ller-Taubenberger, E., Lupas, A. N., Li, H., Ecke, M., Simmeth, E., & Gerisch, G. E. N. (2001). Calreticulin and calnexin in the endoplasmic reticulum are important for phagocytosis. *The EMBO Journal*, 20, 6772–6782.

Müller, I., Šubert, N., Otto, H., Herbst, R., Rühling, H., Maniak, M., & Leippe, M. (2005). A dictyostelium mutant with reduced lysozyme levels compensates by increased phagocytic activity. *Journal of Biological Chemistry*, 280, 10435–10443.

Münch, C., O'Brien, J., & Bertolotti, A. (2011). Prion-like propagation of mutant superoxide dismutase-1 misfolding in neuronal cells. *Proceedings of the National Academy of Sciences of the United States of America*, 108, 3548–3553.

Nakase, I., Kobayashi, N. B., Takatani-Nakase, T., & Yoshida, T. (2015). Active macropinocytosis induction by stimulation of epidermal growth factor receptor and oncogenic ras expression potentiates cellular uptake efficacy of exosomes. *Scientific Reports 2015 5:1*, 5, 1–14.

Nasser, W., Santhanam, B., Miranda, E. R., Parikh, A., Juneja, K., Rot, G., Dinh, C., Chen, R., Zupan, B., Shaulsky, G., & Kuspa, A. (2013). Bacterial discrimination by dictyostelid amoebae reveals the complexity of ancient interspecies interactions. *Current Biology*, 23, 862–872.

Neuhaus, E. M., Almers, W., & Soldati, T. (2002). Morphology and dynamics of the endocytic pathway in dictyostelium discoideum. *Molecular Biology of the Cell*, 13, 1390–1407.

Neuhaus, E. M. & Soldati, T. (2000). A myosin i is involved in membrane recycling from early endosomes. *The Journal of cell biology*, 150, 1013–26.

Neumeister, B., Faigle, M., Spitznagel, D., Mainka, A., Ograbek, A., Wieland, H., Mannowetz, N., & Rammensee, H. G. (2005). Legionella pneumophila down-regulates mhc class i expression of human monocytic host cells and thereby inhibits t cell activation. *Cellular and molecular life sciences : CMLS*, 62, 578–588.

Nicot, A.-S., Fares, H., Payrastre, B., Chisholm, A. D., Labouesse, M., & Laporte, J. (2006). The phosphoinositide kinase pikfyve/fab1p regulates terminal lysosome maturation in caenorhabditis elegans. *Molecular Biology of the Cell*, 17, 3062–3074.

Nielsen, E., Severin, F., Backer, J. M., Hyman, A. A., & Zerial, M. (1999). Rab5 regulates motility of early endosomes on microtubules. *Nature cell biology*, 1, 376–382.

Nolta, K. V., Padh, H., Steck, T. L., Allen, R. D., O'Halloran, T., Ruscetti, T., Temesvari, L., Steck., T., & Cardelli, J. (1996). An immunocytochemical analysis of the vacuolar proton pump in dictyostelium discoideum. *Journal of Cell Science*, 105, 849–859.

Nunes, P., Cornut, D., Bochet, V., Hasler, U., Oh-Hora, M., Waldburger, J. M., & Demaurex, N. (2012). Stim1 juxtaposes er to phagosomes, generating ca2+ hotspots that boost phagocytosis. *Current Biology*, 22, 1990–1997.

Nunes, P. & Demaurex, N. (2010). The role of calcium signaling in phagocytosis. *Journal of Leukocyte Biology*, 88, 57–68.

Nunes-Hasler, P. & Demaurex, N. (2017). The er phagosome connection in the era of membrane contact sites. *Biochimica et Biophysica Acta (BBA) - Molecular Cell Research*, 1864, 1513–1524.

Ostrowicz, C. W., Bröcker, C., Ahnert, F., Nordmann, M., Lachmann, J., Peplowska, K., Perz, A., Auffarth, K., Engelbrecht-Vandré, S., & Ungermann, C. (2010). Defined subunit arrangement and rab interactions are required for functionality of the hops tethering complex. *Traffic*, 11, 1334–1346.

Pearse, B. M. (1976). Clathrin: A unique protein associated with intracellular transfer of membrane by coated vesicles. *Proceedings of the National Academy of Sciences of the United States of America*, 73, 1255–1259.

Peracino, B., Wagner, C., Balest, A., Balbo, A., Pergolizzi, B., Noegel, A. A., Steinert, M., & Bozzaro, S. (2006). Function and mechanism of action of dictyostelium nramp1 (slc11a1) in bacterial infection. *Traffic*, 7, 22–38.

Perini, E. D., Schaefer, R., Stöter, M., Kalaidzidis, Y., & Zerial, M. (2014). Mammalian corvet is required for fusion and conversion of distinct early endosome subpopulations. *Traffic*, 15, 1366–1389.

Racoosin, E. L. & Swanson, J. A. (1989). Macrophage colony stimulating factor (rm-csf) stimulates pinocytosis in bone marrow-derived macrophages. *J. Exp. Med.*, 170, 1635–1648.

Rai, A., Pathak, D., Thakur, S., Singh, S., Dubey, A. K., & Mallik, R. (2016). Dynein clusters into lipid microdomains on phagosomes to drive rapid transport toward lysosomes. *Cell*, 164, 722–734.

Raper, K. (1935). Dictyostelium discoideum, a new species of slime mold from decaying forestleaves. *Journal of Agricultural Research*, 50, 135–147.

Raper, K. & Thom, C. (1932). The distribution of dictyostelium and other slime molds in soil. *Journal of the Washington Academy of Sciences*, 22, 92–96.

Rauchenberger, R., Hacker, U., Murphy, J., Niewöhner, J., & Maniak, M. (1997). Coronin and vacuolin identify consecutive stages of a late, actin-coated endocytic compartment in dictyostelium. *Current biology : CB*, 7, 215–218.

Ravanel, K. (2001). Membrane sorting in the endocytic and phagocytic pathway of dictyostelium discoideum. *European Journal of Cell Biology*, 80, 754–764.

Reddy, A., Caler, E. V., & Andrews, N. W. (2001). Plasma membrane repair is mediated by ca2+-regulated exocytosis of lysosomes. *Cell*, 106, 157–169.

Repnik, U., Česen, M. H., & Turk, B. (2013). The endolysosomal system in cell death and survival. *Cold Spring Harbor Perspectives in Biology*, 5, a008755.

Rieger, R., Michaelis, A., & Green, M. M. (1991). *Glossary of Genetics: Classical and Molecular*. Springer-Verlag, 5th edition.

Roberts, R., Barbieri, M., Pryse, K., Chua, M., Morisaki, J., & Stahl, P. (1999). Endosome fusion in living cells overexpressing gfp-rab5. *Journal of cell science*, 112 (Pt 21), 3667–3675.

Roche, P. A. & Furuta, K. (2015). The ins and outs of mhc class ii-mediated antigen processing and presentation. *Nature reviews. Immunology*, 15, 203–216.

Rosales-Reyes, R., Pérez-López, A., Sánchez-Gómez, C., Hernández-Mote, R. R., Castro-Eguiluz, D., Ortiz-Navarrete, V., & Alpuche-Aranda, C. M. (2012). Salmonella infects b cells by macropinocytosis and formation of spacious phagosomes but does not induce pyroptosis in favor of its survival. *Microbial pathogenesis*, 52, 367–374.

Roth, T. F. & Porter, K. R. (1964). Yolk protein uptake in the oocyte of the mosquito aedes aegypti. l. *The Journal of Cell Biology*, 20, 313.

Rupper, A., Grove, B., & Cardelli, J. (2001a). Rab7 regulates phagosome maturation in dictyostelium. *J. Cell Sci.*, 109, 1479–1495.

Rupper, A. C., Rodriguez-Paris, J. M., Grove, B. D., & Cardelli, J. A. (2001b). p110-related pi 3-kinases regulate phagosome-phagosome fusion and phagosomal ph through a pkb/akt dependent pathway in dictyostelium. *Journal of Cell Science*, 114, 1283–1295.

Rusten, T. E., Rodahl, L. M., Pattni, K., Englund, C., Samakovlis, C., Dove, S., Brech, A., & Stenmark, H. (2006). Fab1 phosphatidylinositol 3-phosphate 5-kinase controls trafficking but not silencing of endocytosed receptors. *Molecular Biology of the Cell*, 17, 3989–4001.

Saffi, G. T., Tang, E., Mamand, S., Inpanathan, S., Fountain, A., Salmena, L., & Botelho, R. J. (2021). Reactive oxygen species prevent lysosome coalescence during pikfyve inhibition. *PLOS ONE*, 16, e0259313.

Samie, M., Wang, X., Zhang, X., Goschka, A., Li, X., Cheng, X., Gregg, E., Azar, M., Zhuo, Y., Garrity, A. G., Gao, Q., Slaugenhaupt, S., Pickel, J., Zolov, S. N., Weisman, L. S., Lenk, G. M., Titus, S., Bryant-Genevier, M., Southall, N., Juan, M., Ferrer, M., & Xu, H. (2013). A trp channel in the lysosome regulates large particle phagocytosis via focal exocytosis. *Developmental cell*, 26, 511–524.

Sattler, N., Bosmani, C., Barisch, C., Guého, A., Gopaldass, N., Dias, M., Leuba, F., Bruckert, F., Cosson, P., & Soldati, T. (2018). Functions of the dictyostelium limp-2 and cd36 homologues in bacteria uptake, phagolysosome biogenesis and host cell defence. *Journal of Cell Science*, 131.

Sbrissa, D., Ikonomov, O. C., Fenner, H., & Shisheva, A. (2008). Arpikfyve homomeric and heteromeric interactions scaffold pikfyve and sac3 in a complex to promote pikfyve activity and functionality. *Journal of Molecular Biology*, 384, 766–779.

Sbrissa, D., Ikonomov, O. C., Fu, Z., Ijuin, T., Gruenberg, J., Takenawa, T., & Shisheva, A. (2007). Core protein machinery for mammalian phosphatidylinositol 3,5-bisphosphate synthesis and turnover that regulates the progression of endosomal transport. *Journal of Biological Chemistry*, 282, 23878–23891.

Sbrissa, D., Ikonomov, O. C., & Shisheva, A. (2000). Pikfyve lipid kinase is a protein kinase: downregulation of 5'-phosphoinositide product formation by autophosphorylation. *Biochemistry*, 39, 15980–9.

Sbrissa, D., Ikonomov, O. C., & Shisheva, A. (2002). Phosphatidylinositol 3-phosphate-interacting domains in pikfyve. binding specificity and role in pikfyve. endomenbrane localization. *The Journal of biological chemistry*, 277, 6073–6079.

Sbrissa, D., Ikonomov, O. C., Strakova, J., Dondapati, R., Mlak, K., Deeb, R., Silver, R., & Shisheva, A. (2004). A mammalian ortholog of saccharomyces cerevisiae vac14 that associates with and up-regulates pikfyve phosphoinositide 5-kinase activity. *Molecular and Cellular Biology*, 24, 10437–10447.

Sbrissa, D., Naisan, G., Ikonomov, O. C., & Shisheva, A. (2018). Apilimod, a candidate anticancer therapeutic, arrests not only ptdins(3,5)p2 but also ptdins5p synthesis by pikfyve and induces bafilomycin a1-reversible aberrant endomembrane dilation. *PLOS ONE*, 13, e0204532.

Seeberg, J. C., Loibl, M., Moser, F., Schwegler, M., Büttner-Herold, M., Daniel, C., Engel, F. B., Hartmann, A., Schlötzer-Schrehardt, U., Goppelt-Struebe, M., Schellerer, V., Naschberger, E., Ganzleben, I., Heinzerling, L., Fietkau, R., & Distel, L. V. (2019). Non-professional phagocytosis: a general feature of normal tissue cells. *Scientific Reports 2019 9:1*, 9, 1–8.

Shisheva, A. (2008). Pikfyve: Partners, significance, debates and paradoxes. *Cell biology international*, 32, 591–604.

Shisheva, A., Sbrissa, D., & Ikonomov, O. (1999). Cloning, characterization, and expression of a novel zn2+-binding fyve finger-containing phosphoinositide kinase in insulin-sensitive cells. *Molecular and cellular biology*, 19, 623–34.

Simonsen, A., Gaullier, J. M., D'Arrigo, A., & Stenmark, H. (1999). The rab5 effector eea1 interacts directly with syntaxin-6. *Journal of Biological Chemistry*, 274, 28857–28860.

Smith, M. E. (1999). Phagocytosis of myelin in demyelinative disease: a review. *Neurochemical research*, 24, 261–268.

Soares, A. C., Ferreira, A., Mariën, J., Delay, C., Lee, E., Trojanowski, J. Q., Moechars, D., Annaert, W., & de Muynck, L. (2021). Pikfyve activity is required for lysosomal trafficking of tau aggregates and tau seeding. *The Journal of biological chemistry*, 296.

Souza, G., Mehta, D., Lammertz, M., Rodriguez-Paris, J., Wu, R., Cardelli, J., & Freeze, H. (1997). Dictyostelium lysosomal proteins with different sugar modifications sort to functionally distinct compartments. *Journal of Cell Science*, 110, 2239–2248.

Spang, A. (2016). Membrane tethering complexes in the endosomal system. *Frontiers in Cell and Developmental Biology*, 4, 35.

Stenmark, H. (2009). Rab gtpases as coordinators of vesicle traffic. *Nature Reviews Molecular Cell Biology 2009 10:8*, 10, 513–525.

Stock, C., Grønlien, H. K., & Allen, R. D. (2002). The ionic composition of the contractile vacuole fluid of paramecium mirrors ion transport across the plasma membrane. *European journal of cell biology*, 81, 505–515.

Stossel, T. P. (1973). Quantitative studies of phagocytosis. kinetic effects of cations and heat-labile opsonin. *The Journal of cell biology*, 58, 346–356.

Sussman, R. & Sussman, M. (1967). Cultivation of dictyostelium discoideum in axenic medium. *Biochemical and biophysical research communications*, 29, 53–55.

Tauber, A. I. (2003). Metchnikoff and the phagocytosis theory. *Nature Reviews Molecular Cell Biology 2003 4:11*, 4, 897–901.

Temesvarisp, L., Rodriguez-Paris, J., Bush, J., Steckn, T. L., & Cardellisii, J. (1994). Characterization of lysosomal membrane proteins of dictyostelium discoideum. *The Journal of Biological Chemistry*, 269, 25719–25727.

Touret, N., Paroutis, P., Terebiznik, M., Harrison, R. E., Trombetta, S., Pypaert, M., Chow, A., Jiang, A., Shaw, J., Yip, C., Moore, H. P., Wel, N. V. D., Houben, D., Peters, P. J., Chastellier, C. D., Mellman, I., & Grinstein, S. (2005). Quantitative and dynamic assessment of the contribution of the er to phagosome formation. *Cell*, 123, 157–170.

Tu, H., Wang, Z., Yuan, Y., Miao, X., Li, D., Guo, H., Yang, Y., & Cai, H. (2022). The pripa-tbcra complex-centered rab gap cascade facilitates macropinosome maturation in dictyostelium. *Nature Communications 2022 13:1*, 13, 1–15.

Ungar, D. & Hughson, F. M. (2003). Snare protein structure and function. *Annual review of cell and developmental biology*, 19, 493–517.

Vieira, O. V., Botelho, R. J., Rameh, L., Brachmann, S. M., Matsuo, T., Davidson, H. W., Schreiber, A., Backer, J. M., Cantley, L. C., & Grinstein, S. (2001). Distinct roles of class i and class iii phosphatidylinositol 3-kinases in phagosome formation and maturation. *The Journal of Cell Biology*, 155, 19.

Vieira, O. V., Bucci, C., Harrison, R. E., Trimble, W. S., Lanzetti, L., Gruenberg, J., Schreiber, A. D., Stahl, P. D., & Grinstein, S. (2003). Modulation of rab5 and rab7 recruitment to phagosomes by phosphatidylinositol 3-kinase. *Molecular and Cellular Biology*, 23, 2501.

Vines, J. H., Buckley, C. M., Maib, H., Gueho, A., Soldati, T., Murray, D., & King, J. S. (2022). A pi(3,5)p2 probe reveals pikfyve is required for rab7 acquisition and the delivery and fusion of early macropinosomes to phagosomes. *bioRxiv*, (pp. 2022.09.19.508510).

Vines, J. H. & King, J. S. (2019). The endocytic pathways of dictyostelium discoideum. *The International Journal of Developmental Biology*, 63, 461–471.

Wang, X., Zhang, X., Dong, X. P., Samie, M., Li, X., Cheng, X., Goschka, A., Shen, D., Zhou, Y., Harlow, J., Zhu, M. X., Clapham, D. E., Ren, D., & Xu, H. (2012). Tpc proteins are phosphoinositide-activated sodium-selective ion channels in endosomes and lysosomes. *Cell*, 151, 372.

Ward, E. S., Martinez, C., Vaccaro, C., Zhou, J., Tang, Q., & Ober, R. J. (2005). From sorting endosomes to exocytosis: Association of rab4 and rab11 gtpases with the fc receptor, fcrn, during recycling. *Molecular Biology of the Cell*, 16, 2028–2038.

Watts, D. J. & Ashworth, J. M. (1970). Growth of myxameobae of the cellular slime mould dictyostelium discoideum in axenic culture. *The Biochemical journal*, 119, 171–174.

Wienke, D. C., Knetsch, M. L., Neuhaus, E. M., Reedy, M. C., & Manstein, D. J. (1999). Disruption of a dynamin homologue affects endocytosis, organelle morphology, and cytokinesis in dictyostelium discoideum. *Molecular Biology of the Cell*, 10, 225.

Worby, C. A. & Dixon, J. E. (2002). Sorting out the cellular functions of sorting nexins. *Nature Reviews Molecular Cell Biology*, 3, 919–931.

Yasuda, S., Morishita, S., Fujita, A., Nanao, T., Wada, N., Waguri, S., Schiavo, G., Fukuda, M., & Nakamura, T. (2016). Mon1-ccz1 activates rab7 only on late endosomes and dissociates from the lysosome in mammalian cells. *Journal of Cell Science*, 129, 329–340.

Yoshida, S., Gaeta, I., Pacitto, R., Krienke, L., Alge, O., Gregorka, B., & Swanson, J. A. (2015). Differential signaling during macropinocytosis in response to m-csf and pma in macrophages. *Frontiers in Physiology*, 6.

Yu, I. M. & Hughson, F. M. (2010). Tethering factors as organizers of intracellular vesicular traffic. *https://doi.org/10.1146/annurev.cellbio.042308.113327*, 26, 137–156.

Yu, Y., Jiao, M., Zhang, Z., & Yu, Y. (2022). Single-phagosome imaging reveals that homotypic fusion impairs phagosome degradative function. *Biophysical journal*, 121, 459–469.

Yuan, Y., Jaślan, D., Rahman, T., Bolsover, S. R., Arige, V., Ii, L. E. W., Abrahamian, C., Tang, R., Keller, M., Hartmann, J., Rosato, A. S., Weiden, E.-M., Bracher, F., Yule, D. I., Grimm, C., & Patel, S. (2022). Segregated cation flux by tpc2 biases ca 2+ signaling through lysosomes. *Nature Communications*, 13.

Zeineddine, R. & Yerbury, J. J. (2015). The role of macropinocytosis in the propagation of protein aggregation associated with neurodegenerative diseases. *Frontiers in physiology*, 6.

Zhang, C., Feng, Y., Balutowski, A., Miner, G. E., Rivera-Kohr, D. A., Hrabak, M. R., Sullivan, K. D., Guo, A., Calderin, J. D., & Fratti, R. A. (2022). The interdependent transport of yeast vacuole ca2+ and h+ and the role of phosphatidylinositol 3,5-bisphosphate. *The Journal of Biological Chemistry*, 298, 102672.

Zhang, X., Li, X., & Xu, H. (2012). Phosphoinositide isoforms determine compartment-specific ion channel activity. *Proceedings of the National Academy of Sciences of the United States of America*, 109, 11384–11389.

Zhen, Y. & Stenmark, H. (2015). Cellular functions of rab gtpases at a glance. *Journal of cell science*, 128, 3171–3176.

Zhou, K., Takegawa, K., Emr, S. D., & Firtel, R. A. (1995). A phosphatidylinositol (pi) kinase gene family in dictyostelium discoideum: biological roles of putative mammalian p110 and yeast vps34p pi 3-kinase homologs during growth and development. *Molecular and cellular biology*, 15, 5645–5656.

Appendices

Appendix A

Glossaries

A.1 Abbreviations and Acronyms

2xFYVE Tandem repeat of the FYVE domain from the human Hrs gene. Acts as a reliable PI(3)P biosensor.. 4, 37, 46, 76, 79, 81, 88, *see* FYVE

ArPIKfyve see: Vac14. 35

ATCC American Type Culture Collection. 36

ATP Adenosine Triphosphate. An energy-rich nucleotide composed of adenosine linked to ribose and three phosphate groups. The energy currency of the cell.. 18

BLAST Basic Local Alignment Search Tool. Finds regions of local similarity between sequences.. 36

bp Base Pairs. 39

BSA Bovine serum albumin. 37, 39

DMEM Dulbecco's Modified Eagle Medium. 36

DNA Deoxyribonucleic acid. Key carrier of genetic information for all living cells.. 36

EHD Eps15 homology domain. Contained in proteins structurally and functionally related to dynamin. 14

FBS Fetal bovine serum. 36

Fig4 A phosphoinositide phosphatase which catalyzes conversion of PI(3,5) P_2 into PI(3)P. Invovled in PIKfyve regulation. Sac3 in yeast.. 35, 50, 103, *see* PAS

GFP Green fluorescent protein. A protein that exhibits green fluorescence when exposed to light.. 26, 36–39, 41, 44, 77, 78, 85, 107

GTP Guanosine Triphosphate. An energy-rich nucleotide composed of guanine linked to ribose and three phosphate groups. Important for Rab GTPase acitvation.. 6

. *see* &

. *see*

NAADP Nicotinic Acid Adenine Dinucleotide Phosphate. A calcium ion releasing secondary messenger. 29

PBS Phosphate-buffered saline. 36, 38, 77

PCR Polymerase Chain Reaction. 36, 39, 76

PFA Paraformaldehyde. 36, 41

. *see*

PIP Phosphatidylinositide Species. A lipid made of an inositol head group, a glycerol backbone, and two non-polar fatty acid tails. Its head group can be phosphylated at three different positions to form 8 different PIP species. Here, PIP also referes to plasmanylinositides found in *Dictyostelium discoideum*. 11, 35, 37, 39, 75, 102

RFP Red fluorescent protein. A protein that exhibits red fluorescence when exposed to light.. 37, 76, 107

RIPA Radioimmunoprecipitation assay buffer. 37

RNA Ribonucleic acid. A nucleic acid present in all living cells that has structural similarities to DNA.. messenger RNA. A single stranded messenger RNA necessary for protein production.. 8. silencing RNA *or* short interfering RNA. A double-stranded RNA molecule that is non-coding, but can knocks down host cell proteins via RNA interference.. 26, 27.

ROS Reactive Oxygen Speices. Chemically reactive chemical species containing oxygen. They have roles in cell signaling and homeostasis, but can also cause significant damage to cell sturcutres if levels are increased. Examples of ROS include peroxides and superoxide.. 17–19, 27

RPE-1 Human retinal pigment epithelial-1 cells. Immortalized cell line.. 36, 44, 102

Sac3 see: Fig4. 35

SDS-PAGE Sodium dodecyl sulfate–polyacrylamide gel electrophoresis. 78

TBS-T Tris-buffered saline with tween. 37

TPC Two Pore Channel. A family of calcium ion channels that localize to endosomes. 29, 75

Vac14 A scaffold protein invovled in PIKfyve regulation. ArPIKfyve in yeast.. 35, 103, *see* PAS

Vps34 Vacuolar Protein Sorting 34. Recruited by Rab5 and responisble for PI(3)P synthesis on early macroendosomes.. 21, 24, 75, 79, 104

A.2 Proteins

BAR Bin, Amphiphysin and Rvs. A protein domain which senses and induces membrane curvature. 14

CatD Cathepsin D. A lysosomal aspartyl protease delivered to *D. discoideum* phagosomes.. 19, 20, 28
ClC7 A chloride ion channel regulated by PI(3,5) P_2.. 35
CORVET Class C Core Vacuole/Endosome Tethering Complex. A tethering complex that promotes fusion of Rab5-positive membranes. 7, 21, 24, 108

EEA1 Early Endosomal Antibody 1. A Rab5 and PI(3)P effector important for early endosome delivery events in mammals.. 4, 21, 24, 26, 106

Fab1 Yeast homolog of PIKfyve. 4, 35, 50, *see* PIKfyve
FYVE Fab1, YOTB, Vac1, and EEA1 (FYVE) domain. A protein domain which binds PI(3)P.. 4, 24, 25, 35, 46, 50, 75, 103, 104

GAP GTPase-activating proteins. A type of protein which is a negative regulator of GTPases.. 6, 24, *see* GEF
GEF Guanine nucleotide Exchange Factor. A type of protein which catalyzes he dissociation of GDP from GTPase proteins, such as Rabs, to activate them.. 6, 21, *see* GAP

HOPS Homotypic fusion and vacuole Protein Sorting Complex. A thethering complex which promotes fusion of Rab7-positive membranes in yeast.. 7, 25, 91, 108

LAMP-1 Lysosomal Associated Membrane Protein 1. A lysosomal marker protein. Commonly used as a lysosomal marker in mammalian cells. 17, 25
LAMP-2 Lysosomal Associated Membrane Protein 1. A lysosomal marker protein. Commonly used as a lysosomal marker in mammalian cells. 17, 25
LmpA Lysosomal membrane protein A. A *D. discoideum* lysosomal marker protein.. 17, 19, 20, 25, 28
LmpB Lysosomal membrane protein B. A glycoprotein in *D. discoideum* which mediates the uptake of mycobacteria. 13
LmpC Lysosomal membrane protein C. A *D. discoideum* lysosomal marker protein.. 17, 19, 20

mTORC1 Target of Rapamycin Complex 1. An essential regulator of cell growth and metabolism.. 27, 30

Nramp1 Natural resistance-associated membrane protein 1. An iron transporter which localizes to macroendosomes as important in killing certain pathogens. 18

PAS PIKfyve-ArPIKfyve-Sac3 Complex. Complex which regulates PIKfyve, ArPIKfyve is Fig14 in mammal, Sac3 is Fig4 in mammals.. 26
PIKfyve A PI-5 kinase responsible for producing PI(3,5) P_2 on early macroendosomes. It is essential for V-ATPase delivery, efficent maturation, and is the principal protein dicussed in the work above!. 35
PX Phox Homology Domain. A phosphoinositide-binding domain involved in targeting of proteins to cell membranes. 14, 36, 39, 41, 102

Rab GTPase Family of proteins of the Ras superfamily of small G proteins. Rab GTPases regulate many steps of membrane trafficking, including vesicle formation, vesicle movement along actin and tubulin networks, and membrane fusion.. *see* GEF &
RSC Retromer Sorting Complex.. 14

SNARE Soluble N-ethylmale-imide-sensitive factor-attachment protein receptors. Large protein complexes whose primary function is to mediate vesicle fusion. 7, 24, 25
  t-SNARE Target-SNARE. Present on target membreanes, for example phagosomes. 7
  v-SNARE Vesicle-SNARE. Present on vesicle membranes being delivered to targets. 7
STIM1 Stromal Interaction Molecule 1. Plays a crucial role in the interaction between phagosomes and the ER.. 16

TRPML1 . 20, 28, 29, 35, 75, 91, 106

V-ATPase Vacuolar-type ATPase. A proton pump used to acidify a wide range of intraceullular organelles. 15, 18, 20, 25, 28, 30, 35, 50, 76, 81, 83, 88, 89, 105, 106, 108

WASH WASP and SCAR homologue complex.. 13, 14, 20

A.3 Organisms & Cell Types

Ax2 Axenic strain 2. A strain of *D. discoideum* subculutred to grow in liquid meida. For this work it is used as a wild type strain.. 11, 36, 39, 76, 107

Dictyostelium discoideum A soil dewlling social ameoba commonly used as a model organism for the study of macropinocytosis and phagocytosis. 14, 15, 18, 19, 127–129

Escherichia coli A Gram-negative, anaeroibic, rod-shaped bacterium. Is commonly used as a model organism, for it has a long history of laboratory culutre and is easy to manipulate. Is a food source of *D. discoideum*. 18

HEK293 Human embryonic kidney 293 cells. Immortalised cell line derived from embryonic kidney cells.. 26, 36, 44

Klebsiella aerogenes A Gram-negative, anaeroibic, rod-shaped bacterium which is the preffered food source of *D. discoideum*. 18

Legionella pneumonia A Gram-negative, aerobic, rod-shaped bacterium. It is a human pathogen, but can also infect *D. discoideum*. 16, 18

MEF Mouse Embryonic Fibroblasts. A type of fibroblast prepared from mouse embryo. 16

MIA PaCa-2 An epithelial cell line that was derived from tumor tissue of the pancreas. 36, 44, 102

Appendix B

Plasmid List

	Plasmid Name	Plasmid Number	Reference
GFP Plasmids	PIKfyve-GFP	pJV0025	Chapter 2
	GFP-Rab5A	pJV0054	Chapter 3
	2xFYVE-GFP	pJSK418	Gillooly et al. (2000)
	GFP-Rab7A	pTH70	Tu et al. (2022)
SnxA Plasmids	DDB_G0285711-GFP	pJSK620	Chapter 2
	SnxA-GFP	pJSK619	Chapter 2
	SnxA-GFP (Integrating)	pCB40	Chapter 2
	1xPX-GFP	pJV0010	Chapter 2
	2xPX-GFP	pJV0016	Chapter 2
hsSnxA Vectors	GFP-hsSnxA	pJSK658	Chapter 2
	GFP-hs1xPX	pJSK663	Chapter 2
	GFP-hs2xPX	pJSK664	Chapter 2
	H6-GFP-hsSnxA	pJV0042	Chapter 2
	H6-GFP-hs1xPX	pJV0048	Chapter 2
	H6-GFP-hs2xPX	pJV0049	Chapter 2
RFP Vectors	2xPX-RFP	pJV0067	Chapter 2
	RFP-Rab7A	pTH363	Tu et al. (2022)
	RFP-VatM	pMJC26	
	RFP-2xFYVE	pCB128	Chapter 2
Dual	RFP-Rab5A + GFP-Rab7A	pJV0057	Chapter 3

Appendix C

Review from The International Journal of Developmental Biology:

The endocytic pathways of *Dictyostelium discoideum*

James H. Vines and Jason S. King

Int. J. Dev. Biol. 63: 461-471 (2019)
https://doi.org/10.1387/ijdb.190236jk

THE INTERNATIONAL JOURNAL OF DEVELOPMENTAL BIOLOGY
www.intjdevbiol.com

The endocytic pathways of *Dictyostelium discoideum*

JAMES H. VINES and JASON S. KING*

Department of Biomedical Sciences, University of Sheffield, Sheffield, UK

ABSTRACT The formation and processing of vesicles from the cell surface serves many important cellular functions ranging from nutrient acquisition to regulating the turnover of membrane components and signalling. In this article, we summarise the endocytic pathways of the social amoeba *Dictyostelium* from the clathrin-dependent and independent internalisation of surface components to the engulfment of bacteria or fluid by phagocytosis and macropinocytosis respectively. Due to similarities with the professional phagocytes of the mammalian immune system *Dictyostelium* has been extensively used to investigate the complex remodelling and trafficking events that occur as phagosomes and macropinosomes transit through the cell. Here we discuss what is known about this maturation process in order to kill any potential pathogens and obtain nutrients for growth. Finally, we aim to put these studies in evolutionary context and highlight some of the many questions that remain in our understanding of these complex and important pathways.

KEY WORDS: *Clathrin, macropinocytosis, phagocytosis, Dictyostelium, phosphoinositide, endocytosis*

The different types and roles of endocytosis

Endocytosis is a collective term, which refers to several different mechanisms of internalisation but can be divided into two main sub-categories based on the size of the vesicles formed: micro- and macro-endocytosis (Fig. 1). The best understood microendocytic pathway is that mediated by the protein clathrin, known as clathrin-mediated endocytosis (CME). Clathrin is a structural protein, which self-assembles to form a lattice shell around vesicles as they invaginate from the cell surface. This clathrin coat binds to adaptor proteins which recruit specific cargo proteins such as activated receptors, allowing them to be selectively internalised. More recently, clathrin-independent microendocytic pathways have also been identified, such as caveolin-associated endocytosis, which has additional functions in regulating membrane tension (Sinha *et al.*, 2011). Microendocytic pathways therefore primarily act as mechanisms to regulate the cell surface and regulate responses to extracellular signals.

In contrast, the main purpose of macroendocytic pathways is to internalise extracellular components, such as the surrounding fluid or particulate matter like microbes, dead cells or debris. The engulfment of both fluid and particles is achieved by mechanistically-related pathways known as macropinocytosis and phagocytosis respectively. In contrast to clathrin-mediated endosomes, which form by invagination of the plasma membrane, macropinosomes and most types of phagosomes are formed by specialised actin-based protrusions (Fig. 1). Whilst non-phagocytic cells are still able to take up fluid, this is mainly through the functionally-distinct (CLIC)/ GEEC pathway (CLathrin-Independent Carriers /Glycosylophosphatidylinositol-anchored protein Enriched Compartment) mediated by elongated tubular invaginations of the plasma membrane (Mayor *et al.*, 2014). Macropinocytosis and phagocytosis play important but specialised roles in diverse processes including nutrient acquisition, immune surveillance, defence against pathogens and the developmental clearance of dead cells (Bloomfield and Kay, 2016; Lim *et al.*, 2017). Therefore, whilst CME is ubiquitous, macroendocytosis is normally performed by specific cells in metazoa, such as those of the immune system.

The different functions of micro- and macro-endocytosis are apparent from the relative size of the vesicles formed. Clathrin-mediated endosomes are small and uniform, averaging 100 nm in diameter. This ensures a high surface area:volume ratio and therefore efficient membrane internalisation, whilst taking up relatively little fluid. Macropinosomes are larger and more heterogeneous in size, (between 200 and 2,000 nm diameter) and therefore take up substantially more fluid whilst minimising turnover of the plasma membrane. Additionally, whilst CME is selective, macropinosomes and phagosomes have no coats or adaptor proteins and therefore largely internalise surface constituents non-specifically. CME is

Abbreviations used in this paper: CLIC, clathrin-independent carriers; CME, clathrin mediated endocytosis; GEEC glycosylophosphatidylinositol-anchored protein enriched compartment; PIP, phosphatidyl inositol phosphate; SNARE, snap receptor; WASH, WASP and SCAR homologue.

***Address correspondence to:** Jason S. King. Department of Biomedical Sciences, University of Sheffield, Sheffield, UK.
E-mail: Jason.king@sheffield.ac.uk

Submitted: 18 June, 2019; *Accepted:* 23 July, 2019.

ISSN: Online 1696-3547, Print 0214-6282
© 2019 UPV/EHU Press
Printed in Spain

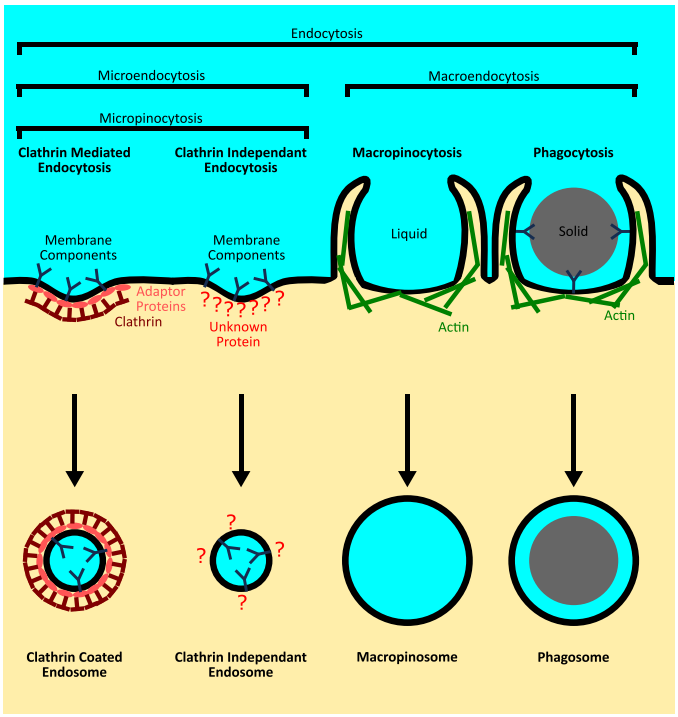

Fig. 1. The endocytic pathways in *Dictyostelium*. *From left to right: (1) In clathrin mediated endocytosis, selected membrane components to be internalized bind to adaptor proteins, which in turn bind intracellular clathrin. This creates an intracellular coat of clathrin and invagination of the plasma membrane, resulting in the formation of a small intracellular vesicle known as a clathrin coated endosome. (2) clathrin-independent endocytosis, whereby membrane components are taken up in the absence of clathrin and independently from macroendocytosis. The mechanism by which this is achieved is unknown (3) In macropinocytosis, extracellular fluid is taken up in large cup formed from spontaneous actin-based protrusions at the cell surface. This forms a large intracellular vesicle. (4) In phagocytosis, an extracellular particle (i.e. bacteria, yeast or latex bead) is taken up upon binding and activation of cell surface receptors, which stimulates actin polymerisation in a similar manner to a macropinocytic cup. This forms a large intracellular endosome known as a phagosome.*

therefore optimised for specific uptake of membrane components, whereas macropinocytosis is better adapted to take up extracellular material using the least possible membrane.

The importance of endocytosis and intracellular vesicle trafficking is highlighted by the prominence of mutations in these pathways associated with human diseases (Aridor and Hannan, 2002; Howell *et al.*, 2006; Mellman and Yarden, 2013; Wang *et al.*, 2014). Over many years of research a broad range of experimental systems have been used to dissect various aspects of endocytosis, most notably the identification of many important trafficking proteins discovered by genetic screens performed in yeast (reviewed in (Weinberg and Drubin, 2012)). However, despite enormous progress, many questions remain. Each model organism has its own particular nuances, and it is essential that studies are interpreted within a broader evolutionary context. In this article we focus on the endocytic pathways of the social amoeba *Dictyostelium discoideum*, which has been extensively used as a model to study many aspects of cell biology, and made a significant contribution to our understanding of intracellular trafficking.

Dictyostelium as a model organism

Dictyostelium discoideum is an amoeba that lives in soil and leaf-litter. When nutrients are plentiful, *Dictyostelium* grow as single cells by binary fission, preying on environmental bacteria for food (Fig. 2). During this life cycle the amoebae are professional phagocytes and, in comparison to mammalian cells, are most similar to the phagocytes of the innate immune system, such as macrophages and neutrophils. Whilst the densely packed, static tissues in multicellular organisms means most cells are not phagocytic, the engulfment machinery and mechanisms used by specialists to kill and digest captured microbes are highly conserved across evolution (Boulais *et al.*, 2010). Phagocytosis therefore first evolved to feed our distant phagotrophic single-celled ancestors such as *Dictyostelium*, before being selectively suppressed in metazoan tissues.

Many studies have therefore taken advantage of the experimental benefits of *Dictyostelium* to model immune cell functions such as bacterial engulfment and killing (Bozzaro and Eichinger, 2011; Dunn *et al.*, 2017).

When food is scarce however, *Dictyostelium* initiate a multicellular developmental cycle (Fig. 2). This involves communication between large numbers of amoebae to form aggregates of over 100,000 cells. These then differentiate into multiple different cell types to initially form a slug, which migrates towards heat and light to reach the soil surface. Remarkably, whilst phagocytosis is suppressed in most cells within the slug, a few hundred retain this capacity and appear to play the role of patrolling immune cells (Chen *et al.*, 2007; Zhang *et al.*, 2016). These cells, known as sentinel cells, are even able to eject extracellular DNA traps to capture and kill pathogens, highly reminiscent of the Neutrophil Extracellular Traps (NET's) important for innate immunity in mammals (Papayannopoulos, 2018).

After the slug stage, the cells differentiate further to generate a fruiting body consisting of a sporehead, which is held aloft by a rigid stem of stalk cells. This structure aids dispersal, whereby the dormant spores can be scattered to find new sources of food whilst the stalk cells are sacrificed for the greater good (Strassmann *et al.*, 2000). This is a complex process, dependent on both inter- and intra-cellular signalling and has thus been the subject of intense research for over 70 years (Loomis, 2014).

The varied life of *Dictyostelium* has made it an attractive organism to investigate many cellular processes. This is aided by a small haploid genome, making it amenable to genetic manipulation and often lacking the redundancy that can be problematic in higher

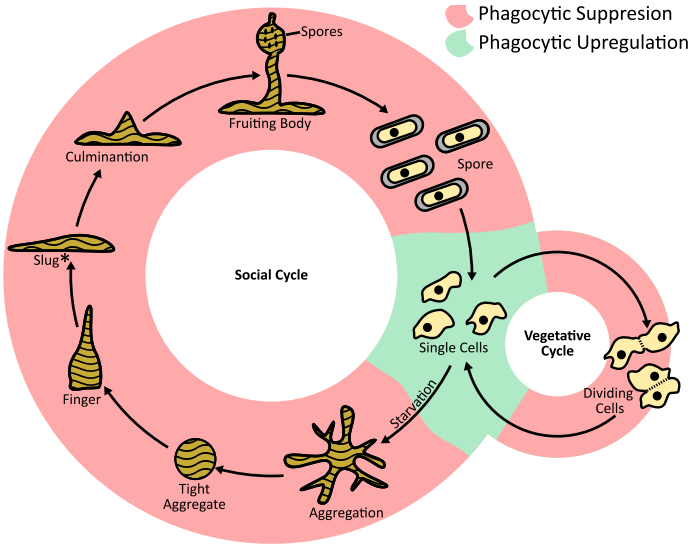

Fig. 2. Endocytosis throughout the *Dictyostelium* life cycles. *In nutrient-replete conditions,* Dictyostelium *will grow in the vegetative cycle where they feed through phagocytosis and macropinocytosis, as highlight by the green background. Upon starvation, macroendocytosis is largely suppressed and large numbers of cells aggregate by chemotaxis and undergo differentiation to form a multicellular structure consisting of >100,000 cells. The purpose of this structure is to aid the distribution of spores to a more nutrient rich environment. Both chemotaxis and development are dependent on clathrin-mediated endocytosis.*

eukaryotes (Eichinger *et al.*, 2005). Although the amoebozoa diverged from the animal lineage before fungi and after plants, the *Dictyostelium* genome appears to have retained much of the ancestral eukaryotic genome. *Dictyostelium* therefore possesses a number of genes that have been subsequently lost in other lineages, most notably in the contracted genome of *Saccharomyces cerevisiae* (Hirst *et al.*, 2014; King, 2012; O'Malley *et al.*, 2016; Roelofs and Van Haastert, 2001).

Simple genetic manipulation coupled with the ability to grow large numbers of isogenic cells for biochemical studies and amenability for fluorescence microscopy, has made *Dictyostelium* a useful system for many trafficking studies. Below, we discuss what is known about the different forms of endocytosis performed by *Dictyostelium,* with a focus on phagocytosis and macropinocytosis, which have been the most extensively investigated.

The endocytic pathways of *Dictyostelium*

Microendocytosis: clathrin dependent and independent

Although the majority of studies have focused on the large-scale endocytic pathways, *Dictyostelium*, like all eukaryotes, also use microendocytosis to internalise the plasma membrane and its constituents. *Dictyostelium* turnover their entire plasma membrane by microendocytosis every ~10 minutes (Aguado-Velasco and Bretscher, 1999), whereas the contribution from macropinocytosis is estimated to be 10-fold less (Aguado-Velasco and Bretscher, 1999; Buckley *et al.*, 2016). Surprisingly, mutants lacking the clathrin heavy chain (chcA), which is essential for lattice formation are only reduced in their membrane turnover by 25% (Aguado-Velasco and Bretscher, 1999; O'Halloran and Anderson, 1992; Ruscetti *et al.*, 1994). This is not due to upregulated macropinocytosis as *chcA*- cells also have significantly reduced fluid uptake, and clathrin-independent membrane internalisation is not aggravated by actin-depolymerising drugs (Neuhaus *et al.*, 2002; O'Halloran and Anderson, 1992). Microendocytosis can therefore occur by a clathrin independent mechanism in *Dictyostelium.* How this is achieved is unknown and whilst the caveolin proteins are able to drive endosome formation in mammalian cells, they only evolved in metazoa and so are not present in *Dictyostelium*(Kirkham *et al.*, 2008).

Whilst disruption of clathrin is not lethal, wild-type *Dictyostelium* cells have several hundred dynamic clathrin-coated pits on their surface at any one time, indicating that high levels of CME occur constitutively (Veltman *et al.*, 2011). Clathrin mutants are also perturbed in a wide range of cellular processes including cytokinesis, cell migration, lysosomal sorting, secretion and osmoregulation (O'Halloran and Anderson, 1992; Ruscetti *et al.*, 1994; Wessels *et al.*, 2000). Clathrin mutants also have severe defects in development (O'Halloran and Anderson, 1992). Many of these defects can be explained by defective trafficking of cell surface receptors and consequent disruption of signal transduction. However, clathrin also plays a role in sorting events within the cell, such as sorting and budding from intracellular compartments like the trans-Golgi network. Therefore phenotypes such as defects in the biogenesis of lysosomes and the specialised contractile vacuole osmoregulatory network found in protists may be due to disruption of intracellular sorting rather than endocytosis *per se* (Lefkir *et al.*, 2003; Poupon *et al.*, 2008; Ruscetti *et al.*, 1994*)*.

Phagocytosis

During vegetative growth, *Dictyostelium* are extremely efficient phagocytes and are able to feed on a broad range of both Gram-positive and Gram-negative bacteria. Phagocytosis is driven by the activation of cell surface receptors by binding to bacterial surface components. This can be mediated by a range of different receptors such as the *Dictyostelium* orthologues of the mammalian β-integrins (Similar to Integrin Beta, SibA and SibC) (Cornillon *et al.*, 2006) or the scavenger receptor LmpB (lysosomal membrane glycoprotein B) (Sattler *et al.*, 2018). Recently it was also shown that the same G-protein coupled receptor that drives chemotaxis to bacterially-secreted folate can also initiate phagocytosis by binding to lipopolysaccharides on the bacterial surface (Pan *et al.*, 2018).

After engulfment, phagosomes rapidly mature to generate an internal antimicrobial environment and kill the captured bacteria. This is achieved by multiple, parallel killing mechanisms involving acidification, digestion, metal ions and oxidative attack and is essential to prevent infection from potential pathogens (described in more detail later). After killing, bacteria are digested and nutrients

extracted to support growth of the amoebae, whilst any indigestible material is subsequently expelled.

As phagosome trafficking is often manipulated by pathogens to facilitate their intracellular survival, *Dictyostelium* have proven to be a useful model host to study a wide range of pathogenic bacteria including *Mycobacterium marinum* (a model for Tuberculosis), *Legionella pneumophila*, *Klebsiella pneumoniae*, *Francisella noatunensis* and *Listeria monocytogenes* (Reviewed in (Bozzaro and Eichinger, 2011; Dunn *et al*., 2017)). Although environmental isolates of *Dictyostelium* are strictly bacterivorous and cannot generate phagocytic cups large enough to engulf fungi, axenic laboratory strains can ingest larger organisms (Bloomfield *et al*., 2015). These strains have therefore also been used to study fungal infections (Hillmann *et al*., 2015; Koller *et al*., 2016; Watkins *et al*., 2018). As many pathogens also have an environmental niche, avoiding predation by amoebae such as *Dictyostelium* or the more common water amoeba *Acanthamoeba castellanii* has been proposed to be an important evolutionary driver of virulence traits - further validating the use of these organisms to study host-pathogen interactions (Casadevall *et al*., 2019; Molmeret *et al*., 2005).

Macropinocytosis

Consistent with a shared evolutionary origin for phagocytosis and macropinocytosis, *Dictyostelium* also constitutively take up fluid from their environment and can use it for food (Kay *et al*., 2019; King and Kay, 2019). Whilst both macropinocytosis and phagocytosis can be used to feed, they were recently shown to be inversely regulated, with macropinocytosis suppressed in the presence of bacteria and upregulated when bacteria were removed (Williams and Kay, 2018). *Dictyostelium* therefore adapt to the nutrient source available, although they prefer bacteria – a richer source of nutrients – over a liquid diet.

Feeding by macropinocytosis is important because like most protists and unlike most metazoan cells, *Dictyostelium* do not directly transport nutrients across the plasma membrane into the cytosol. This is most likely because living free in the environment inevitably exposes amoebae to the huge diversity of chemicals generated by the soil microbiota, including many potentially harmful molecules. This problem is circumvented by centralised nutrient extraction and detoxification in metazoa, but organisms such as *Dictyostelium* must attempt to control the absorption of extracellular molecules by first confining them within vesicles. Recently it has become clear that this original role for macropinocytosis in acquiring nutrients still occurs in mammals, and is used by cancer cells to enable the use of extracellular proteins as an additional food source to support their rapid growth (Commisso *et al*., 2013).

Whilst *Dictyostelium* can use macropinocytosis to feed, the amount of fluid taken up by wild-type environmental isolates is insufficient to support growth in liquid media unless heavily supplemented with protein (i.e. 10% fetal calf serum (FCS)(Bloomfield *et al*., 2015)). However, after prolonged incubation or mutagenesis, mutants can be selected that form much larger cups and engulf enough nutrients to grow (Sussman and Sussman, 1967; Watts and Ashworth, 1970). The ability to grow pure cultures of cells in the absence of bacteria has advantages for both genetic and biochemical studies. Therefore axenic mutant strains (known as Ax2-4) were widely adopted by the *Dictyostelium* community since their isolation (Watts and Ashworth, 1970). Surprisingly, the key mutation that enables axenic growth was only recently identified as loss of function of the *Dictyostelium* orthologue of neurofibromin (NF1) (Bloomfield *et al*., 2015). NF1 is a GTPase Activating Protein (GAP) that deactivates the small GTPase known as Ras. Ras is a key regulator of macropinosome formation in both *Dictyostelium* and mammals (Bar-Sagi and Feramisco, 1986). Disruption of *Dictyostelium* NF1 causes hyperactivation of Ras, increasing the size of the cup-shaped protrusions that generate macropinosomes and therefore the volume of fluid engulfed (Bloomfield *et al*., 2015). Importantly, this regulatory role in macropinocytosis and therefore inflammatory signalling was also recently confirmed in mouse macrophages (Ghoshal *et al*., 2019). Mutations in NF1 also cause the genetic condition Neurofibratomatosis type 1 in humans, resulting in tumours in the nervous system (Xu *et al*., 1990). Whether these two observations are causally linked remains to be determined, but the conserved role of NF1 emphasises how the mechanisms underlying macropinosome formation have been preserved across evolution.

The prominence of phagocytosis and macropinocytosis in *Dictyostelium,* combined with obvious parallels in the cell biology of amoebae and phagocytic cells of the immune system has meant that this is where the majority of endocytic studies have been focused in *Dictyostelium*. Indeed, the technical challenges faced in studies using mammalian macrophages and neutrophils have made *Dictyostelium* a valuable alternative experimental system to explore the basic mechanisms of engulfment, killing and digestion (Bozzaro and Eichinger, 2011). Engulfment is driven by the generation of actin-rich protrusions, sharing much of the same machinery used to drive cell migration. Macropinosome formation is particularly interesting, as the cups are able to spontaneously self-organise in the absence of any spatial or physical signals from a particulate template. This is described elsewhere, including in this issue (Buckley and King, 2017; Kay *et al*., 2019; Williams *et al*., 2019). The focus of this review will instead be on the maturation pathway of these compartments in *Dictyostelium* from the moment the phagosomes and macropinosomes have formed, until their eventual resolution.

The trafficking of macropinosomes and phagosomes

Phagocytosis and macropinocytosis co-evolved as feeding mechanisms in early eukaryotes (King and Kay, 2019). Therefore the mechanisms used to process and extract nutrients from the internalised fluid or bacteria are very similar. Whether the activation of membrane receptors during phagocytosis affects subsequent maturation is unclear. However, as *Dictyostelium* are clearly able to discriminate between different bacteria (Nasser *et al*., 2013) it is possible that phagosomes generate a more antimicrobial environment than macropinosomes.

Broadly, maturation can be divided into four distinct stages: (1) nascent recycling events, (2) early maturation (3) late maturation and (4) expulsion of indigestible waste (Figs. 3,4). Within each stage a variety of fusion and fission events occur, principally regulated through inositol phospholipids within the vesicle membrane, and Rab-family small GTPases present on the vesicle surface. Both of these act to mark different endocytic compartments and recruit specific effectors as they progress through the maturation pathway. As progression occurs, the luminal contents of both macropinosomes and phagosomes become acidified and digested to liberate nutrients before the final stage where any indigestible

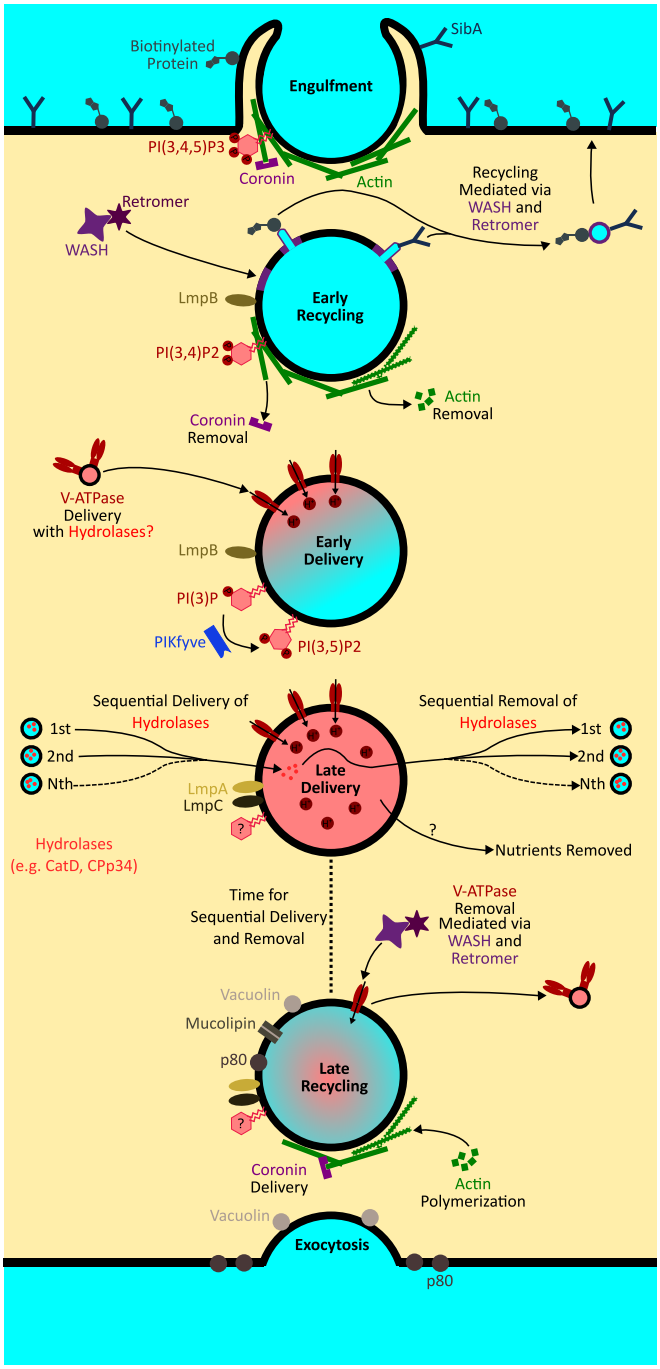

fragments are expelled from the cell. In *D. discoideum* this complete process takes around an hour. This pathway is highly conserved with mammalian leukocytes, with the exception of the final expulsion stage as both macrophages and neutrophils can retain engulfed material indefinitely, presumably to prevent an inflammatory response (Bai *et al.*, 2015).

The nascent macropinosome/ phagosome

Nascent macropinosomes and phagosomes are those which have just formed and separated from the plasma membrane. How the point of scission is detected is unknown, but the vesicles formed will be large, with a pH equal to that of their extracellular environment and a membrane consisting primarily of proteins and lipids found in the plasma membrane. Initially they are surrounded by actin filaments, which are required for the cup formation and sealing process (Rupper *et al.*, 2001). These filaments dissociate within 30-60 seconds following cup closure (Clarke *et al.*, 2010; Rupper *et al.*, 2001) along with actin associated proteins, such as coronin (Lu and Clarke, 2005; Maniak *et al.*, 1995). This process coincides with the movement of the nascent macropinosome/phagosome away from the plasma membrane and the initiation of subsequent membrane rearrangement events.

The inositol phospholipid (PIP) content of the membrane also changes during this time-period. PIPs are a family of lipids whereby the inositol sugar head-group can be phosphorylated at any of three

Fig. 3. Macropinosome and phagosome maturation in *Dictyostelium*. *The cartoon shows the progress of macroendosomes as they mature. Upon engulfment, the PI(3,4)P2 positive nascent vesicle is surrounded by actin which is rapidly removed. In an early recycling phase, plasma membrane proteins are rapidly recycled back to the plasma membrane by the WASH and retromer complexes. During this process, the compartment accumulates PI(3)P, and an early delivery phase also begins as the V-ATPase is delivered on small acidic vesicles. V-ATPase activity causes acidification of the vesicle lumen (represents by red colouring), and over time PI(3)P is converted to PI(3,5)P2 by the activity of PIKfyve. In a later delivery phase, when the lumen is acidified, hydrolases such as CatD and CP-p34 are sequentially delivered over an extended, digestive period. At this time, nutrients are presumably removed from the lumen via an unknown mechanism. Finally, after digestion is complete, the macroendosome is prepared for exocytosis in a late recycling phase. Here, WASH-stimulated actin re-forms around the compartment to retrieve the V-ATPase and form a neutral post-lysosome. The retromer complex is also present and potentially plays a role in hydrolase retrieval. Other important proteins such as vacuolin and mucolipin also accumulate on this late compartment, although are most probably retrieved before exocytosis, unlike p80 which is present during exocytosis and can be seen in high concentrations at the plasma membrane immediately after.*

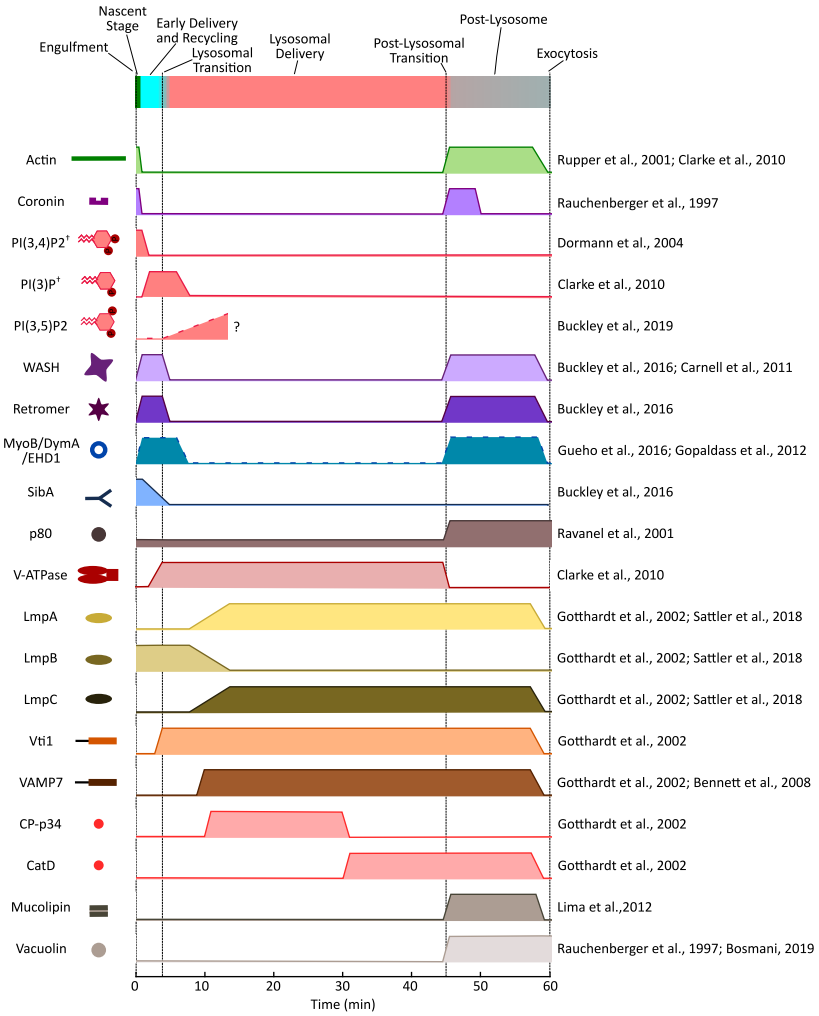

Fig. 4. Timings of components of phagosome and macropinosome maturation in *Dictyostelium*. *Each line represents the dynamics of the components (protein or lipid) covered by this review over a 60-minute maturation event. When the line of the time-courses is high, the respective component is at/on/in the endosome at this time-point. When the line of the time-course is low, the component is not present. This diagram has been pieced together from the existing literature, combining both microscopy and biochemical data. We have made the assumption that phagosome and macropinosome maturation are comparable and integrated data from studies of both pathways. The large majority of the studies cited support this, with the exception of minor differences in phosphoinositide dynamics discussed in the main text. It should be noted that in general, biochemical analysis of purified phagosomes often indicates slower maturation than that observed by live-cell imaging, with maturation occuring over an almost 3 hour period (Buckley* et al., *2016; Gopaldass* et al., *2012; Gotthardt* et al., *2002a). Microscopy studies in contrast, indicate exocytosis of yeast and bead-containing phagosomes, as well as macropinosomes occurs at around 60-90 minutes after engulfment (Clarke* et al., *2010; Lima* et al., *2012; Ravanel* et al., *2001; Watkins* et al., *2018). We have consolidated and corollated data from both techniques to an "average" 60-minute transit. With this in mind, this figure is best viewed in the context of our review as a whole and combined with the references provided for each individual component. "†" indicates that retrieval phase is known to be longer in phagosomes containing yeast. Time courses with dashed lines indicate an even greater level of uncertainty.*

positions. The different phosphorylation states can be interconverted by a family of PIP kinases and phosphatases to generate seven different forms of the lipid. Each PIP is able to recruit different target proteins, resulting in an elegant system to identify different membranes and regulate endocytic trafficking (Bohdanowicz and Grinstein, 2013). Both macropinosome and phagosome membranes initially contain high levels of $PI(3,4)P_2$. $PI(3,4)P_2$ is generated by the rapid de-phosphorylation of $PI(3,4,5)P_3$ by the PI-5 phosphatase called Oculocerebrorenal syndrome of Lowe (OCRL), during and immediately following cup closure (Dormann *et al.*, 2004; Li *et al.*, 2018; Loovers *et al.*, 2007; Luscher *et al.*, 2019). On phagosomal membranes $PI(3,4)P_2$ content peaks immediately following cup closure and is gradually lost over time (Dormann *et al.*, 2004). There are however conflicting reports of how long $PI(3,4)P_2$ is retained. Studies following phagocytosed yeast show that $PI(3,4)P_2$ is only transiently present on the phagosome, between 60 and 120 seconds post-engulfment (Dormann *et al.*, 2004; Giorgione and Clarke, 2008). In contrast, latex-bead containing phagosomes maintain $PI(3,4)P_2$ much longer - upwards of 360 seconds suggesting that the pathways regulating phagosomal maturation may be cargo-dependent (Giorgione and Clarke, 2008).

Early recycling events

One of the first key events in maturation is the recycling of plasma membrane components back to the cell surface. Several

studies have shown that cell surface proteins are non-specifically internalised on both phagosomes and macropinosomes, but rapidly removed following engulfment (Buckley *et al*., 2016; Gotthardt *et al*., 2002b; Ravanel *et al*., 2001). This appears to occur over 2 phases, with an early myoB-independent phase followed by slower myoB-dependent recycling (Neuhaus and Soldati, 2000). Although the majority of proteins appear to be internalised non-specifically, there is also evidence that a subset can be specifically excluded from cups, although how this might be achieved is not known (Mercanti *et al*., 2006).

As the contents of macroendosomes are destined for degradation the rescue of cell surface components before their digestion is important for continued cell function. This is achieved by the combined action of sorting and recycling complexes. One such complex is the WASP and SCAR Homolog (WASH) complex, which is recruited to nascent macropinosomes and phagosomes in both *D. discoideum* and mammalian macrophages immediately following cup closure (Buckley *et al*., 2016). The WASH complex is able to generate patches of polymerised actin on the surface of vesicles via activation of the Arp2/3 complex (Derivery *et al*., 2009; Gomez and Billadeau, 2009). WASH enables the formation of actin-rich subdomains, which can both sequester specific proteins, as well as aid the formation of tubules and removal of the membrane. This is assisted by a direct interaction between the FAM21 subunit of the WASH complex and the vacuolar protein sorting-35 (VPS35) subunit of the retromer sorting complex (RSC), known to promote recycling (Jia *et al*., 2012). This is a general mechanism, and in recent years, studies in mammalian cells have shown WASH and the RSC mediate sorting from several different endosomal compartments (Seaman, 2012).

In *D. discoideum*, the WASH and retromer complexes co-localise on nascent phagosomes and macropinosomes, and disruption of *WASH* causes defects in the retrieval of surface proteins (Buckley *et al*., 2016). In the absence of this step, levels of surface proteins such as the Sib integrin-like receptors important for both substrate adhesion and phagocytosis are severely depleted (Buckley *et al*., 2016). Consequently, the phagocytosis efficiency of *WASH*-null cells is significantly reduced, demonstrating the importance of early surface protein retrieval in maintaining cellular functions.

Class I non-muscle myosins have also been shown to be important for early recycling events. Myosin IB heavy chain (MyoB) has also been identified as localising to nascent phagosomes, and disruption of both myosin I isoforms known as myosin IA heavy chain (MyoA) and MyoB or treatment with the myosin I inhibitor, butanedione monoxime, results in a build-up of cell surface proteins on intracellular compartments (Neuhaus and Soldati, 2000). How myosin I contributes to recycling mechanistically, or interacts with the WASH/Retromer complexes is yet to be determined. An additional class I myosin, myoK is also involved during early maturation, but plays a distinct role in regulating the association and delivery of ER components to the phagosome, although the functional significance of ER delivery is unclear (Dieckmann *et al*., 2012).

Another element important in early recycling from phagosomes and macropinosomes is the machinery to mediate the final stages of membrane scission as vesicles pinch off from endosomes (Gopaldass *et al*., 2012). The most well understood of these is the large GTPase dynamin, necessary for pinching off clathrin-coated vesicles from the plasma membrane and scission of vesicles from elongated endosomal tubules in mammalian cells and yeast (Ferguson and De Camilli, 2012). Disruption of the *Dictyostelium* dynamin orthologue DymA disrupts multiple membrane scission events making it problematic to differentiate between direct and indirect roles (Wienke *et al*., 1999). Nonetheless, DymA localises to phagosomes during the early recycling phase and *DymA* mutants have very slow acidification and reduced proteolysis rates in later stages of maturation (Gopaldass *et al*., 2012).

Recently it was also shown that the *Dictyostelium* orthologue of EHD (Eps15 homology domain containing protein) is also recruited very early to phagosomes (Gueho *et al*., 2016). EHD proteins are structurally and functionally related to dynamin. *Dictyostelium* EHD and DymA physically interact and are recruited to the nascent phagosome simultaneously, but independently (Gueho *et al*., 2016). In mammals, EHD1 has been shown to regulate retromer-mediated trafficking (Zhang *et al*., 2012). Whilst disruption of DymA or EHD both result in hyper-tubulation of endosomal compartments, they appear to play functionally independent roles in phagosome maturation as in contrast to *DymA* mutants, *EHD* knockout phagosomes acidify more rapidly (Gueho *et al*., 2016).

Whilst it is easy to imagine a role for dynamin and EHD in the scission of recycling vesicles from nascent phagosomes and macropinosomes, this is yet to be directly tested. As WASH and the retromer are only present for the first 2-3 minutes following engulfment, but DymA and EHD remain for as long as 30 minutes, there are also likely to be a number of additional trafficking steps regulated by this membrane cleavage machinery (Buckley *et al*., 2016; Gueho *et al*., 2016).

Early delivery events

Following internalisation, and somewhat overlapping with early recycling, macroendosomes then undergo various fusions to deliver the digestive, acidification and killing machinery. This is often referred to as early maturation and occurs within the first 10 minutes post-engulfment. During this period phagosomes and macropinosomes are marked by the lipid PI(3)P (Buckley *et al*., 2019; Clarke *et al*., 2010). Although it has not been confirmed in *Dictyostelium,* in mammalian cells this is generated by activation of the class III PI-3 kinase by Rab5 (Christoforidis *et al*., 1999b; Vieira *et al*., 2001).

PI(3)P is not identifiable on the nascent phagosomes/macropinosome while it is still surrounded by actin, but appears almost immediately after internalisation (Clarke *et al*., 2010). PI(3)P is lost gradually from early phagosomes containing bacteria over the next six minutes (Clarke *et al*., 2010) and similar dynamics are also observed in macropinosomes (Clarke *et al*., 2010; King and Kay, 2019). In contrast, engulfed yeast retain PI(3)P much longer, again indicating cargo-dependent signalling dynamics (our unpublished observations and (Clarke *et al*., 2010)).

In mammalian cells, the best known Rab5/PI(3)P effector is EEA1 (Early Endosomal Autoantigen 1), which can lead to endosomal docking and fusion in collaboration with SNARE (Soluble NSF attachment Protein Receptor) membrane fusion complexes (Christoforidis *et al*., 1999a; Simonsen *et al*., 1998). Whilst *Dictyostelium* Rab5 has not been studied in detail, and there is no obvious EEA1 orthologue the presence of PI(3)P coincides with the fusion of several different compartments with phagosomes and macropinosomes. The role for PI(3)P in the fusion of endosomal compartments and delivery of maturation components is therefore

likely to be conserved.

SNAREs are membrane bound proteins present in all eukaryotic cells, which function to fuse intracellular compartments. Fusion occurs when one vesicle-SNARE forms a complex with two or three specific target-SNAREs to form an alpha helix coiled-coil bundle (reviewed in (Hong, 2005)). The first target-SNARE found in *Dictyostelium* was the orthologue of syntaxin 7, required for endosome-endosome fusion (Bogdanovic *et al.*, 2002). In complex with its co-target SNARES, syntaxin 8 and Vti1, syntaxin 7 is able to bind to a single vesicle-SNARE called VAMP7. Binding facilitates the fusion of the two respective compartments. VAMP7-GFP labels all *D. discoideum* early endocytic compartments, suggesting that these SNAREs mediate most early fusion events (Bennett *et al.*, 2008). However, the precise fusions in which these SNAREs are used are not well characterised.

One of the best characterised complexes delivered to the phagosome and macropinosome within its early stages is the vacuolar ATPase (V-ATPase) (Clarke *et al.*, 2002; Gotthardt *et al.*, 2002b). The V-ATPase is responsible for the translocation of protons across membranes and consequently it is the key component leading to lumen acidification. The V-ATPase complex is formed of multiple subunits, including the large 100 kDa transmembrane subunit VatM. Studies following the trafficking of GFP-tagged VatM showed that it is delivered to early phagosomes and macropinosomes over the first 1 to 2 minutes after engulfment (Clarke *et al.*, 2002; Clarke *et al.*, 2010). Delivery occurs via small GFP-VatM-positive acidic vesicles, which cluster around the early phagosome before fusing (Clarke *et al.*, 2002). These pre-existing, acidic compartments stem from the endosomal system as they can be labelled with the endosomal dye TRITC-dextran, which becomes visible in the lumen of the phagosome within 3 to 4 minutes post engulfment (Clarke *et al.*, 2002; Clarke *et al.*, 2010).

V-ATPase delivery coincides with the rapid acidification of macroendosomes, which begins around 60 seconds after engulfment. VatM concentrations increase until a peak around 4 minutes after cup closure, coinciding with the end of the WASH/retromer recycling phase (Buckley *et al.*, 2016). Luminal pH continues to drop to a low of pH 3.5 over about 10 minutes, where it is maintained for a further 30 minutes to allow for digestion (Gopaldass *et al.*, 2012). Whilst VatM is essential for cell viability, knock-down of the protein shows slow cell growth, reduced phagocytosis, and a mis-localisation of other V-ATPase subunits, including the catalytic subunit, VatA (Liu *et al.*, 2002).

More recent studies have implicated PIKfyve, a PI-5 kinase, in the efficient delivery of V-ATPase (Buckley *et al.*, 2019). PIKfyve catalyses the conversion of PI(3)P to PI(3,5)P_2, and knockouts of PIKfyve have slower V-ATPase delivery to early phagosomes, and consequently are defective in acidification (Buckley *et al.*, 2019). PIKfyve is also important for hydrolase delivery and proteolysis (see below). Cells lacking PIKfyve are therefore poor at killing engulfed bacteria and are thus highly susceptible to pathogens, such as *Legionella pneumphila* (Buckley *et al.*, 2019). Despite this importance, the role of PI(3,5,)P_2 is poorly characterised, with a paucity of known effector proteins.

Delivery of lysosomal enzymes

As maturation progresses, the lysosomal enzymes important for digestion are delivered to the phagosome/macropinosome. Acid hydrolyses are some of the best characterised proteins known to be delivered during this stage and depend on the low pH generated by the V-ATPase for activity. Contrary to a model whereby a lysosome containing the entire gamut of digestive enzymes and the V-ATPase deliver them to phagosomes all at once, imaging of lysosomal enzymes with different sugar modifications and proteomics of purified phagosomes both indicate multiple phases of delivery and retrieval throughout the 45 minute digestive period (Gotthardt *et al.*, 2002b; Souza *et al.*, 1997). For example, the cysteine protease CP-p34 is amongst the first hydrolases delivered, coinciding with delivery of the two Lysosomal Membrane Proteins LmpA and LmpC (Gotthardt *et al.*, 2002b). This is subsequently followed by CP-p34 retrieval and delivery of cathepsin D (CatD), a second hydrolase, which is retained until just before exocytosis, along with LmpA and LmpC (Gotthardt *et al.*, 2002b). How specific luminal enzymes are selectively trafficked is not known, and the reason for sequential delivery and retrieval is not entirely clear. However, it may be possible that digestion is more efficient if early hydrolases partially digest the luminal contents for later ones with different cleavage specificity.

The post-lysosomal transition and exocytosis

The final stage of maturation ends in the expulsion of indigestible luminal contents into the extracellular space. However, before this can happen, various proteins must be retrieved from the compartment, which at this stage is referred to as the post-lysosome. The transition from a digestive compartment to a post-lysosome is precipitated by retrieval of the V-ATPase and subsequent neutralisation. Over a three minute period, the V-ATPase is sequestered from the membrane into small vesicles and recycled (Clarke *et al.*, 2010). The mammalian V-ATPase directly binds actin (Holliday *et al.*, 2000; Vitavska *et al.*, 2003), and although this interaction has not been confirmed in *Dictyostelium,* V-ATPase retrieval is dependent on actin polymerisation (Clarke *et al.*, 2010). Surprisingly, this is mediated by a second, independent phase of WASH complex activity, which occurs 40-50 minutes after engulfment (Carnell *et al.*, 2011). In the absence of WASH, phagosomes and macropinosomes never neutralise and cells have a complete block in exocytosis (Carnell *et al.*, 2011). In *WASH* null cells, hydrolases also accumulate in this late compartment, blocking their recycling and delivery to nascent endosomes (King *et al.*, 2013). Exocytosis, neutralisation and hydrolase retention are also all defective in cells expressing dominant-negative Rab7 (Buczynski *et al.*, 1997). It is therefore likely that an additional mechanism to retrieve hydrolases before they are lost by exocytosis exists, potentially via the activity of the retromer, which is also present at this time (Buckley *et al.*, 2016).

As the V-ATPase is removed the luminal pH neutralises and additional components are gained such as the putative copper transporter p80, which is commonly used to identify the post-lysosomal compartment (Ravanel *et al.*, 2001). The metal ion composition of post-lysosomes appears to be highly regulated as mucolipin-1, a calcium ion channel, is also specifically found on this compartment (Lima *et al.*, 2012). Disruption of mucolipin results in decreased calcium within the post-lysosome and increased exocytosis, although how this is mediated by calcium is unclear (Lima *et al.*, 2012). Another important late protein seems to be lvsB (Large Volume Sphere), a *Dictyostelium* homologue of the LYST/Beige (Lysosomal Trafficking Regulator) protein which is important

in endosomal fusion in mammals and mutated in Chediak-Higashi syndrome (Charette *et al.*, 2007). In *lvsB* mutants the lysosome/post-lysosomal transition is defective, resulting in decreased post-lysosomal numbers and exocytosis (Charette *et al.*, 2007).

Post-lysosomes also likely have unique lipid properties as they specifically accumulate the *Dictyostelium* orthologues of flotillin (known as the vacuolins) which partly reside in detergent-resistant lipid microdomains known as lipid rafts (Bosmani *et al.*, 2019; Jenne *et al.*, 1998; Rauchenberger *et al.*, 1997). In mammalian cells, these microdomains are found on both the plasma membrane and endosomal compartment, where they function as platforms for signalling and recycling of specific cargoes (Stuermer and Plattner, 2015). Despite their predominantly post-lysosomal localisation, disruption of the vacuolin causes defects throughout the endocytic cycle, including faster maturation, defective recycling of membrane proteins and strong defects in phagocytosis (Bosmani *et al.*, 2019). It is therefore likely that lipid-microdomain mediated sorting and recycling has pleiotropic functions throughout the *Dictyostelium* endocytic pathway.

Conclusions and perspectives

The studies described above demonstrate complex remodelling of endosomes throughout their transit through the cell. Multiple mechanisms are employed to retrieve and deliver both soluble and transmembrane components at specific points to achieve the orderly capture of extracellular nutrients whilst protecting the cell from environmental toxins, potential pathogens, or the accidental degradation of surface components. Much of this machinery is conserved throughout evolution and *Dictyostelium* has proven a useful model for the phagocytic cells of the human immune system.

Many questions still remain. For example, scission from the plasma membrane instigates the immediate start of maturation, but the events surrounding cup closure and the transition from formation to maturation are very poorly understood. Whilst macroendocytic transit follows a consistent maturation programme with defined transitions, how this is timed and translated into abrupt changes in vesicle identity is not known. There are also many mechanistic questions about how specific components are delivered and retrieved that will only be elucidated by future studies.

Importantly, *Dictyostelium* provides a highly accessible system to manipulate and dissect these pathways using both *in vivo* and biochemical techniques. As many recent studies have demonstrated, the ability to extend such investigations to interactions with potential pathogens has uncovered many fascinating aspects of the constant competition between phagocytes and their prey. Whilst new techniques such as CRISPR-Cas9 gene editing have opened up new possibilities to manipulate mammalian cells, the relative simplicity, reduced functional redundancy and ease of use mean there is still much we can learn from these humble amoebae.

References

AGUADO-VELASCO, C. and BRETSCHER, M. S. (1999). Circulation of the plasma membrane in Dictyostelium. *Mol Biol Cell* 10: 4419–4427.

ARIDOR, M. and HANNAN, L. A. (2002). Traffic jams II: an update of diseases of intracellular transport. *Traffic* 3: 781–790.

BAI, Y., BRUGHA, R. E., JACOBS, L., GRIGG, J., NAWROT, T. S. and NEMERY, B. (2015). Carbon loading in airway macrophages as a biomarker for individual exposure to particulate matter air pollution - A critical review. *Env. Int* 74: 32–41.

BAR-SAGI, D. and FERAMISCO, J. R. (1986). Induction of membrane ruffling and fluid-phase pinocytosis in quiescent fibroblasts by ras proteins. *Science* 233: 1061–1068.

BENNETT, N., LETOURNEUR, F., RAGNO, M. and LOUWAGIE, M. (2008). Sorting of the v-SNARE VAMP7 in Dictyostelium discoideum: A role for more than one Adaptor Protein (AP) complex. *Exp. Cell Res.* 314: 2822–2833.

BLOOMFIELD, G. and KAY, R. R. (2016). Uses and abuses of macropinocytosis. *J Cell Sci* 129: 2697–2705.

BLOOMFIELD, G., TRAYNOR, D., SANDER, S. P., VELTMAN, D. M., PACHEBAT, J. A. and KAY, R. R. (2015). Neurofibromin controls macropinocytosis and phagocytosis in Dictyostelium. *Elife 4,* e04940.

BOGDANOVIC, A., BENNETT, N., KIEFFER, S., LOUWAGIE, M., MORIO, T., GARIN, J., SATRE, M. AND BRUCKERT, F. (2002). Syntaxin 7, syntaxin 8, Vti1 and VAMP7 (vesicle-associated membrane protein 7) form an active SNARE complex for early macropinocytic compartment fusion in *Dictyostelium discoideum. Biochem. J.* 368: 29–39.

BOHDANOWICZ, M. and GRINSTEIN, S. (2013). Role of phospholipids in endocytosis, phagocytosis, and macropinocytosis. *Physiol Rev* 93: 69–106.

BOSMANI, C., BACH, F., LEUBA, F., HANNA, N., BURDET, F., PAGNI, M., HAGEDORN, M. and SOLDATI, T. (2019). Dictyostelium discoideum flotillin homologues are essential for phagocytosis and participate in plasma membrane recycling and lysosome biogenesis. *bioRxiv* 582049.

BOULAIS, J., TROST, M., LANDRY, C. R., DIECKMANN, R., LEVY, E. D., SOLDATI, T., MICHNICK, S. W., THIBAULT, P. and DESJARDINS, M. (2010). Molecular characterization of the evolution of phagosomes. *Mol Syst Biol* 6: 423.

BOZZARO, S. and EICHINGER, L. (2011). The professional phagocyte Dictyostelium discoideum as a model host for bacterial pathogens. *Curr Drug Targets* 12: 942–954.

BUCKLEY, C. M. and KING, J. S. (2017). Drinking problems: mechanisms of macropinosome formation and maturation. *FEBS J.* 284: 3778–3790.

BUCKLEY, C. M. C. M., GOPALDASS, N., BOSMANI, C., JOHNSTON, S. A. S. A., SOLDATI, T., INSALL, R. H. R. H. and KING, J. S. (2016). WASH drives early recycling from macropinosomes and phagosomes to maintain surface phagocytic receptors. *Proc. Natl. Acad. Sci. USA* 113: 201524532.

BUCKLEY, C. M., HEATH, V. L., GUÉHO, A., BOSMANI, C., KNOBLOCH, P., SIKAKANA, P., PERSONNIC, N., DOVE, S. K., MICHELL, R. H., MEIER, R., *et al.,* (2019). PIKfyve/Fab1 is required for efficient V-ATPase and hydrolase delivery to phagosomes, phagosomal killing, and restriction of Legionella infection. *PLoS Pathog.* 15: e1007551.

BUCZYNSKI, G., BUSH, J., ZHANG, L., RODRIGUEZ-PARIS, J. and CARDELLI, J. (1997). Evidence for a recycling role for Rab7 in regulating a late step in endocytosis and in retention of lysosomal enzymes in Dictyostelium discoideum. *Mol Biol Cell* 8: 1343–1360.

CARNELL, M., ZECH, T., CALAMINUS, S. D., URA, S., HAGEDORN, M., JOHNSTON, S. A., MAY, R. C., SOLDATI, T., MACHESKY, L. M. and INSALL, R. H. (2011). Actin polymerization driven by WASH causes V-ATPase retrieval and vesicle neutralization before exocytosis. *J Cell Biol* 193: 831–839.

CASADEVALL, A., FU, M. S., GUIMARAES, A. J. and ALBUQUERQUE, P. (2019). The "Amoeboid Predator-Fungal Animal Virulence" Hypothesis. *J Fungi* 5: 10.

CHARETTE, S. J., COSSON, P., KISTLER, C., HENKEL, A. W. and SOLDATI, T. (2007). ALYST/beige homolog is involved in biogenesis of Dictyostelium secretory lysosomes. *J. Cell Sci.* 120: 2338–2343.

CHEN, G., ZHUCHENKO, O. and KUSPA, A. (2007). Immune-like phagocyte activity in the social amoeba. *Science* 317: 678–681.

CHRISTOFORIDIS, S., MCBRIDE, H. M., BURGOYNE, R. D. and ZERIAL, M. (1999a). The rab5 effector EEA1 is a core component of endosome docking. *Nature* 397: 621–625.

CHRISTOFORIDIS, S., MIACZYNSKA, M., ASHMAN, K., WILM, M., ZHAO, L., YIP, S.-C., WATERFIELD, M. D., BACKER, J. M. and ZERIAL, M. (1999b). Phosphatidylinositol-3-OH kinases are Rab5 effectors. *Nat. Cell Biol.* 1: 249–252.

CLARKE, M., KÖHLER, J., ARANA, Q., LIU, T., HEUSER, J. and GERISCH, G. (2002). Dynamics of the vacuolar H+-ATPase in the contractile vacuole complex and the endosomal pathway of Dictyostelium cells. *J. Cell Sci.* 115: 2893–2905.

CLARKE, M., MADDERA, L., ENGEL, U. and GERISCH, G. (2010). Retrieval of the vacuolar H-ATPase from phagosomes revealed by live cell imaging. *PLoS One* 5: e8585.

COMMISSO, C., DAVIDSON, S. M., SOYDANER-AZELOGLU, R. G., PARKER, S.

J., KAMPHORST, J. J., HACKETT, S., GRABOCKA, E., NOFAL, M., DREBIN, J. A., THOMPSON, C. B., *et al.,* (2013). Macropinocytosis of protein is an amino acid supply route in Ras-transformed cells. *Nature* 497: 633–637.

CORNILLON, S., GEBBIE, L., BENGHEZAL, M., NAIR, P., KELLER, S., WEHRLE-HALLER, B., CHARETTE, S. J., BRUCKERT, F., LETOURNEUR, F. and COSSON, P. (2006). An adhesion molecule in free-living Dictyostelium amoebae with integrin beta features. *EMBO J. Rep* 7: 617–621.

DERIVERY, E., SOUSA, C., GAUTIER, J. J., LOMBARD, B., LOEW, D. and GAUTREAU, A. (2009). The Arp2/3 activator WASH controls the fission of endosomes through a large multiprotein complex. *Dev Cell* 17: 712–723.

DIECKMANN, R., GUEHO, A., MONROY, R., RUPPERT, T., BLOOMFIELD, G. and SOLDATI, T. (2012). The balance in the delivery of ER components and the vacuolar proton pump to the phagosome depends on myosin IK in Dictyostelium. *Mol Cell Proteom.*11: 886–900.

DORMANN, D., WEIJER, G., DOWLER, S. and WEIJER, C. J. (2004). *In vivo* analysis of 3-phosphoinositide dynamics during Dictyostelium phagocytosis and chemotaxis. *J Cell Sci* 117: 6497–6509.

DUNN, J. D., BOSMANI, C., BARISCH, C., RAYKOV, L., LEFRANCOIS, L. H., CARDENAL-MUNOZ, E., LOPEZ-JIMENEZ, A. T. and SOLDATI, T. (2017). Eat Prey, Live: Dictyostelium discoideum As a Model for Cell-Autonomous Defenses. *Front Immunol* 8: 1906.

EICHINGER, I., PACHEBAT, J. A., GLÖCKNER, G., RAJANDREAM, M. A., SUCGANG, R., BERRIMAN, M., SONG, J., OLSEN, R., SZAFRANSKI, K., XU, Q., *et al.,* (2005). The genome of the social amoeba Dictyostelium discoideum. *Nature.* 435: 43–57.

FERGUSON, S. M. and DE CAMILLI, P. (2012). Dynamin, a membrane-remodelling GTPase. *Nat. Rev. Mol. Cell Biol.* 13, 75–88.

GHOSHAL, P., SINGLA, B., LIN, H., CHERIAN-SHAW, M., TRITZ, R., PADGETT, C. A., HUDSON, F., ZHANG, H., STANSFIELD, B. K. and CSÁNYI, G. (2019). Loss of GTPase activating protein neurofibromin stimulates paracrine cell communication via macropinocytosis. *Redox Biol.* 101224.

GIORGIONE, J. and CLARKE, M. (2008). Heterogeneous modes of uptake for latex beads revealed through live cell imaging of phagocytes expressing a probe for phosphatidylinositol-(3,4,5)-trisphosphate and phosphatidylinositol-(3,4)-bisphosphate. *Cell Motil. Cytoskeleton* 65: 721–733.

GOMEZ, T. S. and BILLADEAU, D. D. (2009). A FAM21-containing WASH complex regulates retromer-dependent sorting. *Dev Cell* 17: 699–711.

GOPALDASS, N., PATEL, D., KRATZKE, R., DIECKMANN, R., HAUSHERR, S., HAGEDORN, M., MONROY, R., KRUGER, J., NEUHAUS, E. M., HOFFMANN, E., *et al.,* (2012). Dynamin A, Myosin IB and Abp1 couple phagosome maturation to F-actin binding. *Traffic* 13: 120–130.

GOTTHARDT, D., WARNATZ, H. J., HENSCHEL, O., BRUCKERT, F., SCHLEICHER, M. and SOLDATI, T. (2002a). High-resolution dissection of phagosome maturation reveals distinct membrane trafficking phases. *Mol Biol Cell* 13: 3508–3520.

GOTTHARDT, D., WARNATZ, H. J., HENSCHEL, O., BRÜCKERT, F., SCHLEICHER, M. and SOLDATI, T. (2002b). High-resolution dissection of phagosome maturation reveals distinct membrane trafficking phases. *Mol. Biol. Cell* 13: 3508–3520.

GUEHO, A., BOSMANI, C., GOPALDASS, N., MOLLE, V., SOLDATI, T. and LETOURNEUR, F. (2016). Dictyostelium EHD associates with Dynamin and participates in phagosome maturation. *J. Cell Sci.* 129: 2354–2367.

HILLMANN, F., NOVOHRADSKA, S., MATTERN, D. J., FORBERGER, T., HEINEKAMP, T., WESTERMANN, M., WINCKLER, T. and BRAKHAGE, A. A. (2015). Virulence determinants of the human pathogenic fungus Aspergillus fumigatus protect against soil amoeba predation. *Env. Microbiol* 17: 2858–2869.

HIRST, J., SCHLACHT, A., NORCOTT, J. P., TRAYNOR, D., BLOOMFIELD, G., ANTROBUS, R., KAY, R. R., DACKS, J. B. and ROBINSON, M. S. (2014). Characterization of TSET, an ancient and widespread membrane trafficking complex. *Elife* 3: e02866.

HOLLIDAY, L. S., LU, M., LEE, B. S., NELSON, R. D., SOLIVAN, S., ZHANG, L. and GLUCK, S. L. (2000). The amino-terminal domain of the B subunit of vacuolar H+-ATPase contains a filamentous actin binding site. *J Biol Chem* 275: 32331–32337.

HONG, W. (2005). SNAREs and traffic. *Biochim. Biophys. Acta - Mol. Cell Res.* 1744: 120–144.

HOWELL, G. J., HOLLOWAY, Z. G., COBBOLD, C., MONACO, A. P. and PONNAMBALAM, S. (2006). Cell biology of membrane trafficking in human disease. *Int Rev Cytol* 252: 1–69.

JENNE, N., RAUCHENBERGER, R., HACKER, U., KAST, T. and MANIAK, M. (1998). Targeted gene disruption reveals a role for vacuolin B in the late endocytic pathway and exocytosis. *J. Cell Sci.* 111: 61–70.

JIA, D., GOMEZ, T. S., BILLADEAU, D. D. and ROSEN, M. K. (2012). Multiple repeat elements within the FAM21 tail link the WASH actin regulatory complex to the retromer. *Mol. Biol. Cell* 23: 2352–2361.

KAY, R. R., WILLIAMS, T. D. and MANTON, J. D. (2019). Living on soup : macropinocytic feeding in amoebae. *Int J Dev Biol* (https://doi.org/10.1387/ijdb.190220rk)

KING, J. S. (2012). Autophagy across the eukaryotes Is S. cerevisiae the odd one out? *Autophagy* 8: 1159–1162.

KING, J. S. and KAY, R. R. (2019). The origins and evolution of macropinocytosis. *Philos Trans R Soc L. B Biol Sci* 374: 20180158.

KING, J. S., GUEHO, A., HAGEDORN, M., GOPALDASS, N., LEUBA, F., SOLDATI, T. and INSALL, R. H. R. H. (2013). WASH is required for lysosomal recycling and efficient autophagic and phagocytic digestione. *Mol. Biol. Cell* 24: 2714–2726.

KIRKHAM, M., NIXON, S. J., HOWES, M. T., ABI-RACHED, L., WAKEHAM, D. E., HANZAL-BAYER, M., FERGUSON, C., HILL, M. M., FERNANDEZ-ROJO, M., BROWN, D. A., *et al.,* (2008). Evolutionary analysis and molecular dissection of caveola biogenesis. *J Cell Sci* 121: 2075–2086.

KOLLER, B., SCHRAMM, C., SIEBERT, S., TRIEBEL, J., DELAND, E., PFEFFER-KORN, A. M., RICKERTS, V. and THEWES, S. (2016). Dictyostelium discoideum as a Novel Host System to Study the Interaction between Phagocytes and Yeasts. *Front Microbiol* 7: 1665.

LEFKIR, Y., DE CHASSEY, B., DUBOIS, A., BOGDANOVIC, A., BRADY, R. J., DESTAING, O., BRUCKERT, F., O'HALLORAN, T. J., COSSON, P. and LETOURNEUR, F. (2003). The AP-1 clathrin-adaptor is required for lysosomal enzymes sorting and biogenesis of the contractile vacuole complex in Dictyostelium cells. *Mol Biol Cell* 14: 1835–1851.

LI, X., EDWARDS, M., SWANEY, K. F., SINGH, N., BHATTACHARYA, S., BORLEIS, J., LONG, Y., IGLESIAS, P. A., CHEN, J. and DEVREOTES, P. N. (2018). Mutually inhibitory Ras-PI(3,4)P 2 feedback loops mediate cell migration. *Proc. Natl. Acad. Sci. USA 115: E9125–E9134.*

LIM, J. J., GRINSTEIN, S. and ROTH, Z. (2017). Diversity and Versatility of Phagocytosis: Roles in Innate Immunity, Tissue Remodeling, and Homeostasis. *Front. Cell. Infect. Microbiol.* 1: 191.

LIMA, W. C., LEUBA, F., SOLDATI, T. and COSSON, P. (2012). Mucolipin controls lysosome exocytosis in Dictyostelium. *J Cell Sci* 125: 2315–2322.

LIU, T., MIRSCHBERGER, C., CHOOBACK, L., ARANA, Q., SACCO, Z. D., MACWILLIAMS, H. and CLARKE, M. (2002). Altered expression of the 100 kDa subunit of the Dictyostelium vacuolar proton pump impairs enzyme assembly, endocytic function and cytosolic pH regulation. *J. Cell Sci.* 109: 489–497.

LOOMIS, W. F. (2014). Cell signaling during development of dictyostelium. *Dev. Biol.* 391: 1–16.

LOOVERS, H. M., KORTHOLT, A., DE GROOTE, H., WHITTY, L., NUSSBAUM, R. L. and VAN HAASTERT, P. J. (2007). Regulation of phagocytosis in Dictyostelium by the inositol 5-phosphatase OCRL homolog Dd5P4. *Traffic* 8: 618–628.

LU, H. and CLARKE, M. (2005). Dynamic properties of Legionella-containing phagosomes in Dictyostelium amoebae. *Cell. Microbiol.* 7: 995–1007.

LUSCHER, A., FRÖHLICH, F., BARISCH, C., LITTLEWOOD, C., METCALFE, J., LEUBA, F., PALMA, A., PIRRUCCELLO, M., CESARENI, G., STAGI, M., *et al.,* (2019). Lowe Syndrome-linked endocytic adaptors direct membrane cycling kinetics with OCRL in Dictyostelium discoideum. *Mol. Biol. Cell.* 30: 2268–2282.

MANIAK, M., RAUCHENBERGER, R., ALBRECHT, R., MURPHY, J. and GERISCH, G. (1995). Coronin involved in phagocytosis: Dynamics of particle-induced relocalization visualized by a green fluorescent protein tag. *Cell* 83: 915–924.

MAYOR, S., PARTON, R. G. and DONALDSON, J. G. (2014). Clathrin-independent pathways of endocytosis. *Cold Spring Harb. Perspect. Biol.* 6: a016758.

MELLMAN, I. and YARDEN, Y. (2013). Endocytosis and Cancer. *Cold Spring Harb Perspect Biol* 5: a016949–a016949.

MERCANTI, V., CHARETTE, S. J., BENNETT, N., RYCKEWAERT, J. J., LETOURNEUR, F. and COSSON, P. (2006). Selective membrane exclusion in phagocytic and macropinocytic cups. *J Cell Sci* 119: 4079–4087.

MOLMERET, M., HORN, M., WAGNER, M., SANTIC, M. and KWAIK, Y. A. (2005). Amoebae as training grounds for intracellular bacterial pathogens. *Appl. Environ. Microbiol.* 71: 20–28.

NASSER, W., SANTHANAM, B., MIRANDA, E. R., PARIKH, A., JUNEJA, K., ROT,

G., DINH, C., CHEN, R., ZUPAN, B., SHAULSKY, G., *et al.,* (2013). Bacterial discrimination by dictyostelid amoebae reveals the complexity of ancient interspecies interactions. *Curr Biol* 23: 862–872.

NEUHAUS, E. M. and SOLDATI, T. (2000). A myosin I is involved in membrane recycling from early endosomes. *J Cell Biol* 150: 1013–1026.

NEUHAUS, E. M., ALMERS, W. and SOLDATI, T. (2002). Morphology and dynamics of the endocytic pathway in Dictyostelium discoideum. *Mol Biol Cell* 13: 1390–1407.

O'HALLORAN, T. J. and ANDERSON, R. G. (1992). Clathrin heavy chain is required for pinocytosis, the presence of large vacuoles, and development in Dictyostelium. *J Cell Biol* 118: 1371–1377.

O'MALLEY, M. A., WIDEMAN, J. G. and RUIZ-TRILLO, I. (2016). Losing Complexity: The Role of Simplification in Macroevolution. *Trends Ecol. Evol.* 31: 608–621.

PAN, M., NEILSON, M. P., GRUNFELD, A. M., CRUZ, P., WEN, X., INSALL, R. H. and JIN, T. (2018). A G-protein-coupled chemoattractant receptor recognizes lipopolysaccharide for bacterial phagocytosis. *PLoS Biol* 16: e2005754.

PAPAYANNOPOULOS, V. (2018). Neutrophil extracellular traps in immunity and disease. *Nat. Rev. Immunol.* 18: 134–147.

POUPON, V., GIRARD, M., LEGENDRE-GUILLEMIN, V., THOMAS, S., BOURBONNIERE, L., PHILIE, J., BRIGHT, N. A. and MCPHERSON, P. S. (2008). Clathrin light chains function in mannose phosphate receptor trafficking via regulation of actin assembly. *Proc Natl Acad Sci U S A* 105: 168–173.

RAUCHENBERGER, R., HACKER, U., MURPHY, J., NIEWÖHNER, J. and MANIAK, M. (1997). Coronin and vacuolin identify consecutive stages of a late, actin-coated endocytic compartment in Dictyostelium. *Curr. Biol.* 7: 215–218.

RAVANEL, K., DE CHASSEY, B., CORNILLON, S., BENGHEZAL, M., ZULIANELLO, L., GEBBIE, L., LETOURNEUR, F. and COSSON, P. (2001). Membrane sorting in the endocytic and phagocytic pathway of Dictyostelium discoideum. *Eur J Cell Biol* 80: 754–764.

ROELOFS, J. and VAN HAASTERT, P. J. M. (2001). Genes lost during evolution. *Nature* 411: 1013–1014.

RUPPER, A., GROVE, B. and CARDELLI, J. (2001). Journal of Cell Science. *J. Cell Sci.* 109: 1479–1495.

RUSCETTI, T., CARDELLI, J. A., NISWONGER, M. L. and O'HALLORAN, T. J. (1994). Clathrin heavy chain functions in sorting and secretion of lysosomal enzymes in Dictyostelium discoideum. *J Cell Biol* 126: 343–352.

SATTLER, N., BOSMANI, C., BARISCH, C., GUÉHO, A., GOPALDASS, N., DIAS, M., LEUBA, F., BRUCKERT, F., COSSON, P. and SOLDATI, T. (2018). Functions of the Dictyostelium LIMP-2 and CD36 homologues in bacteria uptake, phagolysosome biogenesis and host cell defence. *J. Cell Sci.* 131: jcs218040.

SEAMAN, M. N. (2012). The retromer complex - endosomal protein recycling and beyond. *J Cell Sci* 125: 4693–4702.

SIMONSEN, A., LIPPE, R., CHRISTOFORIDIS, S., GAULLIER, J. M., BRECH, A., CALLAGHAN, J., TOH, B. H., MURPHY, C., ZERIAL, M. and STENMARK, H. (1998). EEA1 links PI(3)K function to Rab5 regulation of endosome fusion. *Nature* 394: 494–498.

SINHA, B., KÖSTER, D., RUEZ, R., GONNORD, P., BASTIANI, M., ABANKWA, D., STAN, R. V, BUTLER-BROWNE, G., VEDIE, B., JOHANNES, L., *et al.,* (2011). Cells respond to mechanical stress by rapid disassembly of caveolae. *Cell* 144: 402–413.

SOUZA, G. M., MEHTA, D. P., LAMMERTZ, M., RODRIGUEZ-PARIS, J., WU, R., CARDELLI, J. A. and FREEZE, H. H. (1997). Dictyostelium lysosomal proteins with different sugar modifications sort to functionally distinct compartments. *J. Cell Sci.* 110: 2239–2248.

STRASSMANN, J. E., ZHU, Y. and QUELLER, D. C. (2000). Altruism and social cheating in the social amoeba Dictyostelium discoideum. *Nature* 408: 965–967.

STUERMER, C. A. O. and PLATTNER, H. (2015). The "lipid raft" microdomain proteins reggie-1 and reggie-2 (flotillins) are scaffolds for protein interaction and signalling. *Biochem. Soc. Symp.* 72: 109–118.

SUSSMAN, R. and SUSSMAN, M. (1967). Cultivation of Dictyostelium discoideum in axenic medium. *Biochem. Biophys. Res. Commun.* 72: 109–118.

VELTMAN, D. M., AUCIELLO, G., SPENCE, H. J., MACHESKY, L. M., RAPPOPORT, J. Z. and INSALL, R. H. (2011). Functional analysis of Dictyostelium IBARa reveals a conserved role of the I-BAR domain in endocytosis. *Biochem J* 436: 45–52.

VIEIRA, O. V., BOTELHO, R. J., RAMEH, L., BRACHMANN, S. M., MATSUO, T., DAVIDSON, H. W., SCHREIBER, A., BACKER, J. M., CANTLEY, L. C. and GRINSTEIN, S. (2001). Distinct roles of class I and class III phosphatidylinositol 3-kinases in phagosome formation and maturation. *J. Cell Biol.* 155: 19–26.

VITAVSKA, O., WIECZOREK, H. and MERZENDORFER, H. (2003). A novel role for subunit C in mediating binding of the H+-V-ATPase to the actin cytoskeleton. *J. Biol. Chem. 278: 18499–18505.*

WANG, X., HUANG, T., BU, G. J. and XU, H. X. (2014). Dysregulation of protein trafficking in neurodegeneration. *Mol. Neurodegener.* 9: 1-9.

WATKINS, R. A., ANDREWS, A., WYNN, C., BARISCH, C., KING, J. S. and JOHNSTON, S. A. (2018). Cryptococcus neoformans escape from Dictyostelium amoeba by both WASH-mediated constitutive exocytosis and vomocytosis. *Front. Cell. Infect. Microbiol.* 8: 108.

WATTS, D. J. and ASHWORTH, J. M. (1970). Growth of myxameobae of the cellular slime mould Dictyostelium discoideum in axenic culture. *Biochem J* 119: 171–174.

WEINBERG, J. and DRUBIN, D. G. (2012). Clathrin-mediated endocytosis in budding yeast. *Trends Cell Biol.* 22: 1-13.

WESSELS, D., REYNOLDS, J., JOHNSON, O., VOSS, E., BURNS, R., DANIELS, K., GARRARD, E., O'HALLORAN, T. J. and SOLL, D. R. (2000). Clathrin plays a novel role in the regulation of cell polarity, pseudopod formation, uropod stability and motility in Dictyostelium. *J Cell Sci* 113: 21–36.

WIENKE, D. C., KNETSCH, M. L., NEUHAUS, E. M., REEDY, M. C. and MANSTEIN, D. J. (1999). Disruption of a dynamin homologue affects endocytosis, organelle morphology, and cytokinesis in Dictyostelium discoideum. *Mol Biol Cell* 10: 225–243.

WILLIAMS, T. D. and KAY, R. R. (2018). The physiological regulation of macropinocytosis during Dictyostelium growth and development. *J. Cell Sci.* 131: jcs213736.

WILLIAMS, T. D., PASCHKE, P. I. and KAY, R. R. (2019). Function of small GTPases in Dictyostelium macropinocytosis. *Philos. Trans. R. Soc. B Biol. Sci.* 374: 20180150.

XU, G. F., OCONNELL, P., VISKOCHIL, D., CAWTHON, R., ROBERTSON, M., CULVER, M., DUNN, D., STEVENS, J., GESTELAND, R., WHITE, R., *et al.,* (1990). The Neurofibromatosis Type-1 Gene Encodes a Protein Related to Gap. *Cell* 62: 599–608.

ZHANG, J., REILING, C., REINECKE, J. B., PRISLAN, I., MARKY, L. A., SORGEN, P. L., NASLAVSKY, N. and CAPLAN, S. (2012). Rabankyrin-5 Interacts with EHD1 and Vps26 to Regulate Endocytic Trafficking and Retromer Function. *Traffic.* 13: 745–757.

ZHANG, X., ZHUCHENKO, O., KUSPA, A. and SOLDATI, T. (2016). Social amoebae trap and kill bacteria by casting DNA nets. *Nat. Commun. 7: 10938.*